Dopaminergic regulation of the somatosensory cortex

Angelica da Silva Lantyer

Printed by: Gildeprint
ISBN: 978-94-6284-177-2

All rights reserved. No part of this publication may be reproduced, stored in a retrieval system, or transmitted in any form or by any means, mechanically, by photocopy, by recording or otherwise, without permission of the author.

Dopaminergic regulation of the somatosensory cortex

Proefschrift ter verkrijging van de graad van doctor
aan de Radboud Universiteit Nijmegen
op gezag van de rector magnificus prof. dr. J.H.J.M. van Krieken,
volgens besluit van het college van decanen
in het openbaar te verdedigen op

woensdag 5 december 2018

om 12:30 uur precies

door

Angelica da Silva Lantyer

geboren op 26 juli 1990

te Sao Paulo, Brazilië

Promotor: Prof. dr. Tansu Celikel
Co-promotoren:
Dr. Fleur Zeldenrust
Dr. Wim Scheenen

Manuscriptcommissie:
Prof. dr. Benno Rozendaal
Prof. dr. Patrik Krieger (Ruhr-Universität Bochum, Duitsland)
Dr. Sharon Kolk

Dopaminergic regulation of the somatosensory cortex

Doctoral thesis
to obtain the degree of doctor
from Radboud University Nijmegen
on the authority of the Rector Magnificus prof. dr. J.H.J.M. van Krieken,
according to the decision of the Council of Deans
to be defended in public on

Wednesday, December 5, 2018,

at 12:30 hours

by

Angelica da Silva Lantyer

born in July 26, 1990

in Sao Paulo, Brazil

Supervisor: Prof. dr. Tansu Celikel
Co-supervisors:
Dr. Fleur Zeldenrust
Dr. Wim Scheenen

Manuscript committee:
Prof. dr. Benno Rozendaal
Prof. dr. Patrik Krieger (Ruhr-Universität Bochum, Germany)
Dr. Sharon Kolk

Dopaminergic regulation of the somatosensory cortex

Angelica da Silva Lantyer[1]

[1] This work was supported by the National Council of Scientific and Technological Development (CNPq) of the Brazilian Ministry of Science, Technology and Communication.

Table of Contents

Chapter 1

Dopaminergic regulation of action potential timing

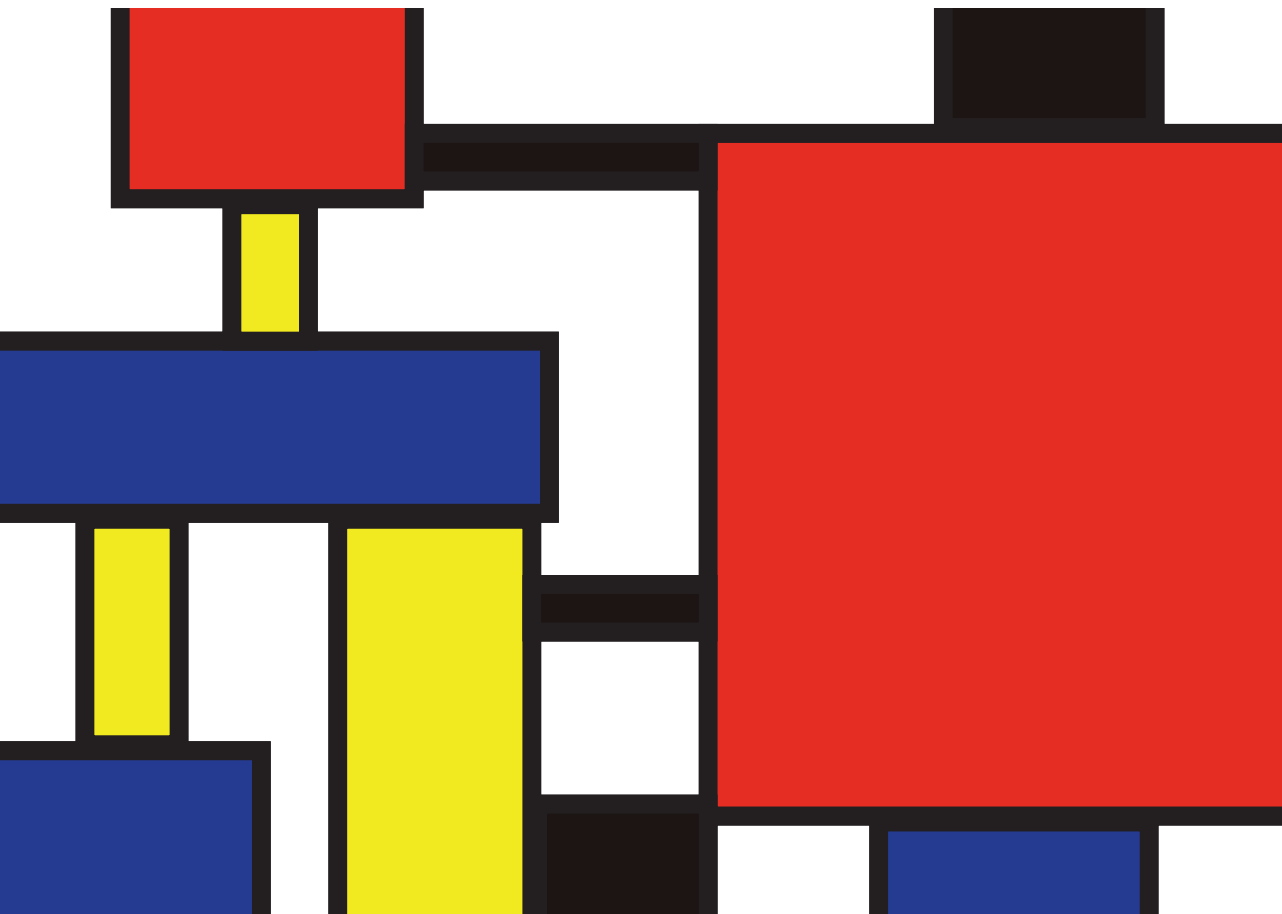

Information processing along sensorimotor pathways requires integration of bottom-up sensory input from the periphery with the top-down computations of the brain. From a sensory processing perspective, adaptive (plausibly neuromodulatory) control of spike timing is of particular interest as rapid propagation of information via ascending sensory pathways requires stimulus-coupled spiking that is correlated across neurons. Here we review the role of dopamine in controlling neuronal excitability and propose that dopaminergic modulation of voltage-gated sodium channels might be an efficient, yet unexplored/unidentified, mechanism for top-down control of spike timing during bottom-up propagation of sensory information. Mechanistic understanding of the contextual control over sensory representations will help to determine how neural representations of the world are shaped by behavioral and perceptual priors.

Dopamine is central to many neural processes including the modulation of the reward system, motor control, pleasure and higher cognitive functions [1–4]. Dysfunctions in the dopaminergic pathways are associated with aggression and violence [5], schizophrenia [6,7], Parkinson's Disease (PD) [8,9], addiction [10–13], anxiety disorders [14] and Attention Deficit Hyperactivity Disorder (ADHD) [7,15].

There are two classes of dopamine receptors that includes five subtypes: D1-like receptors are composed of the subfamily of D1 and D5 receptors (D1R, D5R), and the D2-like receptors that include the D2R, D3R and D4R [16,17]. Dopamine receptors are also found as D1-D2 heteromers [18], and as heteromers with various other G-protein coupled receptors (GPCR)[19,20]. Furthermore, dopamine can bind to Trace Amine Associated Receptor 1 (TAAR1) which modulates presynaptic dopaminergic transmission [21,22]. Considering that dopaminergic neurons might release dopamine extra-synaptically (including somato-dendritically [23,24]) and might release neurotransmitters other than dopamine, such as glutamate, serotonin, endocannabinoids, neurotensin and cholecystokinin [25,26], it is not surprising that dopamine contributes to numerous behaviorally relevant computations throughout the brain, including state dependent changes in neuronal communication [27,28].

State-dependent computations are critical for an animal to adapt its behavior to the ever-changing environment and to create appropriate motor actions. Although the role of dopamine in controlling motor behavior is well documented (see e.g. [29,30]), dopaminergic modulation of sensory processing is yet to be mechanistically understood [31–33]. Here we provide a critical review of the literature on the dopaminergic regulation of neural activity, experience-dependent plasticity and network activity, focusing on sensorimotor circuits. We argue that one key, albeit not yet explored, mechanism with which dopamine could shape sensory representations of the world is the modulation of voltage-gated sodium channels to control action potential timing. Understanding the mechanisms of top/down regulation of sensory representations might help to differentiate the mechanisms of perceptual and experience-dependent plasticity in the sensory systems [34], while providing a mechanistic insight into how adaptive sensorimotor computations emerge in a context dependent manner.

Dopaminergic control of neuronal communication

In the rodent brain, dopaminergic projections mature postnatally, targeting virtually the entire brain, including ascending and descending sensorimotor circuits [31]. Depending on the receptor localization, the neuronal classes they are expressed in, and the dopaminergic receptors types that are (in)activated, dopamine release may result in excitation or inhibition. For example, in the medial prefrontal cortex (mPFC), dopamine release inhibits glutamatergic signaling [35]; in the entorhinal cortex, phasic dopamine release after reward leads to the suppression

of excitatory synaptic responses via the D2-like receptors [36]. Although dopamine readily suppresses action potential backpropagation, if D2 receptors are inactivated simultaneously, the dendritic T-type calcium channels can be recruited, resulting in increased dendritic excitability and calcium inflow during dopaminergic transmission [37].

Dopamine contributes to sensory information processing. In the olfactory bulb, dopamine reduces spontaneous excitatory synaptic events by reducing evoked presynaptic calcium currents, suggesting that dopamine inhibits neurotransmission via presynaptic mechanisms in the mitral/tufted cells [38]. In the striatum, D1 neurons respond to ipsilateral somatosensory stimulation with earlier latency and higher firing rates than D2 neurons, which argues that D1 and D2 may have complementary functions for sensory stimulus processing [39]; D1 neurons might act as a comparator for the sensory information on the ipsilateral and contralateral whiskers [33], while D2 neurons seem to act as integrators [39]. Interestingly, midbrain dopaminergic neurons regulate their spike rate based on the sensory features of the expected rewarded stimulus [32]. Given that these neurons send projections to the extragranular layers of the somatosensory cortex [31], where cross-columnar topographic sensory integration takes place [40,41], dopamine might also shape the topographical (map) representations of the sensory organs, contributing to integration of sensory information across whiskers [42] already in the primary somatosensory cortex.

One of the best studied functional roles for dopamine is its contribution to motor control (see e.g. [43–45] for recent reviews). D2R activation modulates firing rates both in Parkinsonian and non-Parkinsonian rats, possibly through the activation of the GABAergic transmission [46]. In the rodent brain stem, suppression of dopaminergic signaling results in the inhibition of oscillatory input in the pedunculopontine nucleus originating from the basal ganglia. This inhibition could help to explain the role of dopamine in the development of motor phenotypes in PD [47]. In PD patients, levodopa application enhances the long range, cross hemispheric temporal correlations in local field potentials, improving neuronal communication in the basal ganglia [48]. The dopaminergic depletion in the nigrostriatal neurons increases coherence in the motor cortex, but decreases the local field potential power in the medial prefrontal cortex and subthalamic nucleus (STN), which might help regulate the communication between motor and cognitive networks [49]. Taken together, dopamine can control neuronal excitability and communication across sensory, motor, cognitive and executive networks in the brain, and altered dopaminergic transmission is relevant to the development of various neuropathological phenotypes.

Intracellular mechanisms for dopaminergic modulation of neuronal excitability

As a neuromodulatory neurotransmitter dopamine's action is not the direct regulation of the membrane potential. It depends on the functional state of neurons [4]. Dopamine receptors are associated with guanosine triphosphate-binding proteins (G-proteins) and mediate their effects in the postsynaptic neurons by controlling surface receptors via (de)phosphorylation, or by modulating downstream enzymatic cascades and transcription factors (Figure 1).

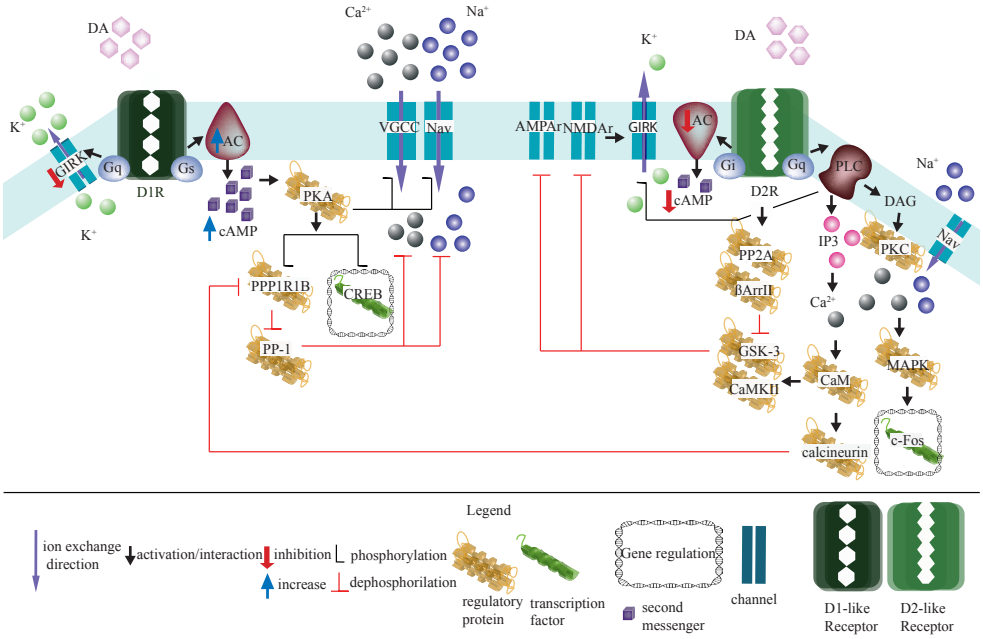

Figure 1. Major intracellular signaling cascades modulated by dopamine. DA receptors are coupled to G-proteins, differentially controlling the (de)phosphorylation of ion channels. **D1R activation** starts a signaling cascade with the activation of AC through Gs. AC increases cAMP concentration and activates PKA, which phosphorylates PPP1R1B. PPP1R1B is an integrator of synaptic input, indirectly increasing Na^+ channels phosphorylation via dephosphorylation of PP-1. PKA directly regulates the phosphorylation of voltage-dependent Na^+ and Ca^{2+} channels. D1R activation also inhibits K^+ channels through Gq. **D2R activation** inhibits AC through Gi, thus reducing intracellular levels of cAMP. Activation of PP2A and βArrII indirectly modulates the phosphorylation of glutamatergic AMPA and NMDA receptors, via dephosphorylation of GSK-3 and CamKII. PLC activation, through Gq, contributes to the phosphorylation of K^+ channels and balances the intracellular Ca^{2+}, through IP3, CaM and calcineurin. The last dephosphorylates PPP1R1B, indirectly contributing to the dephosphorylation of Na^+ channels. PLC interacts with DAG in the membrane, activating PKC, modulating Na^+ channels, and increasing intracellular Ca^{2+}. The latter leads to the activation of MAPK and the transcription factor C-Fos. Abbreviations: *Neurotransmitter*: DA: dopamine; *Ions*: K^+: potassium; Ca^{2+}: calcium; Na^+: sodium; *Ion channels*: GIRK: G-protein coupled inwardly rectifying potassium channel; VGCC: voltage-gated calcium channel; Na_V: voltage-gated sodium channel; *Ligand gated channels*:

D1R: D1-like receptor; D2R: D2-like receptor; AMPAr: α-amino-3-hydroxy-5-methyl-4- isoxazolepropionic acid receptor; NMDAr: *N*-methyl-D-aspartate receptor; *G-protein receptor subunits*: Gq: subunit q; Gs: subunit alpha s; Gi: subunit alpha i; *Biochemical regulators (enzymes and intracellular proteins)*: AC: adenylyl cyclase; cAMP: cyclic adenosine monophosphate; PKA: protein kinase A; PPP1R1B: protein phosphatase 1 regulatory subunit 1B; CREB: cAMP response element-binding protein; PP-1: protein phosphatase 1; PLC: phospholipase C; DAG: diacylglycerol; IP3: inositol triphosphate; PKC: protein kinase C; MAPK: mitogen-activated protein kinase; PP2A: protein phosphatase 2; βArrII: β arrestin II; GSK-3: glycogen synthase kinase 3; CaM: calmodulin; CaMKII: Ca^{2+}/calmodulin-dependent protein kinase II.

Dopamine controls ion channel dynamics via (de)phosphorylation. Dopaminergic activation of the D1R increases cAMP concentration leading to PKA activation (see Figure 1). Because PKA is an enzyme that phosphorylates a large variety of downstream protein targets, it mediates both short- and long-term dynamics of the cellular responses to neuromodulation. For example, PKA is bound to sodium channels via 15 kDa cAMP-dependent protein kinase-anchoring protein (AKAP-15) [50,51] and phosphorylates voltage-gated Na^+ (Na_V) channels in four sites [52–54]. The D1R activation reduces the Na^+ peak transient without changing its kinetics or voltage-dependence in neocortical neurons [52]. This dopamine-mediated "gain modulation" of sodium conductance is conserved throughout evolution, as it is also found in amphibians [55]. D1 receptor activation can modulate ionic flow across the membrane also via phosphorylation of the protein phosphatase 1 regulatory subunit 1B (PPP1R1B, also known as DARPP-32, dopamine and cAMP regulated neuronal phosphoprotein) [56]. PPP1R1B acts as an integrator of synaptic input in dopamine neurons [57]. Glutamate induces dephosphorylation of PPP1R1B and this mechanism of phosphorylation/dephosphorylation of PPP1R1B dynamically and powerfully modulates Na_V channels [58]. The control over the spike after-hyperpolarization suggests that dopamine might modulate potassium conductance in postsynaptic neurons (Figure 1): while D1-like receptors mediate the membrane depolarization (through a G protein-coupled K+ channel or inwardly rectifying K+ channel), the D2-like receptors activation increase the action potential discharge, possibly involving slowly inactivating K+ channels (e.g. Kv.1)[63].

Dopaminergic regulation of spiking is cell-type specific. In striatal low-threshold interneurons, dopamine increases spike frequency by membrane depolarization upon D1R activation [64]. Dopamine might regulate GABAergic currents in medium spiny neurons (MSNs), as dopamine depletion generates burst spiking of GABAergic interneurons [65]. In the STN, dopaminergic regulation of the inhibitory currents is modulated by T-type calcium currents, which depolarize the membrane potential to the spike threshold, increasing burst firing [66]. Dopaminergic neurons in the midbrain have a slow irregular firing pattern that is generated by a slow depolarization current and by a calcium-activated potassium after-hyperpolarization

current (IK(Ca)), the former enabling the membrane potential to reach the spike threshold [67]. The slow depolarization is voltage-dependent and TTX-sensitive, suggesting that early dopaminergic action is mediated through Na_V; the spike after-hyperpolarization depends on high-threshold dendritic calcium spikes [68].

Dopamine controls neuronal excitability through the regulation of action potential generation (see above) as well as through membrane hyperpolarization through inhibition of hyperpolarization-activated, cyclic nucleotide-modulated (HCN) channels. HCN channels are potent regulators of excitability in various cell types in the heart and the brain, including the somatosensory neurons [69]. In olfactory receptor neurons, dopamine suppresses the slowly activated current I_h through D2R, leading to more hyperpolarized potentials and reduced peak currents, while cAMP activation through D1R depolarizes the I_h [70,71]. Dopamine enhances I_h in cortical interneurons in layer 1, involving a cooperative interaction between D1-like and D2-like receptors that also requires GPCR signaling through the G-protein beta-gamma complex [72,73]. Interestingly, D3R-mediated suppression of high frequency spiking does not involve GPCR signaling. Instead, D3R regulate the neuronal excitability via calcium voltage-dependent channels (Cav3) in the axonal initial segment [74].

The empirical observations covered thus far argue that dopaminergic action on the membrane excitability is mediated through two membrane bound enzymes: AC and PLC. They are differentially recruited by the D1-like and D2-like receptors (Figure 1), regulating the calcium release from the intracellular calcium stores.

Considering the complex dopaminergic action on the postsynaptic excitability, computational modelling might help to reduce the dimensionality and shed light onto the critical biochemical events that lead to neuronal modulation by dopamine. Accordingly, a recent biophysical model of dopaminergic circuits argued that the key mechanism that is responsible for the dopamine-mediated reduction in excitability, is the inhibition of calcium activated potassium channels (SK), which subsequently results in a reduction of the number of open Na^+ channels [75] because of their greater inactivation. Combined with the phosphorylation of Na_V channels by dopamine [76] (see Figure 1), these mechanisms could potently control cell excitability and postsynaptic evoked responses. In support of these findings, recordings from the neocortical layer 5 excitatory neurons already showed that dopamine attenuates evoked excitatory postsynaptic potentials (EPSP) as the area and the duration of the EPSP are reduced upon D1R activation through reduction of persistent Na^+ currents (I_{NAP}) [77]. With multiple Na_V subunits, e.g. $Na_V1.1$, $Na_V1.2$ or $Na_V1.6$ α, that might give rise to both I_{NAP} and fast Na^+ currents as a response to dopamine, further research will be required to identify the receptor basis of dopaminergic regulation of the sodium currents.

In summary, although dopamine acts through GPCRs, and dopaminergic receptor

activation does not result in a direct ionic exchange across the membrane, dopamine potently modulates sodium, potassium and calcium conductances in the postsynaptic neurons, gating action potential generation. Because this sustained change in ion channel conductance is a key step in the regulation of synaptic efficacy, dopaminergic control of neuronal excitability might also contribute to bidirectional changes in synaptic plasticity.

A modulatory close-loop between dopaminergic and sensorimotor circuits

Dopaminergic regulation of neuronal, including sensorimotor, excitability (see Section 1) and experience-dependent regulation of dopamine signaling in the somatosensory cortex (see Chapter 4) both argue that there is a modulatory close-loop between dopaminergic transmission and sensory processing. Considering the monosynaptic projections originating from somatosensory- and motor-cortical neurons, and targeting VTA and SNc [78], this close-loop might have a short latency. Dopamine release from VTA and SNc, in return, could influence with the neural activity throughout the brain (Figure 3), including sensorimotor circuits in brainstem, thalamus and cortex [31], completing the close-loop.

A common property of close-loop neuronal circuits is that the activity along the circuit could be regulated by both ascending (bottom-up) and descending (top-down) projections. Although there is ample empirical evidence in support of descending dopaminergic control of sensorimotor circuits, contribution of the sensorimotor projections to dopaminergic neurons' spiking is yet to be systematically studied. Just to give a few examples: high frequency VTA stimulation *in vivo* leads to prolonged calcium transients in the secondary motor cortex (in the prefrontal cortex) while low frequency stimulation induces brief (tonic) transients [79]. Increased dopamine availability decreases the excitability of pyramidal tract neurons in the primary motor cortex, where both D1 and D2 receptors expressed [80]. Electrical stimulations in the ventral midbrain dopaminergic neurons leads to short-latency phasic activations in the auditory cortex through D1R-mediated activation [81]. D2R activation via quinpirole reduces stimulus (tone) evoked spiking, and subsequently auditory sensory gating of aversive events [82]. In the olfactory (piriform) cortex of rats, dopamine suppresses excitatory responses after reward via D2R[36]. In the somatosensory cortex, the blockade of D1 and D2R increases sensory evoked potential amplitudes by 107.5% and 82.1%, respectively [83]. Dopaminergic modulation of sensorimotor neuronal activity is not limited to the central nervous system. In the periphery, e.g. adult sensory neurons, dopamine regulates calcium channels in a voltage-(in)dependent manner [84].

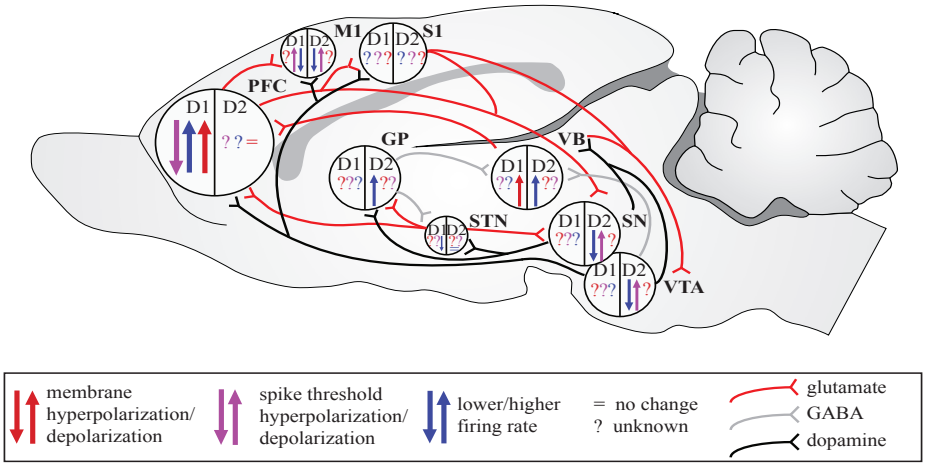

Figure 2. Regulatory close-loops between dopaminergic and key sensorimotor nuclei. Symbols in circles depict the physiological role of dopaminergic signaling in controlling neuronal excitability. Experimental evidence on the simplified anatomical circuit includes **PFC** (prefrontal cortex): D1R, but not D2R, activation reduces AP-evoked calcium influx in the dendrites [85], decreases the spike threshold and first interspike interval in the soma [86]. **GP** (globus pallidus): Dopamine in GP decreases firing rate in the STN and SN[87] which might be mediated through the increased excitability of inhibitory neurons after D2R stimulation [46]; **VB** (ventrobasal thalamus): Selective D1R and D2R activation results in membrane depolarization and increased firing rates [63]; **SN** (substantia nigra): DA in SN increases the firing rate of GP neurons. D2R activation decreases firing via increasing spike threshold in the SN and in the **VTA** (ventral tegmental area) [88–90]; **STN** (subthalamic nucleus): D1R, but not D2R, agonist reduces spontaneous firing while either one increases frequency of bursting [91]; **M1** (Primary motor cortex): Both D1R and D2R activation results in inhibition of pyramidal tract neurons in the motor cortex [80].

The broad extent of dopaminergic projections indicates a spatial and temporal significance for the dopamine signaling. In the hypothalamus, reward increases dopamine release in the entorhinal cortex phasically, following a D2R-mediated suppression of excitatory postsynaptic responses [36]. In the auditory cortex, dopamine is necessary for controlling the frequency of responses to rhythmic sensory inputs [92]. In the basal ganglia, dopamine increases long range temporal correlations across motor nuclei interfering with the motor communication processing [48]. Dopaminergic loss in the basal ganglia increases the inhibitory oscillatory communication between basal ganglia and PPN (pedunculopontine nucleus)[47], and increases synchronization between the SN and the motor cortex during ongoing motor activity [93], showing the relevance of dopamine signaling in bottom-up and top-down temporal and spatial coherence for the brain signaling. Therefore, higher cortical areas seem to modulate motor and sensory circuits throughout the dopaminergic tuning of respectively, the nigrostriatal and the basal-ganglia-thalamocortical network activity.

Conclusions

Sensory neurons represent the world that surrounds us by varying the rate and timing of their action potentials. Because information from the sensory periphery propagates through feed-forward excitatory projections, and is shaped by inhibitory circuit motives, previous research in sensory cortices focused on the roles of glutamatergic and GABAergic signaling in shaping neural representations.

Sensory neurons, however, integrate information from the sensory periphery with the information (e.g. expectations, memories, emotional states) generated internally, elsewhere in the brain. These top-down projections are mediated through neuromodulatory neurotransmitters which alter postsynaptic signaling through slower G-protein signaling. Here, we reviewed the experimental evidence which argues that one of the cardinal neuromodulatory neurotransmitters, dopamine, could potently and rapidly regulate action potential timing (also see Chapter 5). Given that sensory experience regulates dopaminergic signaling in the primary somatosensory cortex (see Chapter 4) and sensorimotor circuits form a close-loop network with dopaminergic circuits (see Section 3), top-down regulation of action potential timing through dopaminergic modulation might mechanistically help to describe how internal neural representations of the external sensory world are shaped by behavioral and perceptual priors. Therefore, in thesis I addressed the top-down regulation of sensory neuronal excitability using mouse somatosensory (barrel) cortex as a model. The main conclusions are:

- Dopamine suppresses neuronal excitability.
- D1 and D2 receptor mediated control of excitability is mediated through voltage-gated sodium channels and manifested through modulation of the action potential threshold.
- D1 mediated control of excitability is cell-type specific. Upon D1 receptor activation excitatory neuron firing rate is decreased while inhibitory neuronal firing rate is increased.
- Sensory deprivation alters transcription of genes in the dopaminergic signaling pathway in a cortical layer specific manner suggesting that there is a functional close-loop between the dopaminergic signaling and sensory experience.
- Corticosterone controls evoked calcium transients in vitro and sensory representations in vivo, which suggests that top-down modulation of sensory neuron excitability is not specific to dopamine

Bibliography

1. Berridge, K. C. & Kringelbach, M. L. Pleasure systems in the brain. *Neuron* **86,** 646–664 (2015).
2. Schultz, W. Reward signaling by dopamine neurons. *Neuroscientist* **7,** 293–302 (2001).
3. Money, K. M. & Stanwood, G. D. Developmental origins of brain disorders: roles for dopamine. *Front. Cell. Neurosci.* **7,** 260 (2013).
4. Girault, J.-A. & Greengard, P. The neurobiology of dopamine signaling. *Arch. Neurol.* **61,** 641–644 (2004).
5. Rosell, D. R. & Siever, L. J. The neurobiology of aggression and violence. *CNS Spectr.* **20,** 254–279 (2015).
6. Meltzer, H. Y. New trends in the treatment of schizophrenia. *CNS Neurol. Disord. Drug Targets* **16,** 900–906 (2017).
7. Arnsten, A. F. T., Wang, M. & Paspalas, C. D. Dopamine's actions in primate prefrontal cortex: challenges for treating cognitive disorders. *Pharmacol. Rev.* **67,** 681–696 (2015).
8. Simms, S. L., Huettner, D. P. & Kortagere, S. In vivo characterization of a novel dopamine D3 receptor agonist to treat motor symptoms of Parkinson's disease. *Neuropharmacology* **100,** 106–115 (2016).
9. Lee, T., Seeman, P., Rajput, A., Farley, I. J. & Hornykiewicz, O. Receptor basis for dopaminergic supersensitivity in Parkinson's disease. *Nature* **273,** 59–61 (1978).
10. Patriquin, M. A., Bauer, I. E., Soares, J. C., Graham, D. P. & Nielsen, D. A. Addiction pharmacogenetics: a systematic review of the genetic variation of the dopaminergic system. *Psychiatr. Genet.* **25,** 181–193 (2015).
11. Berry, A. S. *et al.* Dopamine Synthesis Capacity is Associated with D2/3 Receptor Binding but Not Dopamine Release. *Neuropsychopharmacology* **43,** 1201–1211 (2018).
12. Blum, K. *et al.* Coupling genetic addiction risk score (GARS) and pro dopamine regulation (KB220) to combat substance use disorder (SUD). *Glob. J. Addict. Rehabil. Med.* **1,** (2017).
13. van Holst, R. J. *et al.* Increased striatal dopamine synthesis capacity in gambling addiction. *Biol. Psychiatry* **83,** 1036–1043 (2018).
14. Lee, J. C., Wang, L. P. & Tsien, J. Z. Dopamine Rebound-Excitation Theory: Putting Brakes on PTSD. *Front. Psychiatry* **7,** 163 (2016).
15. Tabatabaei, S. M. *et al.* DRD4 Gene Polymorphisms as a Risk Factor for Children with Attention Deficit Hyperactivity Disorder in Iranian Population. *Int. Sch. Res. Notices* **2017,** 2494537 (2017).
16. Newton, C. L., Wood, M. D. & Strange, P. G. Examining the effects of sodium ions on the binding of antagonists to dopamine D2 and D3 receptors. *PLoS ONE* **11,** e0158808 (2016).
17. Strange, B. A. *et al.* Dopamine receptor 4 promoter polymorphism modulates memory and neuronal responses to salience. *Neuroimage* **84,** 922–931 (2014).
18. Hasbi, A., O'Dowd, B. F. & George, S. R. Heteromerization of dopamine D2 receptors with dopamine D1 or D5 receptors generates intracellular calcium signaling by different mechanisms. *Curr. Opin. Pharmacol.* **10,** 93–99 (2010).
19. George, S. R., Kern, A., Smith, R. G. & Franco, R. Dopamine receptor heteromeric complexes and their emerging functions. *Prog. Brain Res.* **211,** 183–200 (2014).
20. Brugarolas, M. *et al.* G-protein-coupled receptor heteromers as key players in the molecular architecture of the central nervous system. *CNS Neurosci. Ther.* **20,** 703–709 (2014).
21. Leo, D. *et al.* Taar1-mediated modulation of presynaptic dopaminergic neurotransmission: role of D2 dopamine autoreceptors. *Neuropharmacology* **81,** 283–291 (2014).

22. Xie, Z. & Miller, G. M. Trace amine-associated receptor 1 is a modulator of the dopamine transporter. *J. Pharmacol. Exp. Ther.* **321,** 128–136 (2007).
23. Rice, M. E. & Patel, J. C. Somatodendritic dopamine release: recent mechanistic insights. *Philos Trans R Soc Lond, B, Biol Sci* **370,** (2015).
24. Cheramy, A., Leviel, V. & Glowinski, J. Dendritic release of dopamine in the substantia nigra. *Nature* **289,** 537–542 (1981).
25. Seutin, V. Dopaminergic neurones: much more than dopamine? *Br. J. Pharmacol.* **146,** 167–169 (2005).
26. Ibáñez-Sandoval, O. *et al.* Electrophysiological and morphological characteristics and synaptic connectivity of tyrosine hydroxylase-expressing neurons in adult mouse striatum. *J. Neurosci.* **30,** 6999–7016 (2010).
27. Mallet, N. *et al.* Disrupted dopamine transmission and the emergence of exaggerated beta oscillations in subthalamic nucleus and cerebral cortex. *J. Neurosci.* **28,** 4795–4806 (2008).
28. Kondabolu, K. *et al.* Striatal cholinergic interneurons generate beta and gamma oscillations in the corticostriatal circuit and produce motor deficits. *Proc Natl Acad Sci USA* **113,** E3159-68 (2016).
29. Crocker, A. D. The regulation of motor control: an evaluation of the role of dopamine receptors in the substantia nigra. *Rev. Neurosci.* **8,** 55–76 (1997).
30. Joshua, M., Adler, A. & Bergman, H. The dynamics of dopamine in control of motor behaviour. *Curr. Opin. Neurobiol.* **19,** 615–620 (2009).
31. Schubert, D., Nadif Kasri, N., Celikel, T. & Homberg, J. in *Sensorimotor Integration in the Whisker System* (eds. Krieger, P. & Groh, A.) 243–273 (Springer, 2015).
32. Takahashi, Y. K. *et al.* Dopamine neurons respond to errors in the prediction of sensory features of expected rewards. *Neuron* **95,** 1395–1405.e3 (2017).
33. Ketzef, M. *et al.* Dopamine Depletion Impairs Bilateral Sensory Processing in the Striatum in a Pathway-Dependent Manner. *Neuron* **94,** 855–865.e5 (2017).
34. Kole, K., Scheenen, W., Tiesinga, P. & Celikel, T. Cellular diversity of the somatosensory cortical map plasticity. *Neurosci. Biobehav. Rev.* **84,** 100–115 (2018).
35. Kodama, T. *et al.* Dopamine and glutamate release in the anterior default system during rest: A monkey microdialysis study. *Behav. Brain Res.* **294,** 194–197 (2015).
36. Hutter, J. A., Martel, A., Trigiani, L., Barrett, S. G. & Chapman, C. A. Rewarding stimulation of the lateral hypothalamus induces a dopamine-dependent suppression of synaptic responses in the entorhinal cortex. *Behav. Brain Res.* **252,** 266–274 (2013).
37. Evans, R. C., Zhu, M. & Khaliq, Z. M. Dopamine Inhibition Differentially Controls Excitability of Substantia Nigra Dopamine Neuron Subpopulations through T-Type Calcium Channels. *J. Neurosci.* **37,** 3704–3720 (2017).
38. Davila, N. G., Blakemore, L. J. & Trombley, P. Q. Dopamine modulates synaptic transmission between rat olfactory bulb neurons in culture. *J. Neurophysiol.* **90,** 395–404 (2003).
39. Reig, R. & Silberberg, G. Multisensory integration in the mouse striatum. *Neuron* **83,** 1200–1212 (2014).
40. Celikel, T., Szostak, V. A. & Feldman, D. E. Modulation of spike timing by sensory deprivation during induction of cortical map plasticity. *Nat. Neurosci.* **7,** 534–541 (2004).
41. Foeller, E., Celikel, T. & Feldman, D. E. Inhibitory sharpening of receptive fields contributes to whisker map plasticity in rat somatosensory cortex. *J. Neurophysiol.* **94,** 4387–4400 (2005).
42. Celikel, T. & Sakmann, B. Sensory integration across space and in time for decision making in the somatosensory system of rodents. *Proc Natl Acad Sci USA* **104,** 1395–1400 (2007).

43. Vitrac, C. & Benoit-Marand, M. Monoaminergic modulation of motor cortex function. *Front. Neural Circuits* **11,** 72 (2017).
44. Marinelli, L., Quartarone, A., Hallett, M., Frazzitta, G. & Ghilardi, M. F. The many facets of motor learning and their relevance for Parkinson's disease. *Clin. Neurophysiol.* **128,** 1127–1141 (2017).
45. Grillner, S. & Robertson, B. The basal ganglia downstream control of brainstem motor centres--an evolutionarily conserved strategy. *Curr. Opin. Neurobiol.* **33,** 47–52 (2015).
46. Zhu, Y.-C. *et al.* Direct modulation of firing activity by dopamine D2 like receptors in the globus pallidus of both normal and parkinsonian rats. *Sheng Li Xue Bao* **68,** 699–707 (2016).
47. Aravamuthan, B. R. *et al.* Altered neuronal activity relationships between the pedunculopontine nucleus and motor cortex in a rodent model of Parkinson's disease. *Exp. Neurol.* **213,** 268–280 (2008).
48. Hohlefeld, F. U. *et al.* Long-range temporal correlations in the subthalamic nucleus of patients with Parkinson's disease. *Eur. J. Neurosci.* **36,** 2812–2821 (2012).
49. Delaville, C., McCoy, A. J., Gerber, C. M., Cruz, A. V. & Walters, J. R. Subthalamic nucleus activity in the awake hemiparkinsonian rat: relationships with motor and cognitive networks. *J. Neurosci.* **35,** 6918–6930 (2015).
50. Tibbs, V. C., Gray, P. C., Catterall, W. A. & Murphy, B. J. AKAP15 anchors cAMP-dependent protein kinase to brain sodium channels. *J. Biol. Chem.* **273,** 25783–25788 (1998).
51. Few, W. P., Scheuer, T. & Catterall, W. A. Dopamine modulation of neuronal Na (+) channels requires binding of A kinase-anchoring protein 15 and PKA by a modified leucine zipper motif. *Proc Natl Acad Sci USA* **104,** 5187–5192 (2007).
52. Cantrell, A. R. & Catterall, W. A. Neuromodulation of Na+ channels: an unexpected form of cellular plasticity. *Nat. Rev. Neurosci.* **2,** 397–407 (2001).
53. Murphy, B. J., Rossie, S., De Jongh, K. S. & Catterall, W. A. Identification of the sites of selective phosphorylation and dephosphorylation of the rat brain Na+ channel alpha subunit by cAMP-dependent protein kinase and phosphoprotein phosphatases. *J. Biol. Chem.* **268,** 27355–27362 (1993).
54. Murphy, B. J. & Catterall, W. A. Phosphorylation of purified rat brain Na+ channel reconstituted into phospholipid vesicles by protein kinase C. *J. Biol. Chem.* **267,** 16129–16134 (1992).
55. Smith, B. J., Côté, P. D. & Tremblay, F. D1 dopamine receptors modulate cone ON bipolar cell Nav channels to control daily rhythms in photopic vision. *Chronobiol. Int.* **32,** 48–58 (2015).
56. Kuroiwa, M. *et al.* Phosphodiesterase 4 inhibition enhances the dopamine D1 receptor/PKA/DARPP-32 signaling cascade in frontal cortex. *Psychopharmacology (Berl)* **219,** 1065–1079 (2012).
57. Svenningsson, P. *et al.* DARPP-32: an integrator of neurotransmission. *Annu. Rev. Pharmacol. Toxicol.* **44,** 269–296 (2004).
58. Schiffmann, S. N. *et al.* Modulation of the voltage-gated sodium current in rat striatal neurons by DARPP-32, an inhibitor of protein phosphatase. *Eur. J. Neurosci.* **10,** 1312–1320 (1998).
59. Stanzione, P., Calabresi, P., Mercuri, N. & Bernardi, G. Dopamine modulates CA1 hippocampal neurons by elevating the threshold for spike generation: an in vitro study. *Neuroscience* **13,** 1105–1116 (1984).
60. Grace, A. A. Evidence for the functional compartmentalization of spike generating regions of rat midbrain dopamine neurons recorded in vitro. *Brain Res.* **524,** 31–41 (1990).
61. Richards, C. D., Shiroyama, T. & Kitai, S. T. Electrophysiological and immunocytochemical characterization of GABA and dopamine neurons in the substantia nigra of the rat. *Neuroscience* **80,** 545–557 (1997).
62. Rutherford, A., Garcia-Munoz, M. & Arbuthnott, G. W. An afterhyperpolarization recorded in striatal cells "in

vitro": effect of dopamine administration. *Exp. Brain Res.* **71,** 399–405 (1988).

63. Govindaiah, G., Wang, T., Gillette, M. U., Crandall, S. R. & Cox, C. L. Regulation of inhibitory synapses by presynaptic D_4 dopamine receptors in thalamus. *J. Neurophysiol.* **104,** 2757–2765 (2010).
64. Centonze, D. *et al.* Activation of dopamine D1-like receptors excites LTS interneurons of the striatum. *Eur. J. Neurosci.* **15,** 2049–2052 (2002).
65. Dehorter, N. *et al.* Dopamine-deprived striatal GABAergic interneurons burst and generate repetitive gigantic IPSCs in medium spiny neurons. *J. Neurosci.* **29,** 7776–7787 (2009).
66. Yang, Y.-C., Tai, C.-H., Pan, M.-K. & Kuo, C.-C. The T-type calcium channel as a new therapeutic target for Parkinson's disease. *Pflugers Arch.* **466,** 747–755 (2014).
67. Grace, A. A. & Bunney, B. S. The control of firing pattern in nigral dopamine neurons: single spike firing. *J. Neurosci.* **4,** 2866–2876 (1984).
68. Grace, A. A. & Onn, S. P. Morphology and electrophysiological properties of immunocytochemically identified rat dopamine neurons recorded in vitro. *J. Neurosci.* **9,** 3463–3481 (1989).
69. Momin, A., Cadiou, H., Mason, A. & McNaughton, P. A. Role of the hyperpolarization-activated current Ih in somatosensory neurons. *J Physiol (Lond)* **586,** 5911–5929 (2008).
70. Vargas, G. & Lucero, M. T. Dopamine modulates inwardly rectifying hyperpolarization-activated current (Ih) in cultured rat olfactory receptor neurons. *J. Neurophysiol.* **81,** 149–158 (1999).
71. He, C., Chen, F., Li, B. & Hu, Z. Neurophysiology of HCN channels: from cellular functions to multiple regulations. *Prog. Neurobiol.* **112,** 1–23 (2014).
72. Wu, J. & Hablitz, J. J. Cooperative activation of D1 and D2 dopamine receptors enhances a hyperpolarization-activated inward current in layer I interneurons. *J. Neurosci.* **25,** 6322–6328 (2005).
73. Dupré, D. J., Robitaille, M., Rebois, R. V. & Hébert, T. E. The role of Gbetagamma subunits in the organization, assembly, and function of GPCR signaling complexes. *Annu. Rev. Pharmacol. Toxicol.* **49,** 31–56 (2009).
74. Yang, S. *et al.* β-Arrestin-Dependent Dopaminergic Regulation of Calcium Channel Activity in the Axon Initial Segment. *Cell Rep.* **16,** 1518–1526 (2016).
75. Iyer, R., Ungless, M. A. & Faisal, A. A. Calcium-activated SK channels control firing regularity by modulating sodium channel availability in midbrain dopamine neurons. *Sci. Rep.* **7,** 5248 (2017).
76. Valdés-Baizabal, C., Soto, E. & Vega, R. Dopaminergic modulation of the voltage-gated sodium current in the cochlear afferent neurons of the rat. *PLoS ONE* **10,** e0120808 (2015).
77. Rotaru, D. C., Lewis, D. A. & Gonzalez-Burgos, G. Dopamine D1 receptor activation regulates sodium channel-dependent EPSP amplification in rat prefrontal cortex pyramidal neurons. *J Physiol (Lond)* **581,** 981–1000 (2007).
78. Watabe-Uchida, M., Zhu, L., Ogawa, S. K., Vamanrao, A. & Uchida, N. Whole-brain mapping of direct inputs to midbrain dopamine neurons. *Neuron* **74,** 858–873 (2012).
79. Iwashita, M. Phasic activation of ventral tegmental neurons increases response and pattern similarity in prefrontal cortex neurons. *elife* **3,** (2014).
80. Awenowicz, P. W. & Porter, L. L. Local application of dopamine inhibits pyramidal tract neuron activity in the rodent motor cortex. *J. Neurophysiol.* **88,** 3439–3451 (2002).
81. Mylius, J. *et al.* Fast transmission from the dopaminergic ventral midbrain to the sensory cortex of awake primates. *Brain Struct. Funct.* **220,** 3273–3294 (2015).
82. Muthuraju, S., Nobre, M. J., Saito, V. M. N. & Brandao, M. L. Distinct effects of haloperidol in the mediation of conditioned fear in the mesolimbic system and processing of unconditioned aversive information in the inferior

colliculus. *Neuroscience* **261,** 195–206 (2014).

83. Hosp, J. A., Hertler, B., Atiemo, C. O. & Luft, A. R. Dopaminergic modulation of receptive fields in rat sensorimotor cortex. *Neuroimage* **54,** 154–160 (2011).
84. Formenti, A., Arrigoni, E. & Mancia, M. Two distinct modulatory effects on calcium channels in adult rat sensory neurons. *Biophys. J.* **64,** 1029–1037 (1993).
85. Zhou, W.-L. & Antic, S. D. Rapid dopaminergic and GABAergic modulation of calcium and voltage transients in dendrites of prefrontal cortex pyramidal neurons. *J Physiol (Lond)* **590,** 3891–3911 (2012).
86. Henze, D. A., González-Burgos, G. R., Urban, N. N., Lewis, D. A. & Barrionuevo, G. Dopamine increases excitability of pyramidal neurons in primate prefrontal cortex. *J. Neurophysiol.* **84,** 2799–2809 (2000).
87. Mamad, O., Delaville, C., Benjelloun, W. & Benazzouz, A. Dopaminergic control of the globus pallidus through activation of D2 receptors and its impact on the electrical activity of subthalamic nucleus and substantia nigra reticulata neurons. *PLoS ONE* **10,** e0119152 (2015).
88. Werkman, T. R., McCreary, A. C., Kruse, C. G. & Wadman, W. J. NK3 receptors mediate an increase in firing rate of midbrain dopamine neurons of the rat and the guinea pig. *Synapse* **65,** 814–826 (2011).
89. Robinson, S., Smith, D. M., Mizumori, S. J. Y. & Palmiter, R. D. Firing properties of dopamine neurons in freely moving dopamine-deficient mice: effects of dopamine receptor activation and anesthesia. *Proc Natl Acad Sci USA* **101,** 13329–13334 (2004).
90. Werkman, T. R., Kruse, C. G., Nievelstein, H., Long, S. K. & Wadman, W. J. Neurotensin attenuates the quinpirole-induced inhibition of the firing rate of dopamine neurons in the rat substantia nigra pars compacta and the ventral tegmental area. *Neuroscience* **95,** 417–423 (2000).
91. Galvan, A. *et al.* Localization and function of dopamine receptors in the subthalamic nucleus of normal and parkinsonian monkeys. *J. Neurophysiol.* **112,** 467–479 (2014).
92. Pérez-Alcázar, M. *et al.* Cortical oscillations scan using chirp-evoked potentials in 6-hydroxydopamine rat model of Parkinson's disease. *Brain Res.* **1310,** 58–67 (2010).
93. Brazhnik, E. *et al.* State-dependent spike and local field synchronization between motor cortex and substantia nigra in hemiparkinsonian rats. J. Neurosci. 32, 7869–7880 (2012).

Chapter 2

A databank for intracellular electrophysiological mapping of the adult somatosensory cortex

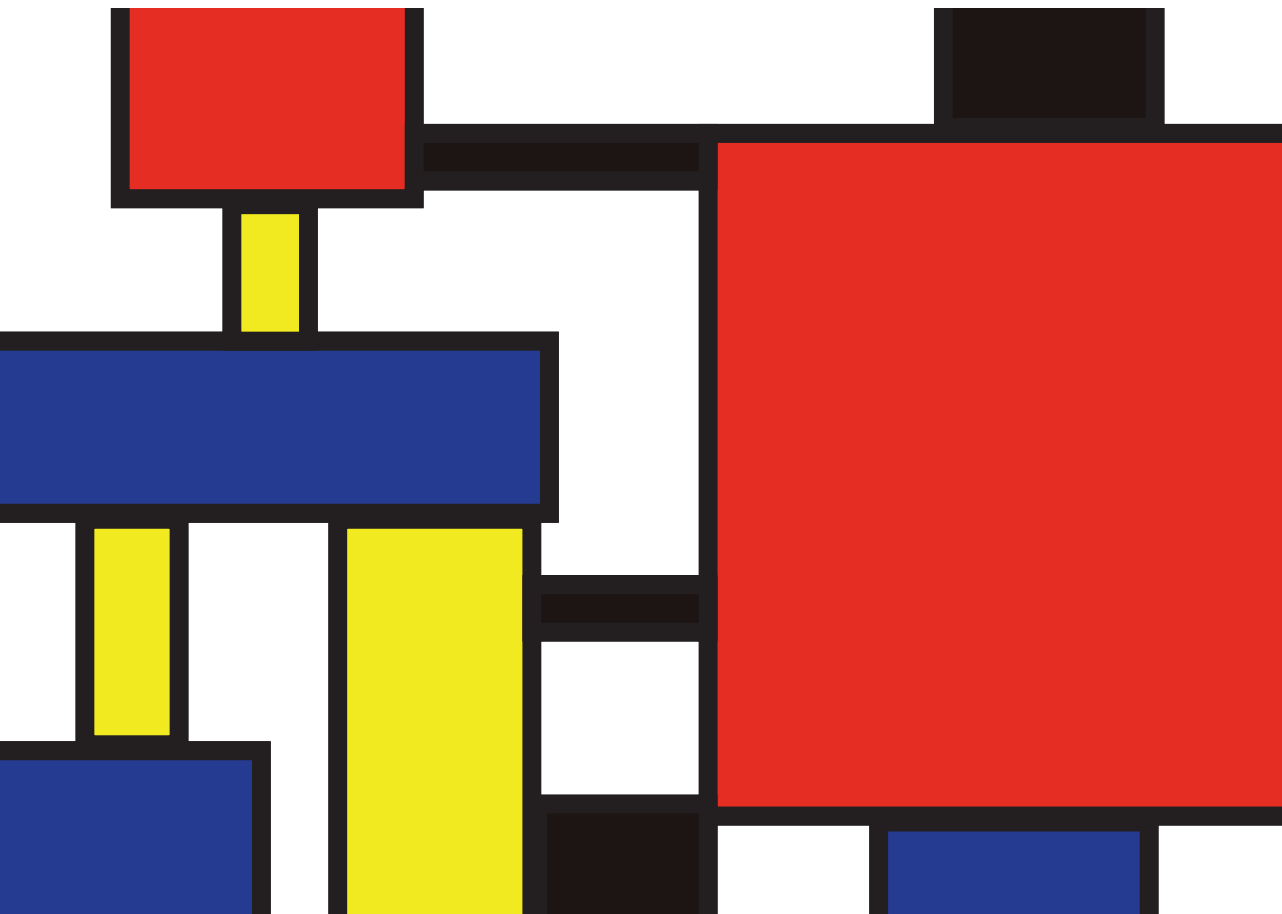

Neurons in the supragranular layers of the somatosensory cortex integrate sensory (bottom-up) and cognitive/perceptual (top-down) information as they orchestrate communication across cortical columns. It has been inferred, based on intracellular recordings from juvenile animals, that supragranular neurons are electrically mature by the fourth postnatal week. However, the dynamics of the neuronal integration in the adulthood is largely unknown. Electrophysiological characterization of the active properties of these neurons throughout adulthood will help to address the biophysical and computational principles of the neuronal integration. Here we provide a database of whole-cell intracellular recordings from 315 neurons located in the supragranular layers (L2/3) of the primary somatosensory cortex in adult mice (9-45 weeks old) from both sexes (females, N=195; males, N=120). Data include 361 somatic current-clamp (CC) and 476 voltage-clamp (VC) experiments, recorded using a step-and-hold protocol (CC, N=257; VC, N=46), frozen noise injections (CC, N=104) and triangular voltage sweeps (VC, 10 (N=132), 50 (N=146) and 100 ms (N=152)), from regular spiking (N=169) and fast-spiking neurons (N=66). The data can be used to systematically study the properties of somatic integration, and the principles of action potential generation across sexes and across electrically characterized neuronal classes in adulthood (see the Chapter 3). Understanding the principles of the somatic transformation of postsynaptic potentials into action potentials will shed light onto the computational principles of intracellular information transfer in single neurons and information processing in neuronal networks, helping to recreate neuronal functions in artificial systems.

Data description

The primary somatosensory cortex (S1) encodes time-varying but spatially well-defined haptic information [1] from the mechanoreceptors in the skin, thereby creating a topographical neuronal representation of the tactile world [2,3]. Rodents, for example, locate tactile targets in their immediate environment by integrating information across these (whisker) representations in the barrel cortex [4], where neurons in each cortical column preferably respond to a single whisker on the contralateral snout [5]. The supragranular layers (cortical layers 2/3, L2/3) of the barrel cortex is the first cortical network that integrates the sensory information across neighboring cortical columns, whiskers and whisk cycles [6–10]. This representation of the whisker contacts undergoes experience-dependent changes [11–14] and is altered in animal models of neurodevelopmental disorders [15–17]. Adaptive changes in the synaptic and modulatory drive could powerfully regulate the transformation of postsynaptic responses into action potentials, ultimately controlling how sensory information is transferred between cortical columns and cortical regions [18].

Understanding the principles of neuronal information transfer in the supragranular layers will require a systematic analysis of the integrative properties of these cortical neurons. Thus far, however, slice experiments primarily focused on juvenile animals as it is widely considered that the neurons mature anatomically and electrophysiologically by the fourth postnatal week [16,19–23]. Here we provide a database of 837 experiments collected from 315 adult supragranular neurons that will help to address the principles of information processing by cortical neurons throughout the adulthood of mice. The database consists of whole-cell intracellular recordings in voltage-clamp (VC) and current-clamp (CC) configurations: while current-clamp somatic measurements bring insight into the properties related to action potential initiation, timing, rate, and pattern, voltage-clamp recordings provide information on the voltage-gated ion-channel dynamics. The database is best utilized to address the principles of information transfer in individual neurons (see e.g. [18,24]) and for the electrical characterization of adult cortical sensory neurons. It will serve synaptic, systems, computational and theoretical neuroscientist in search of the principles of information processing, transfer, and recovery in neuronal networks. The database is expected to create synergy with 1) the recently completed transcriptome [25,26] and proteome [27,28] of the supragranular layers of the barrel cortex, 2) computational models of the molecular changes that contribute to the maturation of synaptic communication in the same cortical region (e.g. [29]), 3) computational models of synaptic integration and action potential generation in the supragranular layers of the barrel cortex [18], and 4) the high-resolution mapping of sensory representations using intrinsic signals in single trial resolution (e.g. [30]) resulting in a multi-scale analysis of the cortical organization, from molecules of chemical communication to network representations.

Methods

Experiments that involve animals were conducted in accordance with the European Directive 2010/63/EU, national regulations in the Netherlands, and international guidelines on animal care and use of animals. Pvalbtm1(cre)Arbr (RRID:MGI:5315557) or Ssttm2.1(cre)Zjh/J mice (RRID:IMSR_JAX:013044) from either sex (N=75 females, N=45 males, aged 9-54 weeks) were used from the local breeding colonies.

The mice were anesthetized with Isoflurane (1.5 ml/mouse) before the tissue was extracted and coronal slices of the primary somatosensory cortex, barrel subfield region is prepared (Figure 1). The procedures were as described before [11,12,14,16,31] with the exception that animals were intracardially perfused with ice-cold dissection solution containing (in mM) 108 choline chloride, 3 KCl, 26 $NaHCO_3$, 1.25 $NaH_2PO_4.H_2O$, 25 Glucose.H_2O, 1 $CaCl_2.2H_2O$, 6 $MgSO_4.7H_2O$, 3 sodium pyruvate, after animals were deeply anesthetized, as assessed by pinch withdrawal reflex, heart and breathing rate. The brain was removed after decapitation and sliced coronally (300 micrometers in thickness) in the same ice-cold perfusion medium. The slices were then transferred to a chamber containing aCSF (in mM): 120 NaCl, 3.5 KCl, 10 Glucose.H_2O, 2.5 $CaCl_2.2H_2O$, 1.3 $MgSO_4.7H_2O$, 25 $NaHCO_3$, 1.25 $NaH_2PO_4.H_2O$, aerated with 95% O_2/ 5% CO_2 at 37°C. After 30 minutes, the slices were transferred to room temperature before whole-cell electrophysiological recordings started.

Whole-cell recordings

Slices were continuously oxygenated and perfused with aCSF during recordings. The barrel cortex was localized and cells of interest in the supragranular layers were patched under 40x magnification in room temperature using HEKA EPC 9 and EPC10 amplifiers in combination with the Patch Master v2x90.2 data acquisition software. Patch clamp electrodes were pulled from glass capillaries (1.00 mm (external diameter), 0.50 mm (internal diameter), 75 mm (length), GC100FS-7.5, Harvard Apparatus) with a P-2000 puller (Sutter Instrument, USA) and used if their initial resistance were between 5 and 10 MOhm. They were filled with intracellular solution containing (in mM) 130 K-Gluconate, 5 KCl, 1.5 $MgCl_2.6H_2O$, 0.4 Na3GTP, 4 Na2ATP, 10 HEPES, 10 Na-phosphocreatine, 0.6 EGTA, and the pH was set at 7.22 with KOH. Current-clamp and voltage-clamp recordings were performed as described before [32, 33] and included four stimulus protocols (Figure 2).

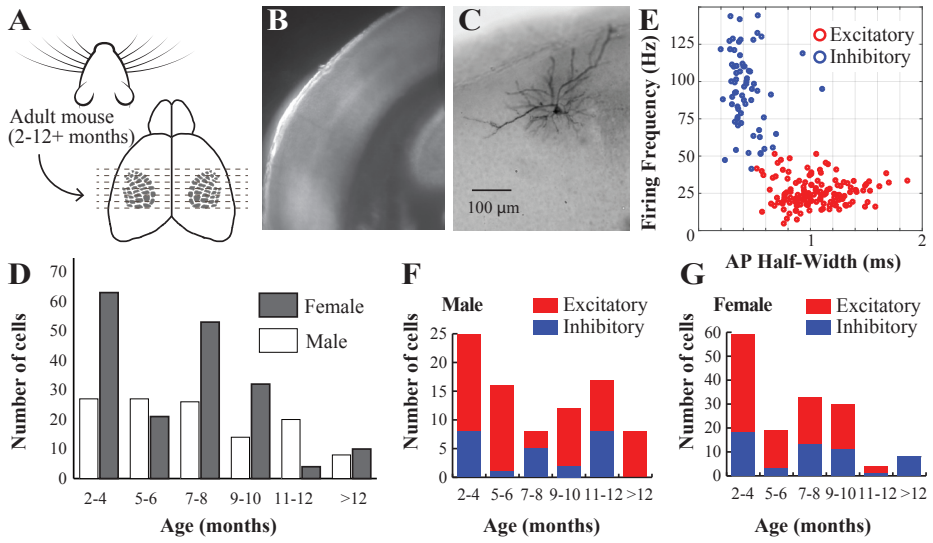

Figure 1. Acute slice preparation. **(A)** Coronal slices (300 micrometers in thickness) were prepared for ex vivo recording from the L2/3 neurons in the mouse primary somatosensory cortex, barrel cortex subregion. **(B)** A low magnification view of the slice in 4x. **(C)** A representative neuron, intracellularly filled with biocytin and visualized with DAB staining (VECTASTAIN Elite ABC Kit, RRID: AB_2336827) according to the manufacturer's guidelines. **(D)** Distribution of the 326 neurons in this database across males (39.9%) and females (60.1%) as well as the ages of the animals. **(E)** Classification of the neurons presumed fast-spiking (FS) and regular spiking (RS) populations based on firing frequency and action potential half-width (see Methods for details). **(F-G).** The distribution of cells across cell type and ages.

Current-clamp protocol

After establishing the current-clamp configuration, the resting membrane potential was set to -70 mV by direct somatic current injections, as required. The step-and-hold stimulation protocol included 10 steps of 500 ms long depolarization pulses (step size: 5, 10, 20, 40 or 60 pA) with an inter-sweep-interval of 6.5 s. The stimulus train was repeated 1-3 times with a 20 s interval. The drift, if any, in resting membrane potential during the recording was not corrected for. However, any neuron whose resting membrane potential varied more than 7 mV was not included in the database. The frozen-noise (FN) stimulation protocol involved somatic injection of the current that is the output of an artificial neural network of 1000 neurons, each firing Poisson spike trains in response to a 'hidden state' (see [34] for details, and [35] on how to generate the frozen noise input and analyze the data).

Voltage-clamp protocol

The voltage-clamp stimulation protocols included step-and-hold and sawtooth (triangular) pulse injections (Figure 2). In both protocols, the membrane potential was clamped at -70 mV prior to somatic depolarization. In the step-and-hold protocols, 14 incremental steps of depolarizing pulses (10 mV/each) were delivered for a period of 250 ms with an interval of 20 s. Sawtooth pulses (range: -70 to 70 mV) were delivered at three frequencies (5, 10, 50 Hz) and consisted of five triangular pulses with peak-to-peak (P2P) distances of 200, 100, 20 ms, respectively. Each trial was repeated twice with 20 s interval.

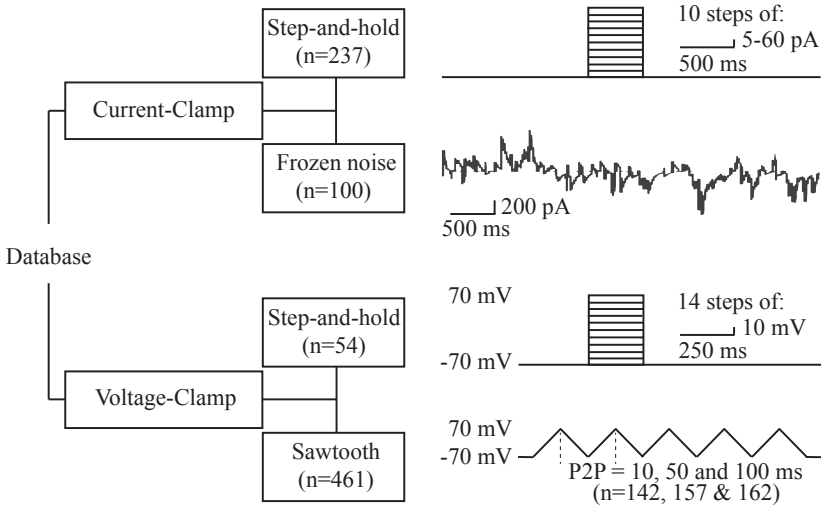

Figure 2. Experimental protocols and the hierarchical organization of the database. The data is available online at https://goo.gl/khkbB4 (DOI comes here). The database contains two subfolders, current-clamp and voltage-clamp, each of which has additional subfolders based on the stimulus protocols utilized in this study. Each dataset is provided in a .mat format and includes both voltage and current channels unless otherwise described. The stimulus delivered to the cells as well as the cell's response can be quantified from these variables.

Data organization

Files in ".mat" (MATLAB) format containing the original traces from each experiment are organized in folders separated by the structure described in Figure 2. Metadata including the date and number of the experiments, the experimenter's initials, the animal's sex and age, the experimental protocol, the cell type, and the animal number are included in a tabulated format (.xlsx, Microsoft Excel; Supplemental Table 1). The experiments are named as the date_prefix_experiment number_protocol number. All cells recorded from the same animal share the same experimental date.

The current clamp data (see "Current Clamp" folder) contains two subfolders, "Step Protocol" and "Frozen Noise". Step Protocol data includes two channels (voltage and current), each of which includes two columns (timestamp and voltage/current values in volt and amp, respectively) for each repetition. Users can visualize both the current injected to clamp the soma and the observed voltage response. Data from each stimulus condition is saved under a separate variable which starts with "Trace_a_b_c_d" and includes information about a) the cell and experiment ID, b) the data type, c) the number of sweeps in each dataset, and d) the channels.

The "Frozen Noise" subfolder contains the voltage trace (i.e. neuronal response to the injected frozen noise), hidden state (activity in the modeled network responds to, see [34] for details) and the injected current trace. In addition, a MATLAB "struct" variable named "settings" is provided. Settings provide metadata under following "fields": condition, experimenter, baseline (membrane potential value (in mV) at which the cell is kept with the baseline current injection), amplidute_scalind (the scaling factor used to translate the output of the neural network, in pA value), tau (the time constant that defines the average switching speed of the hidden state), mean_firing_rate (of the artificial neurons), sampling_rate (the acquisition rate (in kHz)), duration (in ms), FLAG_convert_to_amphere (a binary value that is 1 if the output was converted into Ampere), and cell_type (regular spiking vs fast spiking).

The voltage clamp folder includes two subfolders: VC Step (voltage step-and-hold) and VC Sawtooth, the latter containing 3 subfolders with recordings from experiments with triangular sweeps at 3 frequencies (5, 10 or 50 Hz). Data in the Voltage Clamp folder is organized similarly to data in the Current Clamp folder, and variable naming follows the formatting rules described above.

Cell type classification

K-means clustering (cluster count=2; the number of repetitions=10) was performed to classify neurons into fast-spiking and regular spiking neurons, using current clamp step-and-hold recordings. The clustering was based on the maximum firing rate reached during the current step injections and on the mean spike half-width across all stimulus steps during the current-clamp, step-and-hold protocol. Please note that the cell classification is solely provided to help the user to navigate the data. We do not claim that neurons can be necessarily electrically classified in a binary fashion, nor do we claim that commonly utilized clustering approaches are optimal for accurate (albeit broad) classification of excitatory (mostly regular spiking) and inhibitory (predominantly fast-spiking) neurons.

Re-use potential

The dataset is rich in information regarding current versus voltage dynamics in adult cortical neurons. The independent variables in the database are the sex and age of the animal. While current-clamp experiments provide information about sub- and suprathreshold voltage dynamics, the voltage-clamp experiments are informative about the ionic conductances that lead to activation or inactivation of neurons.

In the step-and-hold current-clamp experiments, the voltage responses can be quantified using subthreshold (e.g. amplitude, latency, duration of the postsynaptic potential) and suprathreshold (e.g. interspike interval adaptation, spike count, spike half-width) responses to somatic current injection (Figure 3). Because multiple stimuli with incrementally increasing current intensities are delivered, cellular responses can be mapped onto stimulation intensities, allowing users to study input/output curves for the parameters of interest.

Action potentials can be studied both in terms of their shape (e.g. waveform, rise and decay slope, amplitude of the positive and negative peaks, the half-width of spike) and temporal response properties (that allow quantification of the rate and timing of action potentials during synaptic activation). Since adaptation to a sustained current injection is commonly used as a criterion to classify neurons, the data provides an inclusive database for the electrical classification of adult neurons, creating synergy with other publicly available databases, e.g. Neurodata Without Borders [36] and the Allen Institute Cell Type database [37]. The data can be used independently or in the context of computational models of neural networks, a broad selection of which can be found in the ModelDB database [38]. In addition to sustained somatic depolarization, the current-clamp database also includes “frozen noise” injections, during which a time-varying current was injected into the recorded neuron (Figure 4). The injected current was generated using an artificial neural network (see [34] for details) of 1000 neurons, each one firing spike trains from an inhomogeneous Poisson process, responding to a binary hidden state which represents the presence or absence of an external stimulus. The activity of all the neurons in the artificial network is integrated and the resulting current is corrected for the baseline current required to keep the patched neuron at -70mV. This summed current is injected to the patched soma. A major utility of the frozen noise protocol is that it allows direct quantification of neuronal information transfer [10,34]. Compared to other metrics of neuronal information transfer [18,39,40], this approach enables bias-free quantification of information with a short (3 or 6 min) stimulation protocol [34].

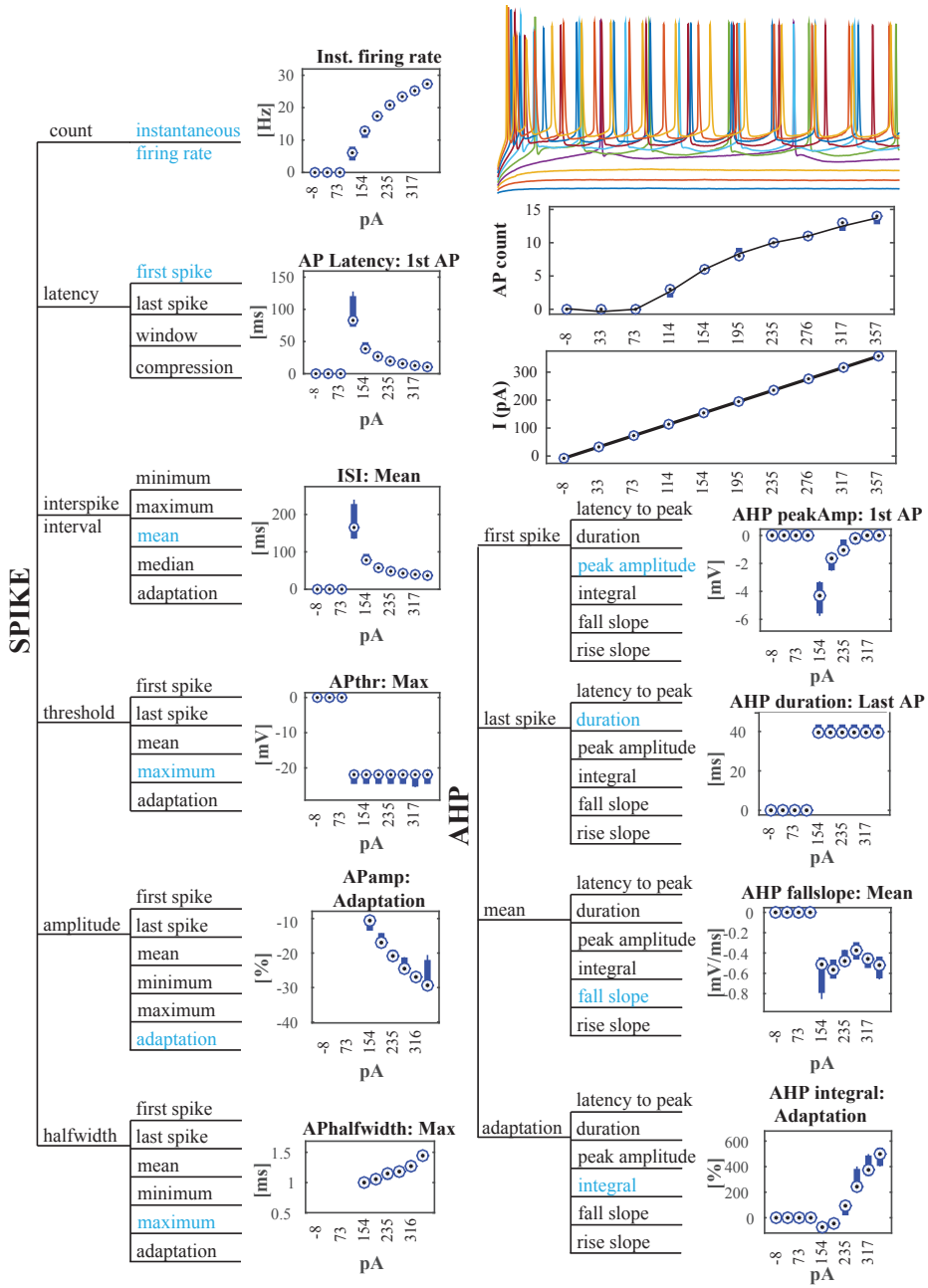

Figure 3. Electrical characterization of the spiking response in current-clamp experiments. The parameter space is shown as a hierarchical tree. Variables shown in blue are used for the data displays. AHP = afterhyperpolarization. "Compression" is a normalized metric that can be calculated as the difference between observations (e.g. spike timing) over the duration of stimulus. In the case of "latency compression" it is calculated as the temporal difference

between the first and last action potential divided by the stimulus duration. “Adaptation” is the relative change in the observed variable, normalized to the first event. For example, in the case of spike amplitude adaptation, it is calculated as (AP_{amp}first-AP_{amp}last) / AP_{amp}first. All characteristics are measured relative to the stimulus amplitude (the current injected, in pA). Membrane potential traces on the top-right are the responses to incremental current injections, superimposed on top of each other. The data below the raw traces represents the number of action potentials and the amplitude of the injected current across the 10 step-and-hold stimuli in this experiment (Filename: 170130_AL_133).

In the database, experimental data recorded from our frozen noise protocol include the recorded membrane potential voltage, the hidden state and the current injected into the neurons (Figure 4). Thus, the user can perform forward and reverse modeling to predict the neuronal response and to study neuronal dynamics in the adult neocortex.

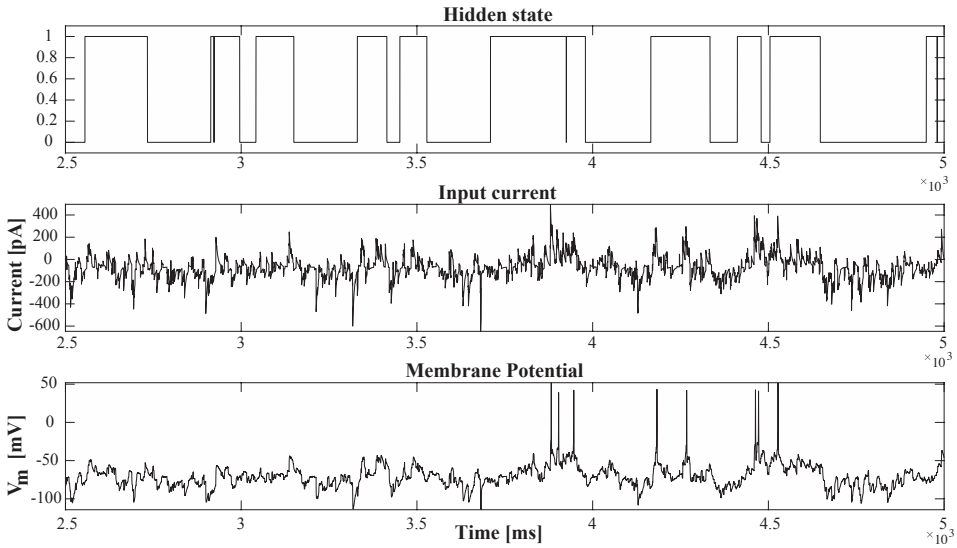

Figure 4. Frozen noise injection in current-clamp configuration. Representative recording from a single neuron (experiment 171207_NC_146). Top row: Binary representation of the hidden state that forms the input to an artificial neural network with 1000 point neurons, firing action potentials following an inhomogeneous Poisson process (see [34] for details). Middle row: the synaptic current generated by the artificial network that was injected into the recorded neuron. Bottom row: the membrane potential response of the recorded neuron.

Going beyond the voltage dynamics in the adult neurons, the database also provides insight into the ionic currents that flow through the membrane. With the triangle shaped VC-Saw protocol (Figure 5), it is possible to measure the activation threshold of the currents flowing through the membrane, by assessing when deviations from the expected sawtooth shape occur. Additionally, it is possible to compute: amplitudes and latencies of the events,

peaks half-widths, the percentage difference between consecutive events and the total number of events in each sweep. Other features could also be extracted from the dataset depending on the researchers' interests.

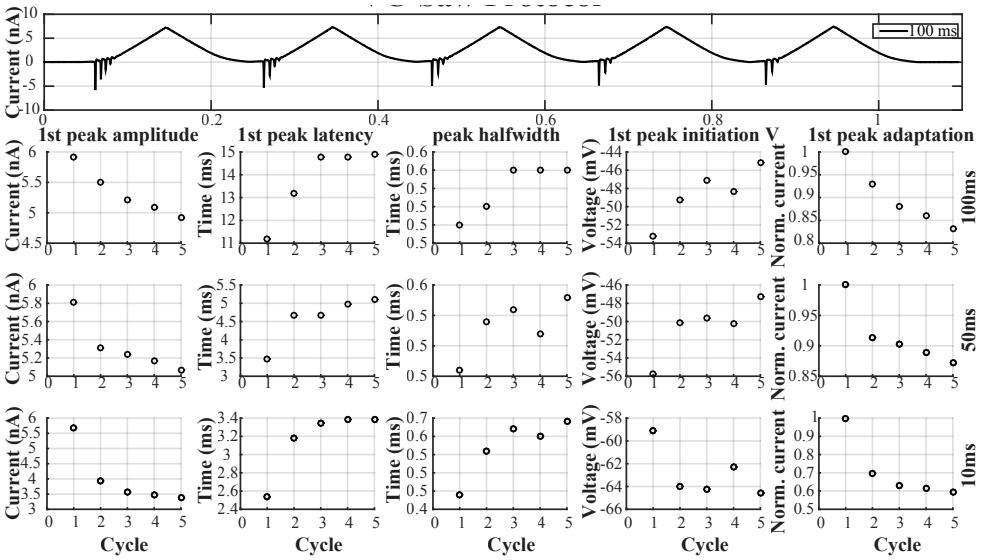

Figure 5. Voltage-clamp sawtooth protocol. Top row: Current trace from a representative experiment (180412_AB_53_ST). Figurines, left to right, are measurements of the first peak amplitude, first peak latency, the half width of the first inward current, membrane potential at which the inward current is initiated, and the adaptation of the first event amplitude across the 5 (triangle) cycles. Data in the bottom three rows are from three different sawtooth speeds (10/50/100 ms, corresponding to 100/20/10 Hz stimulation). The five points in each figurine are calculated from the first inward current in each (triangle) cycle.

The current-voltage relationship was measured with voltage-clamp steps (Figure 6), which could be used to produce an I/V curve. The peak amplitude, latency, and peak half width can be extracted for the inward currents observed during the sustained depolarization of the soma.

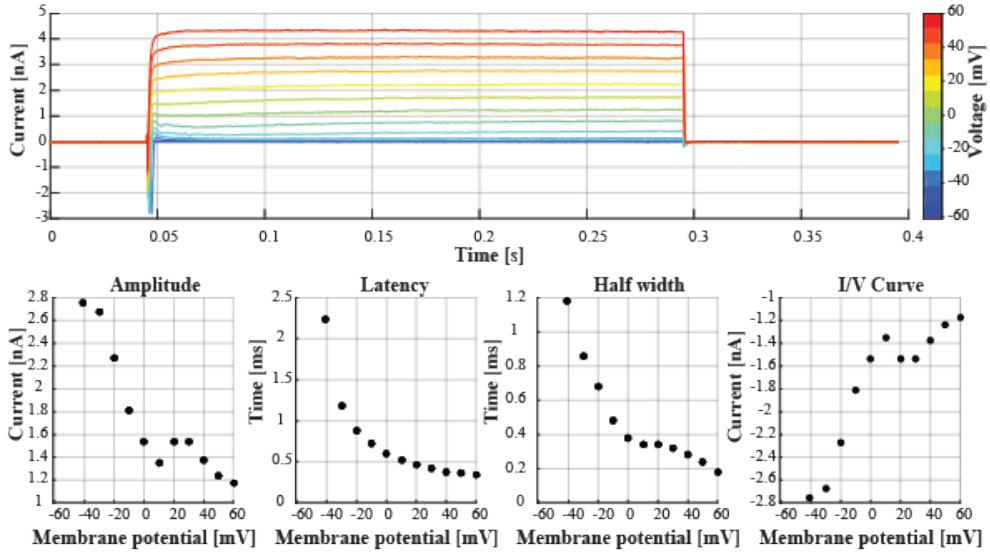

Figure 6. Step-and-hold protocol in voltage-clamp preparation. Top panel shows data from a representative experiment (170915_AB_5_VC). Every other figurine shows one of the analyzed features, including the amplitude of the peak, temporal delay between the stimulus onset and the peak amplitude (i.e. latency), width of the evoked transient measured at half maximum as well as the current at every holding potential (I/V curve).

Availability of Source Code and Requirements

Project name: Rapid mutual information calculation using frozen noise injection

Project home page: [35]

Operating system: Platform independent

Programming language: MATLAB

Other requirements: MATLAB version 2017a or higher.

License: GNU GPL

RRID: SCR_016558

Availability of supporting data

Snapshots of the database and code, including further supporting data is available in the GigaScience repository.

Application scenarios

From the recordings available in this database, it is possible to quantify active the membrane properties of supragranular layer neurons to infer current and voltage dynamics during somatic depolarization.

Network development is based on processes of self-organization that are highly dependent on sensory stimuli and experience [2]. Such plasticity is not limited to early life development. From the voltage-clamp and current-clamp experiments, it is possible to infer the biophysical properties of layer 2/3 pyramidal neurons of the adult somatosensory cortex under baseline conditions, in the absence of altered sensory experience.

The focus on adult neurons brings a new perspective to the study of membrane properties, as data from these mature ages are still scarce. The dynamics of the active electrical properties of the membrane can be accessed as a function of different developmental time points and/or sex, and the recorded data can be used as virtual neurons in dynamic-clamp experiments.

In a computational approach, spiking properties described herein could be used for biomimetic modeling of diverse networks, facilitating the study of computational roles of circuit motives. Moreover, applying the principles of information transfer and recovery to the data might help recreate neuronal functions in artificial systems.

Limitations

Neurons in this dataset originate from regular spiking and fast spiking neurons, however, there is no anatomical characterization of the neuron type studied. The database is focused on Layer 2/3 of the somatosensory cortex as a model region and does not allow the study of neuronal information processing across different cortical regions in isolation. However, the user might consider comparing data across different regions and species by utilizing the other publicly available databases, e.g. Neurodata Without Borders [36], the Cell Type database [37] of the Allen Institute and the Collaborative Research in Computational Neuroscience data sharing initiative [41].

References

1. Azarfar, A. *et al.* An open-source high-speed infrared videography database to study the principles of active sensing in freely navigating rodents. *GigaScience*
2. Kole, K., Scheenen, W., Tiesinga, P. & Celikel, T. Cellular diversity of the somatosensory cortical map plasticity. *Neurosci. Biobehav. Rev.* **84,** 100–115 (2018).
3. Diamond, M. E., Petersen, R. S. & Harris, J. A. Learning through maps: functional significance of topographic organization in primary sensory cortex. *J. Neurobiol.* **41,** 64–68 (1999).
4. Celikel, T. & Sakmann, B. Sensory integration across space and in time for decision making in the somatosensory system of rodents. *Proc Natl Acad Sci USA* **104,** 1395–1400 (2007).
5. Van der Loos, H. & Woolsey, T. A. Somatosensory cortex: structural alterations following early injury to sense organs. *Science* **179,** 395–398 (1973).
6. Voigts, J., Herman, D. H. & Celikel, T. Tactile object localization by anticipatory whisker motion. *J. Neurophysiol.* **113,** 620–632 (2015).
7. Carvell, G. E. & Simons, D. J. Task- and subject-related differences in sensorimotor behaviour during active touch. *Somatosens. Mot. Res.* **12,** 1–9 (1995).
8. Voigts, J., Sakmann, B. & Celikel, T. Unsupervised whisker tracking in unrestrained behaving animals. *J. Neurophysiol.* **100,** 504–515 (2008).
9. Carvell, G. E. & Simons, D. J. Effect of whisker geometry on contact force produced by vibrissae moving at different velocities. *J. Neurophysiol.* **118,** 1637–1649 (2017).
10. Azarfar, A., Calcini, N., Huang, C., Zeldenrust, F. & Celikel, T. Neural coding: A single neuron's perspective. *Neurosci. Biobehav. Rev.* (2018). doi:10.1016/j.neubiorev.2018.09.007
11. Allen, C. B., Celikel, T. & Feldman, D. E. Long-term depression induced by sensory deprivation during cortical map plasticity in vivo. *Nat. Neurosci.* **6,** 291–299 (2003).
12. Celikel, T., Szostak, V. A. & Feldman, D. E. Modulation of spike timing by sensory deprivation during induction of cortical map plasticity. *Nat. Neurosci.* **7,** 534–541 (2004).
13. Foeller, E., Celikel, T. & Feldman, D. E. Inhibitory sharpening of receptive fields contributes to whisker map plasticity in rat somatosensory cortex. *J. Neurophysiol.* **94,** 4387–4400 (2005).
14. Clem, R. L., Celikel, T. & Barth, A. L. Ongoing in vivo experience triggers synaptic metaplasticity in the neocortex. *Science* **319,** 101–104 (2008).
15. Juczewski, K. *et al.* Somatosensory map expansion and altered processing of tactile inputs in a mouse model of fragile X syndrome. *Neurobiol. Dis.* **96,** 201–215 (2016).
16. Miceli, S. *et al.* Reduced Inhibition within Layer IV of Sert Knockout Rat Barrel Cortex is Associated with Faster Sensory Integration. *Cereb. Cortex* **27,** 933–949 (2017).
17. Pang, R. D. *et al.* Mapping functional brain activation using [14C]-iodoantipyrine in male serotonin transporter knockout mice. *PLoS ONE* **6,** e23869 (2011).
18. Huang, C., Resnik, A., Celikel, T. & Englitz, B. Adaptive spike threshold enables robust and temporally precise neuronal encoding. *PLoS Comput. Biol.* **12,** e1004984 (2016).
19. Zhang, Z., Jiao, Y. Y. & Sun, Q. Q. Developmental maturation of excitation and inhibition balance in principal neurons across four layers of somatosensory cortex. *Neuroscience* **174,** 10–25 (2011).
20. Ashby, M. C. & Isaac, J. T. R. Maturation of a recurrent excitatory neocortical circuit by experience-dependent

unsilencing of newly formed dendritic spines. *Neuron* **70,** 510–521 (2011).

21. Cheetham, C. E. J. & Fox, K. Presynaptic development at L4 to l2/3 excitatory synapses follows different time courses in visual and somatosensory cortex. *J. Neurosci.* **30,** 12566–12571 (2010).
22. Stern, E. A., Maravall, M. & Svoboda, K. Rapid development and plasticity of layer 2/3 maps in rat barrel cortex in vivo. *Neuron* **31,** 305–315 (2001).
23. Lo, S. Q., Sng, J. C. G. & Augustine, G. J. Defining a critical period for inhibitory circuits within the somatosensory cortex. *Sci. Rep.* **7,** 7271 (2017).
24. Diamond, M. E., Petersen, R. S., Harris, J. A. & Panzeri, S. Investigations into the organization of information in sensory cortex. *J. Physiol. Paris* **97,** 529–536 (2003).
25. Kole, K. *et al.* Transcriptional mapping of the primary somatosensory cortex upon sensory deprivation. *Gigascience* (2017).
26. Kole, K. *et al.* Supporting data for "Transcriptional mapping of the primary somatosensory cortex upon sensory deprivation." *GigaDB* (2017).
27. Kole, K. *et al.* Proteomic landscape of the primary somatosensory cortex upon sensory deprivation. *Gigascience* **6,** 1–10 (2017).
28. Kole, K. *et al.* Supporting data for "Proteomic landscape of the primary somatosensory cortex upon sensory deprivation." *GigaDB* (2017).
29. Martens, M. B., Celikel, T. & Tiesinga, P. H. E. A developmental switch for hebbian plasticity. *PLoS Comput. Biol.* **11,** e1004386 (2015).
30. Stewart, R. S., Huang, C., Arnett, M. T. & Celikel, T. Spontaneous oscillations in intrinsic signals reveal the structure of cerebral vasculature. *J. Neurophysiol.* **109,** 3094–3104 (2013).
31. Kole, K. & Celikel, T. Neocortical microdissection at columnar and laminar resolution for molecular interrogation. *Curr. Protoc. Neurosci.* e55 (2018). doi:10.1002/cpns.55
32. Blanton, M. G., Lo Turco, J. J. & Kriegstein, A. R. Whole cell recording from neurons in slices of reptilian and mammalian cerebral cortex. *J. Neurosci. Methods* **30,** 203–210 (1989).
33. Margrie, T. W., Brecht, M. & Sakmann, B. In vivo, low-resistance, whole-cell recordings from neurons in the anaesthetized and awake mammalian brain. *Pflugers Arch.* **444,** 491–498 (2002).
34. Zeldenrust, F., de Knecht, S., Wadman, W. J., Denève, S. & Gutkin, B. Estimating the Information Extracted by a Single Spiking Neuron from a Continuous Input Time Series. *Front. Comput. Neurosci.* **11,** 49 (2017).
35. Rapid mutual information calculation using frozen noise injection. at <https://github.com/Departmentof-Neurophysiology/Analysis-tools-for-electrophysiological-somatosensory-cortex-databank/tree/master/Frozen%20Noise>
36. Neurodata without borders. at <https://www.nwb.org>
37. Allen Institute Cell Types database. at <http://celltypes.brain-map.org>
38. ModelDB database. at <https://senselab.med.yale.edu/ModelDB/>
39. Ince, R. A. A. *et al.* Information-theoretic methods for studying population codes. *Neural Netw.* **23,** 713–727 (2010).
40. Quian Quiroga, R. & Panzeri, S. Extracting information from neuronal populations: information theory and decoding approaches. *Nat. Rev. Neurosci.* **10,** 173–185 (2009).
41. Collaborative Research in Computational Neuroscience data sharing initiative. at <https://crcns.org/>

Supplemental Table 1: Metadata

Date	*Experiment Number*	*Prefix*	*Age (P)*	*Sex*	*Experiment Protocol*	*Classification*	*Animal number*
170130	133	AL	226	F	CC 40pA	Excitatory	5
170202	9	NC	229	M	CC 40pA	Excitatory	8
170220	192	AL	84	F	CC 40pA, ST	Excitatory	11
170220	194	AL	84	F	CC 20pA, ST	Excitatory	11
170221	243	AB	85	F	CC 40pA, ST	Excitatory	12
170222	195	AL	86	F	CC 20pA, ST	Excitatory	13
170223	196	AB	87	F	CC 40pA, ST	Excitatory	14
170308	200	AL	253	F	CC 40pA, ST	Excitatory	16
170308	201	AL	253	F	CC 40pA, ST	Excitatory	16
170309	203	AL	254	F	CC 40pA, ST	Excitatory	17
170310	210	AL	255	M	CC 40pA, ST	Excitatory	18
170310	255	AB	255	M	CC 20pA, ST	Excitatory	18
170314	214	AL	275	F	CC 20 pA, ST, VC	Excitatory	19
170314	215	AL	275	F	CC 20 pA, ST, VC	Excitatory	19
170315	215	AL	276	F	CC 40pA, ST, VC	Excitatory	20
170315	216	AL	276	F	CC 20pA, ST, VC	Excitatory	20
170321	222	AL	282	F	CC 40pA, ST	Excitatory	24
170321	223	AL	282	F	CC 40pA, ST, VC	Excitatory	24
170323	227	AL	284	M	CC 40pA, ST, VC	Excitatory	26
170328	233	AL	316	M	CC 40pA, ST, VC	Excitatory	28
170328	234	AL	316	M	CC 40pA, ST, VC	Excitatory	28
170328	237	AL	316	M	CC 40pA, ST, VC	Excitatory	28
170328	238	AL	316	M	CC 40pA, ST, VC	Excitatory	28
170405	282	AB	324	M	CC 20pA, ST, VC	Excitatory	30
170420	246	AL	160	M	CC 20pA, ST, VC	Excitatory	34
170420	294	AB	160	M	CC 20pA, ST	Excitatory	34
170421	246	AL	305	M	CC 40pA, ST, VC	Excitatory	35
170424	247	AL	164	M	CC 40pA, ST, VC	Excitatory	36
170425	251	AL	165	F	CC 20pA, ST	Excitatory	37
170425	300	AB	165	F	CC 20pA, ST	Excitatory	37
170426	255	AL	166	F	CC 40pA, ST, VC	Excitatory	38

Date	*Experiment Number*	*Prefix*	*Age (P)*	*Sex*	*Experiment Protocol*	*Classification*	*Animal number*
170502	258	AL	248	F	CC 40pA, ST, VC	Excitatory	39
170502	303	AB	248	F	CC 40pA, ST	Excitatory	39
170503	304	AB	249	F	CC 20pA, ST	Excitatory	40
170503	305	AB	249	F	CC 20pA, ST, VC	Excitatory	40
170508	258	AL	254	M	CC 20pA, ST, VC	Excitatory	41
170509	260	AL	179	M	CC 20pA, ST, VC	Excitatory	42
170509	310	AB	179	M	CC 40pA, ST	Excitatory	42
170510	312	AB	163	M	CC 40pA, ST	Excitatory	43
170510	314	AB	163	M	CC 20pA, ST	Excitatory	43
170511	317	AB	164	M	CC 20pA, ST	Excitatory	44
170516	322	AB	224	F	CC 20pA, ST	Excitatory	46
170516	324	AB	224	F	CC 40pA, ST, VC	Excitatory	46
170615	19	NC	218	M	CC 40pA, FN	Excitatory	60
170620	22	NC	213	M	CC 40pA, FN	Excitatory	62
170623	23	NC	110	M	CC 40pA	Excitatory	63
170626	28	NC	113	M	CC 40pA	Excitatory	64
170627	31	NC	71	F	CC 40pA	Excitatory	65
170628	32	NC	95	F	CC 40pA, FN	Excitatory	66
170628	33	NC	95	F	CC 40pA, FN	Excitatory	66
170630	34	NC	97	M	CC 40pA	Excitatory	67
170630	36	NC	97	M	CC 40pA, FN	Excitatory	67
170703	38	NC	100	M	CC 40pA, FN	Excitatory	68
170703	39	NC	100	M	CC 40pA	Excitatory	68
170703	41	NC	100	M	CC 40pA, FN	Excitatory	68
170703	42	NC	100	M	CC 40pA	Excitatory	68
170704	43	NC	101	F	CC 40pA	Excitatory	69
170705	46	NC	102	F	CC 40pA	Excitatory	70
170705	47	NC	102	F	CC 40pA	Excitatory	70
170710	48	NC	108	F	CC 40pA	Excitatory	71
170710	49	NC	108	F	CC 40pA	Excitatory	71
170711	51	NC	89	M	CC 40pA, FN	Excitatory	72
170711	52	NC	89	M	CC 40pA, FN	Excitatory	72

Date	*Experiment Number*	*Prefix*	*Age (P)*	*Sex*	*Experiment Protocol*	*Classification*	*Animal number*
170711	53	NC	89	M	CC 40pA	Excitatory	72
170711	54	NC	89	M	CC 40pA, FN	Excitatory	72
170712	55	NC	84	F	CC 40pA, FN	Excitatory	73
170712	56	NC	84	F	CC 40pA, FN	Excitatory	73
170713	57	NC	227	F	CC 40pA	Excitatory	74
170713	58	NC	227	F	CC 40pA, FN	Excitatory	74
170713	59	NC	227	F	CC 20pA, FN	Excitatory	74
170714	60	NC	178	F	CC 40pA	Excitatory	75
170714	61	NC	178	F	CC 40pA	Excitatory	75
170714	62	NC	178	F	CC 40pA	Excitatory	75
170714	63	NC	178	F	CC 40pA	Excitatory	75
170714	64	NC	178	F	CC 20pA, FN	Excitatory	75
170717	66	NC	104	F	CC 40pA	Excitatory	76
170718	68	NC	105	F	CC 40pA, FN	Excitatory	77
170719	70	NC	169	F	CC 40pA, FN	Excitatory	78
170719	71	NC	169	F	CC 40pA	Excitatory	78
170720	72	NC	204	F	CC 40pA, FN	Excitatory	79
170720	73	NC	204	F	CC 40pA	Excitatory	79
170720	74	NC	204	F	CC 40pA, FN	Excitatory	79
170720	75	NC	204	F	CC 40pA, FN	Excitatory	79
170724	76	NC	103	F	CC 20pA, FN	Excitatory	80
170724	77	NC	103	F	CC 40pA, FN	Excitatory	80
170724	78	NC	103	F	CC 40pA	Excitatory	80
170724	79	NC	103	F	CC 40pA, FN	Excitatory	80
170725	80	NC	104	F	CC 40pA	Excitatory	81
170725	81	NC	104	F	CC 20pA, FN	Excitatory	81
170726	85	NC	229	F	CC 40pA	Excitatory	82
170728	89	NC	100	F	CC 40pA, FN	Excitatory	84
170728	91	NC	100	F	CC 40pA, FN	Excitatory	84
170801	92	NC	104	F	CC 40pA	Excitatory	85
170811	94	NC	114	M	CC 40pA, FN	Excitatory	86
170811	95	NC	114	M	CC 40pA, FN	Excitatory	86

Date	*Experiment Number*	*Prefix*	*Age (P)*	*Sex*	*Experiment Protocol*	*Classification*	*Animal number*
170811	96	NC	114	M	CC 20pA	Excitatory	86
170811	97	NC	114	M	CC 20pA, FN	Excitatory	86
170811	98	NC	114	M	CC 40pA, FN	Excitatory	86
170814	99	NC	117	F	CC 20pA	Excitatory	87
170814	101	NC	117	F	CC 40pA	Excitatory	87
170814	102	NC	117	F	CC 40pA	Excitatory	87
170814	103	NC	117	F	CC 40pA, FN	Excitatory	87
170814	105	NC	117	F	CC 40pA, FN	Excitatory	87
170815	107	NC	118	F	CC 40pA, FN	Excitatory	88
170815	109	NC	118	F	CC 40pA, FN	Excitatory	88
170816	112	NC	79	F	CC 40pA, FN	Excitatory	89
170821	113	NC	84	F	CC 40pA, FN	Excitatory	90
170821	114	NC	84	F	CC 40pA, FN	Excitatory	90
170821	115	NC	84	F	CC 40pA, FN	Excitatory	90
170830	118	NC	285	F	CC 40pA, FN	Excitatory	91
170830	119	NC	285	F	CC 40pA, FN	Excitatory	91
170914	4	AB	309	F	CC 20pA, ST, VC	Excitatory	92
170926	7	AB	288	M	CC 40pA, ST, VC	Excitatory	94
171006	125	NC	143	F	CC 40pA, FN	Excitatory	95
171010	127	NC	335	M	CC 40pA, FN	Excitatory	96
171010	129	NC	335	M	CC 40pA, FN	Excitatory	96
171011	130	NC	372	M	CC 40pA, FN	Excitatory	97
171011	131	NC	372	M	CC 40pA, FN	Excitatory	97
171011	132	NC	372	M	CC 40pA, FN	Excitatory	97
171012	134	NC	373	M	CC 40pA	Excitatory	98
171012	135	NC	373	M	CC 40pA, FN	Excitatory	98
171012	136	NC	373	M	CC 40pA	Excitatory	98
171012	137	NC	373	M	CC 40pA, FN	Excitatory	98
171012	138	NC	373	M	CC 40pA, FN	Excitatory	98
171017	140	NC	154	F	CC 40pA, FN	Excitatory	98
171017	141	NC	154	F	CC 40pA, FN	Excitatory	98
171017	142	NC	154	F	CC 40pA, FN	Excitatory	98

Date	*Experiment Number*	*Prefix*	*Age (P)*	*Sex*	*Experiment Protocol*	*Classification*	*Animal number*
171220	156	NC	218	F	CC 40pA, ST, FN	Excitatory	103
171220	157	NC	218	F	CC 40pA	Excitatory	103
171220	158	NC	218	F	CC 40pA, ST, FN	Excitatory	103
171220	159	NC	218	F	CC 40pA, ST, FN	Excitatory	103
171222	160	NC	208	F	CC 40pA, ST, FN	Excitatory	104
171222	161	NC	208	F	CC 40pA, ST, FN	Excitatory	104
170623	24	NC	110	M	CC 40pA	Excitatory	63
170815	108	NC	118	F	CC 20pA, FN	Excitatory	88
171207	149	NC	384	F	CC 40pA, ST, FN	Excitatory	100
171207	148	NC	384	F	CC 20pA, ST, FN	Excitatory	100
170316	263	AB	273	F	CC 20pA, ST, VC	Inhibitory	21
170424	297	AB	164	M	CC 20pA, ST	Inhibitory	36
170515	319	AB	176	M	CC 20pA, ST	Inhibitory	45
161104	3	NC	192	M	CC 40pA	Inhibitory	1
161214	7	NC	210	M	CC 40pA	Inhibitory	4
161214	113	AL	210	M	CC 40pA	Inhibitory	4
170130	134	AL	226	F	CC 40pA	Inhibitory	5
170308	203	AL	253	F	CC 40pA, ST	Inhibitory	16
170309	252	AB	254	F	CC 20pA, ST	Inhibitory	17
170315	261	AB	276	F	CC 40pA, ST, VC	Inhibitory	20
170316	217	AL	273	F	CC 40pA, ST, VC	Inhibitory	21
170317	218	AL	274	F	CC 40pA, ST	Inhibitory	22
170328	235	AL	316	M	CC 40pA, ST, VC	Inhibitory	28
170410	288	AB	202	F	CC 40pA, ST	Inhibitory	31
170420	293	AB	160	M	CC 20pA, ST, VC	Inhibitory	34
170421	296	AB	305	M	CC 20pA, ST	Inhibitory	35
170426	301	AB	166	F	CC 40pA, ST	Inhibitory	38
170502	257	AL	248	F	CC 40pA, ST	Inhibitory	39
170508	308	AB	254	M	CC 20pA, ST, VC	Inhibitory	41
170518	18	NC	226	F	CC 20pA	Inhibitory	48
170616	20	NC	209	M	CC 40pA, FN	Inhibitory	61
170616	21	NC	209	M	CC 40pA, FN	Inhibitory	61

Date	*Experiment Number*	*Prefix*	*Age (P)*	*Sex*	*Experiment Protocol*	*Classification*	*Animal number*
170623	25	NC	110	M	CC 40pA, FN	Inhibitory	63
170626	26	NC	113	M	CC 40pA, FN	Inhibitory	64
170626	27	NC	113	M	CC 40pA, FN	Inhibitory	64
170626	29	NC	113	M	CC 40pA, FN	Inhibitory	64
170627	30	NC	71	F	CC 40pA, FN	Inhibitory	65
170630	35	NC	97	M	CC 40pA	Inhibitory	67
170630	37	NC	97	M	CC 40pA, FN	Inhibitory	67
170703	40	NC	100	M	CC 40pA	Inhibitory	68
170704	44	NC	101	F	CC 20pA, FN	Inhibitory	69
170704	45	NC	101	F	CC 40pA	Inhibitory	69
170710	50	NC	108	F	CC 40pA	Inhibitory	71
170717	65	NC	104	F	CC 40pA, FN	Inhibitory	76
170718	67	NC	105	F	CC 40pA, FN	Inhibitory	77
170718	69	NC	105	F	CC 40pA, FN	Inhibitory	77
170725	82	NC	104	F	CC 40pA, FN	Inhibitory	81
170726	83	NC	229	F	CC 40pA, FN	Inhibitory	82
170726	86	NC	229	F	CC 40pA, FN	Inhibitory	82
170726	87	NC	229	F	CC 40pA, FN	Inhibitory	82
170727	88	NC	230	F	CC 40pA, FN	Inhibitory	83
170728	90	NC	100	F	CC 40pA, FN	Inhibitory	84
170801	93	NC	104	F	CC 40pA, FN	Inhibitory	85
170814	100	NC	117	F	CC 40pA, FN	Inhibitory	87
170814	104	NC	117	F	CC 20pA, FN	Inhibitory	87
170815	106	NC	118	F	CC 40pA, FN	Inhibitory	88
170830	116	NC	285	F	CC 40pA, FN	Inhibitory	91
170914	123	NC	309	F	CC 40pA, FN	Inhibitory	92
170918	6	AB	155	F	CC 20pA, ST, VC	Inhibitory	93
171006	124	NC	143	F	CC 40pA, FN	Inhibitory	95
171010	126	NC	335	M	CC 40pA, FN	Inhibitory	96
171010	128	NC	335	M	CC 40pA, FN	Inhibitory	96
171110	143	NC	356	M	CC 40pA, ST, FN	Inhibitory	99
171110	144	NC	356	M	CC 40pA, ST, FN	Inhibitory	99

Date	*Experiment Number*	*Prefix*	*Age (P)*	*Sex*	*Experiment Protocol*	*Classification*	*Animal number*
171110	145	NC	356	M	CC 40pA, ST, FN	Inhibitory	99
171207	22	AB	384	F	CC 40pA, ST, FN	Inhibitory	100
171207	146	NC	384	F	CC 40pA, ST, FN	Inhibitory	100
171207	147	NC	384	F	CC 40pA	Inhibitory	100
171207	150	NC	384	F	CC 40pA, ST, FN	Inhibitory	100
171208	151	NC	385	F	CC 40pA, ST	Inhibitory	101
171208	152	NC	385	F	CC 40pA, ST	Inhibitory	101
171211	153	NC	197	F	CC 40pA, ST, FN	Inhibitory	102
171211	154	NC	197	F	CC 40pA, ST, FN	Inhibitory	102
171220	155	NC	218	F	CC 20pA, ST, FN	Inhibitory	103
180412	53	AB	212	F	CC 40pA, ST, VC	Inhibitory	105
170222	196	AL	86	F	CC 10pA, ST	Unknown	13
170224	197	AL	163	M	CC 10pA, ST	Unknown	15
170310	213	AL	255	M	CC 5pA, ST	Unknown	18
170315	260	AB	276	F	CC 10pA, ST, VC	Unknown	20
170322	227	AL	283	M	CC 5pA, ST, VC	Unknown	25
170323	229	AL	284	M	CC 10pA, ST, VC	Unknown	26
170324	232	AL	285	M	CC 10pA, ST	Unknown	27
170424	249	AL	164	M	CC 5pA, ST, VC	Unknown	36
170502	302	AB	248	F	CC 10pA, ST	Unknown	39
170509	309	AB	179	M	CC 10pA, ST	Unknown	42
170517	17	NC	225	F	CC 10pA	Unknown	47
170914	5	AB	309	F	CC 10pA, ST, VC	Unknown	92
170926	8	AB	288	M	CC 60pA, ST, VC	Unknown	94
171010	343	AB	335	M	ST, VC	Unknown	96
171017	139	NC	154	F	CC 40pA, FN	Unknown	98
171222	162	NC	208	F	CC 40pA, ST, FN	Unknown	104
170310	256	AB	255	M	CC 10pA, ST	Unknown	18
170315	259	AB	276	F	ST, VC	Unknown	20
170317	265	AB	274	F	ST	Unknown	22
170320	223	AL	281	F	CC 5pA, ST	Unknown	23
170405	284	AB	324	M	CC 10pA, ST	Unknown	30

Date	*Experiment Number*	*Prefix*	*Age (P)*	*Sex*	*Experiment Protocol*	*Classification*	*Animal number*
170410	287	AB	202	F	ST	Unknown	31
170726	84	NC	229	F	CC 60pA	Unknown	82
170816	110	NC	79	F	CC 10pA, FN	Unknown	89
170816	111	NC	79	F	CC 20pA, FN	Unknown	89
171207	23	AB	384	F	ST	Unknown	100
170131	216	AB	227	F	ST	Unknown	6
170131	218	AB	227	F	ST	Unknown	6
170201	220	AB	228	F	ST	Unknown	7
170201	221	AB	228	F	ST	Unknown	7
170201	222	AB	228	F	ST	Unknown	7
170208	231	AB	235	M	ST	Unknown	9
170208	232	AB	235	M	ST	Unknown	9
170209	237	AB	222	F	ST	Unknown	10
170220	240	AB	84	F	ST, VC	Unknown	11
170221	241	AB	85	F	ST, VC	Unknown	12
170308	250	AB	253	F	ST	Unknown	16
170314	258	AB	275	F	CC 60pA, ST, VC	Unknown	19
170323	268	AB	284	M	ST	Unknown	26
170328	276	AB	316	M	ST	Unknown	28
170328	277	AB	316	M	ST	Unknown	28
170329	279	AB	377	F	ST	Unknown	29
170329	280	AB	317	F	ST	Unknown	29
170405	285	AB	324	M	VC	Unknown	30
170410	289	AB	202	F	ST, VC	Unknown	31
170516	323	AB	224	F	VC	Unknown	46
170516	326	AB	224	F	ST, VC	Unknown	46
170518	332	AB	227	F	ST	Unknown	48
170519	329	AB	227	F	ST	Unknown	49
170519	330	AB	227	F	ST	Unknown	49
170519	333	AB	227	F	ST	Unknown	49
170522	334	AB	175	M	ST	Unknown	50
170522	335	AB	175	M	ST	Unknown	50

Date	*Experiment Number*	*Prefix*	*Age (P)*	*Sex*	*Experiment Protocol*	*Classification*	*Animal number*
170522	336	AB	175	M	ST	Unknown	50
170523	337	AB	176	M	ST	Unknown	51
170523	338	AB	176	M	ST	Unknown	51
170523	339	AB	176	M	ST	Unknown	51
170524	340	AB	169	F	ST	Unknown	52
170524	341	AB	169	F	ST	Unknown	52
170529	342	AB	195	F	ST	Unknown	53
170529	344	AB	195	F	ST	Unknown	53
170530	347	AB	206	F	ST, VC	Unknown	54
170530	348	AB	206	F	ST	Unknown	54
170531	349	AB	207	F	ST	Unknown	55
170531	350	AB	207	F	ST	Unknown	55
170531	351	AB	207	F	ST	Unknown	55
170608	360	AB	211	M	ST	Unknown	56
170609	361	AB	147	M	ST	Unknown	57
170612	362	AB	150	M	ST	Unknown	58
170612	363	AB	150	M	ST	Unknown	58
170612	364	AB	150	M	ST	Unknown	58
170612	365	AB	150	M	ST	Unknown	58
170613	366	AB	216	M	ST	Unknown	59
170615	367	AB	218	M	ST	Unknown	60
170615	369	AB	218	M	ST	Unknown	60
170615	370	AB	218	M	ST	Unknown	60
170626	373	AB	113	M	ST	Unknown	64
170626	374	AB	113	M	ST	Unknown	64
170627	376	AB	71	F	ST	Unknown	65
170627	378	AB	71	F	ST	Unknown	65

Chapter 3

Electrical characterization of the supragranular layer neurons in the adult mouse barrel cortex

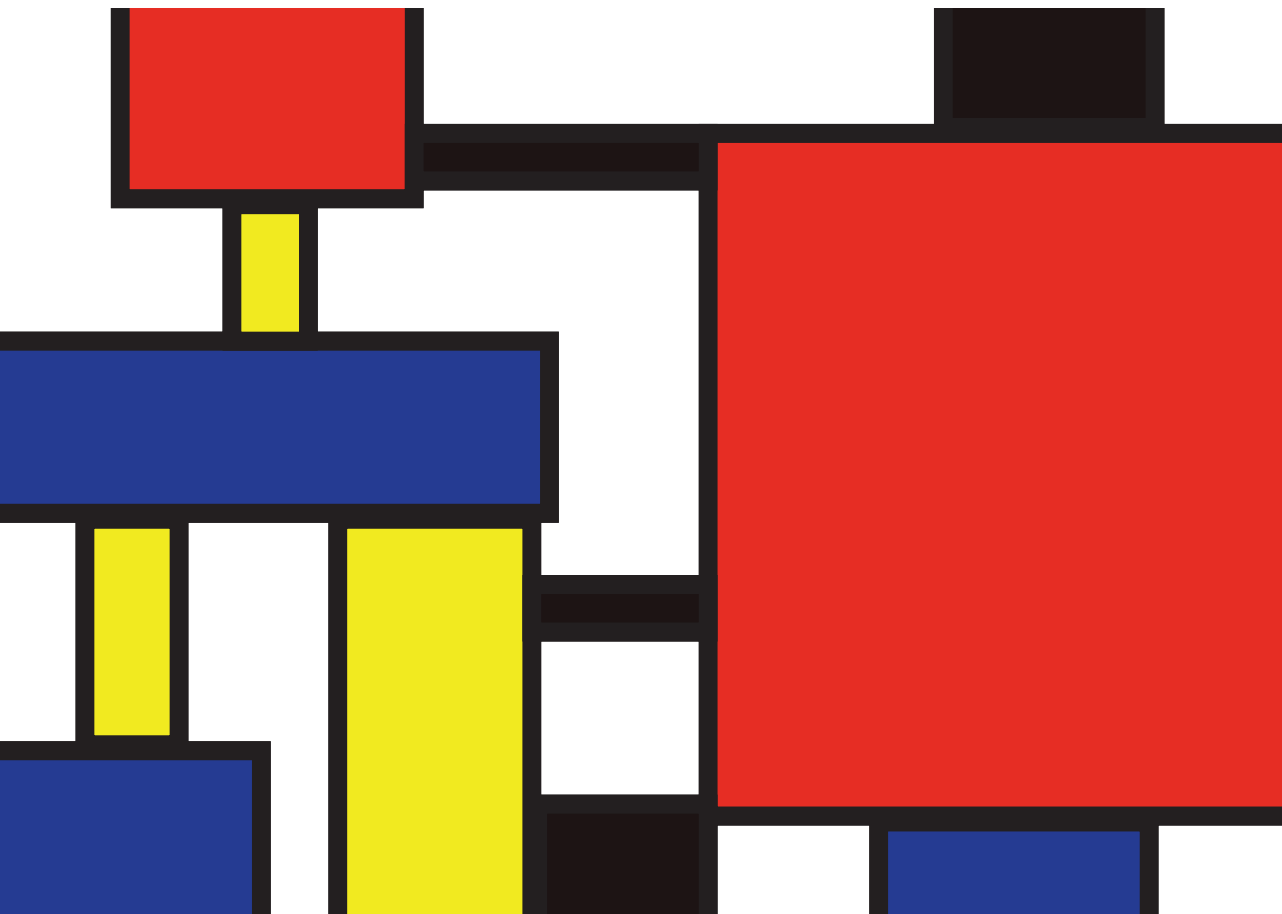

Neurons have diverse molecular, anatomical and electrical characteristics throughout the brain. Functional classification of neurons will help to determine the building blocks of neuronal circuits, in particular in heterogenous circuits like the sensory cortices in the neocortex. Here, taking advantage of a recently introduced intracellular recording database (see Chapter 2), we perform a systematic classification of the cell-types in the supragranular layers of the barrel cortex. Unlike the prior efforts for electrical classification of the neuronal cell-types, we define the neuronal sub- and suprathreshold responses to varying, but bandwidth limited, somatic depolarization in a high dimensional space (N=139). We determine the minimum number of dimensions that are required to represent the data (N=15), reduce the dimensionality while maintaining cluster separation and finally electrically compare the cell-classes. The results show that the best predictor for cell classification is the adaptive change observed in the membrane potential during varying somatic depolarization. The neurons can be classified into 10 cell-classes using 5 dimensions. These results argue that systematic variations in neural responses upon varying somatic depolarization states is an understudied but an important dimension in cellular classification.

The neurons in layer 2/3 the barrel cortex of rodents are involved in integrating information that originates from the sensory periphery with the information generated elsewhere in the brain [1–4]. They carry spatial and temporal information about contacts with an object, tactile features of the object and the whisker position in parallel [5]. Given their importance for the neural processing of sensory information, one of the major goals of systems neuroscience is to identify the building blocks of the somatosensory circuits.

Neurons are commonly classified according to their anatomical features, molecular fingerprints, as well as passive and active electrical properties [6–11]. For example, inhibitory neurons in the supragranular (L2/3) of the juvenile primary somatosensory cortex can be anatomically divided into 8 distinct classes based on their shape, organization, and localization of the projections, while 5 sub-classes can be distinguished among the pyramidal neurons [6,12,13]. Given the considerable molecular and biochemical diversity of neurons [6,9,10,14,15], the combinatorial classification of neurons based on molecular fingerprints and anatomical features arguably results in the overestimation of the functional subclasses in the network. For example, neurogliaform neurons can be classified as a single subpopulation of inhibitory neurons when both their anatomical features and the expression of the 5-Hydroxytryptamine Receptor 3A receptors are considered. However, because these neurons also express Glutamate Decarboxylase 1 and Vasoactive Intestinal Peptide at varying rates, the neurogliaform neurons can be further sub-classified [10]. The expression of the molecular markers is often subject to experience-dependent plasticity [1], therefore, cellular classification based solely on molecular markers might confound the clustering efforts. Considering that action potential rate and timing are the means of neuronal communication in synaptically coupled networks, active electrical properties of neurons could instead be used to determine the functional subclasses of neurons.

Cellular classification based on active electrical properties of neurons necessarily requires redefining continuous voltage (or current) time-series into variables (also known as descriptors, features, dimensions), e.g. action potential threshold, amplitude, spike half-width. Although the selection of features is arbitrary, this approach, combined with various clustering methods, has been successfully used to electrically classify neurons before [14,16–21].

In previous studies, the neural responses to sustained somatic activation (or inactivation) have been studied upon depolarization (or hyperpolarization) at a constant single stimulus intensity. However, given the prominent voltage-gated conductances the integrative properties of neurons are likely to vary depending on the amplitude of the sustained depolarization.

1 The transcriptome and the proteome of the supragranular and granular layers of the barrel cortex in control conditions and after sensory deprivation are freely available at barrelomics.science.ru.nl

Therefore, in this study, we electrically characterized the supragranular neurons in the primary somatosensory cortex using the database of 213 neurons described in Chapter 2. Current-clamp recordings across discrete steps of somatic depolarizations resulted in a varying number, rate, and pattern of action potentials in single neurons. Clustering performed after the identification of the features that describe supra- and subthreshold voltage dynamics within and across depolarization steps showed that adaptive changes in voltage dynamics are a powerful predictor of cell classes in the somatosensory cortex. Based on the classification performed in this dataset, we argue that the supragranular layers of the barrel cortex consist of 10 electrically distinguishable cell types.

Materials and methods

Animal experiments were realized as approved by the European Directive 2010/63/EU, national regulations in the Netherlands, and international guidelines on animal care and use of animals.

The electrophysiological methods are described in detail in Chapter 2. In short, Pval-cre and SSt-cre mice (n = 120) between 9 and 54 weeks, 37.5% male were anesthetized with Isoflurane (10 ml/mouse) and the depth of the anesthesia was assessed by pinch withdrawal before perfusion in cooled solution containing (in mM): 10.8 choline chloride, 0.3 KCl, 2.6 $NaHCO_3$, 0.125 $NaH_2PO_4.H_2O$, 2.5 Glucose.H_2O, 0.1 $CaCl_2.2H_2O$, 0.6 $MgSO_4.7H_2O$, 0.3 Na.pyruvate. After extraction, the barrel cortex was sectioned coronally in (thickness: 400 μm) and slices were transferred to a chamber containing ACSF (in mM): 120 NaCl, 3.5 KCl, 10 Glucose.H_2O, 2.5 $CaCl_2.2H_2O$, 1.3 $MgSO_4.7H_2O$, 25 $NaHCO_3$, 1.25 $NaH_2PO_4.H_2O$, aerated with 95% O_2/ 5% CO_2 as described before [22,23]. The slices were then kept in 37°C for 30 minutes and subsequently another 30 minutes (minimum) in room temperature before the whole-cell recordings. During incubation and electrical recordings, the slices were continuously oxygenated and perfused with ACSF. The barrel cortex was located using the 20x lens and the pyramidal cells were patched with a 40x lens.

For the electrophysiological recordings, pipettes were pulled from borosilicate glass tubing with a P-2000 puller (Sutter Instrument, USA) and used if their initial resistance were between 5-9 MOhm. They were filled with (mM): 130 K-Gluconate, 5 KCl, 1.5 $MgCl_2.6H_2O$, 0.4 Na3GTP, 4 Na2ATP, 10 HEPES, 10 Na-phosphocreatine, 0.6 EGTA, and the pH was set at 7.22 with KOH. We used conventional current and voltage clamp [24,25] configurations. Series resistances were between 10-75 MOhm and bridge balance was not compensated. After establishing the current-clamp configuration, the current was kept constant to keep the membrane potential at -70 mV and 10 steps of 20-40 pA current injections were somatically delivered for a duration of 500 ms. Each stimulus intensity was repeated 1-3 times with a 20 s

interval. If the membrane potential varied more than 7 mV during the course of the recording the cell was excluded from the database.

Description of the feature space

All data analysis was performed off-line using custom-written routines in MATLAB. Voltage traces corresponding to somatic current injection epochs (500 ms/sweep) were used for the quantification of the active electrophysiological properties of neurons (Figure 1). A total of 139 features were extracted from each neuron (see Supplemental Table 1). Seventy of these features were descriptors of the sub- and suprathreshold responses in single depolarization sweeps. The remaining 69 captured the dynamical nature of the change in somatic voltage dynamics across depolarization states.

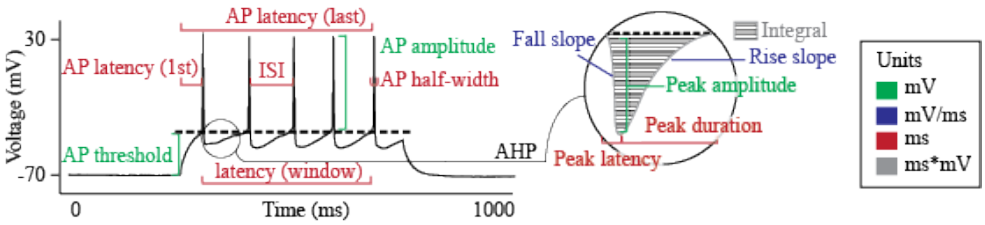

Figure 1. Primary features of somatically evoked action potentials. An example voltage trace and the description of primary features. See Supplemental Table 1 for a complete description. AP = action potential, ISI = interspike interval; AHP = afterhyperpolarization peak.

To estimate the adaptive changes in membrane potential across the 10 somatic depolarization states, we performed a "best fit" analysis. The results showed that the overwhelming majority (i.e. 67/70) of the dynamics can be best approximated by a linear fit, although the slope across the feature space varied. Those features that are best estimated with a logistic or exponential function, can also be approximated with a linear fit albeit at a cost of increased residuals. To ensure a uniform comparison across the feature space, we fitted all dynamical parameters (i.e. varying with stimulus amplitude) with linear kernel, and used the slope and onset value of each fit as descriptors, obtaining a total of 139 parameters (the parameter representing the "lowest current step at which the cell fired an AP" does not have a fit value).

Dimensionality reduction

Dimensionality reduction prior to clustering allows maximum occupancy of each cluster and smaller cluster boundaries, given that those clusters that are weakly connected are unlikely

to converge if clusters are undersampled. Therefore, to estimate the minimum number of dimensions required to describe the data, we performed a Principal Component Analysis (PCA). We computed the eigenvalues of the whitened PCA covariance matrix, obtaining the lower boundary estimation, i.e. 15, as described before [26]: Dim $=(\sum_i \lambda_i)^2/(\sum_i \lambda_i^2)$.

To reduce the dimensionality in the feature space, we applied an empirically defined threshold of 0.6 on the Pearson correlation coefficients, computed pairwise across all parameters. The remaining 35 parameters are listed in Supplemental Table 1. Given the lower limit estimate of 15 and the higher limit of 139, and a dataset of 213 neurons, this feature space represents a sufficiently small dimensionality to perform the initial clustering.

Clustering

To sort neurons into cell-classes, we used a hierarchical clustering approach where neurons were first sorted into 50 classes using k-means clustering [27], which were subsequently merged iteratively using maximum likelihood estimations as described below and before [28]. This approach ensured that the similarity within cell-clusters and dissimilarity between clusters were maximized.

K-means clustering was performed after standardizing the data so that each feature had a mean of zero and a standard deviation of one. After clustering, those cell-clusters that had less than 10 cells were removed and its members were reassigned to the closest cluster based on Z-distance minimization [26]. This entire process was repeated 10000 times to calculate the variance in cluster assignments, which was subsequently used to determine the final cell-clusters based on maximum likelihood (ML) estimations, assigning each cell to the cluster with the highest probability of containing it. If, after the ML assignment, there were any clusters with less than 10 cells, the entire procedure was repeated again but this time ML clusters were used as the starting clusters.

Feature ranking

To systematically evaluate what features are most informative for the classification of neurons, and provide a simplified set of criteria for post-hoc replicability across different datasets, we searched for the most informative features. To do so we computed the mean Z-distance between any given clusters for any combination of 5 features that survived that dimensionality reduction (from 139 to 35). As the final step, we ran the standard k-means algorithm, with the number of clusters estimated with the maximum likelihood agglomerative clustering, for all feature sets (Ns = [139 35 5]) and compared them by computing the Z-distance between them.

Results

To approximate the number of cell classes in the supragranular layers of the adult barrel cortex, we employed a hierarchical clustering approach on voltage traces recorded intracellularly in acute cortical slices.

Dimensionality reduction for neuronal classification

The neuronal response to somatic current injections was approximated by 139 dimensions that represent the response dynamics within and across stimulus intensities (i.e. the amplitude of the current injection, see Supplemental Table 1). To determine whether neurons can be clustered with high confidence in this high-dimensional feature space, we performed the k-means clustering and a single iteration of ML-based cluster merging (see Materials and Methods for details). The quantification of the occupancy for each cluster (Figure 1A) showed a heteroscedastic distribution. The probability of a given neuron to be assigned to any given cluster (Figure 1B) did not follow a uniform distribution, and only a subset of neurons was clustered with high confidence (Figure 1C). These observations support the notion that clustering in a high-dimensional space results in clusters with a small (minimal) inter-cluster distance. Accordingly, under these constraints, cluster identification is a probabilistic inference where each neuron has a particular probability distribution to be associated with a finite number of clusters (Figure 1C).

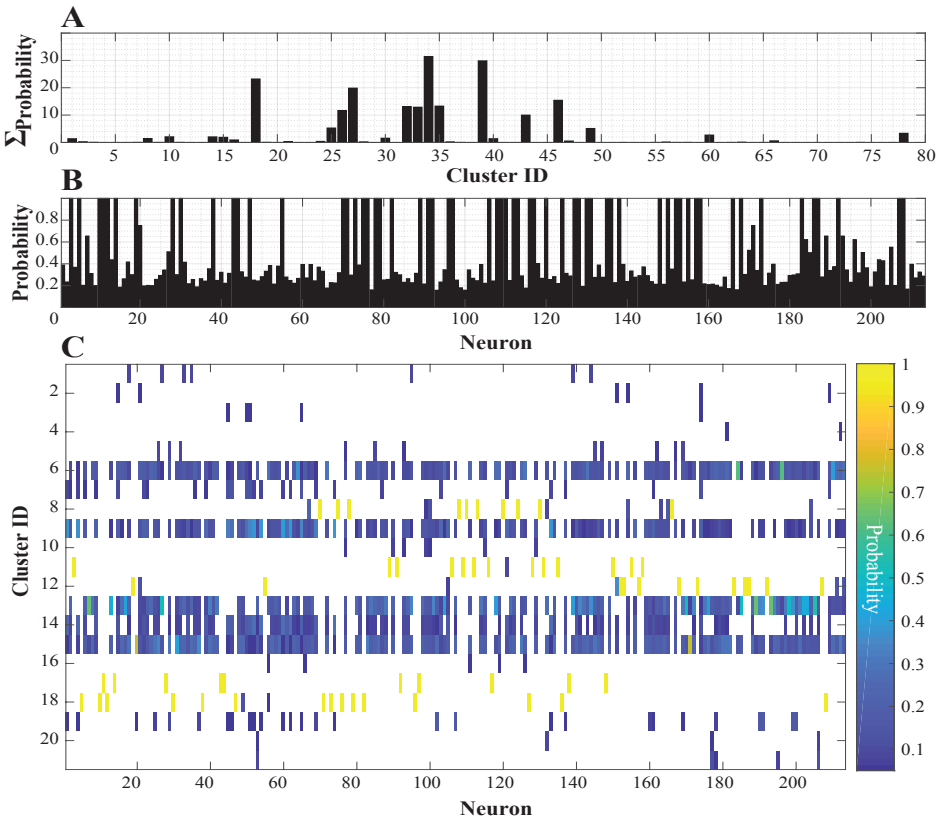

Figure 2. Clustering in high-dimensional feature space is a probabilistic approach to cell-type identification. **(A)** Sum of the probabilities of all the neurons to belong to a specific cluster. **(B)** The maximum probability for each neuron to belong to any cluster (indicative of certainty of cluster assignment). **(C)** The probability of each cell to be assigned to a specific cluster after the merging procedure, counted after 20000 mergings iterations.

Clustering performance can be improved by either reducing the dimensionality of the feature space or by increasing the sampling size (i.e. number of neurons) to minimize the distance between the members of a given cluster while increasing the inter-cluster distance. Given the 213 neurons available in this dataset, we opted to reduce the dimensionality of the feature space.

To estimate the minimum number of features required to describe the data, we computed the dimensionality of the dataset based on the eigenvalues of the covariance matrix (see Materials and Methods for details), which showed that a minimum of 15 features is required to maximally reconstruct the data defined in 139 dimensions. To identify these features

we computed the pairwise Pearson correlation across all variables. The correlation matrix (Figure 3A) showed that 12 subsets of features are highly correlated. Using an empirically determined threshold of 0.6, we identified "weakly" correlated parameters (N=35; see Supplemental Table 1) and repeated the neuronal clustering in this lower-dimensional feature space. The 213 neurons were grouped into 10 clusters (Figure 3B) that are well separated from one another (Figure 3C).

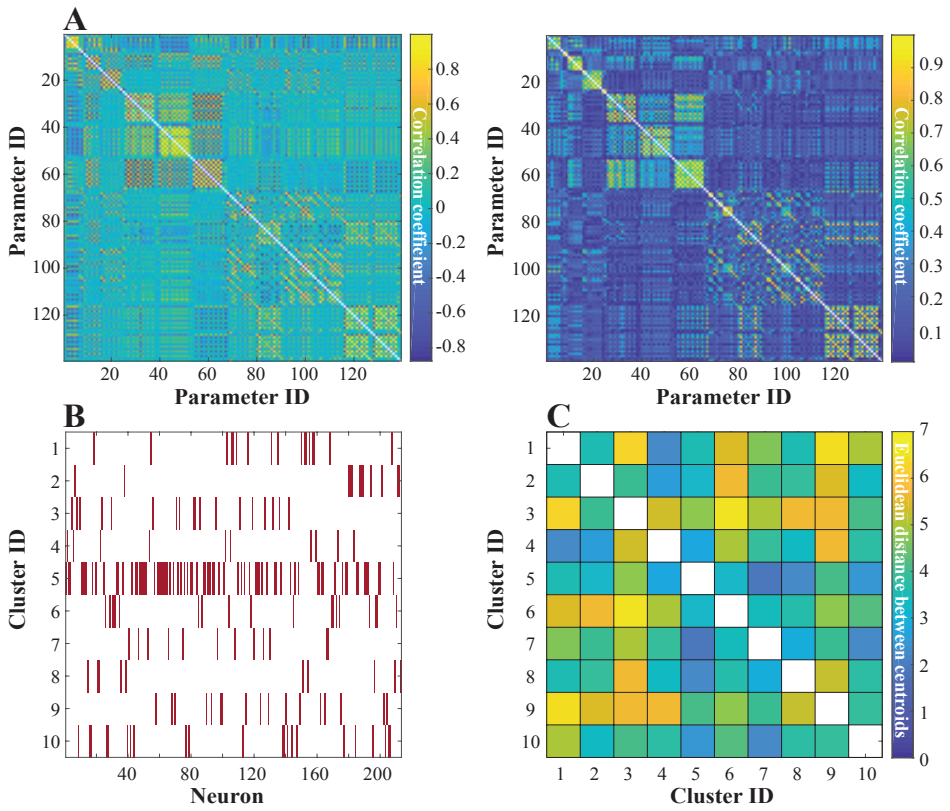

Figure 3. Dimensionality reduction in the feature space and neuronal clustering in a lower dimension. (A) The pairwise correlation coefficient between all 139 variables represented as a matrix. Left: Bidirectional correlation coefficient. Right: The correlation matrix on an absolute scale. **(B)** The distribution of the neurons across 10 clusters identified after clustering using 35 spike features. **(C)** The pairwise Euclidean distance between the cluster centroids after standardization.

The 35 features used for clustering is still significantly larger than the theoretical minimum number of features (i.e. 15) required to describe this dataset. To rank the relevant contribution of each feature to the clustering performance we have repeated clustering using only 5

features at a time in a combinatorial space. Across the 324632 combinations, all informative features are the variables which approximate the cell behavior across current injection steps (Figure 4A).

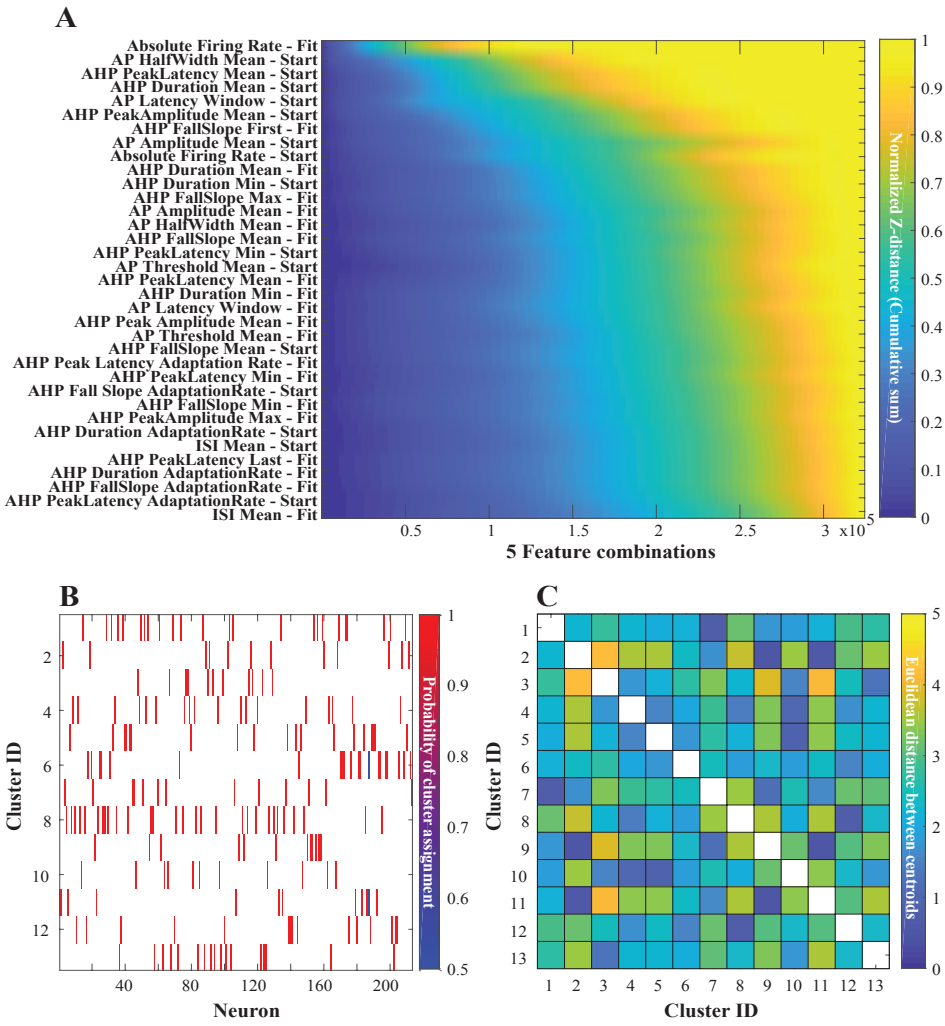

Figure 4. Ranking features for their contribution to cluster separation and clustering with 5 most informative features. We considered every possible combination of 5 parameters, in the 35 remaining after the correlation analysis. We computed new cluster assignments, using the method described before, but in the 35-parameter space, next we computed the Z-distance between the clusters in the space that is given by the projection on each of these 5-parameter subspaces. The combination of 5 parameters that results in the highest average Z-distance between clusters is considered to be the most informative. **(A)** Ranked order of features, computed by counting the appearance of each one, in the 5 parameters combinations, ordered by their averaged Z-distance. **(B)** Neurons were

sorted into 13 clusters. **(C)** The pairwise Euclidean distance between the cluster centroids.

To quantify the clustering performance with a subset of features, we repeated the clustering one final time but with five features (i.e. slope of the linear fit of the Absolute Firing Rate and Maximum AHP Peak Amplitude, the onset values of AP Latency Window, AP HalfWidth Mean and AHP Peak Latency Mean). The results showed that except for one neuron (appears in blue in Figure 4B), all neurons had a unique cluster identity, suggesting that in the 5 dimensional space neurons can still be grouped with high-confidence into well-separated clusters (Figure 4C).

Neuronal electrical identity depends on the somatic depolarization amplitude

The feature space that best predicts the clustering performance, i.e. most informative feature combination, exclusively includes variables that are analytical descriptions of the adaptive changes observed in spiking across somatic (membrane) depolarization states (Figure 4A). This observation suggests that the separation between clusters might depend on stimulus amplitude. Because voltage-gated conductances help maintain membrane depolarization, ensure repolarization and contribute to the action potential generation, a sustained depolarization of the membrane potential might change the electrical signature of the neuron [29–31]. Therefore, to quantify the discriminability of the clusters across the discrete somatic depolarization states, we calculated the average pairwise Z-distance between clusters (Figure 5).

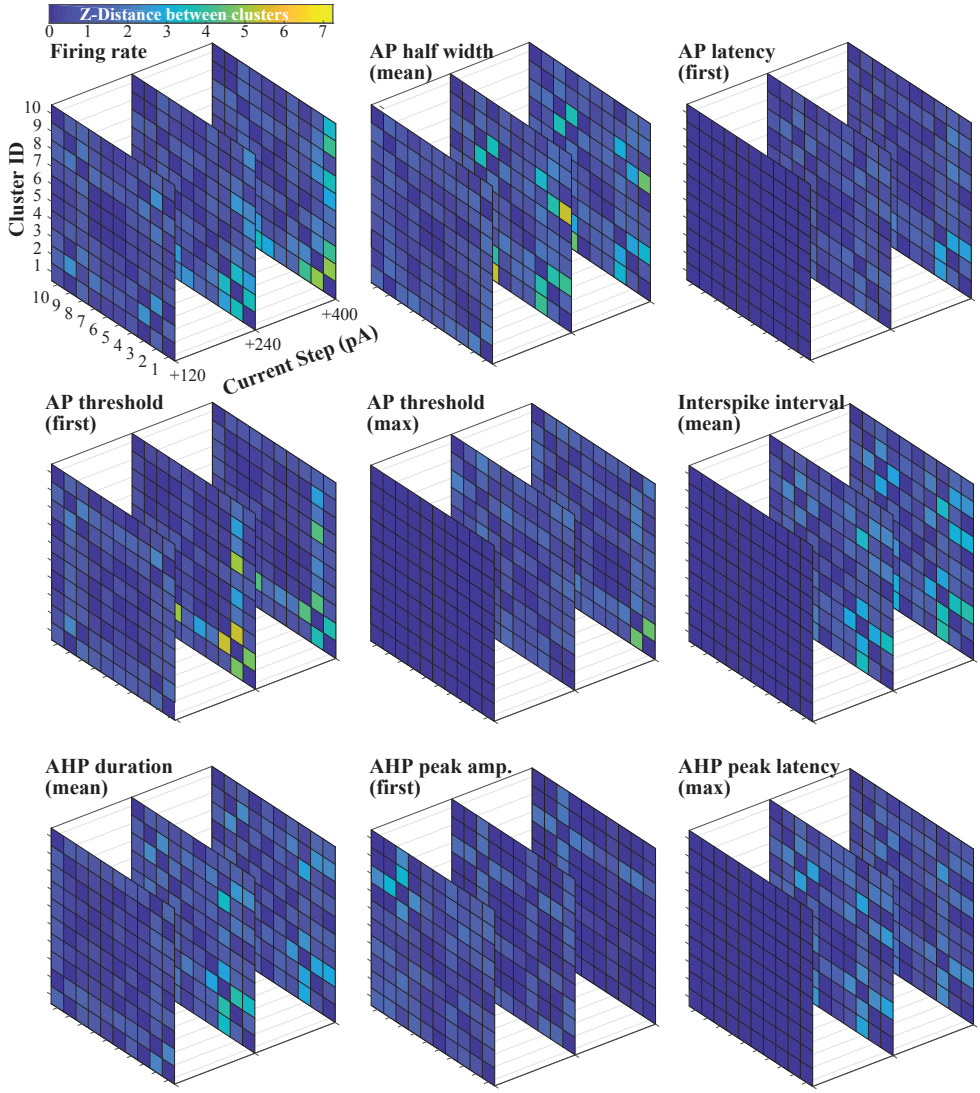

Figure 5. Cluster separation varies with membrane polarization state. The Z-distance between clusters were calculated across all clusters and across stimulus amplitude. Nine representative features and the degree of separation between clusters are shown.

The results show that the cluster separation varies with the membrane potential such that in those feature spaces based on spike timing and its derivatives, the cluster separation

gradually improves as the amplitude of somatic current injection is increased. Spike threshold and firing rate across somatic depolarization states distinguish a non-overlapping subset of clusters which differentially adapt to the changes in the membrane states. The duration, amplitude, and latency of the after-spike hyperpolarization (AHP) are all regulated, expectedly, across the different membrane potentials; while the suppression of the AHP peak amplitude in more depolarized membrane states results in better discriminability of the clusters during weak somatic depolarization; both the peak latency and the duration of the AHP contribute to better cluster separation in more depolarized membrane states. These results argue that the electrical signature of neurons, hence the performance of clustering based on the spiking dynamics of neurons, varies across the membrane states.

Neuronal classes in the adult primary somatosensory cortex in layers 2/3

To identify the functional classes of adult cortical neurons in the supragranular layers of the primary somatosensory cortex, we have deployed the hierarchical clustering described above and assigned each neuron to a cluster. Ten clusters contained 10 or more units. To systematically compare the changes in the spiking responses across the membrane states, we described the electrical responses to somatic current injections using features that are among the most informative dimensions for clustering.

As previously shown [14,19,20,32], binary classification of putative excitatory (regularly spiking) and putative inhibitory (fast-spiking) neurons can be achieved using firing rate/inter-spike interval, action potential half-width, or any combination thereof (Figure 6). The amplitude of the afterhyperpolarization (AHP) peak allows further classification of the putative inhibitory neurons into three sub-classes based on the rate adaptation upon somatic depolarization (Figure 6). Although all three sub-classes have a comparable AHP duration, which is shorter than that of all putative excitatory neurons, and quickly reach the peak latency during membrane repolarization, their AHP amplitude follows a gradient and is not suppressed considerably with the increased depolarization of the membrane (Figure 6).

In terms of the molecular and biochemical complexity, inhibitory neurons are significantly more diverse than their excitatory counterparts [6,9,10,14,15]. Electrophysiologically, however, our findings now indicate that excitatory neurons are more diverse. Seven of the ten clusters generate action potentials at lower rates than putative inhibitory neurons, and the AP width is at least twice as large as that of inhibitory neurons. The significant variability among excitatory neurons' spiking patterns (Figure 6) might be attributed to the properties (i.e. subchannel composition), density and distribution of voltage-gated sodium and potassium channels (e.g. in the case of action potential half-width, action potential latency, action potential threshold), the adaptive changes in voltage-gated conductances across depolarization states (resulting in

action potential threshold variation) or differences in the membrane integration time constant (e.g. interspike interval). This variability between the putative excitatory neurons might also be due to anatomical or experience-dependent changes across cortical neurons. Independent from the underlying cause, these results argue that adult excitatory neurons are more diverse than the inhibitory neurons in the primary somatosensory cortex.

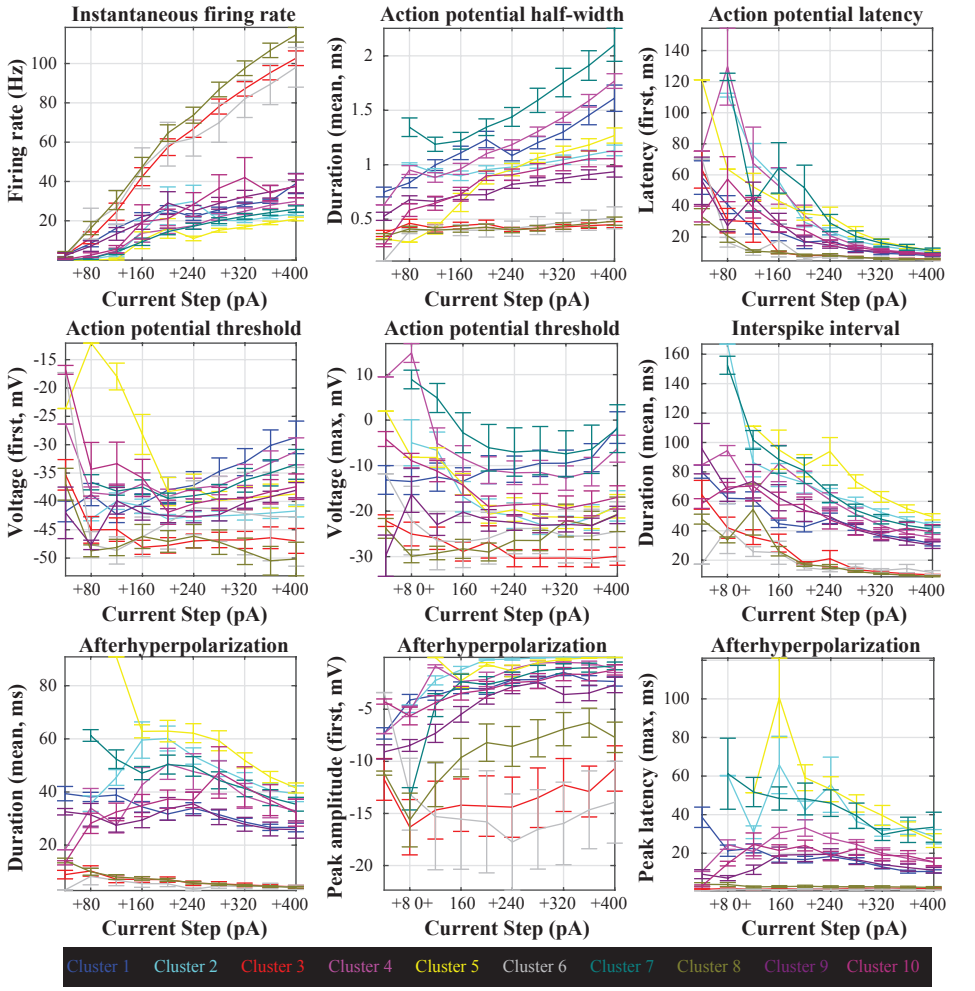

Figure 6. Spiking characteristics of identified clusters in the primary somatosensory cortex of the adult mouse. All data is from the cortical layers 2/3 of the barrel cortex. Clusters 3,6,8 are putatively inhibitory.

Discussion

The responses of (cortical) neurons are shaped by both their intrinsic biophysical properties and their position and connectivity in the network [33–35]. During development, but also throughout the adult life of an animal, several mechanisms including homeostatic and neural plasticity mechanisms constantly update the neuron's properties in order for the neuron to be able to function properly. These changing properties include its biophysical properties (i.e. what ion channels and receptors are expressed in the membrane and in what quantities, see for instance [36]), its connectivity (i.e. to what neurons it is connected and how strongly) as well as its morphology. Therefore, we expect that structural and functional correlations between neurons [18,37,38] results in neural properties that group together so that the cell can perform its functions, corresponding to 'neural cell classes'. Here we described such a grouping of neurons, as we identify three putative inhibitory and seven putative excitatory cell classes in the cortical layers 2/3 of the adult primary somatosensory cortex.

Neurons in a cluster can plausibly adopt different strategies in order to perform certain functions [39,40], resulting in gradual differences between neurons rather than well-separated 'clusters' of properties as we observed among the excitatory neurons (also see [41]). Finding the neural properties that group together, i.e. 'clustering' our high-dimensional dataset, is a non-trivial task, where the experimenter necessarily has to make non-obvious choices about which clustering method to use and how to set the meta-parameters of the clustering algorithm. Often, the 'ground-truth' is not known, so it is difficult to assess the quality of the chosen method. Therefore, it is important to choose the method with some knowledge of the dataset [42]. For instance, because of the continuous nature of our data, clustering methods purely based on distance, such as tSNE [43], do not perform well. An extra difficulty in our dataset is that it is large for an in vitro dataset, but relatively small in relation to the number of dimensions. Therefore, we chose a combination of a simple but well understood and easy to interpret automatic method (k-means clustering) together with a method that was specific for this dataset (merging small clusters until each cluster had at least 10). This approach allowed us to perform clustering in a lower dimensional space, i.e. by considering less number of features. Repeating the clustering in a larger dataset, when it becomes available, will help to identify those neuronal clusters that are sparsely populated in our iteration of the clustering.

Even though the high-dimensional clustering of cell properties gives many insights on its own, it is not always feasible in an experimental setup to measure so many cellular properties. Therefore, we asked: 'How can we minimize the number of measured cell properties, and still perform a cluster analysis with the same results as the high-dimensional clustering?'. For this, we had to perform dimensionality reduction. With the recent improvement of high-dimensional recording techniques, dimensionality reduction methods

beyond ‘simple’ principal component analysis have moved into the spotlight. Even though these types of analysis are mostly used for population recordings [44,45], the same steps apply for high-dimensional in vitro single-cell data. The first step is looking into the ‘underlying’ dimensionality of the dataset: one should check that even though a (typically large) dataset is high-dimensional, the underlying principles are probably low-dimensional, allowing for a low-dimensional description. We showed here through the dimensionality calculation (see Materials and Methods) and the correlations between the measured parameters in our dataset that a lower-dimensional representation should be possible (Figure 3). The second step is to identify informative and less informative dimensions (Figure 4). Finally, one should perform a check on the dimensionality reduction: does the representation in low-dimensional space yield the same properties as in the high-dimensional space? Here we performed our clustering analysis both on the high- and low-dimensional representations of our data, and showed that neurons are classified into well separated clusters before and after the dimensionality reduction (see Figure 3 vs 4). Thus, the clustering approach presented herein is unlikely to be biased by the sampling size or the number of features used for the classification. Future application of this clustering approach in neurons recorded across brain regions and developmental periods will help to address whether these cell classes are universal. Using these identified cell classes and their response properties in computational network models will help to develop more advanced, biologically realistic networks, starting with a model of the somatosensory cortex of the rodents.

Supplementary materials

Supplemental Table 1. Principal features of action potentials. Each quantity is measured over increasing current injections step. For each quantity (with the exception of the 1st, which has only a single scalar value) both the starting value as well as the slope of the linear fit over the current injections are used as parameters (for a total of 139 parameters). AP = action potential; AHP = afterhyperpolarization current; ISI: interspike interval. The 35 parameters that were selected after the correlation analysis are in italics.

1	Current necessary for 1st AP [pA]	the lowest current step at which the cell fired an AP [pA]
2	AP count	the number of APs fired through the stimulation
3	*Absolute FR* [Hz]	the number of APs divided by the stimulus duration
4	Instantaneous FR [Hz]	the instantaneous firing rate over the stimulation
5	AP Latency of 1st spike [ms]	the time interval between the start of the stimulation and the 1st AP generated.
6	AP Latency of last spike [ms]	the time interval between the start of the stimulation and the last AP generated.
7	*AP Latency of window* [ms]	the time interval between first and last AP generated
8	AP Latency compression	onset latency between the first and last spikes, divided by the stimulus length
9	ISI minimum [ms]	the minimum ISI between 2 consecutive APs over the stimulation
10	ISI maximum [ms]	the maximum ISI between 2 consecutive APs over the stimulation
11	*ISI mean* [ms]	the mean ISI between 2 consecutive APs over the stimulation
12	ISI median [ms]	the median ISI between 2 consecutive APs over the stimulation
13	ISI adaptation rate [%]	(First ISI - Last ISI) / First ISI
14	AP Threshold of 1st spike [mV]	the threshold at which the 1st AP of the AP train is generated, computed as the peak of the 2nd derivative of the membrane potential.
15	AP Threshold of last spike [mV]	the threshold at which the last AP of the AP train is generated, computed as the peak of the 2nd derivative of the membrane potential.
16	AP Threshold minimum [mV]	the minimum threshold at which an AP is generated during the AP train, computed as the peak of the 2nd derivative of the membrane potential.
17	AP Threshold maximum [mV]	the maximum threshold at which an AP is generated during the AP train, computed as the peak of the 2nd derivative of the membrane potential.
18	*AP Threshold mean* [mV]	the mean threshold at which an AP is generated during the AP train, computed as the peak of the 2nd derivative of the membrane potential.

19	AP Threshold median [mV]	the median threshold at which an AP is generated during the AP train, computed as the peak of the 2nd derivative of the membrane potential.
20	AP Threshold adaptation rate [%]	(First AP Threshold - Last AP Threshold)/ First AP Threshold
21	AP Half-Width of 1st spike [ms]	the width of the 1st AP at half height
22	AP Half-Width of last spike [ms]	the width of the last AP at half height
23	AP Half-Width minimum [ms]	the minimum half-width of the whole AP train
24	AP Half-Width maximum [ms]	the maximum half-width of the whole AP train
25	*AP Half-Width mean* [ms]	the mean half-width of the whole AP train
26	AP Half-Width median [ms]	the median half-width of the whole AP train
27	AP Half-Width adaptation rate [%]	(First AP Half-Width- Last AP Half-Width)/ First AP Half-Width
28	AP Amplitude of 1st spike [mV]	the amplitude of the 1st AP of the AP train, computed as |max - baseline|
29	AP Amplitude of last spike [mV]	the amplitude of the last AP of the AP train, computed as |max - baseline|
30	AP Amplitude minimum [mV]	the minimum amplitude of the whole AP train, computed as |max - baseline|
31	AP Amplitude maximum [mV]	the maximum amplitude of the whole AP train, computed as |max - baseline|
32	*AP Amplitude mean* [mV]	the mean amplitude of the whole AP train, computed as |max - baseline|
33	AP Amplitude median [mV]	the median amplitude of the whole AP train, computed as |max - baseline|
34	AP Amplitude of adaptation rate [%]	(First AP Amplitude - Last AP Amplitude)/ First AP Amplitude
35	AHP Peak Latency of 1st spike [ms]	the time interval between the return to baseline of the voltage after the 1st AP of the APs train, and its corresponding AHP peak.
36	*AHP Peak Latency of last spike* [ms]	the time interval between the return to baseline of the voltage after the last AP of the APs train, and its corresponding AHP peak.
37	*AHP Peak Latency minimum* [ms]	the minimum time interval between the return to baseline of the voltage after the APs of the APs train, and its corresponding AHP peak.
38	AHP Peak Latency maximum [ms]	the maximum time interval between the return to baseline of the voltage after the APs of the APs train, and its corresponding AHP peak.
39	*AHP Peak Latency mean* [ms]	the maximum time interval between the return to baseline of the voltage after the APs of the APs train, and its corresponding AHP peak.
40	*AHP Peak Latency adaptation rate* [%]	(First AHP Peak Latency - Last AHP Peak Latency)/ First AHP Peak Latency

41	AHP Peak Amplitude of 1st spike [mV]	the difference between the peak of the AHP corresponding to the 1st AP of the APs train, and the baseline membrane potential.
42	AHP Peak Amplitude of last spike [mV]	the difference between the peak of the AHP corresponding to the last AP of the APs train, and the baseline membrane potential.
43	AHP Peak Amplitude minimum [mV]	the minimum difference between the peak of the AHP corresponding to the APs of the APs train, and the baseline membrane potential.
44	*AHP Peak Amplitude maximum* [mV]	the maximum difference between the peak of the AHP corresponding to the APs of the APs train, and the baseline membrane potential.
45	*AHP Peak Amplitude mean* [mV]	the mean difference between the peak of the AHP corresponding to the APs of the APs train, and the baseline membrane potential.
46	AHP Peak Amplitude adaptation rate [%]	(First AHP Amplitude - Last AHP Amplitude)/ First AHP Amplitude
47	AHP Duration of 1st spike [ms]	the time interval between the point where the membrane potential reaches baseline value, after an AP, and when it reaches baseline value, after the corresponding AHP, measured for the 1st AP of the APs train.
48	AHP Duration of last spike [ms]	the time interval between the point where the membrane potential reaches baseline value, after an AP, and when it reaches baseline value, after the corresponding AHP, measured for the last AP of the APs train.
49	*AHP Duration minimum* [ms]	the minimal time interval between the point where the membrane potential reaches baseline value, after an AP, and when it reaches baseline value, after the corresponding AHP, for the whole APs train.
50	AHP Duration maximum [ms]	the maximum time interval between the point where the membrane potential reaches baseline value, after an AP, and when it reaches baseline value, after the corresponding AHP, for the whole APs train.
51	*AHP Duration mean* [ms]	the mean time interval between the point where the membrane potential reaches baseline value, after an AP, and when it reaches baseline value, after the corresponding AHP, for the whole APs train.
52	*AHP Duration adaptation rate* [%]	(First AHP Duration - Last AHP Duration)/ First AHP Duration
53	AHP Integral of 1st spike [ms*mV]	the integral of the AHP of the 1st AP in the APs train.
54	AHP Integral of last spike [ms*mV]	the integral of the AHP of the last AP in the APs train.
55	AHP Integral minimum [ms*mV]	the minimum integral of the AHP of the APs train.
56	AHP Integral maximum [ms*mV]	the maximum integral of the AHP of the APs train.
57	AHP Integral mean [ms*mV]	the mean integral of the AHP of the APs train.

58	AHP Integral adaptation rate [%]	(First AHP Integral - Last AHP Integral)/ First AHP Integral
59	*AHP Fall Slope of 1st spike* [mV/ms]	the slope of the decay phase of the AHP of the 1st AP in the APs train.
60	AHP Fall Slope of last spike [mV/ms]	the slope of the decay phase of the AHP of the last AP in the APs train.
61	*AHP Fall Slope minimum* [mV/ms]	the minimum slope of the decay phase of the AHP of the APs train.
62	*AHP Fall Slope maximum* [mV/ms]	the maximum slope of the decay phase of the AHP of the APs train.
63	*AHP Fall Slope mean* [mV/ms]	the mean slope of the decay phase of the AHP of the APs train.
64	*AHP Fall Slope adaptation rate* [%]	(First AHP Fall Slope - Last AHP Fall Slope)/ First AHP Fall Slope
65	AHP Rise Slope of 1st spike [mV/ms]	the slope of the rising phase of the AHP of the 1st AP in the APs train.
66	AHP Rise Slope of last spike [mV/ms]	the slope of the rising phase of the AHP of the last AP in the APs train.
67	AHP Rise Slope minimum [mV/ms]	the minimum slope of the rising phase of the AHP of the APs train.
68	AHP Rise Slope maximum [mV/ms]	the maximum slope of the rising phase of the AHP of the APs train.
69	AHP Rise Slope mean [mV/ms]	the mean slope of the rising phase of the AHP of the APs train.
70	AHP Rise Slope adaptation rate [%]	(First AHP Rise Slope - Last AHP Rise Slope)/ First AHP Rise Slope

Bibliography

1. Ahissar, E., Sosnik, R., Bagdasarian, K. & Haidarliu, S. Temporal frequency of whisker movement. II. Laminar organization of cortical representations. *J. Neurophysiol.* **86,** 354–367 (2001).
2. Kim, U. & Ebner, F. F. Barrels and septa: separate circuits in rat barrels field cortex. *J. Comp. Neurol.* **408,** 489–505 (1999).
3. Azarfar, A., Calcini, N., Huang, C., Zeldenrust, F. & Celikel, T. Neural coding: A single neuron's perspective. *Neurosci. Biobehav. Rev.* (2018). doi:10.1016/j.neubiorev.2018.09.007
4. Kole, K., Scheenen, W., Tiesinga, P. & Celikel, T. Cellular diversity of the somatosensory cortical map plasticity. *Neurosci. Biobehav. Rev.* **84,** 100–115 (2018).
5. Yu, C., Derdikman, D., Haidarliu, S. & Ahissar, E. Parallel thalamic pathways for whisking and touch signals in the rat. *PLoS Biol.* **4,** e124 (2006).
6. Markram, H. *et al.* Interneurons of the neocortical inhibitory system. *Nat. Rev. Neurosci.* **5,** 793–807 (2004).
7. Tremblay, R., Lee, S. & Rudy, B. Gabaergic interneurons in the neocortex: from cellular properties to circuits. *Neuron* **91,** 260–292 (2016).
8. Sharpee, T. O. Toward functional classification of neuronal types. *Neuron* **83,** 1329–1334 (2014).
9. Luo, L., Callaway, E. M. & Svoboda, K. Genetic dissection of neural circuits: A decade of progress. *Neuron* **98,** 256–281 (2018).
10. Zeng, H. & Sanes, J. R. Neuronal cell-type classification: challenges, opportunities and the path forward. *Nat. Rev. Neurosci.* **18,** 530–546 (2017).
11. Poulin, J.-F., Tasic, B., Hjerling-Leffler, J., Trimarchi, J. M. & Awatramani, R. Disentangling neural cell diversity using single-cell transcriptomics. *Nat. Neurosci.* **19,** 1131–1141 (2016).
12. Feldmeyer, D., Qi, G., Emmenegger, V. & Staiger, J. F. Inhibitory interneurons and their circuit motifs in the many layers of the barrel cortex. *Neuroscience* **368,** 132–151 (2018).
13. Wang, Y., Ye, M., Kuang, X., Li, Y. & Hu, S. A Simplified Morphological Classification Scheme for Pyramidal Cells in Six Layers of Primary Somatosensory Cortex of Juvenile rats. *IBRO Rep.* (2018). doi:10.1016/j.ibror.2018.10.001
14. Petilla Interneuron Nomenclature Group *et al.* Petilla terminology: nomenclature of features of GABAergic interneurons of the cerebral cortex. *Nat. Rev. Neurosci.* **9,** 557–568 (2008).
15. Johnson, M. B. & Walsh, C. A. Cerebral cortical neuron diversity and development at single-cell resolution. *Curr. Opin. Neurobiol.* **42,** 9–16 (2017).
16. Connors, B. W. & Gutnick, M. J. Intrinsic firing patterns of diverse neocortical neurons. *Trends Neurosci.* **13,** 99–104 (1990).
17. Nowak, L. G., Azouz, R., Sanchez-Vives, M. V., Gray, C. M. & McCormick, D. A. Electrophysiological classes of cat primary visual cortical neurons in vivo as revealed by quantitative analyses. *J. Neurophysiol.* **89,** 1541–1566 (2003).
18. Somogyi, P. & Klausberger, T. Defined types of cortical interneurone structure space and spike timing in the hippocampus. *J Physiol (Lond)* **562,** 9–26 (2005).
19. Druckmann, S., Hill, S., Schürmann, F., Markram, H. & Segev, I. A hierarchical structure of cortical interneuron electrical diversity revealed by automated statistical analysis. *Cereb. Cortex* **23,** 2994–3006 (2013).
20. Armañanzas, R. & Ascoli, G. A. Towards the automatic classification of neurons. *Trends Neurosci.* **38,** 307–318

(2015).

21. Deitcher, Y. *et al.* Comprehensive Morpho-Electrotonic Analysis Shows 2 Distinct Classes of L2 and L3 Pyramidal Neurons in Human Temporal Cortex. *Cereb. Cortex* **27,** 5398–5414 (2017).
22. Kole, K. & Celikel, T. Neocortical microdissection at columnar and laminar resolution for molecular interrogation. *Curr. Protoc. Neurosci.* e55 (2018). doi:10.1002/cpns.55
23. Celikel, T., Szostak, V. A. & Feldman, D. E. Modulation of spike timing by sensory deprivation during induction of cortical map plasticity. *Nat. Neurosci.* **7,** 534–541 (2004).
24. Blanton, M. G., Lo Turco, J. J. & Kriegstein, A. R. Whole cell recording from neurons in slices of reptilian and mammalian cerebral cortex. *J. Neurosci. Methods* **30,** 203–210 (1989).
25. Margrie, T. W., Brecht, M. & Sakmann, B. In vivo, low-resistance, whole-cell recordings from neurons in the anaesthetized and awake mammalian brain. *Pflugers Arch.* **444,** 491–498 (2002).
26. Gao, P. *et al.* A theory of multineuronal dimensionality, dynamics and measurement. *BioRxiv* (2017). doi:10.1101/214262
27. Lloyd, S. Least squares quantization in PCM. *IEEE Trans. Inform. Theory* **28,** 129–137 (1982).
28. Castro, R. M., Coates, M. J. & Nowak, R. D. Likelihood based hierarchical clustering. *IEEE Trans. Signal Process.* **52,** 2308–2321 (2004).
29. Tomaselli, G. F. & Farinelli, F. Nav channels: assaying biosynthesis, trafficking, function. *Methods Mol. Biol.* **1722,** 167–184 (2018).
30. Wang, J., Ou, S.-W. & Wang, Y.-J. Distribution and function of voltage-gated sodium channels in the nervous system. *Channels (Austin)* **11,** 534–554 (2017).
31. Greene, D. L. & Hoshi, N. Modulation of Kv7 channels and excitability in the brain. *Cell. Mol. Life Sci.* **74,** 495–508 (2017).
32. Tripathy, S. J., Burton, S. D., Geramita, M., Gerkin, R. C. & Urban, N. N. Brain-wide analysis of electrophysiological diversity yields novel categorization of mammalian neuron types. *J. Neurophysiol.* **113,** 3474–3489 (2015).
33. Harris, K. D. & Mrsic-Flogel, T. D. Cortical connectivity and sensory coding. *Nature* **503,** 51–58 (2013).
34. Ko, H. *et al.* The emergence of functional microcircuits in visual cortex. *Nature* **496,** 96–100 (2013).
35. Ko, H. *et al.* Functional specificity of local synaptic connections in neocortical networks. *Nature* **473,** 87–91 (2011).
36. Taylor, A. L., Hickey, T. J., Prinz, A. A. & Marder, E. Structure and visualization of high-dimensional conductance spaces. *J. Neurophysiol.* **96,** 891–905 (2006).
37. Jinno, S. *et al.* Neuronal diversity in GABAergic long-range projections from the hippocampus. *J. Neurosci.* **27,** 8790–8804 (2007).
38. Tukker, J. J., Fuentealba, P., Hartwich, K., Somogyi, P. & Klausberger, T. Cell type-specific tuning of hippocampal interneuron firing during gamma oscillations in vivo. *J. Neurosci.* **27,** 8184–8189 (2007).
39. Golowasch, J., Goldman, M. S., Abbott, L. F. & Marder, E. Failure of averaging in the construction of a conductance-based neuron model. *J. Neurophysiol.* **87,** 1129–1131 (2002).
40. Swensen, A. M. & Bean, B. P. Robustness of burst firing in dissociated purkinje neurons with acute or long-term reductions in sodium conductance. *J. Neurosci.* **25,** 3509–3520 (2005).
41. Marder, E. & Goaillard, J.-M. Variability, compensation and homeostasis in neuron and network function. *Nat. Rev. Neurosci.* **7,** 563–574 (2006).
42. von Luxburg, U., Williamson, R. C. & Guyon, I. Clustering: Science or Art. in **27,** 65–79 (JMLR, 2012).

43. van der Maaten, L. J. P. & Hinton, G. E. Visualizing High-Dimensional Data Using t-SNE. *J Mach Learn Res* **9,** 2579–2605 (2008).
44. Cunningham, J. P. & Yu, B. M. Dimensionality reduction for large-scale neural recordings. *Nat. Neurosci.* **17,** 1500–1509 (2014).
45. Gao, P. & Ganguli, S. On simplicity and complexity in the brave new world of large-scale neuroscience. *Curr. Opin. Neurobiol.* **32,** 148–155 (2015).

Chapter 4

Activity dependent transcriptional regulation of the dopaminergic signaling in the somatosensory cortex

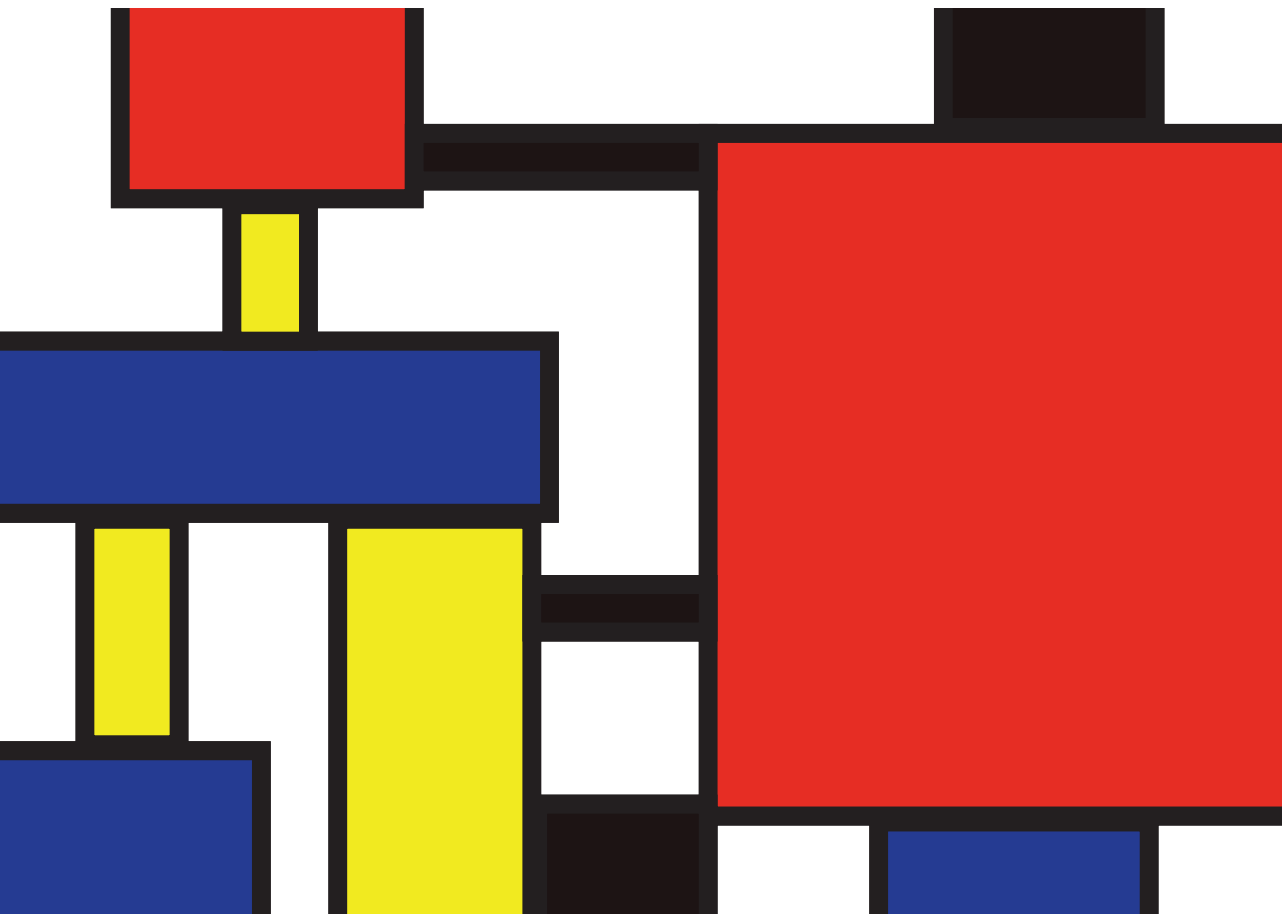

Dopamine is a principal neuromodulator that contributes to various brain functions ranging from motor planning, coordination and execution to processing of reward and sensory stimulus. Whether dopaminergic signaling in sensory cortices is regulated by sensory experience is unknown. Here we addressed this question in the adult mouse primary somatosensory cortex by performing RNA sequencing in cortical columnar and laminae resolution after animals' sensory experience was controlled with bilateral single row whisker deprivation. The results showed that gene transcription in the dopaminergic signaling pathway (DSP) undergoes experience-dependent plasticity both in granular and supragranular layers. Sensory experience and sensory deprivation compete for the regulation of DSP transcription across the neighboring cortical columns, and that sensory deprivation induced changes in DSP signaling are topographically constrained. These results argue that dopaminergic drive originating from the midbrain dopaminergic neurons, targeting the sensory cortex, is subject to experience-dependent regulation and might contribute to the sensory deficits observed after dopaminergic cell loss in Parkinson patients.

Dopamine is a monoaminergic neurotransmitter that contributes to processing of sensory, motor, emotional states and higher cognitive functions 1–5. Dysfunctions of the dopaminergic synthesis and release are associated with various disorders that impair sensory processing, e.g. aggression and violence 6 , Parkinson's Disease 7, addiction 8, attention deficit hyperactivity disorder 9,10.

Although how dopamine alters sensory processing is yet to be mechanistically understood, recent experiments 11 in the monkey prefrontal cortex showed that local application of dopamine regulates the integration of sensory information. Considering that sensory information (experience) powerfully modulates neuronal excitability in the primary somatosensory cortex 12–15 which projects to midbrain nuclei that release dopamine 16,17 if the dopaminergic signaling in the sensory cortices is modulated by experience, this would create a powerful close-loop between dopaminergic signaling and sensory processing. Such a regulatory close-loop might be the mechanism behind sensory integration loss upon dopaminergic depletion 18.

With its columnar organization and topographic representations, the whisker system of the rodents is a widely studied model of sensory information processing and its plasticity by sensory experience 19,20. Previous studies showed that apomorphine injection increases proto-oncogene transcription in the striatum and the barrel cortex 21, suggesting that dopaminergic receptor activation can alter gene transcription in the somatosensory cortex. Surgical transection of the infraorbital nerve, disrupting the sensory flow from the periphery, results in elevated dopamine release in the barrel cortex 22, plausibly contributing to the experience-dependent reorganization of the cortex. Despite these observations, it is not yet known whether dopaminergic signaling in the barrel cortex is differentially altered upon sensory experience. Here we took advantage of the recently completed transcriptomic mapping of the barrel cortex 23 to study this question. After identifying the 187 genes in the dopaminergic signaling pathway (DSP), we addressed 1) whether transcription of the DSP is regulated across cortical layers in the absence of sensory deprivation, 2) does prolong (two-week long) sensory deprivation alter DSP in a cortical column and layer specific manner, 3) is there a competition between sensory experience and sensory deprivation in controlling DSP and 4) the topography of the experience-dependent changes in DSP signaling. The results showed that in the absence of whisker deprivation, DSP signaling is uniform and comparable across the supragranular and granular layers of the barrel cortex. Whisker deprivation systematically reduces DSP signaling across the laminae which dominate gene transcription even in the spared whiskers' cortical columns neighboring the deprived column. Experience-dependent changes in DSP signaling are specific topographic, albeit broad. These results are the first direct observation and systematic analysis of the dopaminergic signaling

pathway in any sensory cortices and argue that whisker deprivation controls neuronal activity beyond the sensorimotor axis in the brain.

Experimental Procedures

All experiments were performed in accordance with the Animal Ethics Committee of the Radboud University in Nijmegen, the Netherlands. The experimental procedures, including sensory deprivation [13,44,45], isolation of cortical columns and laminae [24], RNA isolation, quality control, and data validation [23] were as described. The RNAseq data is available for download [46] and can be searched and visualized online at barrelomics.science.ru.nl.

Animals

Wild-type female C57Bl6 mice (Charles River: Wilmington, Massachusetts, United States, stock number 000664; RRID:NCBITaxon_10090) were used for the experiments described herein. Animals (N=8; 4 mice/group) were randomly assigned to control and whisker deprivation groups 12 days after birth (P12). Experience-dependent plasticity was induced by whisker deprivation. Bilateral plucking of their C-row whiskers was performed under isoflurane anesthesia starting from P12, and repeated as necessary. Control animals were not plucked but anesthetized and handled similarly (sham plucked).

Slice preparation and sample collection

Slice preparation was performed as described [24] on P23-P24. In short, pups were anaesthetized using isoflurane and perfused with ice-cold carbogenated slicing medium (108 mM ChCl, 3 mM KCl, 26 mM NaHCO3, 1.25 mM NaH2PO4, 25 mM glucose, 1 mM CaCl2, 6 mM MgSO4, and 3 mM Na-pyruvate). Acute thalamocortical slices (thickness 400 μm) from each hemisphere were prepared as described before [12,13,24]. Slices were incubated in carbogenated artificial cerebrospinal fluid (ACSF) (120 mM NaCl, 3.5 mM KCl, 10 mM glucose, 2.5 mM CaCl2, 1.3 mM MgSO4, 25 mM NaHCO3, and 1.25 mM NaH2PO4) at 37°C for 30 minutes. After which they were gradually returned to room temperature prior to sample collection.

Cortical columns, A through E, were incised before granular layers (Layer, L, 4) and supragranular layers (L2/3) were isolated while the tissue was continuously perfused with carbogenated ACSF in room temperature as described [24]. Samples from columns A/E and B/D, which respectively correspond to the second- and first-order spared whiskers, were pooled. Thus giving 8 tissue clusters across two groups of animals (See Figure 1). Immediately after dissection, samples were snap-frozen in liquid nitrogen and stored at −80°C until further use. All tools that came into direct contact with brain tissue were treated using RNAseZap (Thermo Fisher Scientific: Waltham, Massachusetts, United States, #AM9780) in order to

minimize RNAse contamination.

RNA isolation and quality control

Details on the RNA sequencing was provided before [25]. In short, tissues were quickly dissolved in Qiazol (Qiagen: Hilden, Germany, #79306) before RNA isolation performed using the miRNeasy Mini kit (Qiagen: Hilden, Germany, #217004). After DNAse (Thermo Fisher Scientific: Waltham, Massachusetts, United States, #EN0521) treatment the tissue samples were cleaned using the RNeasy MinElute kit (Qiagen: Hilden, Germany, #74204) and subsequently stored at –80°C until further processing.

RNA sample integrity was determined using Agilent Tapestation (Agilent: Santa Clara, USA, High Sensitivity RNA Screentape, #5067-5581). All samples had an RNA integrity (RIN) value >7.1, range 7.1-8.8. To confirm cDNA production and to ensure that a large (~1000 bp) amplicon could be obtained from the samples reverse transcription polymerase chain reaction (RT-PCR) was performed. cDNA was produced using SuperScript II Reverse Transcriptase (Thermo Fisher Scientific: Waltham, Massachusetts, United States, #18064014) with random hexamer primers (Roche: Basel, Switzerland, #11034731001). The resulting cDNA was then added to a PCR reaction mix, including Jumpstart Ready Mix (Sigma P2893) and exon-exon junction-spanning CamKII primers (FW TCCAACATTGTACGCCTCCAT; RV TGTTGGTGCTGTCGGAAGAT). From all cDNA samples, a fragment of the expected size could be amplified, suggesting that the RNA samples contained pure RNA of sufficient integrity.

RNA sequencing

RNA sequencing was conducted at the Genomics Core Facility of the EMBL, Heidelberg, Germany (RRID:SCR_004473) as detailed before 25. In short, the cDNA library was generated using the non-stranded NEBNext Ultra RNA Library Preparation Kit for Illumina (NEB: Ipswich, Massachusetts, United States, #E7530) via oligo-dT bead selection of mRNA. 13–14 PCR cycles were performed for library enrichment. Pooled libraries were sequenced on the Illumina: NextSeq 500 instrument (Illumina: San Diego, California, United States of America) (RRID:SCR_014983) in a 75-bp paired-end mode using high-output flow cells. The data is available for download 46 and can be explored online at barrelomics.science.ru.nl

Data validation and quality control

Sequencing read quality was assessed using FastQC (Babraham Bioinformatics: Babraham, England; RRID:SCR_014583), the results of which were merged using MultiQC (RRID:SCR_014982) as detailed in 25. Per base quality (phred) scores ranged from 34.80 to

35.15, indicating a base call accuracy better than >99.9% . Reads were mapped to the mm10 reference genome using STAR (RRID:SCR_005622), which uniquely mapped between 39-59 million reads.

The library preparation required a PCR enrichment step which might lead to overestimation of observed transcripts. Analysis of the read density, using Seqmonk (Babraham Bioinformatics: Babraham, England; RRID:SCR_001913), showed that a positive relation between read density and duplication levels and argued that the origin of read duplication is biological rather than technical.

Analysis of gene expression

To identify the genes in the dopaminergic signaling pathway (DSP), we performed a Mouse Genome Informatics gene ontology search at http://www.informatics.jax.org/vocab/gene_ontology/. DSP genes and their functional annotations are provided in Supplemental Table 1. The differential transcription analysis across experimental groups for the DSP genes was performed using transcript counts in MATLAB with custom written routines. Laminar analysis of the transcription was performed within each column across granular and supragranular layers. Within laminae analyses were performed across independent cortical columns. Statistical comparisons between groups were performed with two sample Kolmogorov-Smirnov test, ANOVA or paired t-test as noted. Hierarchical clustering of the expression data was performed using the *clustergram* function in MATLAB after normalizing the data within laminae across whisker deprivation conditions. See Figure legends for specific data handling procedures.

Results

To address whether dopaminergic signaling pathway undergoes experience-dependent regulation here we studied the transcriptome in the mouse primary somatosensory cortex in a columnar and laminar resolution. Animals were divided into two groups, Control vs Whisker Deprived (Figure 1A). Whisker deprived mice received bilateral C-row deprivation for two weeks; Control animals received sham plucking (see Experimental Procedures for details).

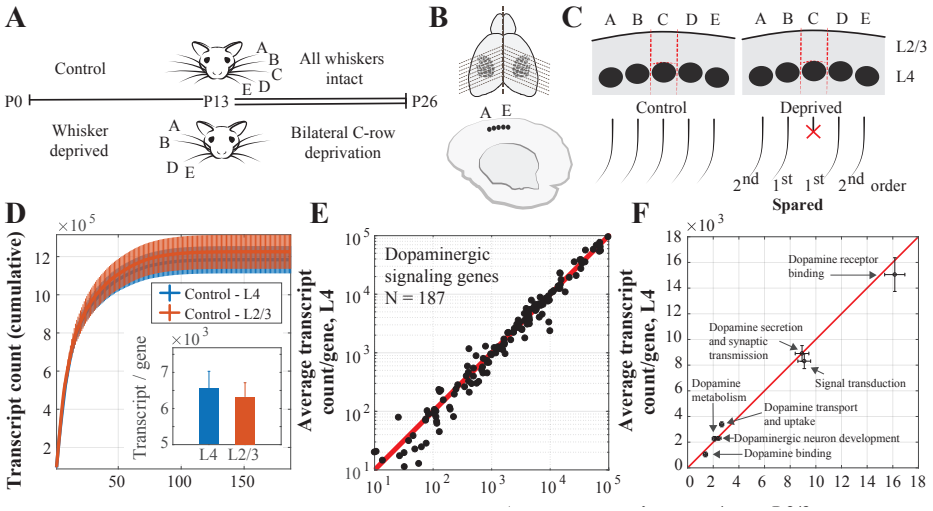

Figure 1. Genes in the Dopaminergic signaling pathway transcribe at comparable rates across layers in control animals. (A) The sensory deprivation protocol (N=4 mice/group). **(B)** Thalamocortical slices of the barrel cortex were prepared from each hemisphere. **(C)** Cortical columns and layers of interest were isolated as described before [24] prior to RNA sequencing. **(D)** Genes in the dopaminergic signaling pathway (DSP, see Supplemental Table 1) were identified via Mouse Genome Informatics gene ontology search. The transcription rate of DSP genes was comparable across layers (p=0.54; Kolmogorov-Smirnov test). Inset: Average number of transcript per gene (N=187) in DSP across granular (L4) and supragranular (L2/3) layers. **(E)** Comparison of gene transcription across layers. Each dot represents a gene in the DSP. Gene transcription did not significantly vary across layers (linear regression, $R^2_{adjusted}$= 0.96, p=0.76, t-test). **(F)** Comparison of gene transcription by function across layers (see Supplemental Table 1 for functional annotations for each gene). None of the pairwise comparisons across layers within functional gene-clusters were significant (0.24<p<0.97, t-test). RNAseq data, read alignments (BAM files), and raw read counts as determined by STAR aligner can be found online http://dx.doi.org/10.5524/100296. Detailed descriptions of the data acquisition, processing, quality control, and validation can be found at [25].

Transcription of the genes in Dopaminergic Signalling Pathway is not cortical laminae specific

Comparison of the transcription across the 187 genes which contribute to dopaminergic signaling (see Supplemental Table 1) across cortical layers (L) 4 and L2/3 showed that gene transcription is not differentially regulated across laminae (Figure 1D). Because there are not any dopaminergic neurons in the neocortex, and dopaminergic axons originating from midbrain nuclei project throughout the cortical layers [26], the observed molecular phenotype supports the existence of diffuse projections across cortical laminae in the juvenile mouse somatosensory cortex. Accordingly, pairwise comparison of the transcription for every

gene across the laminae showed that the transcriptional profile of DSP in the upper layers was predictive of one another (Figure 1E). Although gene transcription was differentially regulated across functional subgroups in the DSP, there was again no systematic change across laminae (Figure 1F).

Experience-dependent regulation of DSP

The transcriptome and proteome of the somatosensory cortex undergo experience-dependent regulation [19,23,27]. Given the extra cortical of origin of dopamine, many of the genes in the DSP are located presynaptically. If their transcription in the somatosensory cortex is regulated by experience, it will shed light onto the consequences of sensory deprivation in structures that are not traditionally considered as nuclei that undergo experience-dependent plasticity.

To address the role of sensory experience in DSP regulation we compared the transcriptome of the DSP within laminae across Control and Whisker Deprived animals. DSP signaling in L4 (Figure 2A) and L2/3 (Figure 2B) were significantly modulated upon sensory deprivation as the lack of sensory input resulted in transcriptional suppression for DSP genes in the primary somatosensory cortex. The pairwise comparison of the gene transcription after normalization of the transcript count (Figure 2C) confirmed these observations and also showed that, except a handful of the genes, the direction and relative change in gene transcription are linearly correlated across the cortical laminae.

To distinguish the laminar expression pattern of the differentially transcribed genes we spatially and functionally classified the DSP (Figure 2D). The results showed that L2/3 is transcriptionally richer. There are relatively more transcripts across all functional classes that are differentially regulated by experience in a layer-specific manner. The relative degree of changes across the functional clusters can be visualized using cluster distance metrics (Figure 2E) which shows genes in the dopaminergic transport and update, dopamine secretion and synaptic transmission, dopaminergic neuron development, and dopamine metabolism are the principal functional classes regulated by sensory experience.

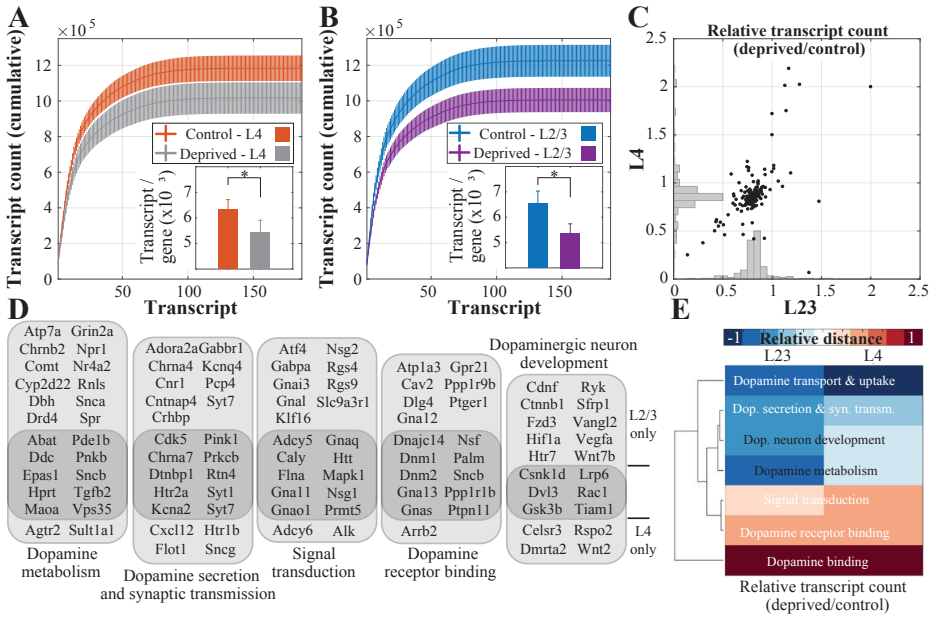

Figure 2. Transcriptional regulation of the Dopaminergic signaling pathway upon whisker deprivation. (A) Whisker deprivation suppresses gene transcription. Data from L4 of the C-columns from control (Control) and whisker deprived (Deprived) animals ($p<0.05$; Kolmogorov-Smirnov test). Inset: Average number of transcript per DSP gene across whisker deprivation conditions ($F(1,186)=12.1639$ $p<0.001$; ANOVA). **(B)** Whisker-deprivation induced suppression in Dopaminergic gene transcription in L2/3 ($p<0.05$; Kolmogorov-Smirnov test). Inset: Average transcript count ($F(1,186)=7.5088$ $p<0.001$; ANOVA). **(C)** Comparison of the relative change in gene transcription across cortical laminae. **(D)** Dopaminergic transcripts whose transcription is altered upon whisker deprivation grouped by simplified functional annotations. See Supplemental Tables 2 and 3 for the transcriptional data, results of the statistical analysis, and functional annotations based on MGI gene ontology. See Supplemental Table 4 for the laminar specificity of the transcriptional regulation for each differentially regulated gene upon whisker deprivation. Note that the intersection of the two rounded rectangles contains transcripts that are regulated by whisker deprivation both in L2/3 and L/4. **(E)** Clustergram shows the relative distance between functional groups in terms of the relative change in transcription upon whisker deprivation. Data is normalized within laminae across whisker deprivation conditions. Whisker deprivation significantly altered the transcription of genes responsible for dopamine secretion and synaptic transmission (L2/3: $p<0.01$; L4: $p=0.01$), dopaminergic neuron development (L2/3: $p<0.005$; L4: $p<0.005$), dopamine metabolism (L2/3: $p<0.001$; L4: $p<0.001$), signal transduction in the dopaminergic pathway (L2/3: $p<0.01$; L4: $p<0.001$) and dopamine receptor binding (L2/3: $p<0.005$; L4:$p<0.005$; All comparisons: t-test).

The competition between sensory experience and sensory deprivation for DSP regulation

Single row whisker deprivation results in synaptic competition in the barrel cortex. Although neurons in a given cortical column are primarily driven by a single whisker, contacts of the

first order neighboring whiskers are also represented by somatosensory neurons, due to broad, multi-whisker subthreshold representations [20,28]. Therefore in the deprived somatosensory cortex, neuronal activity in the first order spared whiskers' cortical columns is a product of the sensory input originating from their principal whisker as well as the adaptive (homeostatic) and long-term changes caused by sensory deprivation affecting their neighboring whisker [12–15,29–33]. To address whether DSP signaling is primarily driven by the sensory experience or deprivation, we compared the DSP transcriptome of the deprived (C) row column and the 1st order spared neighboring column. The transcription in L4 (Figure 3A) and L2/3 (Figure 3B) across the two groups were statistically comparable (Figure 3C). Although the transcriptional bias that we showed across the different functional subclasses in the DSP in the control animals was preserved (Figure 3D) only a small fraction of the transcripts (11/187) were differentially regulated across columns and layers (see Supplemental Tables 5-7 for differentially regulated transcripts). These results argue that there is a competition between sensory experience and deprivation for transcriptional regulation of the DSP, and sensory deprivation is the primary cause for the experience-dependent regulation in transcription.

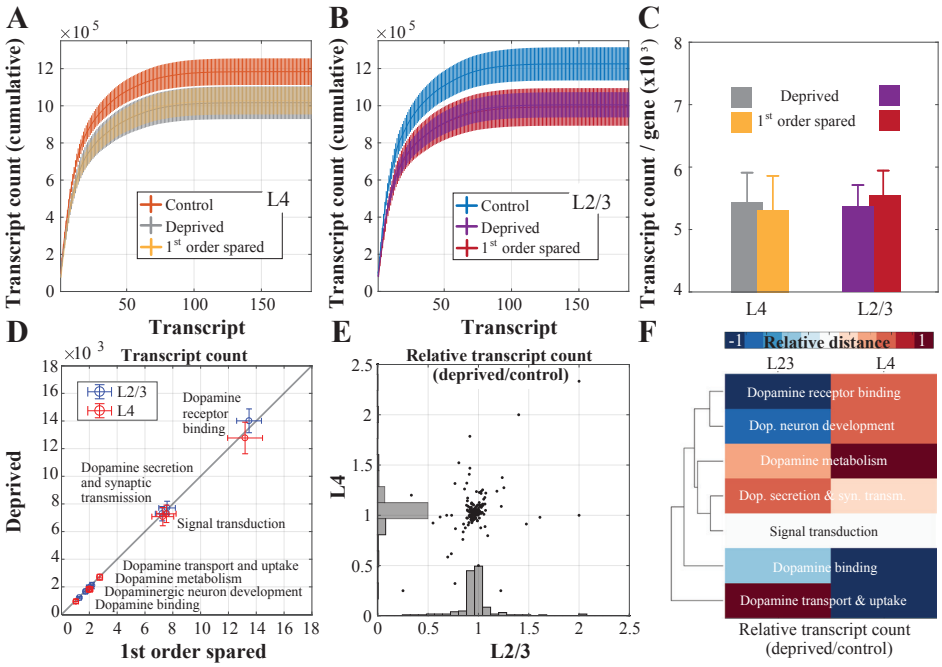

Figure 3. Competition between sensory experience and sensory deprivation in driving DSP signaling. First order neighboring cortical columns (B/D) to the deprived C column are compared against the C column. **(A-B)** DSP signaling is not regulated by the sensory input in the 1st order spared whiskers' cortical columns neither in L4 (p=0.53; Kolmogorov-Smirnov test) nor in L2/3 (p=0.99; Kolmogorov-Smirnov test). Data from Control laminae are shown

in Figure 2 and are provided for herein for comparison. **(C)** Comparison of the relative change in gene transcription across cortical laminae per gene. L4: F(1,186)=0.8789 p=0.87; ANOVA. L2/3: (F(1,186)=0.2418 p=1; ANOVA. **(D)** Comparison of gene transcription by function across layers (see Supplemental Table 1 for functional annotations for each gene). None of the pairwise comparisons across layers within functional gene-clusters were significant (paired t-test). **(E)** Comparison of the relative change in gene transcription across cortical laminae for each gene. See Supplemental Tables 5 and 6 for genes that are differentially transcribed in L4 and L2/3. **(F)** Clustergram shows the relative distance between functional groups in terms of the relative change in transcription across the deprived and the 1st order spared columns in animals that received whisker deprivation. Unlike the visualization in D, this analysis removes the co-variance within animal across cortical columns. Whisker deprivation significantly altered the transcription of genes responsible for dopamine receptor binding (L2/3: $p<0.05$; L4:$p<0.05$) and dopaminergic neuron development (L2/3: $p<0.05$; L4: $p<0.005$) both in L2/3 and L4 (All comparisons: t-test). See Supplemental Table 7 for the laminar distribution of transcripts that are differentially transcribed across the deprived and 1st order spared columns, organized by function.

The topography of the transcriptional regulation of the DSP

Neuromodulatory projections into the somatosensory cortex are diffused and considered to lack the topography that exists in the ascending projections originating from the sensory periphery [34,35]. In the absence of topography, changes in the presynaptic dopaminergic drive might alter the neural function throughout the somatosensory cortex. Although this could be a powerful gain modulation mechanism, it could also impair behavior during partial sensory deprivation, like the single row deprivation protocol employed herein. Therefore, we compared the DSP transcriptome across the deprived and 2nd order spared cortical columns. Two cortical columns away from the deprived whisker, the DSP transcriptome fully recovered to the control levels (Figure 4A-C), and in L4 the transcription was up-regulated (Figure 4A,C). Pairwise comparison of the relative gene transcription across layers (Figure 4D) showed correlated changes across the laminae suggesting that DSP signaling is regulated topographically but independent from columnar identity. Accordingly, the majority of the upregulation in DSP transcription was observed in genes that are co-regulated both in L4 as well as L2/3 (Figure 4E).

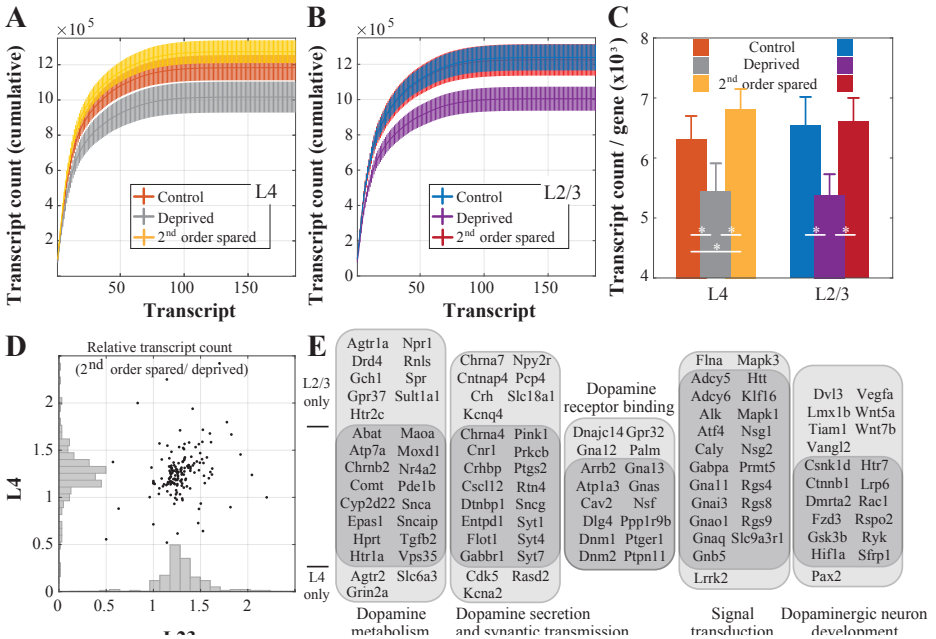

Figure 4. The topography of experience-dependent changes in DSP signaling. Second order neighboring cortical columns (A/E) to the deprived C column are compared against the C column. **(A-B)** DSP signaling is transcriptionally potentiated in the second order spared column compared to the deprived column both in L4 and L2/3 (p=0.01; Kolmogorov-Smirnov test). Data from Control laminae are shown in Figure 2 and are provided for herein for comparison. **(C)** Comparison of the relative change in gene transcription. Statistically significant comparisons are shown. Data from within animal across columns are compared using the paired t-test, data between animals is with ANOVA. **(D)** Comparison of the relative change in gene transcription across cortical laminae for each gene. See Supplemental Tables 8 and 9 for genes that are differentially transcribed in L4 and L2/3 across the deprived and second order spared columns. **(E)** Dopaminergic transcripts whose transcription is altered upon whisker deprivation grouped by simplified functional annotations. See Supplemental Table 10 for the laminar specificity of the transcriptional regulation for each differentially regulated gene upon whisker deprivation. Note that the intersection of the two rounded rectangles contains transcripts that are regulated by whisker deprivation both in L2/3 and L/4.

Discussion

Here we studied the gene transcription involved with dopaminergic signaling and showed that experience powerfully regulates the DSP transcription in the granular and supragranular layers of the cortex. The changes observed are driven by sensory deprivation as the DSP transcriptome of the 1st order spared whiskers' cortical columns is statistically indistinguishable from the deprived cortical columns'. Partial sensory deprivation does not

alter the transcription of the genes in DSP as cortical columns two order away from the deprived whisker have DSP transcriptome generally comparable to control animals.

Experience and layer dependent regulation of dopaminergic gene transcription contributes to complementary aspects of the pre and postsynaptic signaling. Genes whose transcription is down-regulated exclusively in L4 upon sensory deprivation (Agtr2, Alk, Arrb2, Flot1 and Cxcl12) are primarily involved in the regulation of extracellular dopamine availability and uptake. Agtr2 is responsible for encoding the angiotensin receptor 2, whose signaling is inhibited by dopamine at least in the striatum and substantia nigra [36]. As angiotensin receptor activation reduces dopaminergic uptake and increases dopamine availability [37], its transcriptional downregulation by sensory deprivation is likely to reduce dopamine availability in L4. Arrb2 and Flot1 might compensate for the reduction in the dopaminergic drive, given their role in the internalization of dopaminergic receptors [38], and localization and reverse transport of dopamine [39], respectively. Cxcl12, on the other hand, encodes the SDF-1 protein that activates the nigrostriatal dopaminergic pathway via GPCR, increases the action potential frequency and induces burst firing of DA neurons [40]. SDF-1 also positively regulates voltage-dependent channels, potassium currents, and neurotransmitter release via calcium dependent mechanisms [41]. Therefore lack of sensory experience inhibits the dopaminergic signaling, localization and transport presynaptically in the principal thalamocortical recipient cortical layer.

Experience-dependent changes in dopaminergic signaling in L2/3 primarily contribute to the homeostasis of (postsynaptic) cellular and network excitability. The balance of neurotransmitters is crucial in order to maintain the homeostasis. Depending on the dopamine-glutamate ratio, Dlg4 controls D1R trafficking at the postsynaptic density [42]. This gene encodes a kinase family, membrane-associated guanylate kinase (MAGUK), critical for co-clustering of NMDA receptors, potassium channels and dopaminergic receptors [43]. Recruitment of D1R to the membrane is likely to be reduced upon sensory deprivation since the down-regulation of Cav2 transcription reduces Caveolin-2 availability [44], which is required for synaptic localization of D1R [45].

Transcriptional suppression of Gabbr1, the gene encoding GABA-B receptor, upon sensory deprivation functionally contributes to the homeostatic changes in GABA release, which depends on complex interactions between NMDAR and D1R [46,47]. Dopamine-dependent regulation of inhibitory drive is also subunit dependent [48], as activation of Dopamine receptor subunit 4 inhibits GABA release via blockage of L-type Ca^{2+} channels [49]. The dopaminergic gating of cellular inhibition might also involve other surface receptors. For example, the cannabinoid receptor 1 (CB1), encoded by the gene Cnr1, has been associated with the homeostatic regulation of dopaminergic release through the control of inhibitory GABAergic

synapses in the PFC [50]. The activation of CB1, which is widely expressed in brain regions projecting to the NAc, leads to the inhibition of excitatory glutamatergic synapses, not only in the NAc [51] but also in the VTA, through interaction with D2R [52]. Experience-dependent downregulation of Cnr1 might, therefore, correlate with increased excitatory (glutamatergic) drive, as D1R transport to the postsynaptic density (due to Dlg4 suppression) and GABA-B availability are reduced (after down-regulation of Gabbr1) upon sensory deprivation, plausibly increasing the cellular excitability.

Experience-dependent dopaminergic regulation of other neurotransmitters' signaling and availability necessarily involves metabolic control of neurotransmitter synthesis and turnover. In L2/3, the sensory deprivation reduces the transcription of Comt and Tor1a, which control dopamine metabolization and contribute to dopamine clearance [53,54]. Dbh encodes dopamine beta-hydroxylase, an enzyme that has been associated with the D2 receptor activation, and converts dopamine into norepinephrine [55]. Considering that the transcription of Chrnb2, which encodes a cholinergic nicotinic receptor [56], is upon sensory deprivation, activity dependent changes in dopaminergic signaling might also have regulatory control over other neuromodulators.

Among the genes commonly found to be down-regulated after sensory deprivation in both L2/3 and L4, most of them are associated with receptor trafficking (Dtnbp1, Flna, Gna11, Gna13, Gnaq, Gnas), membrane localization (Nat81, Nsf, Palm, Vps35) and the metabolic control of neurotransmitter synthesis and turnover (Dtnbp1, Maoa). Thus sensory experience regulates dopaminergic signaling also in a cortical layer independent manner.

Bibliography

1. Berridge, K. C. & Kringelbach, M. L. Pleasure systems in the brain. *Neuron* **86,** 646–664 (2015).
2. Girault, J.-A. & Greengard, P. The neurobiology of dopamine signaling. *Arch. Neurol.* **61,** 641–644 (2004).
3. Money, K. M. & Stanwood, G. D. Developmental origins of brain disorders: roles for dopamine. *Front. Cell. Neurosci.* **7,** 260 (2013).
4. Volkow, N. D., Wise, R. A. & Baler, R. The dopamine motive system: implications for drug and food addiction. *Nat. Rev. Neurosci.* **18,** 741–752 (2017).
5. Schultz, W. Dopamine reward prediction-error signalling: a two-component response. *Nat. Rev. Neurosci.* **17,** 183–195 (2016).
6. Rosell, D. R. & Siever, L. J. The neurobiology of aggression and violence. *CNS Spectr.* **20,** 254–279 (2015).
7. Lee, T., Seeman, P., Rajput, A., Farley, I. J. & Hornykiewicz, O. Receptor basis for dopaminergic supersensitivity in Parkinson's disease. *Nature* **273,** 59–61 (1978).
8. van Holst, R. J. *et al.* Increased striatal dopamine synthesis capacity in gambling addiction. *Biol. Psychiatry* **83,** 1036–1043 (2018).
9. Arnsten, A. F. T., Wang, M. & Paspalas, C. D. Dopamine's actions in primate prefrontal cortex: challenges for treating cognitive disorders. *Pharmacol. Rev.* **67,** 681–696 (2015).
10. Tabatabaei, S. M. *et al.* DRD4 Gene Polymorphisms as a Risk Factor for Children with Attention Deficit Hyperactivity Disorder in Iranian Population. *Int. Sch. Res. Notices* **2017,** 2494537 (2017).
11. Jacob, S. N., Ott, T. & Nieder, A. Dopamine regulates two classes of primate prefrontal neurons that represent sensory signals. *J. Neurosci.* **33,** 13724–13734 (2013).
12. Allen, C. B., Celikel, T. & Feldman, D. E. Long-term depression induced by sensory deprivation during cortical map plasticity in vivo. *Nat. Neurosci.* **6,** 291–299 (2003).
13. Celikel, T., Szostak, V. A. & Feldman, D. E. Modulation of spike timing by sensory deprivation during induction of cortical map plasticity. *Nat. Neurosci.* **7,** 534–541 (2004).
14. Foeller, E., Celikel, T. & Feldman, D. E. Inhibitory sharpening of receptive fields contributes to whisker map plasticity in rat somatosensory cortex. *J. Neurophysiol.* **94,** 4387–4400 (2005).
15. Clem, R. L., Celikel, T. & Barth, A. L. Ongoing in vivo experience triggers synaptic metaplasticity in the neocortex. *Science* **319,** 101–104 (2008).
16. Syed, E. C. J., Sharott, A., Moll, C. K. E., Engel, A. K. & Kral, A. Effect of sensory stimulation in rat barrel cortex, dorsolateral striatum and on corticostriatal functional connectivity. *Eur. J. Neurosci.* **33,** 461–470 (2011).
17. Pidoux, M., Mahon, S., Deniau, J.-M. & Charpier, S. Integration and propagation of somatosensory responses in the corticostriatal pathway: an intracellular study in vivo. *J Physiol (Lond)* **589,** 263–281 (2011).
18. Ketzef, M. *et al.* Dopamine Depletion Impairs Bilateral Sensory Processing in the Striatum in a Pathway-Dependent Manner. *Neuron* **94,** 855–865.e5 (2017).
19. Kole, K., Scheenen, W., Tiesinga, P. & Celikel, T. Cellular diversity of the somatosensory cortical map plasticity. *Neurosci. Biobehav. Rev.* **84,** 100–115 (2018).
20. Azarfar, A., Calcini, N., Huang, C., Zeldenrust, F. & Celikel, T. Neural coding: A single neuron's perspective. *Neurosci. Biobehav. Rev.* **94,** 238–247 (2018).
21. Steiner, H. & Gerfen, C. R. Tactile sensory input regulates basal and apomorphine-induced immediate-early gene expression in rat barrel cortex. *J. Comp. Neurol.* **344,** 297–304 (1994).

22. Jiménez-Capdeville, M. E., Reader, T. A., Molina-Holgado, E. & Dykes, R. W. Changes in extracellular levels of dopamine metabolites in somatosensory cortex after peripheral denervation. *Neurochem. Res.* **21,** 1–6 (1996).
23. Kole, K. *et al.* Transcriptional mapping of the primary somatosensory cortex upon sensory deprivation. *Gigascience* **6,** 1–6 (2017).
24. Kole, K. & Celikel, T. Neocortical microdissection at columnar and laminar resolution for molecular interrogation. *Curr. Protoc. Neurosci.* e55 (2018). doi:10.1002/cpns.55
25. Kole, K. *et al.* Transcriptional mapping of the primary somatosensory cortex upon sensory deprivation. *Gigascience* (2017).
26. Beier, K. T. *et al.* Circuit Architecture of VTA Dopamine Neurons Revealed by Systematic Input-Output Mapping. *Cell* **162,** 622–634 (2015).
27. Kole, K. *et al.* Proteomic landscape of the primary somatosensory cortex upon sensory deprivation. *Gigascience* **6,** 1–10 (2017).
28. Brecht, M., Roth, A. & Sakmann, B. Dynamic receptive fields of reconstructed pyramidal cells in layers 3 and 2 of rat somatosensory barrel cortex. *J Physiol (Lond)* **553,** 243–265 (2003).
29. Shao, Y. R. *et al.* Plasticity of recurrent l2/3 inhibition and gamma oscillations by whisker experience. *Neuron* **80,** 210–222 (2013).
30. Li, L., Gainey, M. A., Goldbeck, J. E. & Feldman, D. E. Rapid homeostasis by disinhibition during whisker map plasticity. *Proc Natl Acad Sci USA* **111,** 1616–1621 (2014).
31. Gainey, M. A., Aman, J. W. & Feldman, D. E. Rapid Disinhibition by Adjustment of PV Intrinsic Excitability during Whisker Map Plasticity in Mouse S1. *J. Neurosci.* **38,** 4749–4761 (2018).
32. Fox, K. Deconstructing the cortical column in the barrel cortex. *Neuroscience* **368,** 17–28 (2018).
33. Glazewski, S., Greenhill, S. & Fox, K. Time-course and mechanisms of homeostatic plasticity in layers 2/3 and 5 of the barrel cortex. *Philos Trans R Soc Lond, B, Biol Sci* **372,** (2017).
34. Schubert, D., Nadif Kasri, N., Celikel, T. & Homberg, J. in *Sensorimotor Integration in the Whisker System* (eds. Krieger, P. & Groh, A.) 243–273 (Springer, 2015).
35. Azarfar, A., Calcini, N., Huang, C., Zeldenrust, F. & Celikel, T. Neural coding: A single neuron's perspective. *Neurosci Biobehav Rev* (2018).
36. Villar-Cheda, B. *et al.* Nigral and striatal regulation of angiotensin receptor expression by dopamine and angiotensin in rodents: implications for progression of Parkinson's disease. *Eur. J. Neurosci.* **32,** 1695–1706 (2010).
37. Choi, M. R., Correa, A. H., del Valle Turco, V., Garcia, F. A. & Fernández, B. E. Angiotensin II regulates extraneuronal dopamine uptake in the kidney. *Nephron Physiol.* **104,** 136–143 (2006).
38. Deming, J. D. *et al.* Dopamine receptor D4 internalization requires a beta-arrestin and a visual arrestin. *Cell. Signal.* **27,** 2002–2013 (2015).
39. Cremona, M. L. *et al.* Flotillin-1 is essential for PKC-triggered endocytosis and membrane microdomain localization of DAT. *Nat. Neurosci.* **14,** 469–477 (2011).
40. Skrzydelski, D. *et al.* The chemokine stromal cell-derived factor-1/CXCL12 activates the nigrostriatal dopamine system. *J. Neurochem.* **102,** 1175–1183 (2007).
41. Guyon, A. & Nahon, J.-L. Multiple actions of the chemokine stromal cell-derived factor-1alpha on neuronal activity. *J. Mol. Endocrinol.* **38,** 365–376 (2007).
42. Jacobs, M. M. *et al.* Dopamine receptor D1 and postsynaptic density gene variants associate with opiate abuse and striatal expression levels. *Mol. Psychiatry* **18,** 1205–1210 (2013).

43. Frank, R. A. & Grant, S. G. Supramolecular organization of NMDA receptors and the postsynaptic density. *Curr. Opin. Neurobiol.* **45,** 139–147 (2017).
44. Trivedi, M., Narkar, V. A., Hussain, T. & Lokhandwala, M. F. Dopamine recruits D1A receptors to Na-K-ATPase-rich caveolar plasma membranes in rat renal proximal tubules. *Am. J. Physiol. Renal Physiol.* **287,** F921-31 (2004).
45. Yu, P. *et al.* D1 dopamine receptor signaling involves caveolin-2 in HEK-293 cells. *Kidney Int.* **66,** 2167–2180 (2004).
46. Schoffelmeer, A. N. *et al.* Synergistically interacting dopamine D1 and NMDA receptors mediate nonvesicular transporter-dependent GABA release from rat striatal medium spiny neurons. *J. Neurosci.* **20,** 3496–3503 (2000).
47. Li, H.-B., Lin, L., Yang, L.-Y. & Xie, C. Dopaminergic facilitation of GABAergic transmission in layer III of rat medial entorhinal cortex. *Chin. J. Physiol.* **58,** 46–54 (2015).
48. Andersson, R., Johnston, A. & Fisahn, A. Dopamine D4 receptor activation increases hippocampal gamma oscillations by enhancing synchronization of fast-spiking interneurons. *PLoS ONE* **7,** e40906 (2012).
49. Recillas-Morales, S. *et al.* L-type Ca^{2+} channel activity determines modulation of GABA release by dopamine in the substantia nigra reticulata and the globus pallidus of the rat. *Neuroscience* **256,** 292–301 (2014).
50. Dazzi, L. *et al.* Involvement of the cannabinoid CB1 receptor in modulation of dopamine output in the prefrontal cortex associated with food restriction in rats. *PLoS ONE* **9,** e92224 (2014).
51. Pistis, M., Muntoni, A. L., Pillolla, G. & Gessa, G. L. Cannabinoids inhibit excitatory inputs to neurons in the shell of the nucleus accumbens: an in vivo electrophysiological study. *Eur. J. Neurosci.* **15,** 1795–1802 (2002).
52. Melis, M. *et al.* Endocannabinoids mediate presynaptic inhibition of glutamatergic transmission in rat ventral tegmental area dopamine neurons through activation of CB1 receptors. *J. Neurosci.* **24,** 53–62 (2004).
53. Käenmäki, M. *et al.* Quantitative role of COMT in dopamine clearance in the prefrontal cortex of freely moving mice. *J. Neurochem.* **114,** 1745–1755 (2010).
54. Wakabayashi-Ito, N. *et al.* Dtorsin, the Drosophila ortholog of the early-onset dystonia TOR1A (DYT1), plays a novel role in dopamine metabolism. *PLoS ONE* **6,** e26183 (2011).
55. Gaval-Cruz, M. *et al.* Chronic loss of noradrenergic tone produces β-arrestin2-mediated cocaine hypersensitivity and alters cellular D2 responses in the nucleus accumbens. *Addict. Biol.* **21,** 35–48 (2016).
56. Wen, L., Yang, Z., Cui, W. & Li, M. D. Crucial roles of the CHRNB3-CHRNA6 gene cluster on chromosome 8 in nicotine dependence: update and subjects for future research. *Transl. Psychiatry* **6,** e843 (2016).
57. Voigts, J., Sakmann, B. & Celikel, T. Unsupervised whisker tracking in unrestrained behaving animals. *J. Neurophysiol.* **100,** 504–515 (2008).
58. Celikel, T. & Sakmann, B. Sensory integration across space and in time for decision making in the somatosensory system of rodents. *Proc Natl Acad Sci USA* **104,** 1395–1400 (2007).
59. Kole, K. *et al.* Supporting data for "Transcriptional mapping of the primary somatosensory cortex upon sensory deprivation." *GigaDB* (2017).

Supplemental Materials

Supplemental Table 1: List of genes associated with the dopaminergic signaling pathway

MGI Gene/ Marker ID	*Gene symbol*	*Gene name*	*Annotated function*	*GoSlim annotation*
MGI:2443582	Abat	4-aminobutyrate aminotransferase	positive regulation of dopamine metabolic process	Dopamine metabolism
MGI:2443582	Abat	4-aminobutyrate aminotransferase	negative regulation of dopamine secretion	Dopamine secretion & synaptic transmission
MGI:99673	Adcy5	adenylate cyclase 5	adenylate cyclase-activating dopamine receptor signaling pathway	Signal transduction
MGI:99673	Adcy5	adenylate cyclase 5	adenylate cyclase-inhibiting dopamine receptor signaling pathway	Signal transduction
MGI:87917	Adcy6	adenylate cyclase 6	dopamine receptor signaling pathway	Signal transduction
MGI:99402	Adora2a	adenosine A2a receptor	synaptic transmission, dopaminergic	Dopamine secretion & synaptic transmission
MGI:87937	Adrb1	Adregeneric receptor, beta 1	dopamine binding	Dopamine binding
MGI:87938	Adrb2	Adregeneric receptor, beta 2	dopamine binding	Dopamine binding
MGI:87964	Agtr1a	angiotensin II receptor, type 1a	dopamine biosynthetic process	Dopamine metabolism
MGI:87964	Agtr1a	angiotensin II receptor, type 1a	D1 dopamine receptor binding	Dopamine receptor binding
MGI:87966	Agtr2	angiotensin II receptor, type 2	dopamine biosynthetic process	Dopamine metabolism
MGI:103305	Alk	anaplastic lymphoma kinase	regulation of dopamine receptor signaling pathway	Signal transduction
MGI:99474	Arrb2	arrestin, beta 2	D1 dopamine receptor binding	Dopamine receptor binding
MGI:99474	Arrb2	arrestin, beta 2	positive regulation of synaptic transmission, dopaminergic	Dopamine secretion & synaptic transmission
MGI:88096	Atf4	activating transcription factor 4	cellular response to dopamine	Signal transduction
MGI:88107	Atp1a3	ATPase, Na+/K+ transporting, alpha 3 polypeptide	D1 dopamine receptor binding	Dopamine receptor binding

MGI Gene/ Marker ID	*Gene symbol*	*Gene name*	*Annotated function*	*GoSlim annotation*
MGI:99400	Atp7a	ATPase, Cu++ transporting, alpha polypeptide	dopamine metabolic process	Dopamine metabolism
MGI:1915816	Caly	calcyon neuron-specific vesicular protein	dopamine receptor signaling pathway	Signal transduction
MGI:107571	Cav2	caveolin 2	D1 dopamine receptor binding	Dopamine receptor binding
MGI:107571	Cav2	caveolin 2	positive regulation of dopamine receptor signaling pathway	Signal transduction
MGI:101765	Cdk5	cyclin-dependent kinase 5	synaptic transmission, dopaminergic	Dopamine secretion & synaptic transmission
MGI:3606576	Cdnf	cerebral dopamine neurotrophic factor	dopaminergic neuron differentiation	Dopaminergic neuron development
MGI:1858236	Celsr3	cadherin, EGF LAG seven-pass G-type receptor 3	dopaminergic neuron axon guidance	Dopaminergic neuron development
MGI:109248	Chrm5	cholinergic receptor, muscarinic 5	dopamine transport	Dopamine transport & uptake
MGI:87888	Chrna4	cholinergic receptor, nicotinic, alpha polypeptide 4	positive regulation of dopamine secretion	Dopamine secretion & synaptic transmission
MGI:87888	Chrna4	cholinergic receptor, nicotinic, alpha polypeptide 4	regulation of dopamine secretion	Dopamine secretion & synaptic transmission
MGI:106213	Chrna6	cholinergic receptor, nicotinic, alpha polypeptide 6	positive regulation of dopamine secretion	Dopamine secretion & synaptic transmission
MGI:106213	Chrna6	cholinergic receptor, nicotinic, alpha polypeptide 6	regulation of dopamine secretion	Dopamine secretion & synaptic transmission
MGI:99779	Chrna7	cholinergic receptor, nicotinic, alpha polypeptide 7	regulation of synaptic transmission, dopaminergic	Dopamine secretion & synaptic transmission
MGI:87891	Chrnb2	cholinergic receptor, nitotinic, beta polypeptide 2 (neuronal)	regulation of dopamine metabolic process	Dopamine metabolism

MGI Gene/ Marker ID	*Gene symbol*	*Gene name*	*Annotated function*	*GoSlim annotation*
MGI:87891	Chrnb2	cholinergic receptor, nicotinic, beta polypeptide 2 (neuronal)	positive regulation of dopamine secretion	Dopamine secretion & synaptic transmission
MGI:87891	Chrnb2	cholinergic receptor, nicotinic, beta polypeptide 2 (neuronal)	positive regulation of synaptic transmission, dopaminergic	Dopamine secretion & synaptic transmission
MGI:87891	Chrnb2	cholinergic receptor, nicotinic, beta polypeptide 2 (neuronal)	regulation of dopamine secretion	Dopamine secretion & synaptic transmission
MGI:87891	Chrnb2	cholinergic receptor, nicotinic, beta polypeptide 2 (neuronal)	regulation of synaptic transmission, dopaminergic	Dopamine secretion & synaptic transmission
MGI:88414	ckr	chakragati	negative regulation of dopamine receptor signaling pathway	Signal transduction
MGI:2146607	Clic6	chloride intracellular channel 6	D2 dopamine receptor binding	Dopamine receptor binding
MGI:2146607	Clic6	chloride intracellular channel 6	D3 dopamine receptor binding	Dopamine receptor binding
MGI:2146607	Clic6	chloride intracellular channel 6	D4 dopamine receptor binding	Dopamine receptor binding
MGI:104615	Cnr1	cannabinoid receptor 1 (brain)	negative regulation of dopamine secretion	Dopamine secretion & synaptic transmission
MGI:2183572	Cntnap4	contactin associated protein-like 4	regulation of synaptic transmission, dopaminergic	Dopamine secretion & synaptic transmission
MGI:88470	Comt	catechol-O-methyltransferase	dopamine catabolic process	Dopamine metabolism
MGI:88470	Comt	catechol-O-methyltransferase	dopamine metabolic process	Dopamine metabolism
MGI:88470	Comt	catechol-O-methyltransferase	negative regulation of dopamine metabolic process	Dopamine metabolism
MGI:88496	Crh	corticotropin releasing hormone	synaptic transmission, dopaminergic	Dopamine secretion & synaptic transmission
MGI:88497	Crhbp	corticotropin releasing hormone binding protein	synaptic transmission, dopaminergic	Dopamine secretion & synaptic transmission

MGI Gene/ Marker ID	*Gene symbol*	*Gene name*	*Annotated function*	*GoSlim annotation*
MGI:1355272	Csnk1d	casein kinase 1, delta	positive regulation of Wnt-mediated midbrain dopaminergic neuron differentiation	Dopaminergic neuron development
MGI:88276	Ctnnb1	catenin (cadherin associated protein), beta 1	midbrain dopaminergic neuron differentiation	Dopaminergic neuron development
MGI:103556	Cxcl12	chemokine (C-X-C motif) ligand 12	positive regulation of dopamine secretion	Dopamine secretion & synaptic transmission
MGI:103556	Cxcl12	chemokine (C-X-C motif) ligand 12	dopaminergic neuron differentiation	Dopaminergic neuron development
MGI:1929474	Cyp2d22	cytochrome P450, family 2, subfamily d, polypeptide 22	dopamine biosynthetic process	Dopamine metabolism
MGI:1929474	Cyp2d22	cytochrome P450, family 2, subfamily d, polypeptide 22	dopamine metabolic process	Dopamine metabolism
MGI:94859	Dao	D-amino acid oxidase	dopamine biosynthetic process	Dopamine metabolism
MGI:94861	Das	dopamine agonist sensitivity	dopamine receptor signaling pathway	Signal transduction
MGI:94864	Dbh	dopamine beta hydroxylase	dopamine beta-monooxygenase activity	Dopamine metabolism
MGI:94864	Dbh	dopamine beta hydroxylase	dopamine catabolic process	Dopamine metabolism
MGI:94876	Ddc	dopa decarboxylase	dopamine biosynthetic process	Dopamine metabolism
MGI:1329040	Dkk1	dickkopf WNT signaling pathway inhibitor 1	positive regulation of midbrain dopaminergic neuron differentiation	Dopaminergic neuron development
MGI:1277959	Dlg4	discs large MAGUK scaffold protein 4	D1 dopamine receptor binding	Dopamine receptor binding
MGI:2653629	Dmrta2	doublesex and mab-3 related transcription factor like family A2	dopaminergic neuron differentiation	Dopaminergic neuron development
MGI:1921580	Dnajc14	DnaJ heat shock protein family (Hsp40) member C14	dopamine receptor binding	Dopamine receptor binding
MGI:107384	Dnm1	dynamin 1	D2 dopamine receptor binding	Dopamine receptor binding
MGI:109547	Dnm2	dynamin 2	D2 dopamine receptor binding	Dopamine receptor binding

MGI Gene/ Marker ID	*Gene symbol*	*Gene name*	*Annotated function*	*GoSlim annotation*
MGI:109547	Dnm2	dynamin 2	cellular response to dopamine	Signal transduction
MGI:99578	Drd1	dopamine receptor D1	dopamine transport	Dopamine transport & uptake
MGI:99578	Drd1	dopamine receptor D1	regulation of dopamine metabolic process	Dopamine metabolism
MGI:99578	Drd1	dopamine receptor D1	D3 dopamine receptor binding	Dopamine receptor binding
MGI:99578	Drd1	dopamine receptor D1	dopamine neurotransmitter receptor activity	Dopamine receptor binding
MGI:99578	Drd1	dopamine receptor D1	dopamine neurotransmitter receptor activity, coupled via Gs	Dopamine receptor binding
MGI:99578	Drd1	dopamine receptor D1	synaptic transmission, dopaminergic	Dopamine secretion & synaptic transmission
MGI:99578	Drd1	dopamine receptor D1	adenylate cyclase-activating dopamine receptor signaling pathway	Signal transduction
MGI:99578	Drd1	dopamine receptor D1	cellular response to dopamine	Signal transduction
MGI:99578	Drd1	dopamine receptor D1	phospholipase C-activating dopamine receptor signaling pathway	Signal transduction
MGI:94924	Drd2	dopamine receptor D2	dopamine metabolic process	Dopamine metabolism
MGI:94924	Drd2	dopamine receptor D2	dopamine neurotransmitter receptor activity	Dopamine receptor binding
MGI:94924	Drd2	dopamine receptor D2	dopamine neurotransmitter receptor activity, coupled via Gi/Go	Dopamine receptor binding
MGI:94924	Drd2	dopamine receptor D2	negative regulation of dopamine secretion	Dopamine secretion & synaptic transmission
MGI:94924	Drd2	dopamine receptor D2	positive regulation of dopamine uptake involved in synaptic transmission	Dopamine transport & uptake
MGI:94924	Drd2	dopamine receptor D2	regulation of dopamine secretion	Dopamine secretion & synaptic transmission
MGI:94924	Drd2	dopamine receptor D2	regulation of dopamine uptake involved in synaptic transmission	Dopamine transport & uptake

MGI Gene/ Marker ID	*Gene symbol*	*Gene name*	*Annotated function*	*GoSlim annotation*
MGI:94924	Drd2	dopamine receptor D2	synaptic transmission, dopaminergic	Dopamine secretion & synaptic transmission
MGI:94924	Drd2	dopamine receptor D2	adenylate cyclase-inhibiting dopamine receptor signaling pathway	Signal transduction
MGI:94924	Drd2	dopamine receptor D2	negative regulation of dopamine receptor signaling pathway	Signal transduction
MGI:94924	Drd2	dopamine receptor D2	phospholipase C-activating dopamine receptor signaling pathway	Signal transduction
MGI:94925	Drd3	dopamine receptor D3	D1 dopamine receptor binding	Dopamine receptor binding
MGI:94925	Drd3	dopamine receptor D3	dopamine neurotransmitter receptor activity	Dopamine receptor binding
MGI:94925	Drd3	dopamine receptor D3	dopamine neurotransmitter receptor activity, coupled via Gi/Go	Dopamine receptor binding
MGI:94925	Drd3	dopamine receptor D3	regulation of dopamine secretion	Dopamine secretion & synaptic transmission
MGI:94925	Drd3	dopamine receptor D3	synaptic transmission, dopaminergic	Dopamine secretion & synaptic transmission
MGI:94925	Drd3	dopamine receptor D3	adenylate cyclase-activating dopamine receptor signaling pathway	Signal transduction
MGI:94925	Drd3	dopamine receptor D3	adenylate cyclase-inhibiting dopamine receptor signaling pathway	Signal transduction
MGI:94925	Drd3	dopamine receptor D3	negative regulation of dopamine receptor signaling pathway	Signal transduction
MGI:94925	Drd3	dopamine receptor D3	positive regulation of dopamine receptor signaling pathway	Signal transduction
MGI:94926	Drd4	dopamine receptor D4	regulation of dopamine metabolic process	Dopamine metabolism
MGI:94926	Drd4	dopamine receptor D4	regulation of dopamine metabolic process	Dopamine metabolism
MGI:94926	Drd4	dopamine receptor D4	dopamine neurotransmitter receptor activity	Dopamine receptor binding
MGI:94926	Drd4	dopamine receptor D4	dopamine neurotransmitter receptor activity, coupled via Gi/Go	Dopamine receptor binding

MGI Gene/ Marker ID	*Gene symbol*	*Gene name*	*Annotated function*	*GoSlim annotation*
MGI:94926	Drd4	dopamine receptor D4	synaptic transmission, dopaminergic	Dopamine secretion & synaptic transmission
MGI:94926	Drd4	dopamine receptor D4	adenylate cyclase-inhibiting dopamine receptor signaling pathway	Signal transduction
MGI:94927	Drd5	dopamine receptor D5	dopamine neurotransmitter receptor activity	Dopamine receptor binding
MGI:94927	Drd5	dopamine receptor D5	dopamine neurotransmitter receptor activity, coupled via Gs	Dopamine receptor binding
MGI:94927	Drd5	dopamine receptor D5	synaptic transmission, dopaminergic	Dopamine secretion & synaptic transmission
MGI:94927	Drd5	dopamine receptor D5	adenylate cyclase-activating dopamine receptor signaling pathway	Signal transduction
MGI:94927	Drd5	dopamine receptor D5	phospholipase C-activating dopamine receptor signaling pathway	Signal transduction
MGI:2137586	Dtnbp1	dystrobrevin binding protein 1	regulation of dopamine secretion	Dopamine secretion & synaptic transmission
MGI:2137586	Dtnbp1	dystrobrevin binding protein 1	regulation of dopamine receptor signaling pathway	Signal transduction
MGI:108100	Dvl3	dishevelled segment polarity protein 3	Wnt signaling pathway involved in midbrain dopaminergic neuron differentiation	Dopaminergic neuron development
MGI:95389	En1	engrailed 1	dopaminergic neuron differentiation	Dopaminergic neuron development
MGI:95390	En2	engrailed 2	dopaminergic neuron differentiation	Dopaminergic neuron development
MGI:102805	Entpd1	ectonucleoside triphosphate diphosphohydrolase 1	negative regulation of dopamine secretion	Dopamine secretion & synaptic transmission
MGI:109169	Epas1	endothelial PAS domain protein 1	positive regulation of dopamine biosynthetic process	Dopamine metabolism
MGI:99604	Fgf8	fibroblast growth factor 8	dopaminergic neuron differentiation	Dopaminergic neuron development
MGI:95556	Flna	filamin, alpha	adenylate cyclase-inhibiting dopamine receptor signaling pathway	Signal transduction

MGI Gene/ Marker ID	*Gene symbol*	*Gene name*	*Annotated function*	*GoSlim annotation*
MGI:1100500	Flot1	flotillin 1	positive regulation of synaptic transmission, dopaminergic	Dopamine secretion & synaptic transmission
MGI:1347476	Foxa2	forkhead box A2	dopaminergic neuron differentiation	Dopaminergic neuron development
MGI:108476	Fzd3	frizzled class receptor 3	dopaminergic neuron axon guidance	Dopaminergic neuron development
MGI:1860139	Gabbr1	gamma-aminobutyric acid (GABA) B receptor, 1	negative regulation of dopamine secretion	Dopamine secretion & synaptic transmission
MGI:14390	Gabpa	GA repeat binding protein, alpha	cellular response to dopamine	Signal transduction
MGI:95675	Gch1	GTP cyclohydrolase 1	dopamine biosynthetic process	Dopamine metabolism
MGI:107430	Gdnf	glial cell line derived neurotrophic factor	regulation of dopamine uptake involved in synaptic transmission	Dopamine transport & uptake
MGI:95766	Gna11	guanine nucleotide binding protein, alpha 11	phospholipase C-activating dopamine receptor signaling pathway	Signal transduction
MGI:95767	Gna12	guanine nucleotide binding protein, alpha 12	D5 dopamine receptor binding	Dopamine receptor binding
MGI:95768	Gna13	guanine nucleotide binding protein, alpha 13	D5 dopamine receptor binding	Dopamine receptor binding
MGI:95769	Gna14	guanine nucleotide binding protein, alpha 14	phospholipase C-activating dopamine receptor signaling pathway	Signal transduction
MGI:95770	Gna15	guanine nucleotide binding protein, alpha 15	phospholipase C-activating dopamine receptor signaling pathway	Signal transduction
MGI:95773	Gnai3	guanine nucleotide binding protein (G protein), alpha inhibiting 3	dopamine receptor signaling pathway	Signal transduction
MGI:95774	Gnal	guanine nucleotide binding protein, alpha stimulating, olfactory type	adenylate cyclase-activating dopamine receptor signaling pathway	Signal transduction
MGI:95775	Gnao1	guanine nucleotide binding protein, alpha O	dopamine receptor signaling pathway	Signal transduction

MGI Gene/ Marker ID	*Gene symbol*	*Gene name*	*Annotated function*	*GoSlim annotation*
MGI:95776	Gnaq	guanine nucleotide binding protein, alpha q polypeptide	phospholipase C-activating dopamine receptor signaling pathway	Signal transduction
MGI:95777	Gnas	GNAS (guanine nucleotide binding protein, alpha stimulating) complex locus	D1 dopamine receptor binding	Dopamine receptor binding
MGI:95777	Gnas	GNAS (guanine nucleotide binding protein, alpha stimulating) complex locus	adenylate cyclase-activating dopamine receptor signaling pathway	Signal transduction
MGI:101848	Gnb5	guanine nucleotide binding protein (G protein), beta 5	dopamine receptor signaling pathway	Signal transduction
MGI:107193	Gpr143	G protein-coupled receptor 143	dopamine binding	Dopamine binding
MGI:338346	Gpr21	G protein-coupled receptor 21	dopamine neurotransmitter receptor activity, coupled via Gs	Dopamine receptor binding
MGI:1313297	Gpr37	G protein-coupled receptor 37	dopamine biosynthetic process	Dopamine metabolism
MGI:1313297	Gpr37	G-protein coupled receptor 37	positive regulation of dopamine metabolic process	Dopamine metabolism
MGI:620246	Gpr52	G protein-coupled receptor 52	dopamine neurotransmitter receptor activity, coupled via Gs	Dopamine receptor binding
MGI:95820	Grin2a	glutamate receptor, ionotropic, NMDA2B (epsilon 1)	dopamine metabolic process	Dopamine metabolism
MGI:95821	Grin2b	glutamate receptor, ionotropic, NMDA2B (epsilon 2)	D2 dopamine receptor binding	Dopamine receptor binding
MGI:87941	Grk3	G protein-coupled receptor kinase 3	D1 dopamine receptor binding	Dopamine receptor binding
MGI:1861437	Gsk3b	glycogen synthase kinase 3 beta	negative regulation of dopaminergic neuron differentiation	Dopaminergic neuron development
MGI:106918	Hif1a	hypoxia inducible factor 1, alpha subunit	dopaminergic neuron differentiation	Dopaminergic neuron development

MGI Gene/ Marker ID	*Gene symbol*	*Gene name*	*Annotated function*	*GoSlim annotation*
MGI:96217	Hprt	hypoxanthine guanine phosphoribosyl transferase	dopamine metabolic process	Dopamine metabolism
MGI:96217	Hprt	hypoxanthine guanine phosphoribosyl transferase	positive regulation of dopamine metabolic process	Dopamine metabolism
MGI:96273	Htr1a	5-hydroxytryptamine (serotonin) receptor 1A	regulation of dopamine metabolic process	Dopamine metabolism
MGI:96274	Htr1b	5-hydroxytryptamine (serotonin) receptor 1B	regulation of dopamine secretion	Dopamine secretion & synaptic transmission
MGI:109521	Htr2a	5-hydroxytryptamine (serotonin) receptor 2A	regulation of dopamine secretion	Dopamine secretion & synaptic transmission
MGI:96281	Htr2c	5-hydroxytryptamine (serotonin) receptor 2C	negative regulation of dopamine metabolic process	Dopamine metabolism
MGI:1196627	Htr6	5-hydroxytryptamine (serotonin) receptor 6	positive regulation of dopamine secretion	Dopamine secretion & synaptic transmission
MGI:99841	Htr7	5-hydroxytryptamine (serotonin) receptor 7	dopaminergic neuron differentiation	Dopaminergic neuron development
MGI:96067	Htt	huntingtin	dopamine receptor signaling pathway	Signal transduction
MGI:96659	Kcna2	potassium voltage-gated channel, shaker-related subfamily, member 2	regulation of dopamine secretion	Dopamine secretion & synaptic transmission
MGI:1926803	Kcnq4	potassium voltage-gated channel, subfamily Q, member 4	negative regulation of synaptic transmission, dopaminergic	Dopamine secretion & synaptic transmission
MGI:2153049	Klf16	kruppel-like factor 16	dopamine receptor signaling pathway	Signal transduction
MGI:1888519	Lmx1a	LIM homeobox transcription factor 1 alpha	dopaminergic neuron differentiation	Dopaminergic neuron development
MGI:1888519	Lmx1a	LIM homeobox transcription factor 1 alpha	midbrain dopaminergic neuron differentiation	Dopaminergic neuron development
MGI:1888519	Lmx1a	LIM homeobox transcription factor 1 alpha	positive regulation of Wnt-mediated midbrain dopaminergic neuron differentiation	Dopaminergic neuron development

MGI Gene/ Marker ID	*Gene symbol*	*Gene name*	*Annotated function*	*GoSlim annotation*
MGI:1100513	Lmx1b	LIM homeobox transcription factor 1 beta	dopaminergic neuron differentiation	Dopaminergic neuron development
MGI:1298218	Lrp6	low density lipoprotein receptor-related protein 6	dopaminergic neuron differentiation	Dopaminergic neuron development
MGI:1913975	Lrrk2	leucine-rich repeat kinase 2	cellular response to dopamine	Signal transduction
MGI:1913975	Lrrk2	leucine-rich repeat kinase 2	positive regulation of dopamine receptor signaling pathway	Signal transduction
MGI:1913975	Lrrk2	leucine-rich repeat kinase 2	regulation of dopamine receptor signaling pathway	Signal transduction
MGI:1922090	Manf	mesencephalic astrocyte-derived neurotrophic factor	dopaminergic neuron differentiation	Dopaminergic neuron development
MGI:96915	Maoa	monoamine oxidase A	dopamine catabolic process	Dopamine metabolism
MGI:1346858	Mapk1	mitogen-activated protein kinase 1	cellular response to dopamine	Signal transduction
MGI:2652894	Mapk15	mitogen-activated protein kinase 15	dopamine uptake	Dopamine transport & uptake
MGI:1346859	Mapk3	mitogen-activated protein kinase 3	cellular response to dopamine	Signal transduction
MGI:96916	Moab	monoamine oxidase B	positive regulation of dopamine metabolic process	Dopamine metabolism
MGI:1921582	Moxd1	monooxygenase, DBH-like 1	dopamine beta-monooxygenase activity	Dopamine metabolism
MGI:1921582	Moxd1	monooxygenase, DBH-like 1	dopamine catabolic process	Dopamine metabolism
MGI:2388042	Moxd2	monooxygenase, DBH-like 2	dopamine beta-monooxygenase activity	Dopamine metabolism
MGI:2388042	Moxd2	monooxygenase, DBH-like 2	dopamine catabolic process	Dopamine metabolism
MGI:2447776	Nat8l	N-acetyltransferase 8-like	positive regulation of dopamine uptake involved in synaptic transmission	Dopamine transport & uptake
MGI:3038234	nm3	neurological mutant 3	dopamine metabolic process	Dopamine metabolism
MGI:97371	Npr1	natriuretic peptide receptor 1	dopamine metabolic process	Dopamine metabolism

MGI Gene/ Marker ID	*Gene symbol*	*Gene name*	*Annotated function*	*GoSlim annotation*
MGI:108418	Npy2r	neuropeptide Y receptor Y2	positive regulation of dopamine secretion	Dopamine secretion & synaptic transmission
MGI:1352456	Nr4a2	nuclear receptor subfamily 4, group A, member 2	dopamine biosynthetic process	Dopamine metabolism
MGI:1352456	Nr4a2	nuclear receptor subfamily 4, group A, member 2	dopamine metabolic process	Dopamine metabolism
MGI:1352456	Nr4a2	nuclear receptor subfamily 4, group A, member 2	regulation of dopamine metabolic process	Dopamine metabolism
MGI:1352456	Nr4a2	nuclear receptor subfamily 4, group A, member 2	dopaminergic neuron differentiation	Dopaminergic neuron development
MGI:104560	Nsf	N-ethylmaleimide sensitive fusion protein	D1 dopamine receptor binding	Dopamine receptor binding
MGI:10949	Nsg1	neuron specific gene family member 1	dopamine receptor signaling pathway	Signal transduction
MGI:1202070	Nsg2	neuron specific gene family member 2	dopamine receptor signaling pathway	Signal transduction
MGI:3030935	Olfr1101	olfactory receptor 1101	dopamine neurotransmitter receptor activity, coupled via Gi/Go	Dopamine receptor binding
MGI:3030935	Olfr1101	olfactory receptor 1101	regulation of dopamine secretion	Dopamine secretion & synaptic transmission
MGI:3030935	Olfr1101	olfactory receptor 1101	synaptic transmission, dopaminergic	Dopamine secretion & synaptic transmission
MGI:3030935	Olfr1101	olfactory receptor 1101	adenylate cyclase-inhibiting dopamine receptor signaling pathway	Signal transduction
MGI:3030935	Olfr1101	olfactory receptor 1101	phospholipase C-activating dopamine receptor signaling pathway	Signal transduction
MGI:2659178	Olfr150	olfactory receptor 150	dopamine neurotransmitter receptor activity, coupled via Gi/Go	Dopamine receptor binding
MGI:2659178	Olfr150	olfactory receptor 150	regulation of dopamine secretion	Dopamine secretion & synaptic transmission
MGI:2659178	Olfr150	olfactory receptor 150	synaptic transmission, dopaminergic	Dopamine secretion & synaptic transmission
MGI:2659178	Olfr150	olfactory receptor 150	adenylate cyclase-inhibiting dopamine receptor signaling pathway	Signal transduction

MGI Gene/ Marker ID	*Gene symbol*	*Gene name*	*Annotated function*	*GoSlim annotation*
MGI:2659178	Olfr150	olfactory receptor 150	phospholipase C-activating dopamine receptor signaling pathway	Signal transduction
MGI:3030109	Olfr275	olfactory receptor 275	dopamine neurotransmitter receptor activity, coupled via Gi/Go	Dopamine receptor binding
MGI:3030109	Olfr275	olfactory receptor 275	regulation of dopamine secretion	Dopamine secretion & synaptic transmission
MGI:3030109	Olfr275	olfactory receptor 275	synaptic transmission, dopaminergic	Dopamine secretion & synaptic transmission
MGI:3030109	Olfr275	olfactory receptor 275	adenylate cyclase-inhibiting dopamine receptor signaling pathway	Signal transduction
MGI:3030109	Olfr275	olfactory receptor 275	phospholipase C-activating dopamine receptor signaling pathway	Signal transduction
MGI:3030517	Olfr683	olfactory receptor 683	dopamine neurotransmitter receptor activity, coupled via Gi/Go	Dopamine receptor binding
MGI:3030517	Olfr683	olfactory receptor 683	regulation of dopamine secretion	Dopamine secretion & synaptic transmission
MGI:3030517	Olfr683	olfactory receptor 683	synaptic transmission, dopaminergic	Dopamine secretion & synaptic transmission
MGI:3030517	Olfr683	olfactory receptor 683	adenylate cyclase-inhibiting dopamine receptor signaling pathway	Signal transduction
MGI:3030517	Olfr683	olfactory receptor 683	phospholipase C-activating dopamine receptor signaling pathway	Signal transduction
MGI:3030518	Olfr684	olfactory receptor 684	dopamine neurotransmitter receptor activity, coupled via Gi/Go	Dopamine receptor binding
MGI:3030518	Olfr684	olfactory receptor 684	regulation of dopamine secretion	Dopamine secretion & synaptic transmission
MGI:3030518	Olfr684	olfactory receptor 684	synaptic transmission, dopaminergic	Dopamine secretion & synaptic transmission
MGI:3030518	Olfr684	olfactory receptor 684	adenylate cyclase-inhibiting dopamine receptor signaling pathway	Signal transduction
MGI:3030518	Olfr684	olfactory receptor 684	phospholipase C-activating dopamine receptor signaling pathway	Signal transduction

MGI Gene/ Marker ID	*Gene symbol*	*Gene name*	*Annotated function*	*GoSlim annotation*
MGI:3030753	Olfr919	olfactory receptor 919	dopamine neurotransmitter receptor activity, coupled via Gi/Go	Dopamine receptor binding
MGI:3030753	Olfr919	olfactory receptor 919	regulation of dopamine secretion	Dopamine secretion & synaptic transmission
MGI:3030753	Olfr919	olfactory receptor 919	synaptic transmission, dopaminergic	Dopamine secretion & synaptic transmission
MGI:3030753	Olfr919	olfactory receptor 919	adenylate cyclase-inhibiting dopamine receptor signaling pathway	Signal transduction
MGI:3030753	Olfr919	olfactory receptor 919	phospholipase C-activating dopamine receptor signaling pathway	Signal transduction
MGI:97439	Oprk1	opioid receptor, kappa 1	positive regulation of dopamine secretion	Dopamine secretion & synaptic transmission
MGI:97451	Otx2	orthodenticle homeobox 2	dopaminergic neuron differentiation	Dopaminergic neuron development
MGI:1261814	Palm	paralemmin	D3 dopamine receptor binding	Dopamine receptor binding
MGI:1261814	Palm	paralemmin	negative regulation of dopamine receptor signaling pathway	Signal transduction
MGI:1355296	Park2	Parkinson disease (autosomal recessive, juvenile) 2, parkin	dopamine uptake involved in synaptic transmission	Dopamine transport & uptake
MGI:2135637	Park7	Parkinson disease (autosomal recessive, early onset) 7	dopamine uptake involved in synaptic transmission	Dopamine transport & uptake
MGI:2135637	Park7	Parkinson disease (autosomal recessive, early onset) 7	positive regulation of dopamine biosynthetic process	Dopamine metabolism
MGI:2135637	Park7	Parkinson disease (autosomal recessive, early onset) 7	synaptic transmission, dopaminergic	Dopamine secretion & synaptic transmission
MGI:97486	Pax2	paired box 2	dopaminergic neuron differentiation	Dopaminergic neuron development
MGI:97489	Pax5	paired box 5	dopaminergic neuron differentiation	Dopaminergic neuron development
MGI:97509	Pcp4	Purkinje cell protein 4	positive regulation of dopamine secretion	Dopamine secretion & synaptic transmission
MGI:97523	Pde1b	phosphodiesterase 1B, Ca2+- calmodulin dependent	regulation of dopamine metabolic process	Dopamine metabolism

MGI Gene/ Marker ID	*Gene symbol*	*Gene name*	*Annotated function*	*GoSlim annotation*
MGI:1100882	Phox2b	paired-like homeobox 2b	dopaminergic neuron differentiation	Dopaminergic neuron development
MGI:1916193	Pink1	PTEN induced putative kinase 1	positive regulation of dopamine secretion	Dopamine secretion & synaptic transmission
MGI:1916193	Pink1	PTEN induced putative kinase 1	positive regulation of synaptic transmission, dopaminergic	Dopamine secretion & synaptic transmission
MGI:1100498	Pitx3	paired-like homeodomain transcription factor 3	dopaminergic neuron differentiation	Dopaminergic neuron development
MGI:97629	Pmch	pro-melanin-concentrating hormone	negative regulation of synaptic transmission, dopaminergic	Dopamine secretion & synaptic transmission
MGI:1930773	Pnkd	paroxysmal nonkinesiogenic dyskinesia	regulation of dopamine metabolic process	Dopamine metabolism
MGI:1930773	Pnkd	paroxysmal nonkinesiogenic dyskinesia	regulation of synaptic transmission, dopaminergic	Dopamine secretion & synaptic transmission
MGI:94860	Ppp1r1b	protein phosphatase 1, regulatory (inhibitor) subunit 1B	D1 dopamine receptor binding	Dopamine receptor binding
MGI:94860	Ppp1r1b	protein phosphatase 1, regulatory (inhibitor) subunit 1B	D2 dopamine receptor binding	Dopamine receptor binding
MGI:94860	Ppp1r1b	protein phosphatase 1, regulatory (inhibitor) subunit 1B	D3 dopamine receptor binding	Dopamine receptor binding
MGI:94860	Ppp1r1b	protein phosphatase 1, regulatory (inhibitor) subunit 1B	D4 dopamine receptor binding	Dopamine receptor binding
MGI:94860	Ppp1r1b	protein phosphatase 1, regulatory (inhibitor) subunit 1B	D5 dopamine receptor binding	Dopamine receptor binding
MGI:2387581	Ppp1r9b	protein phosphatase 1, regulatory subunit 9B	D2 dopamine receptor binding	Dopamine receptor binding
MGI:97596	Prkcb	protein kinase C, beta	regulation of dopamine secretion	Dopamine secretion & synaptic transmission
MGI:1355296	Prkn	parkin RBR E3 ubiquitin protein ligase	dopamine metabolic process	Dopamine metabolism
MGI:1355296	Prkn	parkin RBR E3 ubiquitin protein ligase	dopamine uptake involved in synaptic transmission	Dopamine transport & uptake

MGI Gene/ Marker ID	*Gene symbol*	*Gene name*	*Annotated function*	*GoSlim annotation*
MGI:1355296	Prkn	parkin RBR E3 ubiquitin protein ligase	regulation of dopamine metabolic process	Dopamine metabolism
MGI:1355296	Prkn	parkin RBR E3 ubiquitin protein ligase	synaptic transmission, dopaminergic	Dopamine secretion & synaptic transmission
MGI:1351645	Prmt5	protein arginine N-methyltransferase 5	positive regulation of adenylate cyclase-inhibiting dopamine receptor signaling pathway	Signal transduction
MGI:97793	Ptger1	prostaglandin E receptor 1 (subtype EP1)	D1 dopamine receptor binding	Dopamine receptor binding
MGI:97793	Ptger1	prostaglandin E receptor 1 (subtype EP1)	adenylate cyclase-activating dopamine receptor signaling pathway	Signal transduction
MGI:97798	Ptgs2	prostaglandin-endoperoxide synthase 2	negative regulation of synaptic transmission, dopaminergic	Dopamine secretion & synaptic transmission
MGI:99511	Ptpn11	protein tyrosine phosphatase, non-receptor type 11	D1 dopamine receptor binding	Dopamine receptor binding
MGI:1917158	Rab3b	RAB3B, member RAS oncogene family	positive regulation of dopamine uptake involved in synaptic transmission	Dopamine transport & uptake
MGI:97845	Rac1	Rac family small GTPase 1	dopaminergic neuron differentiation	Dopaminergic neuron development
MGI:97845	Rac1	Rac family small GTPase 1	midbrain dopaminergic neuron differentiation	Dopaminergic neuron development
MGI:1922391	Rasd2	RASD family, member 2	synaptic transmission, dopaminergic	Dopamine secretion & synaptic transmission
MGI:108409	Rgs4	regulator of G-protein signaling 4	negative regulation of dopamine receptor signaling pathway	Signal transduction
MGI:108408	Rgs8	regulator of G-protein signaling 8	regulation of dopamine receptor signaling pathway	Signal transduction
MGI:1338824	Rgs9	regulator of G-protein signaling 9	dopamine receptor signaling pathway	Signal transduction
MGI:1915045	Rnls	renalase, FAD-dependent amine oxidase	dopamine metabolic process	Dopamine metabolism
MGI:1922667	Rspo2	R-spondin 2	dopaminergic neuron differentiation	Dopaminergic neuron development
MGI:1915835	Rtn4	reticulon 4	positive regulation of dopamine secretion	Dopamine secretion & synaptic transmission

MGI Gene/ Marker ID	*Gene symbol*	*Gene name*	*Annotated function*	*GoSlim annotation*
MGI:101766	Ryk	receptor-like tyrosine kinase	chemorepulsion of dopaminergic neuron axon	Dopaminergic neuron development
MGI:101766	Ryk	receptor-like tyrosine kinase	midbrain dopaminergic neuron differentiation	Dopaminergic neuron development
MGI:892014	Sfrp1	secreted frizzled-related protein 1	dopaminergic neuron differentiation	Dopaminergic neuron development
MGI:892014	Sfrp1	secreted frizzled-related protein 1	regulation of midbrain dopaminergic neuron differentiation	Dopaminergic neuron development
MGI:108078	Sfrp2	secreted frizzled-related protein 2	regulation of midbrain dopaminergic neuron differentiation	Dopaminergic neuron development
MGI:98297	Shh	sonic hedgehog	dopaminergic neuron differentiation	Dopaminergic neuron development
MGI:98297	Shh	sonic hedgehog	negative regulation of dopaminergic neuron differentiation	Dopaminergic neuron development
MGI:106684	Slc18a1	solute carrier family 18 (vesicular monoamine), member 1	positive regulation of dopamine secretion	Dopamine secretion & synaptic transmission
MGI:108111	Slc22a1	solute carrier family 22 (organic cation transporter), member 1	dopamine transmembrane transporter activity	Dopamine transport & uptake
MGI:108111	Slc22a1	solute carrier family 22 (organic cation transporter), member 1	dopamine transport	Dopamine transport & uptake
MGI:1335072	Slc22a2	solute carrier family 22 (organic cation transporter), member 2	dopamine transmembrane transporter activity	Dopamine transport & uptake
MGI:1335072	Slc22a2	solute carrier family 22 (organic cation transporter), member 2	dopamine transport	Dopamine transport & uptake
MGI:1333817	Slc22a3	solute carrier family 22 (organic cation transporter), member 3	dopamine transmembrane transporter activity	Dopamine transport & uptake
MGI:1333817	Slc22a3	solute carrier family 22 (organic cation transporter), member 3	dopamine transport	Dopamine transport & uptake
MGI:94862	Slc6a3	solute carrier family 6 (neurotransmitter transporter, dopamine), member 3	dopamine biosynthetic process	Dopamine metabolism

MGI Gene/ Marker ID	*Gene symbol*	*Gene name*	*Annotated function*	*GoSlim annotation*
MGI:94862	Slc6a3	solute carrier family 6 (neurotransmitter transporter, dopamine), member 3	dopamine catabolic process	Dopamine metabolism
MGI:94862	Slc6a3	solute carrier family 6 (neurotransmitter transporter, dopamine), member 3	dopamine transmembrane transporter activity	Dopamine transport & uptake
MGI:94862	Slc6a3	solute carrier family 6 (neurotransmitter transporter, dopamine), member 3	dopamine transport	Dopamine transport & uptake
MGI:94862	Slc6a3	solute carrier family 6 (neurotransmitter transporter, dopamine), member 3	dopamine uptake	Dopamine transport & uptake
MGI:94862	Slc6a3	solute carrier family 6 (neurotransmitter transporter, dopamine), member 3	dopamine uptake involved in synaptic transmission	Dopamine transport & uptake
MGI:94862	Slc6a3	solute carrier family 6 (neurotransmitter transporter, dopamine), member 3	dopamine: sodium symporter activity	Dopamine transport & uptake
MGI:94862	Slc6a3	solute carrier family 6 (neurotransmitter transporter, dopamine), member 3	regulation of dopamine metabolic process	Dopamine metabolism
MGI:96285	Slc6a4	solute carrier family 6 (neurotransmitter transporter, serotonin), member 4	dopamine uptake involved in synaptic transmission	Dopamine transport & uptake
MGI:96285	Slc6a4	solute carrier family 6 (neurotransmitter transporter, serotonin), member 4	dopamine: sodium symporter activity	Dopamine transport & uptake
MGI:96285	Slc6a4	solute carrier family 6 (neurotransmitter transporter, serotonin), member 4	negative regulation of synaptic transmission, dopaminergic	Dopamine secretion & synaptic transmission

MGI Gene/ Marker ID	*Gene symbol*	*Gene name*	*Annotated function*	*GoSlim annotation*
MGI:96285	Slc6a4	solute carrier family 6 (neurotransmitter transporter, serotonin), member 4	negative regulation of synaptic transmission, dopaminergic	Dopamine secretion & synaptic transmission
MGI:1349482	Slc9a3r1	solute carrier family 9 (sodium/hydrogen exchanger), member 3 regulator 1	adenylate cyclase-activating dopamine receptor signaling pathway	Signal transduction
MGI:1349482	Slc9a3r1	solute carrier family 9 (sodium/hydrogen exchanger), member 3 regulator 1	phospholipase C-activating dopamine receptor signaling pathway	Signal transduction
MGI:1927578	Smpd3	sphingomyelin phosphodiesterase 3, neutral	dopamine uptake	Dopamine transport & uptake
MGI:1277151	Snca	synuclein, alpha	dopamine biosynthetic process	Dopamine metabolism
MGI:1277151	Snca	synuclein, alpha	dopamine metabolic process	Dopamine metabolism
MGI:1277151	Snca	synuclein, alpha	negative regulation of dopamine metabolic process	Dopamine metabolism
MGI:1277151	Snca	synuclein, alpha	negative regulation of dopamine uptake involved in synaptic transmission	Dopamine transport & uptake
MGI:1277151	Snca	synuclein, alpha	regulation of dopamine secretion	Dopamine secretion & synaptic transmission
MGI:1277151	Snca	synuclein, alpha	synaptic transmission, dopaminergic	Dopamine secretion & synaptic transmission
MGI:1915097	Sncaip	synuclein, alpha interacting protein (synphilin)	dopamine metabolic process	Dopamine metabolism
MGI:1889011	Sncb	synuclein, beta	dopamine metabolic process	Dopamine metabolism
MGI:1298397	Sncg	synuclein, gamma	regulation of dopamine secretion	Dopamine secretion & synaptic transmission
MGI:103078	Spr	sepiapterin reductase	dopamine metabolic process	Dopamine metabolism
MGI:102896	Sult1a1	sulfotransferase family 1A, phenol-preferring, member 1	aryl sulfotransferase activity	Dopamine metabolism
MGI:2136282	Sult1b1	sulfotransferase family 1B, member 1	aryl sulfotransferase activity	Dopamine metabolism

MGI Gene/ Marker ID	*Gene symbol*	*Gene name*	*Annotated function*	*GoSlim annotation*
MGI:102928	Sult1c1	sulfotransferase family, cytosolic, 1C, member 1	aryl sulfotransferase activity	Dopamine metabolism
MGI:1926341	Sult1d1	sulfotransferase family 1D, member 1	aryl sulfotransferase activity	Dopamine metabolism
MGI:99667	Syt1	synaptotagmin I	regulation of dopamine secretion	Dopamine secretion & synaptic transmission
MGI:101759	Syt4	synaptotagmin IV	regulation of dopamine secretion	Dopamine secretion & synaptic transmission
MGI:1859545	Syt7	synaptotagmin VII	regulation of dopamine secretion	Dopamine secretion & synaptic transmission
MGI:2148258	Taar1	trace amine-associated receptor 1	adenylate cyclase-activating dopamine receptor signaling pathway	Signal transduction
MGI:892968	Tacr3	tachykinin receptor 3	regulation of dopamine metabolic process	Dopamine metabolism
MGI:98726	Tgfb2	transforming growth factor, beta 2	dopamine biosynthetic process	Dopamine metabolism
MGI:98735	Th	tyrosine hydroxylase	dopamine biosynthetic process	Dopamine metabolism
MGI:98735	Th	tyrosine hydroxylase	synaptic transmission, dopaminergic	Dopamine secretion & synaptic transmission
MGI:103306	Tiam1	T cell lymphoma invasion and metastasis 1	regulation of dopaminergic neuron differentiation	Dopaminergic neuron development
MGI:1353568	Tor1a	torsin family 1, member A (torsin A)	regulation of dopamine uptake involved in synaptic transmission	Dopamine transport & uptake
MGI:98849	Tshr	thyroid stimulating hormone receptor	dopaminergic neuron differentiation	Dopaminergic neuron development
MGI:2135272	Vangl2	VANGL planar cell polarity 2	dopaminergic neuron axon guidance	Dopaminergic neuron development
MGI:103178	Vegfa	vascular endothelial growth factor A	dopaminergic neuron differentiation	Dopaminergic neuron development
MGI:108037	Vegfd	vascular endothelial growth factor D	dopaminergic neuron differentiation	Dopaminergic neuron development
MGI:1890467	Vps35	VPS35 retromer complex component	positive regulation of dopamine biosynthetic process	Dopamine metabolism
MGI:1890467	Vps35	VPS35 retromer complex component	D1 dopamine receptor binding	Dopamine receptor binding

MGI Gene/ Marker ID	*Gene symbol*	*Gene name*	*Annotated function*	*GoSlim annotation*
MGI:1890467	Vps35	VPS35 retromer complex component	positive regulation of dopamine receptor signaling pathway	Signal transduction
MGI:98953	Wnt1	wingless-type MMTV integration site family, member 1	astrocyte-dopaminergic neuron signaling	Dopaminergic neuron development
MGI:98953	Wnt1	wingless-type MMTV integration site family, member 1	canonical Wnt signaling pathway involved in midbrain dopaminergic neuron differentiation	Dopaminergic neuron development
MGI:98953	Wnt1	wingless-type MMTV integration site family, member 1	dopaminergic neuron differentiation	Dopaminergic neuron development
MGI:98953	Wnt1	wingless-type MMTV integration site family, member 1	midbrain dopaminergic neuron differentiation	Dopaminergic neuron development
MGI:98954	Wnt2	wingless-type MMTV integration site family, member 2	canonical Wnt signaling pathway involved in midbrain dopaminergic neuron differentiation	Dopaminergic neuron development
MGI:98954	Wnt2	wingless-type MMTV integration site family, member 2	midbrain dopaminergic neuron differentiation	Dopaminergic neuron development
MGI:98955	Wnt3	wingless-type MMTV integration site family, member 3	canonical Wnt signaling pathway involved in midbrain dopaminergic neuron differentiation	Dopaminergic neuron development
MGI:98956	Wnt3a	wingless-type MMTV integration site family, member 3A	dopaminergic neuron differentiation	Dopaminergic neuron development
MGI:98956	Wnt3a	wingless-type MMTV integration site family, member 3A	negative regulation of dopaminergic neuron differentiation	Dopaminergic neuron development
MGI:98958	Wnt5a	wingless-type MMTV integration site family, member 5A	chemorepulsion of dopaminergic neuron axon	Dopaminergic neuron development
MGI:98958	Wnt5a	wingless-type MMTV integration site family, member 5A	dopaminergic neuron differentiation	Dopaminergic neuron development
MGI:98958	Wnt5a	wingless-type MMTV integration site family, member 5A	midbrain dopaminergic neuron differentiation	Dopaminergic neuron development

MGI Gene/ Marker ID	*Gene symbol*	*Gene name*	*Annotated function*	*GoSlim annotation*
MGI:98958	Wnt5a	wingless-type MMTV integration site family, member 5A	Wnt signaling pathway involved in midbrain dopaminergic neuron differentiation	Dopaminergic neuron development
MGI:98962	Wnt7b	wingless-type MMTV integration site family, member 7B	chemoattraction of dopaminergic neuron axon	Dopaminergic neuron development
MGI:1197020	Wnt9b	wingless-type MMTV integration site family, member 9B	midbrain dopaminergic neuron differentiation	Dopaminergic neuron development
MGI:1197020	Wnt9b	wingless-type MMTV integration site family, member 9B	non-canonical Wnt signaling pathway involved in midbrain dopaminergic neuron differentiation	Dopaminergic neuron development

Supplemental Table 2: DSP transcripts that are regulated by experience in Layer 4

Gene	*Control Mean*	*Control STD*	*Deprived Mean*	*Deprived STD*	*Deprived Control*	*p*	*Annotation*	*Simplified Annotation*
Abat	12433	1095.79	10442.75	1036.9	0.84	0.02	positive regulation of dopamine metabolic process	Dopamine metabolism
Adcy5	5218.5	248	4334.5	291.87	0.831	0.02	adenylate cyclase-activating dopamine receptor signaling pathway	Signal transduction
Adcy6	3543.75	180.92	3100.75	261.38	0.875	0.02	dopamine receptor signaling pathway	Signal transduction
Agtr2	9.75	3.3	4.5	1.29	0.5	0.03	dopamine biosynthetic process	Dopamine metabolism

Gene	*Control Mean*	*Control STD*	*Deprived Mean*	*Deprived STD*	*Deprived Control*	*p*	*Annotation*	*Simplified Annotation*
Alk	320	35.29	239.75	18.7	0.75	0.02	regulation of dopamine receptor signaling pathway	Signal transduction
Arrb2	1449.25	103.29	1230	70.58	0.849	0.04	D1 dopamine receptor binding	Dopamine receptor binding
Caly	3604.25	222.67	3064.75	79.97	0.85	0.02	dopamine receptor signaling pathway	Signal transduction
Cdk5	4638.75	171.48	3795.5	163.66	0.818	0.02	synaptic transmission, dopaminergic	Dopamine secretion & synaptic transmission
Celsr3	6461.5	712	4975.5	209.38	0.77	0.02	dopaminergic neuron axon guidance	Dopaminergic neuron development
Chrna7	501.75	35.47	408	73.11	0.813	0.04	regulation of synaptic transmission, dopaminergic	Dopamine secretion & synaptic transmission
Csnk1d	7071	641.07	6028.75	345.17	0.853	0.02	positive regulation of Wnt-mediated midbrain dopaminergic neuron differentiation	Dopaminergic neuron development
Cxcl12	1696.25	257.92	1318.5	181.48	0.778	0.02	positive regulation of dopamine secretion	Dopamine secretion & synaptic transmission
Ddc	233.25	33.23	131.25	20.69	0.562	0.02	dopamine biosynthetic process	Dopamine metabolism
Dmrta2	259.75	17.04	218.75	22.74	0.842	0.02	dopaminergic neuron differentiation	Dopaminergic neuron development

Gene	*Control Mean*	*Control STD*	*Deprived Mean*	*Deprived STD*	*Deprived Control*	*p*	*Annotation*	*Simplified Annotation*
Dnajc14	2218.25	148.53	1913.75	151.05	0.863	0.04	dopamine receptor binding	Dopamine receptor binding
Dnm1	75977	2516.02	66992.5	3443.36	0.882	0.02	D2 dopamine receptor binding	Dopamine receptor binding
Dnm2	2758.5	169.83	2336.25	134.11	0.847	0.02	D2 dopamine receptor binding	Dopamine receptor binding
Dtnbp1	2176.5	212.64	1910.5	114.78	0.878	0.04	regulation of dopamine secretion	Dopamine secretion & synaptic transmission
Dvl3	4069.5	185.76	3721	257.16	0.914	0.04	Wnt signaling pathway involved in midbrain dopaminergic neuron differentiation	Dopaminergic neuron development
Epas1	7541.75	603.01	5910	371.05	0.784	0.02	positive regulation of dopamine biosynthetic process	Dopamine metabolism
Flna	3484.5	284.75	2806.25	178.2	0.805	0.02	adenylate cyclase-inhibiting dopamine receptor signaling pathway	Signal transduction
Flot1	3960.25	242.13	3595.25	156.29	0.908	0.04	positive regulation of synaptic transmission, dopaminergic	Dopamine secretion & synaptic transmission

Gene	*Control Mean*	*Control STD*	*Deprived Mean*	*Deprived STD*	*Deprived Control*	*p*	*Annotation*	*Simplified Annotation*
Gna11	6642	251.42	5669	388.3	0.854	0.02	phospholipase C-activating dopamine receptor signaling pathway	Signal transduction
Gna13	2530.75	336.83	2076.75	240.74	0.821	0.04	D5 dopamine receptor binding	Dopamine receptor binding
Gnao1	35292.25	1266.72	30041.75	2072.49	0.851	0.02	dopamine receptor signaling pathway	Signal transduction
Gnaq	14442.5	544.48	12844.5	1185.72	0.889	0.04	phospholipase C-activating dopamine receptor signaling pathway	Signal transduction
Gnas	57953	1476.13	50840.75	2235.83	0.877	0.02	D1 dopamine receptor binding	Dopamine receptor binding
Gsk3b	13640.25	685.19	11525.5	892.5	0.845	0.02	negative regulation of dopaminergic neuron differentiation	Dopaminergic neuron development
Hprt	4631.75	175.63	3833.75	178.08	0.828	0.02	dopamine metabolic process	Dopamine metabolism
Htr1b	31.25	12.31	63.25	13.94	2.032	0.02	regulation of dopamine secretion	Dopamine secretion & synaptic transmission
Htr2a	880.25	24.76	718.5	124.74	0.817	0.04	regulation of dopamine secretion	Dopamine secretion & synaptic transmission

Gene	*Control Mean*	*Control STD*	*Deprived Mean*	*Deprived STD*	*Deprived Control*	*p*	*Annotation*	*Simplified Annotation*
Htt	10600.5	769.97	8861	809.49	0.836	0.04	dopamine receptor signaling pathway	Signal transduction
Kcna2	22898.5	2076.99	17503.25	800.84	0.764	0.02	regulation of dopamine secretion	Dopamine secretion & synaptic transmission
Lrp6	2627.25	141.69	2185.5	283.93	0.832	0.04	dopaminergic neuron differentiation	Dopaminergic neuron development
Maoa	983.5	114.09	749.25	53.07	0.761	0.02	dopamine catabolic process	Dopamine metabolism
Mapk1	27162.25	1101.66	22163.25	2199.38	0.816	0.02	cellular response to dopamine	Signal transduction
Nat8l	35366.25	1116.27	27845.5	2296.42	0.787	0.02	positive regulation of dopamine uptake involved in synaptic transmission	Dopamine transport & uptake
Nsf	38488	1763.08	33046.25	1893.91	0.859	0.02	D1 dopamine receptor binding	Dopamine receptor binding
Nsg1	10867.75	344.4	9548.5	733.47	0.879	0.04	dopamine receptor signaling pathway	Signal transduction
Palm	12423.25	830.14	10411.25	1001.45	0.838	0.04	D3 dopamine receptor binding	Dopamine receptor binding
Park7	3315.75	230.39	2756.25	136.29	0.831	0.02	dopamine uptake involved in synaptic transmission	Dopamine transport & uptake

Gene	*Control Mean*	*Control STD*	*Deprived Mean*	*Deprived STD*	*Deprived Control*	*p*	*Annotation*	*Simplified Annotation*
Pde1b	6781.5	229.49	5617.75	245.81	0.828	0.02	regulation of dopamine metabolic process	Dopamine metabolism
Pink1	17597.25	746.22	14907	690.59	0.847	0.02	positive regulation of dopamine secretion	Dopamine secretion & synaptic transmission
Pnkd	6712.75	436.05	5775.25	295.54	0.86	0.02	regulation of dopamine metabolic process	Dopamine metabolism
Ppp1r1b	5428.5	498.36	4564.5	597.89	0.841	0.02	D1 dopamine receptor binding	Dopamine receptor binding
Prkcb	64249	4046.23	51872.25	5531.43	0.807	0.02	regulation of dopamine secretion	Dopamine secretion & synaptic transmission
Prmt5	2578.25	221.79	2082	79.53	0.808	0.02	positive regulation of adenylate cyclase-inhibiting dopamine receptor signaling pathway	Signal transduction
Ptpn11	8409.75	86.45	7068.75	359.35	0.841	0.02	D1 dopamine receptor binding	Dopamine receptor binding
Rac1	11389	536.09	10066.25	603.72	0.884	0.04	dopaminergic neuron differentiation	Dopaminergic neuron development
Rspo2	38	24.26	76.5	8.58	2.026	0.03	dopaminergic neuron differentiation	Dopaminergic neuron development
Rtn4	38429.5	1689.54	32169.75	1857.11	0.837	0.02	positive regulation of dopamine secretion	Dopamine secretion & synaptic transmission

Gene	*Control Mean*	*Control STD*	*Deprived Mean*	*Deprived STD*	*Deprived Control*	*p*	*Annotation*	*Simplified Annotation*
Smpd3	5774	626.83	4422.75	221.47	0.766	0.02	dopamine uptake	Dopamine transport & uptake
Sncb	22496.25	1523.84	19760.25	1182.76	0.878	0.04	dopamine metabolic process	Dopamine metabolism
Sncg	11.25	4.27	4.75	3.3	0.455	0.04	regulation of dopamine secretion	Dopamine secretion & synaptic transmission
Sult1a1	395	122.53	233	42.34	0.59	0.02	aryl sulfotransferase activity	Dopamine metabolism
Syt1	67977.25	1926.07	56713	3979.46	0.834	0.02	regulation of dopamine secretion	Dopamine secretion & synaptic transmission
Syt7	10836.5	782.01	8804.5	1103.29	0.812	0.02	regulation of dopamine secretion	Dopamine secretion & synaptic transmission
Tgfb2	294.25	18.25	242.5	29.56	0.827	0.04	dopamine biosynthetic process	Dopamine metabolism
Tiam1	7834.5	764.03	5727.25	350.66	0.731	0.02	regulation of dopaminergic neuron differentiation	Dopaminergic neuron development
Vps35	6385.5	300.69	5463	479.09	0.855	0.04	positive regulation of dopamine biosynthetic process	Dopamine metabolism
Wnt2	106.5	40.17	233.25	41.96	2.178	0.02	canonical Wnt signaling pathway involved in midbrain dopaminergic neuron differentiation	Dopaminergic neuron development

Supplemental Table 3: DSP transcripts that are regulated by experience in Layer 2/3

Gene	*Control Mean*	*Control STD*	*Deprived Mean*	*Deprived STD*	*Deprived/ Control*	*p*	*Annotation*	*Simplified Annotation*
Abat	14048	1370.6	11111.5	200.03	0.791	0.02	positive regulation of dopamine metabolic process	Dopamine metabolism
Adcy5	5697.75	506.31	4698.25	228.1	0.824	0.02	adenylate cyclase-activating dopamine receptor signaling pathway	Signal transduction
Adora2a	116	2.58	94.25	3.1	0.81	0.02	synaptic transmission, dopaminergic	Dopamine secretion & synaptic transmission
Atf4	6979.5	290.96	5338.5	454.79	0.765	0.02	cellular response to dopamine	Signal transduction
Atp1a3	98113.5	6894.87	82678.75	5509.73	0.843	0.04	D1 dopamine receptor binding	Dopamine receptor binding
Atp7a	494.25	79.67	371.75	28.11	0.753	0.04	dopamine metabolic process	Dopamine metabolism
Caly	4480.5	469.23	3556.75	370.87	0.794	0.04	dopamine receptor signaling pathway	Signal transduction
Cav2	1474	119.27	1269	60.39	0.861	0.02	D1 dopamine receptor binding	Dopamine receptor binding
Cdk5	4294.25	326.36	3384	306.92	0.788	0.02	synaptic transmission, dopaminergic	Dopamine secretion & synaptic transmission
Cdnf	75.25	25.24	32.5	7.85	0.44	0.02	dopaminergic neuron differentiation	Dopaminergic neuron development
Chrna4	904.75	78.86	678.25	32.67	0.749	0.02	positive regulation of dopamine secretion	Dopamine secretion & synaptic transmission
Chrna7	684.5	109.99	568.75	42.17	0.831	0.04	regulation of synaptic transmission, dopaminergic	Dopamine secretion & synaptic transmission

Gene	*Control Mean*	*Control STD*	*Deprived Mean*	*Deprived STD*	*Deprived/ Control*	*p*	*Annotation*	*Simplified Annotation*
Chrnb2	1958	181.14	1572.75	155.48	0.803	0.04	regulation of dopamine metabolic process	Dopamine metabolism
Cnr1	9583.5	1513.18	7764.75	295.14	0.81	0.02	negative regulation of dopamine secretion	Dopamine secretion & synaptic transmission
Cntnap4	390.75	16.46	335.75	49.4	0.859	0.03	regulation of synaptic transmission, dopaminergic	Dopamine secretion & synaptic transmission
Comt	2866	146.11	2540.75	175.25	0.887	0.04	dopamine catabolic process	Dopamine metabolism
Crhbp	726.75	82.79	548.5	115.36	0.755	0.02	synaptic transmission, dopaminergic	Dopamine secretion & synaptic transmission
Csnk1d	7401.25	131.68	6445.25	540.97	0.871	0.02	positive regulation of Wnt-mediated midbrain dopaminergic neuron differentiation	Dopaminergic neuron development
Ctnnb1	21394.75	982.6	16776.75	342.75	0.784	0.02	midbrain dopaminergic neuron differentiation	Dopaminergic neuron development
Cyp2d22	1286.5	140.41	1013.75	34.99	0.788	0.02	dopamine biosynthetic process	Dopamine metabolism
Dbh	32.25	10.75	13.5	5.2	0.438	0.04	dopamine beta-monooxygenase activity	Dopamine metabolism
Ddc	126.5	26.79	64.25	16.68	0.504	0.02	dopamine biosynthetic process	Dopamine metabolism
Dlg4	73298.25	6629.59	61278	2536.78	0.836	0.04	D1 dopamine receptor binding	Dopamine receptor binding
Dnajc14	2398.75	152.35	1945.25	78.99	0.811	0.02	dopamine receptor binding	Dopamine receptor binding

Gene	*Control Mean*	*Control STD*	*Deprived Mean*	*Deprived STD*	*Deprived/ Control*	*p*	*Annotation*	*Simplified Annotation*
Dnm1	70790.5	5579.07	59844	4894.96	0.845	0.04	D2 dopamine receptor binding	Dopamine receptor binding
Dnm2	2708	257.28	2259.75	106	0.835	0.02	D2 dopamine receptor binding	Dopamine receptor binding
Drd4	77	15.14	35.25	10.63	0.455	0.02	regulation of dopamine metabolic process	Dopamine metabolism
Dtnbp1	1902.5	136.33	1599	76.67	0.84	0.02	regulation of dopamine secretion	Dopamine secretion & synaptic transmission
Dvl3	4338.5	309.53	3665.25	243.52	0.845	0.02	Wnt signaling pathway involved in midbrain dopaminergic neuron differentiation	Dopaminergic neuron development
Epas1	9253	1171.95	6847	421.41	0.74	0.02	positive regulation of dopamine biosynthetic process	Dopamine metabolism
Flna	3934.75	208.69	3268.75	248.78	0.831	0.02	adenylate cyclase-inhibiting dopamine receptor signaling pathway	Signal transduction
Fzd3	9806.75	449.27	7209	720.46	0.735	0.02	dopaminergic neuron axon guidance	Dopaminergic neuron development
Gabbr1	35228	2720.57	29889.5	1780.02	0.848	0.04	negative regulation of dopamine secretion	Dopamine secretion & synaptic transmission
Gabpa	1005.5	38.93	856.25	77.21	0.851	0.02	cellular response to dopamine	Signal transduction
Gna11	7650.5	417.09	6249.75	348.2	0.817	0.02	phospholipase C-activating dopamine receptor signaling pathway	Signal transduction

Gene	*Control Mean*	*Control STD*	*Deprived Mean*	*Deprived STD*	*Deprived/ Control*	*p*	*Annotation*	*Simplified Annotation*
Gna12	2723.25	123.14	2447.5	60.39	0.899	0.02	D5 dopamine receptor binding	Dopamine receptor binding
Gna13	3318.5	140.12	2484.25	147.92	0.748	0.02	D5 dopamine receptor binding	Dopamine receptor binding
Gnai3	1626.75	77.27	1364.5	98.49	0.839	0.02	dopamine receptor signaling pathway	Signal transduction
Gnal	6584.25	439.54	5319.5	162.67	0.808	0.02	adenylate cyclase-activating dopamine receptor signaling pathway	Signal transduction
Gnao1	39903.5	1913.77	33228	1647.21	0.833	0.02	dopamine receptor signaling pathway	Signal transduction
Gnaq	15059.75	417.32	12561.25	472.6	0.834	0.02	phospholipase C-activating dopamine receptor signaling pathway	Signal transduction
Gnas	55141	2431.46	45711.25	3836.78	0.829	0.02	D1 dopamine receptor binding	Dopamine receptor binding
Gpr21	137	18.74	102.25	15.52	0.745	0.04	dopamine neurotransmitter receptor activity, coupled via Gs	Dopamine receptor binding
Grin2a	2141.5	254.5	1598	271.14	0.746	0.02	dopamine metabolic process	Dopamine metabolism
Gsk3b	13804.75	511.38	11186.25	550.29	0.81	0.02	negative regulation of dopaminergic neuron differentiation	Dopaminergic neuron development
Hif1a	4100	192.05	3248.5	131.68	0.792	0.02	dopaminergic neuron differentiation	Dopaminergic neuron development
Hprt	3658.25	154.6	2939	232.57	0.803	0.02	dopamine metabolic process	Dopamine metabolism

Gene	*Control Mean*	*Control STD*	*Deprived Mean*	*Deprived STD*	*Deprived/ Control*	*p*	*Annotation*	*Simplified Annotation*
Htr2a	547.75	52.73	406.25	35.37	0.741	0.02	regulation of dopamine secretion	Dopamine secretion & synaptic transmission
Htr7	718.25	119.21	520.75	72.69	0.726	0.04	dopaminergic neuron differentiation	Dopaminergic neuron development
Htt	10536.75	784.17	8448	618.94	0.802	0.02	dopamine receptor signaling pathway	Signal transduction
Kcna2	14800.25	1494.72	10777	1233.92	0.728	0.02	regulation of dopamine secretion	Dopamine secretion & synaptic transmission
Kcnq4	404.25	27.1	351.5	18.21	0.871	0.02	negative regulation of synaptic transmission, dopaminergic	Dopamine secretion & synaptic transmission
Klf16	3725	204.22	3189.25	201.71	0.856	0.02	dopamine receptor signaling pathway	Signal transduction
Lrp6	2999.5	289.89	2223.5	87.75	0.741	0.02	dopaminergic neuron differentiation	Dopaminergic neuron development
Maoa	1189	131.31	834	90.4	0.701	0.02	dopamine catabolic process	Dopamine metabolism
Mapk1	33835.25	1492.65	26602.75	1147.62	0.786	0.02	cellular response to dopamine	Signal transduction
Nat8l	26036.5	1736.46	20632	2486.03	0.792	0.02	positive regulation of dopamine uptake involved in synaptic transmission	Dopamine transport & uptake
Npr1	198	28.2	124	16.57	0.626	0.02	dopamine metabolic process	Dopamine metabolism
Nr4a2	1562.5	274.06	1176	158.16	0.752	0.04	dopamine biosynthetic process	Dopamine metabolism
Nsf	33947	1752.59	27791.5	2195.9	0.819	0.02	D1 dopamine receptor binding	Dopamine receptor binding

Gene	*Control Mean*	*Control STD*	*Deprived Mean*	*Deprived STD*	*Deprived/ Control*	*p*	*Annotation*	*Simplified Annotation*
Nsg1	11183.5	446.17	9139.25	711.3	0.817	0.02	dopamine receptor signaling pathway	Signal transduction
Nsg2	28109.25	1875.37	23648.25	1628.51	0.841	0.04	dopamine receptor signaling pathway	Signal transduction
Palm	14897.75	1416.72	12113.5	472.56	0.813	0.02	D3 dopamine receptor binding	Dopamine receptor binding
Park2	248.75	24.1	183.75	26.69	0.739	0.02	dopamine uptake involved in synaptic transmission	Dopamine transport & uptake
Park7	3064.25	182.54	2519	203.96	0.822	0.02	dopamine uptake involved in synaptic transmission	Dopamine transport & uptake
Pcp4	794.5	69.29	605.5	48.56	0.762	0.02	positive regulation of dopamine secretion	Dopamine secretion & synaptic transmission
Pde1b	6529.75	459.47	5072.75	403.99	0.777	0.02	regulation of dopamine metabolic process	Dopamine metabolism
Pink1	15524.25	1066.31	12763	950.4	0.822	0.04	positive regulation of dopamine secretion	Dopamine secretion & synaptic transmission
Pnkd	5530.25	296.03	4386	532.24	0.793	0.02	regulation of dopamine metabolic process	Dopamine metabolism
Ppp1r1b	4550.75	674.32	3184.5	548.64	0.7	0.04	D1 dopamine receptor binding	Dopamine receptor binding
Ppp1r9b	69927.5	8336.48	58363.5	1635.93	0.835	0.04	D2 dopamine receptor binding	Dopamine receptor binding
Prkcb	72420	5020.88	56077.25	3467.21	0.774	0.02	regulation of dopamine secretion	Dopamine secretion & synaptic transmission

Gene	*Control Mean*	*Control STD*	*Deprived Mean*	*Deprived STD*	*Deprived/ Control*	*p*	*Annotation*	*Simplified Annotation*
Prmt5	2468.75	90.65	2000	137.33	0.81	0.02	positive regulation of adenylate cyclase-inhibiting dopamine receptor signaling pathway	Signal transduction
Ptger1	1399	85.31	1152.25	98.11	0.823	0.02	D1 dopamine receptor binding	Dopamine receptor binding
Ptpn11	8402.75	437.66	6726.5	508.84	0.801	0.02	D1 dopamine receptor binding	Dopamine receptor binding
Rac1	11543.75	389.59	9651	560.43	0.836	0.02	dopaminergic neuron differentiation	Dopaminergic neuron development
Rgs4	40472.75	1986.12	34026.75	2529.18	0.841	0.02	negative regulation of dopamine receptor signaling pathway	Signal transduction
Rgs9	559.75	69.43	434	40.9	0.775	0.02	dopamine receptor signaling pathway	Signal transduction
Rnls	104.25	18.19	71.75	13.3	0.692	0.04	dopamine metabolic process	Dopamine metabolism
Rtn4	32643.75	1217.76	26323.25	1945.21	0.806	0.02	positive regulation of dopamine secretion	Dopamine secretion & synaptic transmission
Ryk	1665.5	110.3	1439.5	75.24	0.864	0.04	chemorepulsion of dopaminergic neuron axon	Dopaminergic neuron development
Sfrp1	373	103	225.75	9.46	0.606	0.02	dopaminergic neuron differentiation	Dopaminergic neuron development
Slc9a3r1	4458.5	398.41	3381.5	132.47	0.758	0.02	adenylate cyclase-activating dopamine receptor signaling pathway	Signal transduction

Gene	*Control Mean*	*Control STD*	*Deprived Mean*	*Deprived STD*	*Deprived/ Control*	*p*	*Annotation*	*Simplified Annotation*
Smpd3	5213.75	493.18	4198	235.91	0.805	0.02	dopamine uptake	Dopamine transport & uptake
Snca	6810.75	219.53	5668.75	178.99	0.832	0.02	dopamine biosynthetic process	Dopamine metabolism
Sncb	15001.75	1032.45	12581.75	1335.77	0.839	0.04	dopamine metabolic process	Dopamine metabolism
Spr	974.5	64.61	817	60.93	0.838	0.04	dopamine metabolic process	Dopamine metabolism
Syt1	61941.25	2857.81	50143.75	3910.56	0.81	0.02	regulation of dopamine secretion	Dopamine secretion & synaptic transmission
Syt4	9435	648.68	7541	459.7	0.799	0.02	regulation of dopamine secretion	Dopamine secretion & synaptic transmission
Syt7	18260.75	1767.65	14025	940.19	0.768	0.02	regulation of dopamine secretion	Dopamine secretion & synaptic transmission
Tgfb2	459	25.34	365.5	39.43	0.797	0.02	dopamine biosynthetic process	Dopamine metabolism
Tiam1	4828.75	414.08	3832.25	116.39	0.794	0.02	regulation of dopaminergic neuron differentiation	Dopaminergic neuron development
Tor1a	1233.5	42.77	1009.5	92.45	0.818	0.02	regulation of dopamine uptake involved in synaptic transmission	Dopamine transport & uptake
Vangl2	408.75	67.53	301.25	25.32	0.736	0.04	dopaminergic neuron axon guidance	Dopaminergic neuron development
Vegfa	4070	71.03	3515	329.03	0.864	0.02	dopaminergic neuron differentiation	Dopaminergic neuron development

Gene	*Control Mean*	*Control STD*	*Deprived Mean*	*Deprived STD*	*Deprived/ Control*	*p*	*Annotation*	*Simplified Annotation*
Vps35	7012	256.77	5859.25	269.42	0.836	0.02	positive regulation of dopamine biosynthetic process	Dopamine metabolism
Wnt7b	840.75	51.8	692	42.79	0.823	0.02	chemoattraction of dopaminergic neuron axon	Dopaminergic neuron development

Supplemental Table 4: Laminar distribution of genes whose transcript is regulated experience

Gene	*Laminae*	*Annotation*	*Simplified Annotation*
Abat	Both	positive regulation of dopamine metabolic process	Dopamine metabolism
Ddc	Both	dopamine biosynthetic process	Dopamine metabolism
Epas1	Both	positive regulation of dopamine biosynthetic process	Dopamine metabolism
Hprt	Both	dopamine metabolic process	Dopamine metabolism
Maoa	Both	dopamine catabolic process	Dopamine metabolism
Pde1b	Both	regulation of dopamine metabolic process	Dopamine metabolism
Pnkd	Both	regulation of dopamine metabolic process	Dopamine metabolism
Sncb	Both	dopamine metabolic process	Dopamine metabolism
Tgfb2	Both	dopamine biosynthetic process	Dopamine metabolism
Vps35	Both	positive regulation of dopamine biosynthetic process	Dopamine metabolism
Atp7a	L2/3 only	dopamine metabolic process	Dopamine metabolism
Chrnb2	L2/3 only	regulation of dopamine metabolic process	Dopamine metabolism
Comt	L2/3 only	dopamine catabolic process	Dopamine metabolism
Cyp2d22	L2/3 only	dopamine biosynthetic process	Dopamine metabolism
Dbh	L2/3 only	dopamine beta-monooxygenase activity	Dopamine metabolism
Drd4	L2/3 only	regulation of dopamine metabolic process	Dopamine metabolism
Grin2a	L2/3 only	dopamine metabolic process	Dopamine metabolism
Npr1	L2/3 only	dopamine metabolic process	Dopamine metabolism
Nr4a2	L2/3 only	dopamine biosynthetic process	Dopamine metabolism
Rnls	L2/3 only	dopamine metabolic process	Dopamine metabolism
Snca	L2/3 only	dopamine biosynthetic process	Dopamine metabolism
Spr	L2/3 only	dopamine metabolic process	Dopamine metabolism
Agtr2	L4 only	dopamine biosynthetic process	Dopamine metabolism

Gene	*Laminae*	*Annotation*	*Simplified Annotation*
Sult1a1	L4 only	aryl sulfotransferase activity	Dopamine metabolism
Dnajc14	Both	dopamine receptor binding	Dopamine receptor binding
Dnm1	Both	D2 dopamine receptor binding	Dopamine receptor binding
Dnm2	Both	D2 dopamine receptor binding	Dopamine receptor binding
Gna13	Both	D5 dopamine receptor binding	Dopamine receptor binding
Gnas	Both	D1 dopamine receptor binding	Dopamine receptor binding
Nsf	Both	D1 dopamine receptor binding	Dopamine receptor binding
Palm	Both	D3 dopamine receptor binding	Dopamine receptor binding
Ppp1r1b	Both	D1 dopamine receptor binding	Dopamine receptor binding
Ptpn11	Both	D1 dopamine receptor binding	Dopamine receptor binding
Atp1a3	L2/3 only	D1 dopamine receptor binding	Dopamine receptor binding
Cav2	L2/3 only	D1 dopamine receptor binding	Dopamine receptor binding
Dlg4	L2/3 only	D1 dopamine receptor binding	Dopamine receptor binding
Gna12	L2/3 only	D5 dopamine receptor binding	Dopamine receptor binding
Gpr21	L2/3 only	dopamine neurotransmitter receptor activity, coupled via Gs	Dopamine receptor binding
Ppp1r9b	L2/3 only	D2 dopamine receptor binding	Dopamine receptor binding
Ptger1	L2/3 only	D1 dopamine receptor binding	Dopamine receptor binding
Arrb2	L4 only	D1 dopamine receptor binding	Dopamine receptor binding
Cdk5	Both	synaptic transmission, dopaminergic	Dopamine secretion & synaptic transmission
Chrna7	Both	regulation of synaptic transmission, dopaminergic	Dopamine secretion & synaptic transmission
Dtnbp1	Both	regulation of dopamine secretion	Dopamine secretion & synaptic transmission
Htr2a	Both	regulation of dopamine secretion	Dopamine secretion & synaptic transmission
Kcna2	Both	regulation of dopamine secretion	Dopamine secretion & synaptic transmission
Pink1	Both	positive regulation of dopamine secretion	Dopamine secretion & synaptic transmission
Prkcb	Both	regulation of dopamine secretion	Dopamine secretion & synaptic transmission
Rtn4	Both	positive regulation of dopamine secretion	Dopamine secretion & synaptic transmission
Syt1	Both	regulation of dopamine secretion	Dopamine secretion & synaptic transmission

Gene	*Laminae*	*Annotation*	*Simplified Annotation*
Syt7	Both	regulation of dopamine secretion	Dopamine secretion & synaptic transmission
Adora2a	L2/3 only	synaptic transmission, dopaminergic	Dopamine secretion & synaptic transmission
Chrna4	L2/3 only	positive regulation of dopamine secretion	Dopamine secretion & synaptic transmission
Cnr1	L2/3 only	negative regulation of dopamine secretion	Dopamine secretion & synaptic transmission
Cntnap4	L2/3 only	regulation of synaptic transmission, dopaminergic	Dopamine secretion & synaptic transmission
Crhbp	L2/3 only	synaptic transmission, dopaminergic	Dopamine secretion & synaptic transmission
Gabbr1	L2/3 only	negative regulation of dopamine secretion	Dopamine secretion & synaptic transmission
Kcnq4	L2/3 only	negative regulation of synaptic transmission, dopaminergic	Dopamine secretion & synaptic transmission
Pcp4	L2/3 only	positive regulation of dopamine secretion	Dopamine secretion & synaptic transmission
Syt4	L2/3 only	regulation of dopamine secretion	Dopamine secretion & synaptic transmission
Cxcl12	L4 only	positive regulation of dopamine secretion	Dopamine secretion & synaptic transmission
Flot1	L4 only	positive regulation of synaptic transmission, dopaminergic	Dopamine secretion & synaptic transmission
Htr1b	L4 only	regulation of dopamine secretion	Dopamine secretion & synaptic transmission
Sncg	L4 only	regulation of dopamine secretion	Dopamine secretion & synaptic transmission
Nat8l	Both	positive regulation of dopamine uptake involved in synaptic transmission	Dopamine transport & uptake
Park7	Both	dopamine uptake involved in synaptic transmission	Dopamine transport & uptake
Smpd3	Both	dopamine uptake	Dopamine transport & uptake
Park2	L2/3 only	dopamine uptake involved in synaptic transmission	Dopamine transport & uptake
Tor1a	L2/3 only	regulation of dopamine uptake involved in synaptic transmission	Dopamine transport & uptake
Csnk1d	Both	positive regulation of Wnt-mediated midbrain dopaminergic neuron differentiation	Dopaminergic neuron development
Dvl3	Both	Wnt signaling pathway involved in midbrain dopaminergic neuron differentiation	Dopaminergic neuron development

Gene	*Laminae*	*Annotation*	*Simplified Annotation*
Gsk3b	Both	negative regulation of dopaminergic neuron differentiation	Dopaminergic neuron development
Lrp6	Both	dopaminergic neuron differentiation	Dopaminergic neuron development
Rac1	Both	dopaminergic neuron differentiation	Dopaminergic neuron development
Tiam1	Both	regulation of dopaminergic neuron differentiation	Dopaminergic neuron development
Cdnf	L2/3 only	dopaminergic neuron differentiation	Dopaminergic neuron development
Ctnnb1	L2/3 only	midbrain dopaminergic neuron differentiation	Dopaminergic neuron development
Fzd3	L2/3 only	dopaminergic neuron axon guidance	Dopaminergic neuron development
Hif1a	L2/3 only	dopaminergic neuron differentiation	Dopaminergic neuron development
Htr7	L2/3 only	dopaminergic neuron differentiation	Dopaminergic neuron development
Ryk	L2/3 only	chemorepulsion of dopaminergic neuron axon	Dopaminergic neuron development
Sfrp1	L2/3 only	dopaminergic neuron differentiation	Dopaminergic neuron development
Vangl2	L2/3 only	dopaminergic neuron axon guidance	Dopaminergic neuron development
Vegfa	L2/3 only	dopaminergic neuron differentiation	Dopaminergic neuron development
Wnt7b	L2/3 only	chemoattraction of dopaminergic neuron axon	Dopaminergic neuron development
Celsr3	L4 only	dopaminergic neuron axon guidance	Dopaminergic neuron development
Dmrta2	L4 only	dopaminergic neuron differentiation	Dopaminergic neuron development
Rspo2	L4 only	dopaminergic neuron differentiation	Dopaminergic neuron development
Wnt2	L4 only	canonical Wnt signaling pathway involved in midbrain dopaminergic neuron differentiation	Dopaminergic neuron development
Adcy5	Both	adenylate cyclase-activating dopamine receptor signaling pathway	Signal transduction
Caly	Both	dopamine receptor signaling pathway	Signal transduction

Gene	*Laminae*	*Annotation*	*Simplified Annotation*
Flna	Both	adenylate cyclase-inhibiting dopamine receptor signaling pathway	Signal transduction
Gna11	Both	phospholipase C-activating dopamine receptor signaling pathway	Signal transduction
Gnao1	Both	dopamine receptor signaling pathway	Signal transduction
Gnaq	Both	phospholipase C-activating dopamine receptor signaling pathway	Signal transduction
Htt	Both	dopamine receptor signaling pathway	Signal transduction
Mapk1	Both	cellular response to dopamine	Signal transduction
Nsg1	Both	dopamine receptor signaling pathway	Signal transduction
Prmt5	Both	positive regulation of adenylate cyclase-inhibiting dopamine receptor signaling pathway	Signal transduction
Atf4	L2/3 only	cellular response to dopamine	Signal transduction
Gabpa	L2/3 only	cellular response to dopamine	Signal transduction
Gnai3	L2/3 only	dopamine receptor signaling pathway	Signal transduction
Gnal	L2/3 only	adenylate cyclase-activating dopamine receptor signaling pathway	Signal transduction
Klf16	L2/3 only	dopamine receptor signaling pathway	Signal transduction
Nsg2	L2/3 only	dopamine receptor signaling pathway	Signal transduction
Rgs4	L2/3 only	negative regulation of dopamine receptor signaling pathway	Signal transduction
Rgs9	L2/3 only	dopamine receptor signaling pathway	Signal transduction
Slc9a3r1	L2/3 only	adenylate cyclase-activating dopamine receptor signaling pathway	Signal transduction
Adcy6	L4 only	dopamine receptor signaling pathway	Signal transduction
Alk	L4 only	regulation of dopamine receptor signaling pathway	Signal transduction

Supplemental Table 5: DSP transcripts that are differentially transcribed across the deprived and first order spared Layer 4

Gene	*Control Mean*	*Control STD*	*Deprived Mean*	*Deprived STD*	*Deprived/ Control*	*p*	*Annotation*	*Simplified Annotation*
Agtr2	14	3.83	4.5	1.29	0.357	0.02	dopamine biosynthetic process	Dopamine metabolism
Gna15	71.25	4.65	86.75	8.77	1.225	0.04	phospholipase C-activating dopamine receptor signaling pathway	Signal transduction
Gpr37	900.25	146.55	1105	73.41	1.228	0.04	dopamine biosynthetic process	Dopamine metabolism
Mapk3	2156.75	263.46	2665.75	365.64	1.236	0.04	cellular response to dopamine	Signal transduction
Npy2r	84	16.37	118.25	15.92	1.405	0.02	positive regulation of dopamine secretion	Dopamine secretion & synaptic transmission
Shh	161.75	13.1	200.5	39.24	1.241	0.04	dopaminergic neuron differentiation	Dopaminergic neuron development
Slc22a2	2.25	1.5	0	0	0	0.04	dopamine transmembrane transporter activity	Dopamine transport & uptake
Wnt3	59.25	9.07	75.5	2.38	1.288	0.02	canonical Wnt signaling pathway involved in midbrain dopaminergic neuron differentiation	Dopaminergic neuron development

Supplemental Table 6: DSP transcripts that are differentially transcribed across the deprived and first order spared Layer 2/3

Gene	*Control Mean*	*Control STD*	*Deprived Mean*	*Deprived STD*	*Deprived/ Control*	*p*	*Annotation*	*Simplified Annotation*
Alk	555.75	31.72	497	28.21	0.894	0.04	regulation of dopamine receptor signaling pathway	Signal transduction
Dmrta2	319	22.35	282	14.49	0.884	0.04	dopaminergic neuron differentiation	Dopaminergic neuron development
Shh	96.75	7.63	114.5	11	1.186	0.04	dopaminergic neuron differentiation	Dopaminergic neuron development
Wnt7b	785	51.46	692	42.79	0.882	0.04	chemoattraction of dopaminergic neuron axon	Dopaminergic neuron development

Supplemental Table 7: Laminar distribution of transcripts that are differentially transcribed across the deprived and first order spared columns, organized by function

Gene	*Laminae*	*Annotation*	*Simplified Annotation*
Alk	L2/3 only	regulation of dopamine receptor signaling pathway	Signal transduction
Dmrta2	L2/3 only	dopaminergic neuron differentiation	Dopaminergic neuron development
Shh	Both	dopaminergic neuron differentiation	Dopaminergic neuron development
Wnt7b	L2/3 only	chemoattraction of dopaminergic neuron axon	Dopaminergic neuron development
Agtr2	L4 only	dopamine biosynthetic process	Dopamine metabolism
Gna15	L4 only	phospholipase C-activating dopamine receptor signaling pathway	Signal transduction
Gpr37	L4 only	dopamine biosynthetic process	Dopamine metabolism
Mapk3	L4 only	cellular response to dopamine	Signal transduction
Npy2r	L4 only	positive regulation of dopamine secretion	Dopamine secretion & synaptic transmission
Slc22a2	L4 only	dopamine transmembrane transporter activity	Dopamine transport & uptake

Wnt3	L4 only	canonical Wnt signaling pathway involved in midbrain dopaminergic neuron differentiation	Dopaminergic neuron development

Supplemental Table 8: DSP transcripts that are differentially transcribed across the deprived and second order spared Layer 2/3

Gene	*Control Mean*	*Control STD*	*Deprived Mean*	*Deprived STD*	*Deprived/ Control*	*p*	*Annotation*	*Simplified Annotation*
Abat	12972.5	574.87	10442.75	1036.9	0.805	0.02	positive regulation of dopamine metabolic process	Dopamine metabolism
Adcy5	5609.25	330.53	4334.5	291.87	0.773	0.02	adenylate cyclase-activating dopamine receptor signaling pathway	Signal transduction
Adcy6	3586.25	127.84	3100.75	261.38	0.865	0.02	dopamine receptor signaling pathway	Signal transduction
Adora2a	85.25	11.44	67.5	5.26	0.8	0.04	synaptic transmission, dopaminergic	Dopamine secretion & synaptic transmission
Adrb1	3804.75	220.12	2839.5	406.43	0.746	0.02	dopamine binding	Dopamine binding
Agtr2	7.5	1.29	4.5	1.29	0.625	0.03	dopamine biosynthetic process	Dopamine metabolism
Alk	338.25	34.12	239.75	18.7	0.71	0.02	regulation of dopamine receptor signaling pathway	Signal transduction
Arrb2	1457.5	104.2	1230	70.58	0.844	0.02	D1 dopamine receptor binding	Dopamine receptor binding

Gene	*Control Mean*	*Control STD*	*Deprived Mean*	*Deprived STD*	*Deprived/ Control*	*p*	*Annotation*	*Simplified Annotation*
Atf4	6601.75	414.03	5741.5	399.8	0.87	0.04	cellular response to dopamine	Signal transduction
Atp1a3	100628	2800.69	84311	9955.54	0.838	0.02	D1 dopamine receptor binding	Dopamine receptor binding
Atp7a	647	30.59	496.25	61.41	0.767	0.02	dopamine metabolic process	Dopamine metabolism
Caly	3578.5	323.62	3064.75	79.97	0.856	0.04	dopamine receptor signaling pathway	Signal transduction
Cav2	1822.25	136.79	1280	43.45	0.703	0.02	D1 dopamine receptor binding	Dopamine receptor binding
Cdk5	4351.75	301.93	3795.5	163.66	0.872	0.04	synaptic transmission, dopaminergic	Dopamine secretion & synaptic transmission
Chrna4	734.75	61.85	552.5	120.8	0.752	0.04	positive regulation of dopamine secretion	Dopamine secretion & synaptic transmission
Chrnb2	2304.25	137.24	1973.75	145.38	0.857	0.04	regulation of dopamine metabolic process	Dopamine metabolism
Cnr1	4718.75	654.04	2749	502.2	0.583	0.02	negative regulation of dopamine secretion	Dopamine secretion & synaptic transmission
Comt	3292.25	144.89	2693	180.52	0.818	0.02	dopamine catabolic process	Dopamine metabolism
Crhbp	871	92.92	576.25	114.6	0.661	0.02	synaptic transmission, dopaminergic	Dopamine secretion & synaptic transmission

Gene	*Control Mean*	*Control STD*	*Deprived Mean*	*Deprived STD*	*Deprived/ Control*	*p*	*Annotation*	*Simplified Annotation*
Csnk1d	7588	317.86	6028.75	345.17	0.795	0.02	positive regulation of Wnt-mediated midbrain dopaminergic neuron differentiation	Dopaminergic neuron development
Ctnnb1	20574.75	686.06	16136.5	1908.37	0.784	0.02	midbrain dopaminergic neuron differentiation	Dopaminergic neuron development
Cxcl12	2021	155.8	1318.5	181.48	0.653	0.02	positive regulation of dopamine secretion	Dopamine secretion & synaptic transmission
Cyp2d22	1175.5	83.84	992.25	137.68	0.844	0.04	dopamine biosynthetic process	Dopamine metabolism
Dlg4	57896.25	3073.03	47781.75	5430.11	0.825	0.04	D1 dopamine receptor binding	Dopamine receptor binding
Dmrta2	302	32.87	218.75	22.74	0.725	0.02	dopaminergic neuron differentiation	Dopaminergic neuron development
Dnm1	77308.5	5741.62	66992.5	3443.36	0.867	0.04	D2 dopamine receptor binding	Dopamine receptor binding
Dnm2	2693.5	131.22	2336.25	134.11	0.867	0.02	D2 dopamine receptor binding	Dopamine receptor binding
Dtnbp1	2134.5	59.05	1910.5	114.78	0.895	0.02	regulation of dopamine secretion	Dopamine secretion & synaptic transmission
Entpd1	744.25	88.13	567.25	105.94	0.762	0.04	negative regulation of dopamine secretion	Dopamine secretion & synaptic transmission
Epas1	7610.25	484.06	5910	371.05	0.777	0.02	positive regulation of dopamine biosynthetic process	Dopamine metabolism

Gene	*Control Mean*	*Control STD*	*Deprived Mean*	*Deprived STD*	*Deprived/ Control*	*p*	*Annotation*	*Simplified Annotation*
Flot1	4514.25	220.95	3595.25	156.29	0.796	0.02	positive regulation of synaptic transmission, dopaminergic	Dopamine secretion & synaptic transmission
Fzd3	10134.5	334.99	6469.5	813.8	0.638	0.02	dopaminergic neuron axon guidance	Dopaminergic neuron development
Gabbr1	37419	1715.28	30369.5	2252.63	0.812	0.02	negative regulation of dopamine secretion	Dopamine secretion & synaptic transmission
Gabpa	1159	36.41	873	96.9	0.753	0.02	cellular response to dopamine	Signal transduction
Gna11	6709	328.71	5669	388.3	0.845	0.02	phospholipase C-activating dopamine receptor signaling pathway	Signal transduction
Gna13	2825.25	100.89	2076.75	240.74	0.735	0.02	D5 dopamine receptor binding	Dopamine receptor binding
Gnai3	1749.25	113.89	1306	155.41	0.747	0.02	dopamine receptor signaling pathway	Signal transduction
Gnal	5571	142.75	3522.75	482.06	0.632	0.02	adenylate cyclase-activating dopamine receptor signaling pathway	Signal transduction
Gnao1	38122.5	1477.63	30041.75	2072.49	0.788	0.02	dopamine receptor signaling pathway	Signal transduction

Gene	*Control Mean*	*Control STD*	*Deprived Mean*	*Deprived STD*	*Deprived/ Control*	*p*	*Annotation*	*Simplified Annotation*
Gnaq	16595.25	157.85	12844.5	1185.72	0.774	0.02	phospholipase C-activating dopamine receptor signaling pathway	Signal transduction
Gnas	62344.75	2175.4	50840.75	2235.83	0.815	0.02	D1 dopamine receptor binding	Dopamine receptor binding
Gnb5	7326	292.8	5588.5	588.34	0.763	0.02	dopamine receptor signaling pathway	Signal transduction
Grin2a	2039.25	284.91	1317	282.52	0.646	0.02	dopamine metabolic process	Dopamine metabolism
Gsk3b	15251.25	293.35	11525.5	892.5	0.756	0.02	negative regulation of dopaminergic neuron differentiation	Dopaminergic neuron development
Hif1a	4158	154.19	2906	289.11	0.699	0.02	dopaminergic neuron differentiation	Dopaminergic neuron development
Hprt	4887	172.89	3833.75	178.08	0.785	0.02	dopamine metabolic process	Dopamine metabolism
Htr1a	629.25	115.29	424.25	61.55	0.674	0.02	regulation of dopamine metabolic process	Dopamine metabolism
Htr7	639	51.04	402.25	34.42	0.629	0.02	dopaminergic neuron differentiation	Dopaminergic neuron development
Htt	11393.5	909.21	8861	809.49	0.778	0.02	dopamine receptor signaling pathway	Signal transduction
Kcna2	23245.25	1951.45	17503.25	800.84	0.753	0.02	regulation of dopamine secretion	Dopamine secretion & synaptic transmission

Gene	*Control Mean*	*Control STD*	*Deprived Mean*	*Deprived STD*	*Deprived/ Control*	*p*	*Annotation*	*Simplified Annotation*
Klf16	2316.25	176.22	1784.25	183.56	0.77	0.02	dopamine receptor signaling pathway	Signal transduction
Lrp6	2873.5	121.35	2185.5	283.93	0.761	0.02	dopaminergic neuron differentiation	Dopaminergic neuron development
Lrrk2	5591.25	244.06	4227.25	229.7	0.756	0.02	cellular response to dopamine	Signal transduction
Maoa	1052.5	39.37	749.25	53.07	0.711	0.02	dopamine catabolic process	Dopamine metabolism
Mapk1	30498.5	1297.41	22163.25	2199.38	0.727	0.02	cellular response to dopamine	Signal transduction
Moxd1	144.5	23.01	74.5	10.47	0.517	0.02	dopamine beta-monooxygenase activity	Dopamine metabolism
Nat8l	35681.75	3890.29	27845.5	2296.42	0.78	0.02	positive regulation of dopamine uptake involved in synaptic transmission	Dopamine transport & uptake
Nr4a2	1168.75	190.32	871	130.66	0.745	0.04	dopamine biosynthetic process	Dopamine metabolism
Nsf	41279.75	1505.19	33046.25	1893.91	0.801	0.02	D1 dopamine receptor binding	Dopamine receptor binding
Nsg1	12084.75	521.54	9548.5	733.47	0.79	0.02	dopamine receptor signaling pathway	Signal transduction
Nsg2	22275.25	1566.46	19024.5	1613.03	0.854	0.04	dopamine receptor signaling pathway	Signal transduction
Park7	3305.75	84.4	2756.25	136.29	0.834	0.02	dopamine uptake involved in synaptic transmission	Dopamine transport & uptake

Gene	*Control Mean*	*Control STD*	*Deprived Mean*	*Deprived STD*	*Deprived/ Control*	*p*	*Annotation*	*Simplified Annotation*
Pax2	7.25	4.72	2.5	1	0.429	0.02	dopaminergic neuron differentiation	Dopaminergic neuron development
Pde1b	6496.25	408.77	5617.75	245.81	0.865	0.02	regulation of dopamine metabolic process	Dopamine metabolism
Pink1	18509	893.96	14907	690.59	0.805	0.02	positive regulation of dopamine secretion	Dopamine secretion & synaptic transmission
Ppp1r9b	55913.25	2109.86	46521.25	5137.74	0.832	0.04	D2 dopamine receptor binding	Dopamine receptor binding
Prkcb	71011.25	4140.4	51872.25	5531.43	0.73	0.02	regulation of dopamine secretion	Dopamine secretion & synaptic transmission
Prmt5	2600.25	17.73	2082	79.53	0.801	0.02	positive regulation of adenylate cyclase-inhibiting dopamine receptor signaling pathway	Signal transduction
Ptger1	1203.25	54.89	955.75	48.51	0.795	0.02	D1 dopamine receptor binding	Dopamine receptor binding
Ptgs2	1413	90.6	842.5	136.49	0.597	0.02	negative regulation of synaptic transmission, dopaminergic	Dopamine secretion & synaptic transmission
Ptpn11	8406.25	618.2	7068.75	359.35	0.841	0.02	D1 dopamine receptor binding	Dopamine receptor binding
Rac1	13224.75	196.32	10066.25	603.72	0.761	0.02	dopaminergic neuron differentiation	Dopaminergic neuron development

Gene	*Control Mean*	*Control STD*	*Deprived Mean*	*Deprived STD*	*Deprived/ Control*	*p*	*Annotation*	*Simplified Annotation*
Rasd2	7418.75	354.37	6492.5	644.69	0.875	0.04	synaptic transmission, dopaminergic	Dopamine secretion & synaptic transmission
Rgs4	68243.75	3190.58	48261.25	5292.64	0.707	0.02	negative regulation of dopamine receptor signaling pathway	Signal transduction
Rgs8	3124.5	533.79	1826.5	400.7	0.585	0.02	regulation of dopamine receptor signaling pathway	Signal transduction
Rgs9	368.75	31.26	278.75	23.43	0.756	0.02	dopamine receptor signaling pathway	Signal transduction
Rspo2	121.25	23.04	76.5	8.58	0.636	0.02	dopaminergic neuron differentiation	Dopaminergic neuron development
Rtn4	41251	933	32169.75	1857.11	0.78	0.02	positive regulation of dopamine secretion	Dopamine secretion & synaptic transmission
Ryk	1549.25	88.71	1208.75	116.78	0.781	0.02	chemorepulsion of dopaminergic neuron axon	Dopaminergic neuron development
Sfrp1	390.25	26.46	314.25	49.95	0.805	0.02	dopaminergic neuron differentiation	Dopaminergic neuron development
Slc6a3	2.75	1.71	0.25	0.5	0	0.03	dopamine biosynthetic process	Dopamine metabolism
Slc9a3r1	3134.5	175.44	2618.25	302.44	0.835	0.04	adenylate cyclase-activating dopamine receptor signaling pathway	Signal transduction

Gene	*Control Mean*	*Control STD*	*Deprived Mean*	*Deprived STD*	*Deprived/ Control*	*p*	*Annotation*	*Simplified Annotation*
Smpd3	5033	373.95	4422.75	221.47	0.879	0.04	dopamine uptake	Dopamine transport & uptake
Snca	9190	347.97	8058.25	833.84	0.877	0.04	dopamine biosynthetic process	Dopamine metabolism
Sncaip	135.75	9.74	99.5	9.88	0.735	0.02	dopamine metabolic process	Dopamine metabolism
Sncg	11.5	2.38	4.75	3.3	0.417	0.02	regulation of dopamine secretion	Dopamine secretion & synaptic transmission
Syt1	77269.25	3406.97	56713	3979.46	0.734	0.02	regulation of dopamine secretion	Dopamine secretion & synaptic transmission
Syt4	10055.75	381.24	7931.75	647.89	0.789	0.02	regulation of dopamine secretion	Dopamine secretion & synaptic transmission
Syt7	12535.75	632.13	8804.5	1103.29	0.702	0.02	regulation of dopamine secretion	Dopamine secretion & synaptic transmission
Tgfb2	356.25	23.14	242.5	29.56	0.683	0.02	dopamine biosynthetic process	Dopamine metabolism
Vps35	7631.75	401.19	5463	479.09	0.716	0.02	positive regulation of dopamine biosynthetic process	Dopamine metabolism

Supplemental Table 9: DSP transcripts that are differentially transcribed across the deprived and second order spared Layer 4

Gene	*Control Mean*	*Control STD*	*Deprived Mean*	*Deprived STD*	*Deprived/ Control*	*p*	*Annotation*
Abat	14451	1019.36	11111.5	200.03	0.769	0.02	positive regulation of dopamine metabolic process
Adcy5	6087.5	286.65	4698.25	228.1	0.772	0.02	adenylate cyclase-activating dopamine receptor signaling pathway
Adcy6	3666.5	216.69	3163.75	206.55	0.863	0.04	dopamine receptor signaling pathway
Adora2a	135.25	32.39	94.25	3.1	0.696	0.02	synaptic transmission, dopaminergic
Adrb1	4424	185.06	3625.25	239.43	0.819	0.02	dopamine binding
Adrb2	94	10.13	51.75	9.6	0.553	0.02	dopamine binding
Agtr1a	11.75	3.1	5.75	1.26	0.5	0.02	dopamine biosynthetic process
Alk	660.75	62.31	497	28.21	0.752	0.02	regulation of dopamine receptor signaling pathway
Arrb2	1740.25	92.6	1388.25	188.07	0.798	0.04	D1 dopamine receptor binding
Atf4	6504	494.3	5338.5	454.79	0.821	0.02	cellular response to dopamine
Atp1a3	100194.25	6244.18	82678.75	5509.73	0.825	0.02	D1 dopamine receptor binding
Atp7a	517.75	40.21	371.75	28.11	0.718	0.02	dopamine metabolic process
Caly	4596.5	160.82	3556.75	370.87	0.774	0.02	dopamine receptor signaling pathway
Cav2	1988.5	141.95	1269	60.39	0.638	0.02	D1 dopamine receptor binding
Chrna4	922	85.04	678.25	32.67	0.735	0.02	positive regulation of dopamine secretion
Chrna7	770.5	44.43	568.75	42.17	0.738	0.02	regulation of synaptic transmission, dopaminergic
Chrnb2	1872.25	160.86	1572.75	155.48	0.84	0.04	regulation of dopamine metabolic process
Cnr1	11834.5	766.86	7764.75	295.14	0.656	0.02	negative regulation of dopamine secretion
Cntnap4	432.25	37.77	335.75	49.4	0.778	0.02	regulation of synaptic transmission, dopaminergic
Comt	3010	117.26	2540.75	175.25	0.844	0.02	dopamine catabolic process
Crh	1299.25	43.96	1007.5	59.44	0.776	0.02	synaptic transmission, dopaminergic
Crhbp	726.25	53.77	548.5	115.36	0.756	0.02	synaptic transmission, dopaminergic

Gene	*Control Mean*	*Control STD*	*Deprived Mean*	*Deprived STD*	*Deprived/ Control*	*p*	*Annotation*
Csnk1d	7735	701.6	6445.25	540.97	0.833	0.04	positive regulation of Wnt-mediated midbrain dopaminergic neuron differentiation
Ctnnb1	22283.75	1265.6	16776.75	342.75	0.753	0.02	midbrain dopaminergic neuron differentiation
Cxcl12	2126.25	62.33	1469.25	126.42	0.691	0.02	positive regulation of dopamine secretion
Cyp2d22	1358.25	167.59	1013.75	34.99	0.747	0.02	dopamine biosynthetic process
Dlg4	72298.5	3467.53	61278	2536.78	0.848	0.02	D1 dopamine receptor binding
Dmrta2	411.75	82.73	282	14.49	0.684	0.04	dopaminergic neuron differentiation
Dnajc14	2331	131.02	1945.25	78.99	0.834	0.02	dopamine receptor binding
Dnm1	69112.25	3662.81	59844	4894.96	0.866	0.04	D2 dopamine receptor binding
Dnm2	2742.5	245.13	2259.75	106	0.824	0.02	D2 dopamine receptor binding
Drd4	50	4.24	35.25	10.63	0.7	0.04	regulation of dopamine metabolic process
Dtnbp1	1760.75	94.51	1599	76.67	0.908	0.04	regulation of dopamine secretion
Dvl3	4206.25	312.26	3665.25	243.52	0.871	0.02	Wnt signaling pathway involved in midbrain dopaminergic neuron differentiation
Entpd1	1005.25	128.61	755.25	56.35	0.751	0.02	negative regulation of dopamine secretion
Epas1	10152	781.29	6847	421.41	0.674	0.02	positive regulation of dopamine biosynthetic process
Flna	4055.5	273.08	3268.75	248.78	0.806	0.02	adenylate cyclase-inhibiting dopamine receptor signaling pathway
Flot1	4661.25	313.69	3949.25	320.24	0.847	0.04	positive regulation of synaptic transmission, dopaminergic
Fzd3	9589.25	896.72	7209	720.46	0.752	0.02	dopaminergic neuron axon guidance
Gabbr1	36825	1890.27	29889.5	1780.02	0.812	0.02	negative regulation of dopamine secretion
Gabpa	1176.25	49.31	856.25	77.21	0.728	0.02	cellular response to dopamine

Gene	*Control Mean*	*Control STD*	*Deprived Mean*	*Deprived STD*	*Deprived/ Control*	*p*	*Annotation*
Gch1	124	19.85	80.75	15.95	0.653	0.04	dopamine biosynthetic process
Gna11	7730.25	437.08	6249.75	348.2	0.809	0.02	phospholipase C-activating dopamine receptor signaling pathway
Gna12	3235.75	174.65	2447.5	60.39	0.756	0.02	D5 dopamine receptor binding
Gna13	3555.75	314.92	2484.25	147.92	0.699	0.02	D5 dopamine receptor binding
Gnai3	1874.75	121.07	1364.5	98.49	0.728	0.02	dopamine receptor signaling pathway
Gnal	7332.5	421.13	5319.5	162.67	0.725	0.02	adenylate cyclase-activating dopamine receptor signaling pathway
Gnao1	41515.5	2162.55	33228	1647.21	0.8	0.02	dopamine receptor signaling pathway
Gnaq	15725.25	892.06	12561.25	472.6	0.799	0.02	phospholipase C-activating dopamine receptor signaling pathway
Gnas	57648	2855.08	45711.25	3836.78	0.793	0.02	D1 dopamine receptor binding
Gnb5	7474.25	498.27	6250	605.77	0.836	0.02	dopamine receptor signaling pathway
Gpr37	457	75.36	371.25	30.87	0.812	0.04	dopamine biosynthetic process
Gpr52	78.25	12.76	44	4.97	0.564	0.02	dopamine neurotransmitter receptor activity, coupled via Gs
Gsk3b	13808	717.13	11186.25	550.29	0.81	0.02	negative regulation of dopaminergic neuron differentiation
Hif1a	4553	109.66	3248.5	131.68	0.714	0.02	dopaminergic neuron differentiation
Hprt	3652.5	176.24	2939	232.57	0.805	0.02	dopamine metabolic process
Htr1a	680.5	66.02	571.25	27.66	0.838	0.02	regulation of dopamine metabolic process
Htr2c	194	23.55	119.5	9.85	0.619	0.02	negative regulation of dopamine metabolic process
Htr7	791	79.04	520.75	72.69	0.659	0.02	dopaminergic neuron differentiation
Htt	10143.5	876.54	8448	618.94	0.833	0.04	dopamine receptor signaling pathway

Gene	*Control Mean*	*Control STD*	*Deprived Mean*	*Deprived STD*	*Deprived/ Control*	*p*	*Annotation*
Kcnq4	435.5	39.75	351.5	18.21	0.807	0.02	negative regulation of synaptic transmission, dopaminergic
Klf16	4110.5	465.01	3189.25	201.71	0.776	0.02	dopamine receptor signaling pathway
Lmx1b	4	0.82	0.25	0.5	0	0.02	dopaminergic neuron differentiation
Lrp6	2885.25	251.68	2223.5	87.75	0.771	0.02	dopaminergic neuron differentiation
Maoa	1263.75	115.03	834	90.4	0.66	0.02	dopamine catabolic process
Mapk1	34862.25	1641.03	26602.75	1147.62	0.763	0.02	cellular response to dopamine
Mapk3	3959.75	380.23	3089	192.02	0.78	0.02	cellular response to dopamine
Moxd1	313.25	53.78	221.25	43.42	0.706	0.04	dopamine beta-monooxygenase activity
Npr1	191.5	49.26	124	16.57	0.646	0.02	dopamine metabolic process
Npy2r	190.75	39.55	127	8.76	0.665	0.02	positive regulation of dopamine secretion
Nr4a2	1614.25	107.7	1176	158.16	0.729	0.02	dopamine biosynthetic process
Nsf	32971	1784.61	27791.5	2195.9	0.843	0.02	D1 dopamine receptor binding
Nsg1	10812	607.73	9139.25	711.3	0.845	0.02	dopamine receptor signaling pathway
Nsg2	27825	954.6	23648.25	1628.51	0.85	0.02	dopamine receptor signaling pathway
Palm	15158	1085.5	12113.5	472.56	0.799	0.02	D3 dopamine receptor binding
Park2	225.25	23.43	183.75	26.69	0.818	0.04	dopamine uptake involved in synaptic transmission
Park7	2941	198.39	2519	203.96	0.857	0.02	dopamine uptake involved in synaptic transmission
Pcp4	893	13.54	605.5	48.56	0.679	0.02	positive regulation of dopamine secretion
Pde1b	6075.75	345.36	5072.75	403.99	0.835	0.02	regulation of dopamine metabolic process
Pink1	16867.25	812.64	12763	950.4	0.757	0.02	positive regulation of dopamine secretion
Ppp1r9b	73588.5	3092.83	58363.5	1635.93	0.793	0.02	D2 dopamine receptor binding
Prkcb	68094.75	3981.41	56077.25	3467.21	0.824	0.02	regulation of dopamine secretion

Gene	*Control Mean*	*Control STD*	*Deprived Mean*	*Deprived STD*	*Deprived/ Control*	*p*	*Annotation*
Prmt5	2511	80.05	2000	137.33	0.796	0.02	positive regulation of adenylate cyclase-inhibiting dopamine receptor signaling pathway
Ptger1	1499.25	140.73	1152.25	98.11	0.769	0.02	D1 dopamine receptor binding
Ptgs2	2477.25	373.19	1549.5	257.6	0.626	0.02	negative regulation of synaptic transmission, dopaminergic
Ptpn11	8320.5	500.3	6726.5	508.84	0.808	0.02	D1 dopamine receptor binding
Rab3b	1200.25	82.56	1041.25	114.47	0.868	0.04	positive regulation of dopamine uptake involved in synaptic transmission
Rac1	13225.75	518.88	9651	560.43	0.73	0.02	dopaminergic neuron differentiation
Rgs4	39776	1402.26	34026.75	2529.18	0.855	0.02	negative regulation of dopamine receptor signaling pathway
Rgs8	9984	801.43	7783.5	987.26	0.78	0.02	regulation of dopamine receptor signaling pathway
Rgs9	604.75	45.49	434	40.9	0.717	0.02	dopamine receptor signaling pathway
Rnls	89.5	5.45	71.75	13.3	0.8	0.03	dopamine metabolic process
Rspo2	83.75	15.33	52	10.86	0.619	0.04	dopaminergic neuron differentiation
Rtn4	32105.25	1805.45	26323.25	1945.21	0.82	0.02	positive regulation of dopamine secretion
Ryk	2003	131.5	1439.5	75.24	0.719	0.02	chemorepulsion of dopaminergic neuron axon
Sfrp1	365.75	33.12	225.75	9.46	0.617	0.02	dopaminergic neuron differentiation
Slc18a1	6.25	1.71	3.25	1.5	0.5	0.05	positive regulation of dopamine secretion
Slc22a2	22.5	7.33	7	4.97	0.304	0.02	dopamine transmembrane transporter activity
Slc9a3r1	4543	440.43	3381.5	132.47	0.744	0.02	adenylate cyclase-activating dopamine receptor signaling pathway
Smpd3	4962	398	4198	235.91	0.846	0.02	dopamine uptake
Snca	7107	343.55	5668.75	178.99	0.798	0.02	dopamine biosynthetic process

Gene	*Control Mean*	*Control STD*	*Deprived Mean*	*Deprived STD*	*Deprived/ Control*	*p*	*Annotation*
Sncaip	226.5	43.18	148	14.85	0.652	0.02	dopamine metabolic process
Sncg	51	7.87	30	5.03	0.588	0.02	regulation of dopamine secretion
Spr	966.75	68.68	817	60.93	0.845	0.04	dopamine metabolic process
Sult1a1	373.5	115.5	235.25	51.46	0.628	0.02	aryl sulfotransferase activity
Syt1	63527.75	4343.52	50143.75	3910.56	0.789	0.02	regulation of dopamine secretion
Syt4	9537.25	185.54	7541	459.7	0.791	0.02	regulation of dopamine secretion
Syt7	18708.25	967.07	14025	940.19	0.75	0.02	regulation of dopamine secretion
Tgfb2	546.75	61.66	365.5	39.43	0.669	0.02	dopamine biosynthetic process
Tiam1	4984.5	263.59	3832.25	116.39	0.769	0.02	regulation of dopaminergic neuron differentiation
Tor1a	1312.5	83.01	1009.5	92.45	0.769	0.02	regulation of dopamine uptake involved in synaptic transmission
Vangl2	393.25	26.59	301.25	25.32	0.766	0.02	dopaminergic neuron axon guidance
Vegfa	4587.5	551.35	3515	329.03	0.766	0.02	dopaminergic neuron differentiation
Vps35	7771.5	456.22	5859.25	269.42	0.754	0.02	positive regulation of dopamine biosynthetic process
Wnt5a	525.5	45.88	327.75	64.65	0.624	0.02	chemorepulsion of dopaminergic neuron axon
Wnt7b	961.25	87.32	692	42.79	0.72	0.02	chemoattraction of dopaminergic neuron axon

Supplemental Table 10: Laminar distribution of transcripts that are differentially transcribed across the deprived and second order spared columns, organized by function

Gene	*Laminae*	*Annotation*	*Simplified Annotation*
Abat	Both	positive regulation of dopamine metabolic process	Dopamine metabolism
Adcy5	Both	adenylate cyclase-activating dopamine receptor signaling pathway	Signal transduction
Adcy6	Both	dopamine receptor signaling pathway	Signal transduction

Gene	*Laminae*	*Annotation*	*Simplified Annotation*
Adora2a	Both	synaptic transmission, dopaminergic	Dopamine secretion & synaptic transmission
Adrb1	Both	dopamine binding	Dopamine binding
Adrb2	L2/3 only	dopamine binding	Dopamine binding
Agtr1a	L2/3 only	dopamine biosynthetic process	Dopamine metabolism
Alk	Both	regulation of dopamine receptor signaling pathway	Signal transduction
Arrb2	Both	D1 dopamine receptor binding	Dopamine receptor binding
Atf4	Both	cellular response to dopamine	Signal transduction
Atp1a3	Both	D1 dopamine receptor binding	Dopamine receptor binding
Atp7a	Both	dopamine metabolic process	Dopamine metabolism
Caly	Both	dopamine receptor signaling pathway	Signal transduction
Cav2	Both	D1 dopamine receptor binding	Dopamine receptor binding
Chrna4	Both	positive regulation of dopamine secretion	Dopamine secretion & synaptic transmission
Chrna7	L2/3 only	regulation of synaptic transmission, dopaminergic	Dopamine secretion & synaptic transmission
Chrnb2	Both	regulation of dopamine metabolic process	Dopamine metabolism
Cnr1	Both	negative regulation of dopamine secretion	Dopamine secretion & synaptic transmission
Cntnap4	L2/3 only	regulation of synaptic transmission, dopaminergic	Dopamine secretion & synaptic transmission
Comt	Both	dopamine catabolic process	Dopamine metabolism
Crh	L2/3 only	synaptic transmission, dopaminergic	Dopamine secretion & synaptic transmission
Crhbp	Both	synaptic transmission, dopaminergic	Dopamine secretion & synaptic transmission
Csnk1d	Both	positive regulation of Wnt-mediated midbrain dopaminergic neuron differentiation	Dopaminergic neuron development
Ctnnb1	Both	midbrain dopaminergic neuron differentiation	Dopaminergic neuron development
Cxcl12	Both	positive regulation of dopamine secretion	Dopamine secretion & synaptic transmission
Cyp2d22	Both	dopamine biosynthetic process	Dopamine metabolism
Dlg4	Both	D1 dopamine receptor binding	Dopamine receptor binding

Gene	*Laminae*	*Annotation*	*Simplified Annotation*
Dmrta2	Both	dopaminergic neuron differentiation	Dopaminergic neuron development
Dnajc14	L2/3 only	dopamine receptor binding	Dopamine receptor binding
Dnm1	Both	D2 dopamine receptor binding	Dopamine receptor binding
Dnm2	Both	D2 dopamine receptor binding	Dopamine receptor binding
Drd4	L2/3 only	regulation of dopamine metabolic process	Dopamine metabolism
Dtnbp1	Both	regulation of dopamine secretion	Dopamine secretion & synaptic transmission
Dvl3	L2/3 only	Wnt signaling pathway involved in midbrain dopaminergic neuron differentiation	Dopaminergic neuron development
Entpd1	Both	negative regulation of dopamine secretion	Dopamine secretion & synaptic transmission
Epas1	Both	positive regulation of dopamine biosynthetic process	Dopamine metabolism
Flna	L2/3 only	adenylate cyclase-inhibiting dopamine receptor signaling pathway	Signal transduction
Flot1	Both	positive regulation of synaptic transmission, dopaminergic	Dopamine secretion & synaptic transmission
Fzd3	Both	dopaminergic neuron axon guidance	Dopaminergic neuron development
Gabbr1	Both	negative regulation of dopamine secretion	Dopamine secretion & synaptic transmission
Gabpa	Both	cellular response to dopamine	Signal transduction
Gch1	L2/3 only	dopamine biosynthetic process	Dopamine metabolism
Gna11	Both	phospholipase C-activating dopamine receptor signaling pathway	Signal transduction
Gna12	L2/3 only	D5 dopamine receptor binding	Dopamine receptor binding
Gna13	Both	D5 dopamine receptor binding	Dopamine receptor binding
Gnai3	Both	dopamine receptor signaling pathway	Signal transduction
Gnal	Both	adenylate cyclase-activating dopamine receptor signaling pathway	Signal transduction
Gnao1	Both	dopamine receptor signaling pathway	Signal transduction
Gnaq	Both	phospholipase C-activating dopamine receptor signaling pathway	Signal transduction
Gnas	Both	D1 dopamine receptor binding	Dopamine receptor binding

Gene	*Laminae*	*Annotation*	*Simplified Annotation*
Gnb5	Both	dopamine receptor signaling pathway	Signal transduction
Gpr37	L2/3 only	dopamine biosynthetic process	Dopamine metabolism
Gpr52	L2/3 only	dopamine neurotransmitter receptor activity, coupled via Gs	Dopamine receptor binding
Gsk3b	Both	negative regulation of dopaminergic neuron differentiation	Dopaminergic neuron development
Hif1a	Both	dopaminergic neuron differentiation	Dopaminergic neuron development
Hprt	Both	dopamine metabolic process	Dopamine metabolism
Htr1a	Both	regulation of dopamine metabolic process	Dopamine metabolism
Htr2c	L2/3 only	negative regulation of dopamine metabolic process	Dopamine metabolism
Htr7	Both	dopaminergic neuron differentiation	Dopaminergic neuron development
Htt	Both	dopamine receptor signaling pathway	Signal transduction
Kcnq4	L2/3 only	negative regulation of synaptic transmission, dopaminergic	Dopamine secretion & synaptic transmission
Klf16	Both	dopamine receptor signaling pathway	Signal transduction
Lmx1b	L2/3 only	dopaminergic neuron differentiation	Dopaminergic neuron development
Lrp6	Both	dopaminergic neuron differentiation	Dopaminergic neuron development
Maoa	Both	dopamine catabolic process	Dopamine metabolism
Mapk1	Both	cellular response to dopamine	Signal transduction
Mapk3	L2/3 only	cellular response to dopamine	Signal transduction
Moxd1	Both	dopamine beta-monooxygenase activity	Dopamine metabolism
Npr1	L2/3 only	dopamine metabolic process	Dopamine metabolism
Npy2r	L2/3 only	positive regulation of dopamine secretion	Dopamine secretion & synaptic transmission
Nr4a2	Both	dopamine biosynthetic process	Dopamine metabolism
Nsf	Both	D1 dopamine receptor binding	Dopamine receptor binding
Nsg1	Both	dopamine receptor signaling pathway	Signal transduction
Nsg2	Both	dopamine receptor signaling pathway	Signal transduction
Palm	L2/3 only	D3 dopamine receptor binding	Dopamine receptor binding

Gene	*Laminae*	*Annotation*	*Simplified Annotation*
Park2	L2/3 only	dopamine uptake involved in synaptic transmission	Dopamine transport & uptake
Park7	Both	dopamine uptake involved in synaptic transmission	Dopamine transport & uptake
Pcp4	L2/3 only	positive regulation of dopamine secretion	Dopamine secretion & synaptic transmission
Pde1b	Both	regulation of dopamine metabolic process	Dopamine metabolism
Pink1	Both	positive regulation of dopamine secretion	Dopamine secretion & synaptic transmission
Ppp1r9b	Both	D2 dopamine receptor binding	Dopamine receptor binding
Prkcb	Both	regulation of dopamine secretion	Dopamine secretion & synaptic transmission
Prmt5	Both	positive regulation of adenylate cyclase-inhibiting dopamine receptor signaling pathway	Signal transduction
Ptger1	Both	D1 dopamine receptor binding	Dopamine receptor binding
Ptgs2	Both	negative regulation of synaptic transmission, dopaminergic	Dopamine secretion & synaptic transmission
Ptpn11	Both	D1 dopamine receptor binding	Dopamine receptor binding
Rab3b	L2/3 only	positive regulation of dopamine uptake involved in synaptic transmission	Dopamine transport & uptake
Rac1	Both	dopaminergic neuron differentiation	Dopaminergic neuron development
Rgs4	Both	negative regulation of dopamine receptor signaling pathway	Signal transduction
Rgs8	Both	regulation of dopamine receptor signaling pathway	Signal transduction
Rgs9	Both	dopamine receptor signaling pathway	Signal transduction
Rnls	L2/3 only	dopamine metabolic process	Dopamine metabolism
Rspo2	Both	dopaminergic neuron differentiation	Dopaminergic neuron development
Rtn4	Both	positive regulation of dopamine secretion	Dopamine secretion & synaptic transmission
Ryk	Both	chemorepulsion of dopaminergic neuron axon	Dopaminergic neuron development
Sfrp1	Both	dopaminergic neuron differentiation	Dopaminergic neuron development
Slc18a1	L2/3 only	positive regulation of dopamine secretion	Dopamine secretion & synaptic transmission

Gene	*Laminae*	*Annotation*	*Simplified Annotation*
Slc22a2	L2/3 only	dopamine transmembrane transporter activity	Dopamine transport & uptake
Slc9a3r1	Both	adenylate cyclase-activating dopamine receptor signaling pathway	Signal transduction
Smpd3	Both	dopamine uptake	Dopamine transport & uptake
Snca	Both	dopamine biosynthetic process	Dopamine metabolism
Sncaip	Both	dopamine metabolic process	Dopamine metabolism
Sncg	Both	regulation of dopamine secretion	Dopamine secretion & synaptic transmission
Spr	L2/3 only	dopamine metabolic process	Dopamine metabolism
Sult1a1	L2/3 only	aryl sulfotransferase activity	Dopamine metabolism
Syt1	Both	regulation of dopamine secretion	Dopamine secretion & synaptic transmission
Syt4	Both	regulation of dopamine secretion	Dopamine secretion & synaptic transmission
Syt7	Both	regulation of dopamine secretion	Dopamine secretion & synaptic transmission
Tgfb2	Both	dopamine biosynthetic process	Dopamine metabolism
Tiam1	L2/3 only	regulation of dopaminergic neuron differentiation	Dopaminergic neuron development
Tor1a	L2/3 only	regulation of dopamine uptake involved in synaptic transmission	Dopamine transport & uptake
Vangl2	L2/3 only	dopaminergic neuron axon guidance	Dopaminergic neuron development
Vegfa	L2/3 only	dopaminergic neuron differentiation	Dopaminergic neuron development
Vps35	Both	positive regulation of dopamine biosynthetic process	Dopamine metabolism
Wnt5a	L2/3 only	chemorepulsion of dopaminergic neuron axon	Dopaminergic neuron development
Wnt7b	L2/3 only	chemoattraction of dopaminergic neuron axon	Dopaminergic neuron development
Agtr2	L4 only	dopamine biosynthetic process	Dopamine metabolism
Cdk5	L4 only	synaptic transmission, dopaminergic	Dopamine secretion & synaptic transmission
Grin2a	L4 only	dopamine metabolic process	Dopamine metabolism

Gene	*Laminae*	*Annotation*	*Simplified Annotation*
Kcna2	L4 only	regulation of dopamine secretion	Dopamine secretion & synaptic transmission
Lrrk2	L4 only	cellular response to dopamine	Signal transduction
Nat8l	L4 only	positive regulation of dopamine uptake involved in synaptic transmission	Dopamine transport & uptake
Pax2	L4 only	dopaminergic neuron differentiation	Dopaminergic neuron development
Rasd2	L4 only	synaptic transmission, dopaminergic	Dopamine secretion & synaptic transmission
Slc6a3	L4 only	dopamine biosynthetic process	Dopamine metabolism

Chapter 5

Sparsification of sensory representations by dopamine

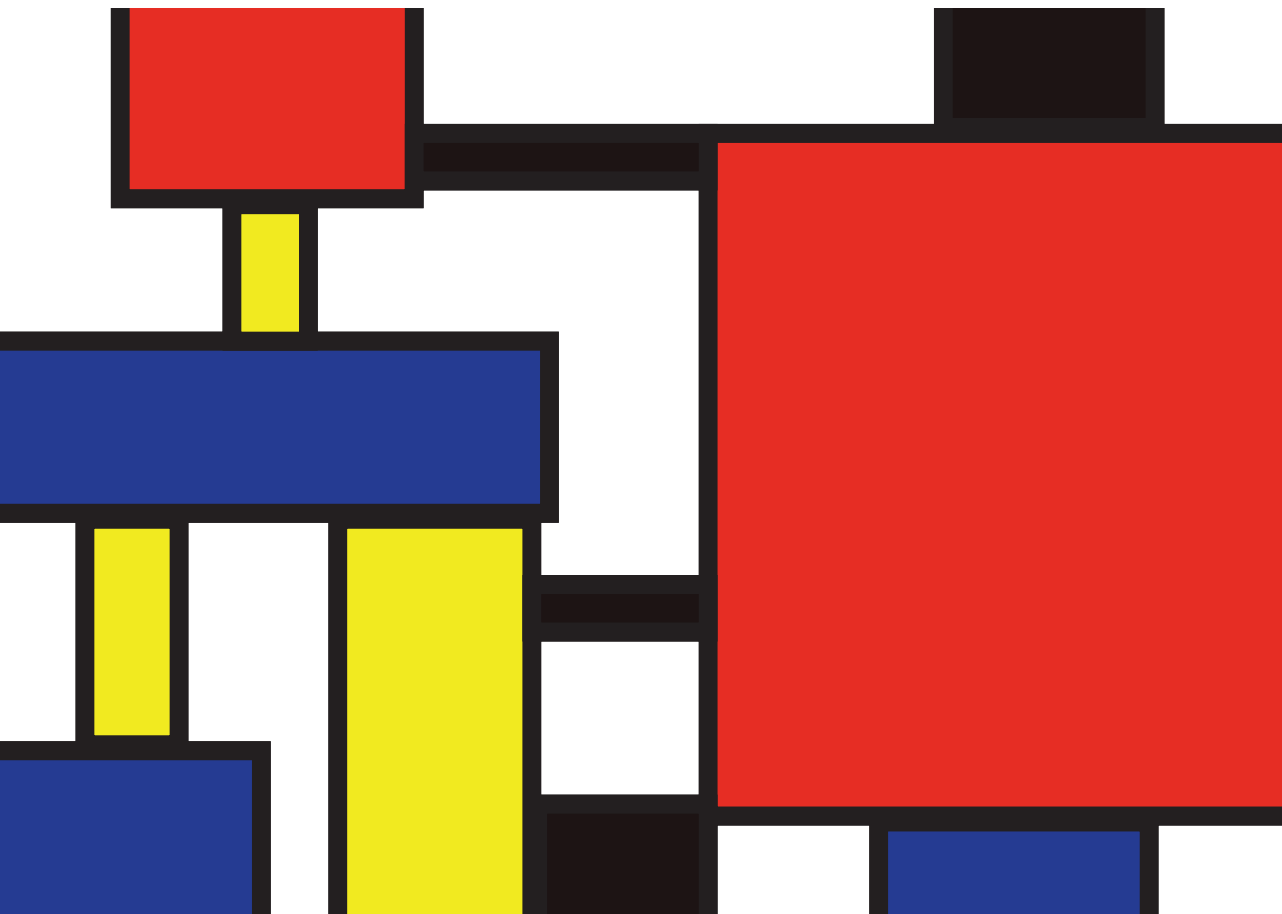

Sensory perception is an orchestrated outcome of the central circuits of the brain. It requires integration of the bottom-up information from the periphery with the top-down, often neuromodulatory, information originating elsewhere in the brain. Recent studies in the whisker system showed that monoamines, particularly serotonin, performs gain-modulation for adaptive control of active sensing. Here we show that another monoamine, dopamine, powerfully controls sensory processing and neural representation of the sensory information in the somatosensory cortex. Specifically, we demonstrate that pharmacological activation of the D1-like dopaminergic receptors (D1R) in the somatosensory cortex from freely-behaving animals results in faster integration of the sensory information. The mechanism underlying this behavioral improvement might be explained by the bidirectional control of neuronal excitability by D1R activation. Intracellular whole-cell recordings before, during and after the activation of the D1R showed that receptor activation results in firing rate suppression in excitatory neurons and facilitation in inhibitory neurons. Intracellularly, this cell-type dependent modulation is regulated by sodium channels and accompanied by the correlated changes in calcium dynamics both in dendrites and soma. Taken together, the results indicate that the D1 signaling in the somatosensory cortex contributes to sensory information processing, improves integration of tactile evidence to reach a perceptual decision and performs cell-type specific gain modulation to enhance inhibitory neurons' contribution to sensory coding in the neocortex.

The perception of the environment is dictated by sensory processing, which depends on the sensory representations in the brain. Dopamine is one of the neurotransmitters mediating this process, heterogeneously affecting neuronal responses both in sensory [1] and motor [2] systems. This is an active process, as evidenced by the dopaminergic regulation of spike-timing-dependent plasticity in structures related to the sensory processing [3,4]. Dopamine is also important for decision-making, reward and memory processing, thus its regulation of the stimulus representation in sensory circuits might have over-arching consequences for the processing and representation of sensory stimuli based on prior experiences.

A subregion of the primary somatosensory cortex (S1), named barrel cortex, is responsible for the processing of sensory inputs coming from the whiskers, and constitute one of the major sensory systems in rodents. As layer 2/3 (L2/3) of the S1 integrates neuronal inputs coming from surrounding cortical columns via horizontal connections, long-range neocortical inputs via L1 and information (including neuromodulatory) originating elsewhere in the brain, it is suitable for studying top-down and bottom-up processing of cortical sensory information. Monoamines are known to interfere with the development of this cortical neurons, modulate the balance between excitation and inhibition, and shape the contribution of these neurons to tactile processing [5–7]. Although they seem to have no influence in the thalamocortical projections that pattern the barrel formations, they are necessary for the maturation of layer (L) 4 and L2/3 of the barrel cortex [8]. Moreover, S1 sends excitatory inputs to the Substantia Nigra (SN), reducing the latency for responding to stimuli predicted to be rewarded [9]. This indicates that the dopaminergic and the somatosensory systems are functionally coupled throughout life.

Dopamine receptors are differentially present in all cortical layers, L1 through L6: D1-like receptors are generally more expressed than D2, in both pyramidal and interneurons [10]. The D1 receptor activates the cAMP/PKA cascade resulting in the activation of many downstream protein targets, such as AKAP-15 [11] and DARPP-32 [12], which phosphorylates/dephosphorylates voltage-gated sodium channels (Na_V), thus modulating sodium conductance in the cortical neurons (also see Chapter 1). Because Na_V channels are responsible for establishing the spike threshold for action potential generation, it is not surprising that in hippocampus [13], midbrain [14] and basal ganglia [15], dopamine is shown to increase the spike threshold and duration, decreasing the postsynaptic excitability via the modulation of sodium and calcium channels. This dopamine-mediated increase in spike threshold is also observed in the striatum, where it mediates inhibition of hyperpolarizing potential, and controls spike latency [16].

Despite the indirect evidence concerning the role of dopamine for sensory processing, and the empirical findings on the dopaminergic control of neuronal excitability and spike timing,

whether dopaminergic signaling controls sensory processing in the somatosensory cortex is not yet known. Therefore, in this study, we studied the contribution of the dopaminergic receptors for neuronal and behavioral information processing. The results showed that dopamine controls excitability in a cell-type specific manner. While D1R activation hyperpolarizes spike-threshold and increases firing rate in inhibitory neurons, it inhibits stimulus-evoked spiking in the excitatory neurons. As a result, information transferred between cortical neurons are shaped bidirectionally by the activation of the D1Rs. The behavioral consequence of this modulatory control by D1Rs is the facilitation of sensory integration, as animals require substantially less sensory information to successfully locate tactile targets. This cell-type specific control of excitability by dopaminergic receptor activation is likely to act as a gain-modulator, increasing the signal-to-noise during goal-directed behavior.

Materials and Methods

The physiology of the dopaminergic activation across the different receptor types was investigated through pharmacological manipulation by dopaminergic agonists (D1: SKF38393, D2: Quinpirole) and antagonists (D1: SCH23390, D2: Sulpiride) both in cell cultures and brain slices using intracellular recordings and calcium imaging. All animal procedures were approved by the Radboud University Animal Experiment Committee.

Experiments in neocortical cell cultures

Cultures of dissociated cortical neurons were prepared from postnatal day 0 mice on C57BL/6J background. The mother was sacrificed by cervical dislocation, pups by decapitation, before their brains were rapidly removed. Brains were put on ice-cold Hank's balanced salts solution (HBBS; pH 7.3) comprising 10% HBSS without magnesium or calcium (Gibco Life Technologies; Catalog number (Cat.nr.): 14175129), 100 U/ml penicillin-streptomycin (Thermo Fisher Scientific; Cat.nr. 15140122) and 500 µM GlutaMAXTM (Thermo Fisher Scientific; Cat.nr. 35050061). Neocortex was removed bilaterally and incubated in HBSS with 5% trypsin solution (Gibco Life Technologies; Cat.nr. 15090046). The solution was removed, and the cells were dissociated using a fire-polished Pasteur's pipette. Dissociated neurons were plated onto 25 mm coverslips, coated with 1% (weight/volume) poly-L-lysine (Sigma-Aldrich; Cat.nr. 25988-63-0), with a density of 1.6 x 105/coverslip. Cultures were maintained at 37°C in culture medium comprising neurobasal medium (Thermo Fisher Scientific; Catalog number: 21103049) and carbonated (95%O_2/ 5% CO_2), supplemented with 2% B27 Supplement (Thermo Fisher Scientific; Cat.nr. 17504044) and 500 µM GlutaMAXTM (Thermo Fisher Scientific; Cat.nr. 35050061). On day 5, the culture medium was replaced with medium without glutamate. Half of the medium was changed twice per week.

Virally expressed GCaMP6s [17] under the CaMK2 promoter was used for visualization of the intracellular calcium dynamics. Viral packaging was adapted from [18–20]. In short, a suspension of 37.5 µg pRVl (AAV2) (6.25 µg/plate), 37.5 µg pH21 (AAV1) (6.25 µg/plate), 125µg pFΔ6 (Ad Helper) (25 µg/plate), 62.5 µg GCamp6 (12.5 µg/plate), 2 ml $CaCl_2$ (2.5 M; Merck; Cat. nr. 1023820500) and 12 ml of ddH_2O were slowly added (5 ml/15 cm plate) to HEK293 cells (density: 800.000 cells/plate) as plates were gently swirled. Viral transfection was confirmed 48 hours later with the Eclipse TS100 light microscope (Nikon) coupled with the epi-fluorescence illuminator Nikon Intensilight C-HGFIE and viral particles were purified with heparin (GE Healthcare; Cat.nr. 170406013). Concentration of the virus was checked with qPCR (fwd ITR primer, 5'-GGAACCCCTAGTGATGGAGTT-3', and rev ITR primer, 5'-CGGCCTCAGTGAGCGA-3'), as in [21]. 2 µl of the virus was transferred to dissociated neuronal cell cultures (plate diameter: 25 mm) on day 2 of the culture (DIV2). For these experiments, two batches of the virus with titers of 4.92×10^{12} and 1.86×10^{12} were used. Transfected neurons were stored in the cell incubator at 37°C until the fluorescence was visible.

Neurons were visualized using LED illumination (Coolled, pE-100) and a camera (Q-imaging, Model number: EXI-BLU-R-F-M-14-C, CA) coupled to a light microscope (Nikon, FN1) placed on an active vibration isolation table (Table Stable; TS-150). Data was acquired full field at 10 fps in MicroManager (https://micro-manager.org/) at 14-bit with a readout time of 30 MHz. Data acquisition was triggered using a custom Arduino interface, coupling whole-cell recording (see below) software Patchmaster (HEKA) with MicroManager, camera, and the excitation light source. Electrical recordings, electrical stimulation and calcium imaging were time aligned with clock signals generated in the Patchmaster.

Cell cultures were used 9-15 days after plating, i.e. 7-13 days after viral transfection. Pyramidal neurons were visually selected according to their somatic shape and dendritic morphology. The culture plate was continuously perfused with Ringer's solutions (in mM): 10 HEPES (Sigma-Aldrich, Cat.nr. 7364459); 150.1 NaCl; 5 KCl; 1.5 $CaCl_2.2H_2O$; 1 $MgCl_2.6H_2O$; 10 Glucose.H_20; pH 7.4 adjusted with NaOH (all last chemicals are from Merck, Cat.nrs., respectively are: 7647145, 7447407, 100350408, 1058330250, 14431437).

Patch pipette electrodes with a resistance of 5-9 MOhm were pulled from borosilicate glass (Multi Channel Systems; Cat.nr. 300034) using a horizontal puller (Sutter instrument CO. Model P-2000). Intra-pipette solution included (in mM): 5 KCl (Merck, Cat.nr. 7447407); 130 K-Gluconate; 1.5 $MgCl_2.6H_2O$; 0.4 Na_3GTP; 4 Na_2ATP; 10 HEPES; 10 Na-phosphocreatine; 0.6 EGTA (Sigma-Aldrich, Cat.nrs., respectively are: 299274, 1058330250, G877, A26209, 7364459, P7936, 67425). pH was set to 7.22 using KOH (1 M; Merck; Cat.nr. 5033). A

chlorided silver wire was used to create electrical continuity between the intra-pipette solution and head-stage, connected to EPC 9 amplifier (HEKA).

Somatic whole-cell configuration was achieved as described before [22]. Current-clamp recordings were performed using step-and-hold pulses, 500 ms in duration. 10 steps of 40 pA current were delivered in every train, and each train was repeated three times. Sweep duration was set to 7 sec. Resting membrane potential was clamped at -70 mV. Evoked calcium dynamics were visualized as described above after binning (x2) with an exposure duration of 100 ms.

Electrophysiology of layer 2/3 pyramidal neurons in slices

Recordings from 47 cells coming from 34 Pval-cre and SSt-cre mice between 11 and 54 weeks (15 male, 19 female) were used in this study. Acute slices of the barrel cortex were prepared as described before [23]. In short, mice were anesthetized with Isoflurane (10 ml/mouse) and the depth of the anesthesia was assessed by pinch withdrawal before perfusion in the cooled solution containing (in mM): 108 choline chloride, 3 KCl, 26 $NaHCO_3$, 1.25 NaH_2PO_4.H2O, 25 Glucose.H_2O, 1 $CaCl_2$.2H_2O, 6 $MgSO_4$.7H_2O, 3 Na-pyruvate. Animals were decapitated for brain extraction and sliced in the same solution. Brain slices were then transferred to a chamber with ACSF (in mM): 1200 NaCl, 35 KCl, 100 Glucose.H2O, 25 CaCl2.2H2O, 13 $MgSO_4$.7H_2O, 250 $NaHCO_3$, 12.5 NaH_2PO_4.H_2O, carbonated with 95% O_2/5% CO_2. The coronal slices were then kept oxygenated at 37°C for 30 minutes and then 30 minutes in room temperature before the whole-cell recordings. The slice was then placed in a chamber under the microscope and was continuously oxygenated and perfused with ACSF. The barrel cortex was localized using the 20x lens and the pyramidal cells were patched with a 40x lens.

For the electrophysiological recordings, conventional current-clamp and voltage-clamp [24,25] configurations were used. All data were collected while somatic membrane potential was clamped at -70 mV. Two types (step-and-hold and frozen noise) current-clamp protocols were used as described in Chapter 2. In the voltage-clamp mode, there were 4 types of protocols used. First, a sawtooth voltage sweep from -70 mV to +70 mV in 100 ms five times was performed. This was repeated twice. Subsequently, the same five sawtooth waves were performed in 50 ms and in 10 ms in cycle duration, corresponding to stimulus frequencies of 10, 20, 100 Hz, respectively. Finally, the membrane voltage was clamped at -70 mV while applying 14 increasing steps of 10 mV for 250 ms, with a 20 s interval. Collectively these protocols allowed me to address the ionic bases of dopaminergic modulation of neuronal activity.

During these experiments select pharmacological agents, such as SKF38393 (D1 agonist,

1 μM), Quinpirole (D2 agonist, 10 μM), Dopamine (50 μM), SCH23390 (D1 antagonist, 1 μM), Sulpiride (D2 antagonist, 10 μM), plus additional tetrodotoxin (TTX, 10 μM), EGTA (Ca^{2+} channels blocker (1, 2 and 20 μM)), $NiCl_2$ (Ca^{2+} channels blocker, 1 μM), $CdCl_2$ (1 μM), targeting specific ion channels were also administered to causally address the mechanisms involved with dopaminergic regulation of the neuronal excitability.

Following data acquisition, we used a custom program in MATLAB to systematically extract the characteristics from the neurons measured. Cell-type classification was performed based on K-means clustering using the maximum firing rate and the mean spike half-width. Comparisons were made with ANOVA repeated measures, Student's t-test and post-hoc analysis with Bonferroni statistical test. Non-parametric comparisons were made with Kruskal-Wallis test and Kolmogorov-Smirnov test.

Behavioral experiments

Adults animals were trained on the spontaneous gap-crossing task as described before [6,18,26–29]. In short, animals were placed on an elevated platform (so called "home" platform) and were allowed to explore their environment in darkness, without light in the visible spectrum to the mammalian eye. A second elevated platform placed with a variable distance to the home platform served as a tactile target (see Figure 4A). A high-speed camera placed above the experimental chamber acquired animal navigation at a rate of 400 frame-per-second (spatial resolution 40 microm/pixel) and this videographic data were analyzed offline for quantification of sensorimotor exploration.

After initial training, the distance between the home and target platforms were set so that the animals could contact the target platform using only their whiskers. Once animals reached this, so-called whisker-distance trials, D1 agonist (SKF38393 in Ringer's solution, 0.25 μg/mouse, volume: 200 nl) or vehicle (Ringer's solution, 200 nl) injections were performed via a cannula implanted in the brain prior to the start of training. The order of the injections was randomized (N=30 trials/condition). The data analysis was performed using custom written routines in MATLAB as described before [6,18,26,27].

Results

Sensory information is encoded by regulation of rate and timing of action potentials [30]. To address whether dopaminergic signaling can modulate generation of action potential, we performed whole-cell recordings in acute slices of the adult mouse barrel cortex (Figure 1). The results showed that D1 receptor activation resulted in reduction in spiking frequency (n=16, ANOVA repeated measures, $p < 0.001$) although the effect size was small ($\eta^2=0.077$) during sustained somatic current injections. D2 activation in pyramidal neurons increases

the spike frequency (n=7, ANOVA repeated measures, p=0.031; Figure 1C). In fast-spiking neurons, activation of D1 receptors increases spiking (D1: (n=16, ANOVA repeated measures, $p < 0.001$, $\eta^2 = 0.254$). Preliminary experiments (N=3) showed that the D2 agonist Quinpirole tends to increase the action potential count in fast-spiking neurons (ANOVA repeated measures, $p < 0.001$, $\eta^2 = 0.586$).

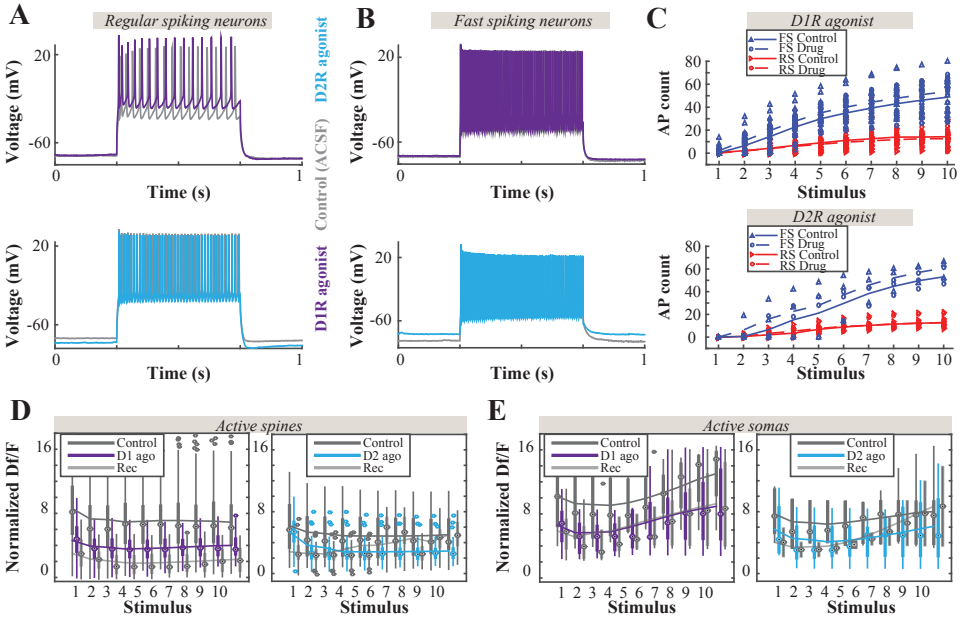

Figure 1. D1 and D2 agonists selectively modulate information transfer in a cell type specific manner. (**A**) Action potential traces of a representative pyramidal neuron under Control, D1 agonist (SKF 38393, 1 µM, in purple) and D2 agonist (Quinpirole, 10 µM, in light blue, bottom row) treatments. (**B**) Representative interneuron under Control, D1 agonist (SKF 38393, 1 µM, purple) and (Quinpirole, 10 µM, in light blue, bottom row) treatments. (**C**) Comparison of D1 and D2 agonist treatments in Regular (red) and Fast Spiking (blue) neurons. Dashed lines show the drug effect in the spike frequency. Minimal effect is observed in regular spiking neurons, while fast spiking neurons show significant increase after both D1 (n=16, Student's t test, $p < 0.001$, ANOVA repeated measures, $p < 0.001$, $\eta^2 = 0.254$) and D2 (n=3, Student's t test, $p < 0.001$, ANOVA repeated measures, $p < 0.001$, $\eta^2 = 0.586$) agonists treatments. (**D-E**) D1 and D2 agonists reduced the change in Df/F in neocortical cell cultures in both active spines (**D**) and somas (**E**). The change in fluorescence (Df/F) was normalized to the maximum change per stimulus. See main text for statistical comparisons. ago = agonist; Rec= recovery.

Dopaminergic regulation of the action potential generation is thought be mediated through T-type calcium channels [31–33]. Therefore, we quantified the changes in intracellular calcium

using genetically encoded calcium indicator, GCaMP6s in dissociated neuronal cultures from the neocortex. Although increasing stimulus intensity was not accompanied by a systematic change in the amplitude of the calcium signals in spines (Figure 1D), D1 agonist (SKF38393, 1 μM) decreased the calcium transients significantly in all stimulus levels (n=191, ANOVA repeated measures, $p=0.01$, Bonferroni, $p<0.001$). Similar to D1, D2 agonist (Quinpirole, 10 μM) decreased evoked calcium transients of active spines significantly and the long-lasting effect remained after the drug administration was ceased (Recovery condition, $p<0.001$). Although the average calcium transients were reduced, the number of active spines and soma varied depending on the dopaminergic receptor activated. The number of active spines increased by 4 folds during D2 agonist administration (Control n = 12, D2 n=48), and slowly reduced post-administration (D2: n=35). However, D1R agonist reduced the number of active spines both during and post administration (Control: n=191, D1: n=55, Recovery: n=41; Figure 1D). The calcium dynamics in soma generally followed the observations in dendritic spines with the exception that D1R activation resulted in uniform reduction of calcium transient across all stimulus conditions, while D2R activation was most effective in lower stimulus intensities (Figure 1E; All comparisons ANOVA for repeated measures $p<0.05$). These observations argue that dopaminergic signaling mediated regulation of calcium might be cell-type dependent.

Although dopaminergic regulation of calcium dynamics contributes to the regulation of cellular excitability, observed changes in spiking dynamics might rather involve voltage-gated sodium (Na_V) channels. As reviewed in Chapter 1, in several subcortical structures, dopamine has been shown to regulate Na_V conductance. We thus quantified the inward currents in whole-cell voltage clamp configuration (Figure 2). Both cell classes displayed prominent inward currents which were suppressed after tetrodotoxin administration (Figure 2A-B). The statistics of the Na_V transients were altered upon D1R activation (Figure 2C). The peak and the total amplitude of the transients were reduced upon D1R activation and the membrane potential at which Na_V opened was hyperpolarized (Figure 2C) when all experiments were considered together.

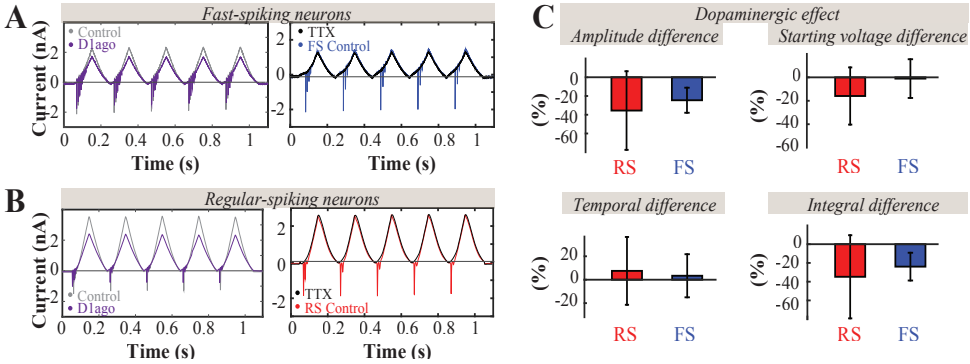

Figure 2. D1 agonist reduces the amplitude of inward currents and affects timing in regular- and fast-spiking neurons. (A) Voltage-clamp recordings of 100 ms triangular sweeps demonstrated that D1 agonist (SKF38393, 1 μM, purple) reduces sodium currents amplitudes in fast-spiking neurons, as sodium blocker tetrodotoxin (TTX) removes the inward currents completely (black). **(B)** The same occurs in regular-spiking neurons, with a higher remission. **(C)** D1R agonist reduced the amplitude of the first current (Student's t-test, p=0.006), starting voltage (Student's t-test, p=0.06) and integral (Student's t-test, p=0.01) of the inward currents, while tending to increase timing (Student's t-test, p=0.10) when all experiments considered together. Splitting data across cell groups reduced the power in the statistical comparisons, thus the cell type specific grouping of the data does not imply cell type specific changes.

Considering that dopaminergic receptor activation results in the reduction of voltage-gated sodium channel conductance, dopamine might control intracellular information transfer as somatic postsynaptic potentials are translated to action potentials. To directly quantify the information transfer we utilized a recently developed information theoretic [36,37] approach that computes the mutual information between a bandwidth limited time-varying current injected into the soma (entitled "frozen noise") with action potentials generated by the neuron (Figure 3A). Both regular-spiking (presumed excitatory) and fast-spiking (presumed inhibitory) neurons responded robustly to the somatic injection of "frozen noise" in control conditions and during drug administration (Figure 3B). D1R caused hyperpolarization of the action potential threshold in both classes of neurons across a large range of inter-spike intervals (Figure 3C) although fast-spiking neurons fired action potentials in more hyperpolarized membrane potentials (Figure 3D).

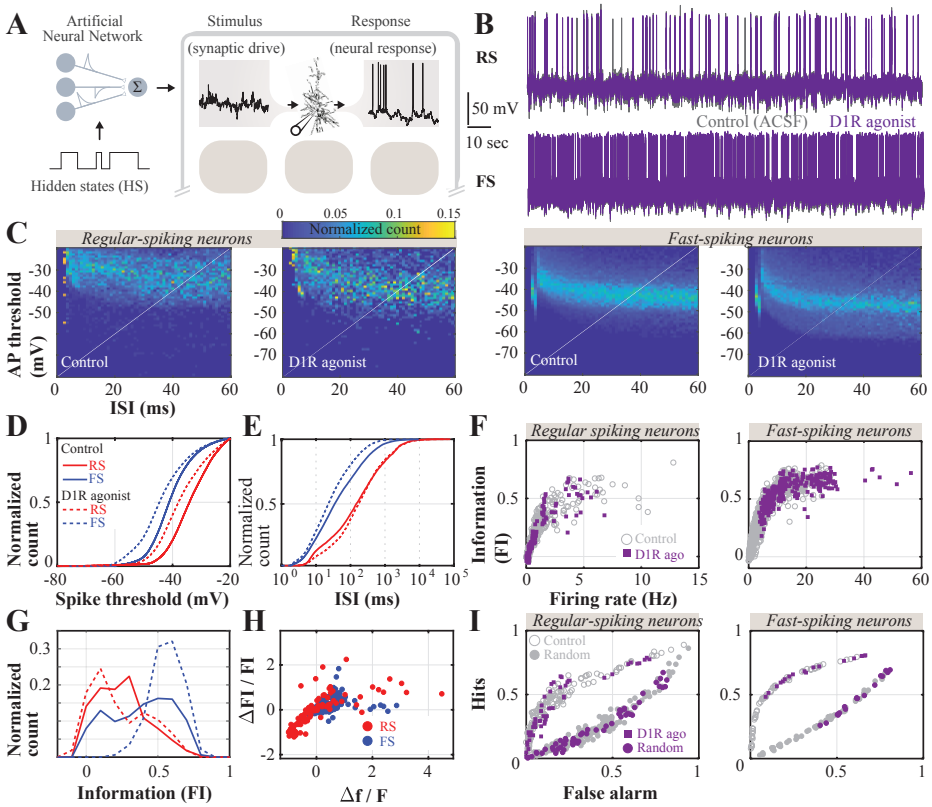

Figure 3. D1R activation controls intracellular information transfer in a cell-type specific manner. (A) Experimental protocol. To calculate the mutual information between current injected in soma ("frozen noise") and the action potentials generated by the neuron, we computed synaptic inputs impinging on the postsynaptic neuron as an output of a 1000 neuron network (see [36] for details). The frozen noise was injected in soma in acute slices of the adult barrel cortex. **(B)** Example of response in regular-spiking (RS) and fast-spiking (FS) neurons, under *Control* (ACSF, gray) and *D1 agonist* (SKF38393, 1 μM, purple) treatments. **(C)** Normalized spike count as a function of per interspike interval (ISI) and action potential (AP) threshold in RS and FS neurons before and during D1R activation. **(D-E)** Change in spike threshold (D) and firing rate, quantified as ISI (E), across drug conditions and cell types. All within cell type across drug conditions are statistically significant, Kruskal-Wallis test, $p<0.05$. **(F-G)** Information content of action potentials. **(F)** Information plotted against the firing rate. **(G)** Change in information transfer across drug conditions in both cell classes. Both within cell type across drug condition comparisons are statistically significant, Kruskal-Wallis test, $p<0.05$. **(H)** Change in information during D1R activation normalized to the change in firing rate across drug conditions. **(I)** Receiver-operating-characteristics of the spiking pattern. Hit: When the postsynaptic neuron fires action potential upon the upstate transition in the frozen noise; False alarm: When postsynaptic action potential is generated in the absence of an upstate.

Similar to our observations made during sustained somatic depolarization with a step-and-hold current pulse, frozen noise injection showed that D1R activation results in firing rate modulation; while the firing rate of regular-spiking neurons was reduced, fast-spiking neurons spiked at higher frequencies (Figure 3E). The change in the firing rate was directly correlated with the degree of information transfer. In regularly spiking neurons D1R activation caused reduction of the information (Figure 3F, left) although inhibitory neurons carried more information in their action potentials (Figure 3F, right). Comparisons of the total information transferred within a cell-type before and during D1R agonist application supported the conclusion that D1R facilitates information processing in presumed inhibitory neurons, while reducing the information content of excitatory neurons (Figure 3G), effectively selectively gating inhibition. Considering that relative change in information content remained constant in respect to the normalized firing rate change (Figure 3H), this differential regulation of information processing by D1R is due to the firing rate modulation of D1R activation.

Change in intracellular information transfer might control barrel cortical neurons' ability to encode the sensory stimulus. We thus quantified receiver-operator-characteristic (ROC) curve for both cell classes before and during D1R stimulation. The results showed that D1R activation increases the sensory encoding in inhibitory neurons and reduced in excitatory neurons (Figure 3I).

The role of D1R in controlling action potential threshold, firing rate and the information transfer between neurons in the somatosensory cortex suggests that dopaminergic signaling ultimately modulates sensory processing in freely behaving animals. Therefore we trained animals on a tactile object localization task, called spontaneous gap-crossing task [6,18,26–29]. On this task animals locate a tactile target, an elevated platform, while standing on another platform located beyond a gap (Figure 4A). A camera located above the gap is used to observe animals and collect the sensory statistics of decision making.

To regulate the D1R activation during task execution, we implanted animals with a guide cannula and trained animals to criteria, i.e. two consecutive sessions with 5+ trials during which animals contacted the target only using their whiskers before successful object localization. After animals reached the criteria, animals received either D1 agonist (SKF38393) or vehicle (Ringer's solution) for 30 trials/drug condition. The animals did not receive any whisker deprivation during these experiments.

Post-hoc analysis of the whisker contacts [38] showed that D1R activation results in faster decision-making as the latency to cross after the first contact was twice as long after vehicle injection (Vehicle vs D1R agonist, 911∓214 vs 417∓54 ms (mean∓sem), ANOVA, $P<0.05$; Figure 4B). The animals required significantly less sensory information to make their decision (Vehicle vs D1R agonist, 931∓115 vs 583∓68 ms (mean∓sem), ANOVA, $P<0.05$; Figure

4D). Although both touch duration per whisker contact (Vehicle vs D1R agonist, 17.3∓0.32 vs 15.9∓0.34 ms (mean∓sem), Kolmogorov-Smirnov Test, P<0.05; Figure 4E, left) and number of whiskers simultaneously in contact with the target (Vehicle vs D1R agonist, 3.1∓0.03 vs 2.9∓0.04 (mean∓sem), Kolmogorov-Smirnov Test, P<0.05; Figure 4E, right) were significantly different, the primary contributor to the reduced sensory exploration was the reduced number of whisker contacts with the target (Vehicle vs D1R agonist, 53.7∓6.62 vs 36.6∓3.7 ms (mean∓sem), ANOVA, P<0.05; Figure 4F). These results argue that D1R activation regulates integration of sensory information during tactile decision making.

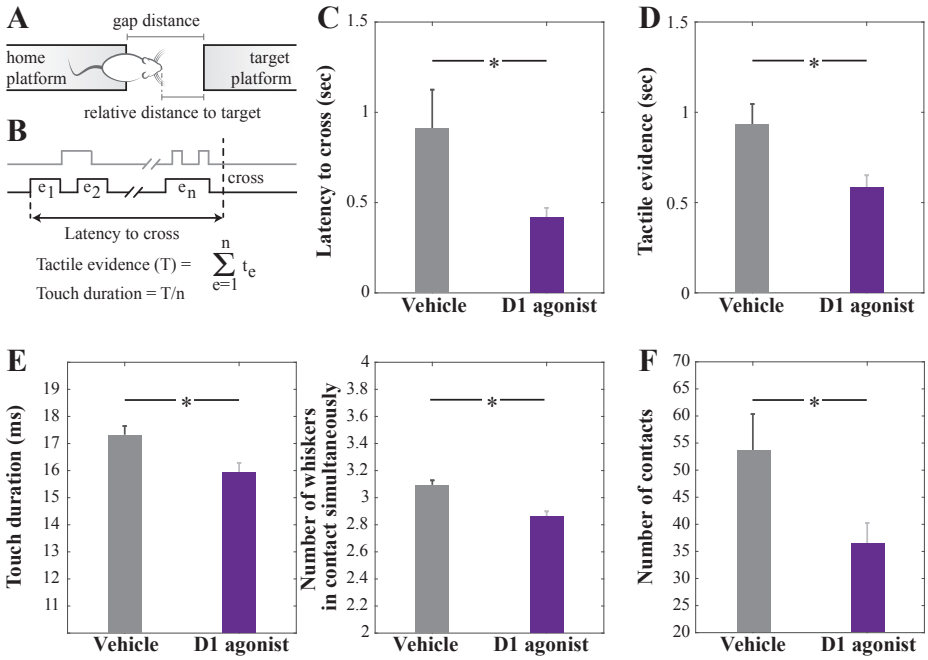

Figure 4. The consequences of D1R activation for tactile decision making. (**A**) Gap-crossing paradigm. **(B)** Quantification of sensory exploration. **(C)** Latency to cross, described as the temporal difference between the very first whisker contact with the target platform and animal's nose crossing the target platform as the animal crosses the gap, jumps on the target. **(D)** Tactile evidence leading to successful target localization across groups. Tactile evidence is calculated as the total duration of whisker contacts with the target. Note that animals had all of their whiskers intact, thus the variable is an integral of all contacts with the target by any whisker. **(E)** Touch duration is calculated as described in B. Number of whisker that are in contact with the target platform is calculated by binning the data in the temporal domain (2.5 ms/bin). **(F)** Total number of contacts made onto the target prior to successful target localization.

Discussion

Decision-making requires precise integration of information coming from various brain systems, demanding selection of relevant sensory inputs and top-down control based on previous knowledge. Tactile information coming from the mouse whiskers during an adequate number of contacts with the object will ultimately result in crossing the gap to explore another space. Here using intracellular recording, calcium imaging, behavioral recordings and pharmacological modulation of receptor activation, we show that dopamine is a potent regulator of cellular and behavioral information processing in the somatosensory cortex.

D1R activation in the somatosensory cortex functions as a top-down control mechanism, reducing the number of contacts required, hence improving performance and facilitating learning. The temporal precision of the neuronal signaling is imperative for sensory and movement constituents coordination by dopaminergic midbrain neurons during learning [39]. In the corticostriatal pathway, D1R activation shortly before pre- and postsynaptic paired stimulation converts LTD into LTP, needing a precise temporal window of maximum 2 seconds [40]. This dopamine-mediated spike-timing-dependent plasticity demonstrates the importance of this neurotransmitter for reinforcement learning [40,41].

At the neuronal network scale, we found dopamine receptors coordinating excitation and inhibition of the somatosensory system in a cell-type-specific manner. Dopaminergic neuromodulation is known to suppress firing in cortical neurons (e.g. [42]). Nevertheless, the novelty of this study is to describe cell-type-specific modulation in L2/3 of the S1. Dopamine release and calcium signaling are intrinsically correlated, as (also) shown herein. Calcium stimulates dopamine release via potassium-dependent depolarization of neurons [43]. Dopaminergic activation of D4 also modulates the information transfer via calcium release after direct activation of IP_3 [44], independently from L-type Ca^{2+} channels [44].

Recent studies now argue for a compartmentalized effect of dopamine, which controls spine excitability by activation of T-type calcium (Ca^{2+}) channels in the substantia nigra (SN) [45]. Neurons with a stronger expression of T-type Ca^{2+} channels display higher responsiveness to excitatory inputs [45]. The information integration of sensory and motor cortices during whisking likewise arise from calcium activity in the dendrites [46], sometimes intervening with the neuronal maturation and plasticity through LTD (for a review see [47]). Furthermore, dopaminergic neurons expressing Calbindin, a calcium binding protein, exhibit a delayed firing pattern during spontaneous activity [48]. Calcium dynamics dependent on L-type and T-type channels can also alter the direction of pre/postsynaptic plasticity if combined with GABAergic activation [49]. Because calcium signals follow sensory stimulation in a specialized subcellular level [50], they complement the voltage response in action potentials and may represent multiple other features in the neuronal network, such as time, location, or contact.

Considering that dopamine is required for corticostriatal plasticity [51,52], understanding the dopaminergic control of internal calcium release would be of use further for explaining memory and plasticity. Conclusively, this powerful influence linking calcium and dopamine circumscribes the firing rate and pattern.

Another possibility for explaining the cell-type-specific response to the dopaminergic drive is the location and engagement of voltage-dependent sodium and potassium channels, which are directly involved in determining the action potential threshold. Membrane configurations as a result of intrinsic properties or repetitive synaptic inputs play a role in firing rate of both cortical pyramidal and interneurons [53]. Sodium and calcium channels also act in the amplification of backpropagating spike trains in neocortical pyramidal neurons dendrites [54], interfering with temporal coding. Moreover, in the mPFC, dopamine enhances excitatory inputs of local circuits of layer V, while blocking the influence of layer I inputs, confirming differential modulation of two subtypes of pyramidal cells, in this instance [55].

Throughout modulation of calcium signaling, voltage-gated channels and spike-timing-dependent plasticity, dopamine presumably serve as a gain-modulator during sensory processing of tactile information and improves behavior execution. Overall, the cell-type-specific dopaminergic control of excitability enables an increase in signal-to-noise ratio during behavior, for performing a modulatory control of the signal through facilitating fast-spiking neurons information transfer while not affecting regular-spiking neurons in the same manner.

Bibliography

1. Gittelman, J. X., Perkel, D. J. & Portfors, C. V. Dopamine modulates auditory responses in the inferior colliculus in a heterogeneous manner. *J. Assoc. Res. Otolaryngol.* **14,** 719–729 (2013).
2. Brazhnik, E. *et al.* State-dependent spike and local field synchronization between motor cortex and substantia nigra in hemiparkinsonian rats. *J. Neurosci.* **32,** 7869–7880 (2012).
3. Schulz, J. M., Redgrave, P. & Reynolds, J. N. J. Corrigendum: Cortico-striatal spike-timing dependent plasticity after activation of subcortical pathways. *Front. Synaptic Neurosci.* **7,** 13 (2015).
4. Ren, Q., Zhang, Y., Wang, R. & Zhao, J. Optical spike-timing-dependent plasticity with weight-dependent learning window and reward modulation. *Opt. Express* **23,** 25247–25258 (2015).
5. Durig, J. & Hornung, J. P. Neonatal serotonin depletion affects developing and mature mouse cortical neurons. *Neuroreport* **11,** 833–837 (2000).
6. Miceli, S. *et al.* Reduced Inhibition within Layer IV of Sert Knockout Rat Barrel Cortex is Associated with Faster Sensory Integration. *Cereb. Cortex* **27,** 933–949 (2017).
7. Schubert, D., Nadif Kasri, N., Celikel, T. & Homberg, J. in *Sensorimotor Integration in the Whisker System* (eds. Krieger, P. & Groh, A.) 243–273 (Springer, 2015).
8. Alvarez, C. *et al.* Effects of genetic depletion of monoamines on somatosensory cortical development. *Neuroscience* **115,** 753–764 (2002).
9. Watabe-Uchida, M., Zhu, L., Ogawa, S. K., Vamanrao, A. & Uchida, N. Whole-brain mapping of direct inputs to midbrain dopamine neurons. *Neuron* **74,** 858–873 (2012).
10. Santana, N., Mengod, G. & Artigas, F. Quantitative analysis of the expression of dopamine D1 and D2 receptors in pyramidal and GABAergic neurons of the rat prefrontal cortex. *Cereb. Cortex* **19,** 849–860 (2009).
11. Few, W. P., Scheuer, T. & Catterall, W. A. Dopamine modulation of neuronal Na(+) channels requires binding of A kinase-anchoring protein 15 and PKA by a modified leucine zipper motif. *Proc Natl Acad Sci USA* **104,** 5187–5192 (2007).
12. Schiffmann, S. N. *et al.* Modulation of the voltage-gated sodium current in rat striatal neurons by DARPP-32, an inhibitor of protein phosphatase. *Eur. J. Neurosci.* **10,** 1312–1320 (1998).
13. Stanzione, P., Calabresi, P., Mercuri, N. & Bernardi, G. Dopamine modulates CA1 hippocampal neurons by elevating the threshold for spike generation: an in vitro study. *Neuroscience* **13,** 1105–1116 (1984).
14. Grace, A. A. Evidence for the functional compartmentalization of spike generating regions of rat midbrain dopamine neurons recorded in vitro. *Brain Res.* **524,** 31–41 (1990).
15. Richards, C. D., Shiroyama, T. & Kitai, S. T. Electrophysiological and immunocytochemical characterization of GABA and dopamine neurons in the substantia nigra of the rat. *Neuroscience* **80,** 545–557 (1997).
16. Rutherford, A., Garcia-Munoz, M. & Arbuthnott, G. W. An afterhyperpolarization recorded in striatal cells “in vitro”: effect of dopamine administration. *Exp. Brain Res.* **71,** 399–405 (1988).
17. Chen, J. L., Carta, S., Soldado-Magraner, J., Schneider, B. L. & Helmchen, F. Behaviour-dependent recruitment of long-range projection neurons in somatosensory cortex. *Nature* **499,** 336–340 (2013).
18. Celikel, T. & Sakmann, B. Sensory integration across space and in time for decision making in the somatosensory system of rodents. *Proc Natl Acad Sci USA* **104,** 1395–1400 (2007).
19. Freudenberg, F., Marx, V., Seeburg, P. H., Sprengel, R. & Celikel, T. Circuit mechanisms of GluA1-dependent spatial working memory. *Hippocampus* **23,** 1359–1366 (2013).

20. Freudenberg, F. *et al.* Hippocampal GluA1 expression in Gria1-/- mice only partially restores spatial memory performance deficits. *Neurobiol. Learn. Mem.* **135,** 83–90 (2016).
21. Aurnhammer, C. *et al.* Universal real-time PCR for the detection and quantification of adeno-associated virus serotype 2-derived inverted terminal repeat sequences. *Hum. Gene Ther. Methods* **23,** 18–28 (2012).
22. Celikel, T., Szostak, V. A. & Feldman, D. E. Modulation of spike timing by sensory deprivation during induction of cortical map plasticity. *Nat. Neurosci.* **7,** 534–541 (2004).
23. Kole, K. & Celikel, T. Neocortical microdissection at columnar and laminar resolution for molecular interrogation. *Curr. Protoc. Neurosci.* e55 (2018). doi:10.1002/cpns.55
24. Blanton, M. G., Lo Turco, J. J. & Kriegstein, A. R. Whole cell recording from neurons in slices of reptilian and mammalian cerebral cortex. *J. Neurosci. Methods* **30,** 203–210 (1989).
25. Margrie, T. W., Brecht, M. & Sakmann, B. In vivo, low-resistance, whole-cell recordings from neurons in the anaesthetized and awake mammalian brain. *Pflugers Arch.* **444,** 491–498 (2002).
26. Voigts, J., Sakmann, B. & Celikel, T. Unsupervised whisker tracking in unrestrained behaving animals. *J. Neurophysiol.* **100,** 504–515 (2008).
27. Voigts, J., Herman, D. H. & Celikel, T. Tactile object localization by anticipatory whisker motion. *J. Neurophysiol.* **113,** 620–632 (2015).
28. Pang, R. D. *et al.* Mapping functional brain activation using [14C]-iodoantipyrine in male serotonin transporter knockout mice. *PLoS ONE* **6,** e23869 (2011).
29. Juczewski, K. *et al.* Somatosensory map expansion and altered processing of tactile inputs in a mouse model of fragile X syndrome. *Neurobiol. Dis.* **96,** 201–215 (2016).
30. Azarfar, A., Calcini, N., Huang, C., Zeldenrust, F. & Celikel, T. Neural coding: A single neuron's perspective. *Neurosci Biobehav Rev* (2018).
31. Bender, K. J., Uebele, V. N., Renger, J. J. & Trussell, L. O. Control of firing patterns through modulation of axon initial segment T-type calcium channels. *J Physiol (Lond)* **590,** 109–118 (2012).
32. Bender, K. J., Ford, C. P. & Trussell, L. O. Dopaminergic modulation of axon initial segment calcium channels regulates action potential initiation. *Neuron* **68,** 500–511 (2010).
33. Yang, S. *et al.* β-Arrestin-Dependent Dopaminergic Regulation of Calcium Channel Activity in the Axon Initial Segment. *Cell Rep.* **16,** 1518–1526 (2016).
34. Kole, K. *et al.* Transcriptional mapping of the primary somatosensory cortex upon sensory deprivation. *Gigascience* (2017).
35. Kole, K. *et al.* Proteomic landscape of the primary somatosensory cortex upon sensory deprivation. *Gigascience* **6,** 1–10 (2017).
36. Zeldenrust, F., de Knecht, S., Wadman, W. J., Denève, S. & Gutkin, B. Estimating the Information Extracted by a Single Spiking Neuron from a Continuous Input Time Series. *Front. Comput. Neurosci.* **11,** 49 (2017).
37. Azarfar, A., Calcini, N., Huang, C., Zeldenrust, F. & Celikel, T. Neural coding: A single neuron's perspective. *Neurosci. Biobehav. Rev.* (2018). doi:10.1016/j.neubiorev.2018.09.007
38. Azarfar, A. *et al.* An open-source high-speed infrared videography database to study the principles of active sensing in freely navigating rodents. *Gigascience*
39. Coddington, L. T. & Dudman, J. T. The timing of action determines reward prediction signals in identified midbrain dopamine neurons. *Nat. Neurosci.* (2018). doi:10.1038/s41593-018-0245-7
40. Shindou, T., Shindou, M., Watanabe, S. & Wickens, J. A silent eligibility trace enables dopamine-dependent synaptic plasticity for reinforcement learning in the mouse striatum. *Eur. J. Neurosci.* (2018). doi:10.1111/

ejn.13921

41. Fisher, S. D. *et al.* Reinforcement determines the timing dependence of corticostriatal synaptic plasticity in vivo. *Nat. Commun.* **8,** 334 (2017).
42. Batallán-Burrowes, A. A. & Chapman, C. A. Dopamine suppresses persistent firing in layer III lateral entorhinal cortex neurons. *Neurosci. Lett.* **674,** 70–74 (2018).
43. Yarom, M., Zurgil, N. & Zisapel, N. Calcium permeability changes and neurotransmitter release in cultured brain neurons. II. Temporal analysis of neurotransmitter release. *J. Biol. Chem.* **260,** 16294–16302 (1985).
44. Wang, Y.-L. *et al.* Selective dopamine receptor 4 activation mediates the hippocampal neuronal calcium response via IP3 and ryanodine receptors. *Brain Res.* **1670,** 1–5 (2017).
45. Evans, R. C., Zhu, M. & Khaliq, Z. M. Dopamine Inhibition Differentially Controls Excitability of Substantia Nigra Dopamine Neuron Subpopulations through T-Type Calcium Channels. *J. Neurosci.* **37,** 3704–3720 (2017).
46. Xu, N. *et al.* Nonlinear dendritic integration of sensory and motor input during an active sensing task. *Nature* **492,** 247–251 (2012).
47. Hlushchenko, I., Koskinen, M. & Hotulainen, P. Dendritic spine actin dynamics in neuronal maturation and synaptic plasticity. *Cytoskeleton (Hoboken)* **73,** 435–441 (2016).
48. Brown, M. T. C., Henny, P., Bolam, J. P. & Magill, P. J. Activity of neurochemically heterogeneous dopaminergic neurons in the substantia nigra during spontaneous and driven changes in brain state. *J. Neurosci.* **29,** 2915–2925 (2009).
49. Jędrzejewska-Szmek, J., Damodaran, S., Dorman, D. B. & Blackwell, K. T. Calcium dynamics predict direction of synaptic plasticity in striatal spiny projection neurons. *Eur. J. Neurosci.* **45,** 1044–1056 (2017).
50. Yang, H. H. *et al.* Subcellular imaging of voltage and calcium signals reveals neural processing in vivo. *Cell* **166,** 245–257 (2016).
51. Kreitzer, A. C. & Malenka, R. C. Striatal plasticity and basal ganglia circuit function. *Neuron* **60,** 543–554 (2008).
52. Yagishita, S. *et al.* A critical time window for dopamine actions on the structural plasticity of dendritic spines. *Science* **345,** 1616–1620 (2014).
53. Lytton, W. W. & Sejnowski, T. J. Simulations of cortical pyramidal neurons synchronized by inhibitory interneurons. *J. Neurophysiol.* **66,** 1059–1079 (1991).
54. Williams, S. R. & Stuart, G. J. Backpropagation of physiological spike trains in neocortical pyramidal neurons: implications for temporal coding in dendrites. *J. Neurosci.* **20,** 8238–8246 (2000).
55. Leyrer-Jackson, J. M. & Thomas, M. P. Layer-specific effects of dopaminergic D1 receptor activation on excitatory synaptic trains in layer V mouse prefrontal cortical pyramidal cells. *Physiol. Rep.* **6,** e13806 (2018).

Chapter 6

Compartmental regulation of calcium by Corticosterone

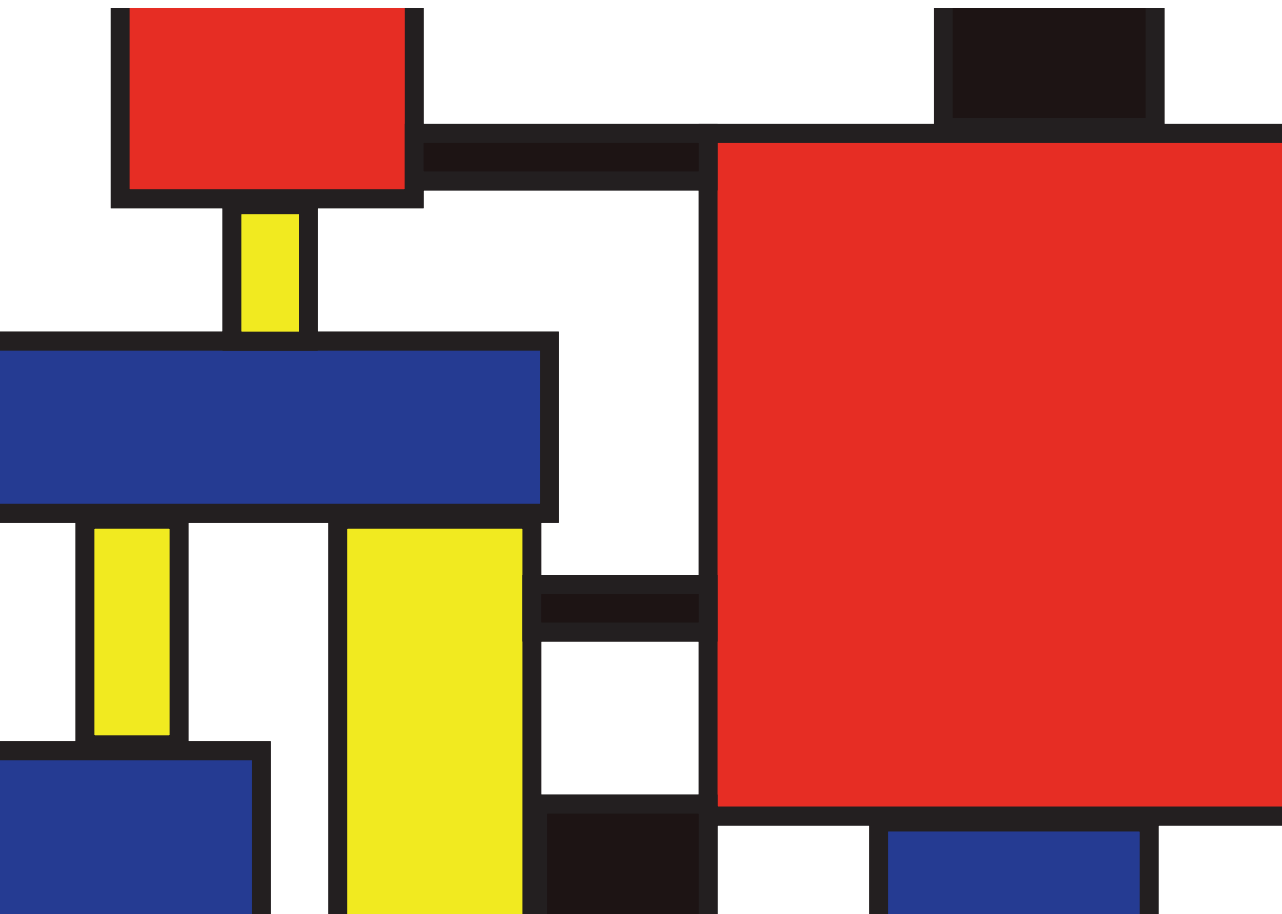

It is estimated that ~90% of the world population suffers from high levels of stress during at least a period in their lifetime. Stress may give rise to major mental disorders such as anxiety, depression and mood disorders either as a contributing or a triggering factor. Cortisol is released from the adrenal cortex during stress. In humans, cortisol release is correlated with enhanced sensory, in particular tactile, processing. The mechanism by which cortisol alters sensation is not yet known. In rodents, it has been shown that corticosterone (Cort), a metabolite of cortisol, controls Ca^{2+} signaling in a region-specific manner. Specifically, Ca^{2+} currents, mediated by high-voltage activated (L-type) Ca^{2+} channels, are augmented in the hippocampal CA1 region and basolateral amygdala upon in vitro Cort administration through genomic mechanisms. However, Cort mediated intracellular Ca^{2+} homeostasis is not ubiquitous, which makes the critical examination of its local effects in sensory circuits crucial. In this chapter, this question is addressed following pharmacological interrogation of GR activation and calcium imaging in acute slices of the somatosensory cortex and in neocortical cell cultures. The results show that Cort modulates evoked calcium transients in soma but not in spines suggesting that Cort action is compartmentalized in individual neurons. These findings have far-reaching implications including adaptive gain modulation of sensory information during the integration of synaptic currents in soma which ultimately controls what information will be transmitted in synaptically coupled networks.

Stress is a physical reaction, plausibly originated from our evolutionary needs to defend ourselves or prevent damage to our body. Reaction to stress differs across individuals. A cue or a context can be interpreted as stressful by someone and still be neutral to another person. If, for example, one once had an accident crossing a street, this experience may trigger more alertness towards all related stimuli, let it be a car, bus, or a screeching sound. Therefore, sensory processing and perception can be regulated by stress, while stress might serve as an active filter for sensory processing.

When our body identifies a stressor, that is, any stimulus threatening the body's homeostasis [1], two systems, i.e. the sympatho-adrenomedullary system and the hypothalamic-pituitary-adrenal (HPA) axis, are activated simultaneously [2]. The former rapidly releases epinephrine and norepinephrine (NE) by the adrenal medulla and the nerve terminals of the sympathetic nervous system [3]. The latter, upon the activation of the vagal nerve, indirectly increases the activity of noradrenergic neurons in the nucleus tractus solitarius and in the locus coeruleus [4], and controls the glucocorticoid levels in the body [5].

The activation of the sympatho-adrenomedullary system is widely considered to trigger the Fight-or-Flight response, increase alertness and attention [6–8]. The HPA-axis activation leads to the secretion of corticotropin-releasing hormone (CRH) and vasopressin (AVP) from the Paraventricular nucleus (PVN) [9]. These hormones reach the anterior pituitary through the portal vessel system, and stimulate the production of pro-opiomelanocortin (POMC). POMC, a precursor to the adrenocorticotropic hormone (ACTH), promotes ACTH release which in turn enhances glucocorticoid release from the adrenal cortex [9]. High levels of glucocorticoid release induce a negative feedback control on the HPA axis [5].

Corticosterone (Cort) and cortisol are the glucocorticoids known as "stress hormones", the former predominant in rodents and the latter in humans [2]. They are synthesized in the adrenal cortex, *zona fasciculata*, a region that regulates many vital functions of the body including immunologic, metabolic and homeostatic functions [2,5]. Because of their lipophilic characteristic, they can cross the brain-blood barrier without any difficulty, being able to reach all cells in the brain, but they can only exert their effects on those cells that express their receptor [1]. During our circadian cycle, corticosteroids are released phasically, however when a stressor is present, there is an increase in their release [2]. In order to generate an effect in the brain, the glucocorticoids bind the mineralocorticoids (MR) and glucocorticoids (GR) receptors [2]. These are nuclear receptors [10] and regulate transcription [1]. The affinity of glucocorticoids is higher for MR, which are recruited even at low concentrations of Cort. GR has a tenfold lower affinity when compared to MR and is activated only when the levels of glucocorticoids are significantly (but often only transiently) elevated, e.g. after a stressful situation or at the high peak of the Cort cycle [11].

Corticosteroids alter brain function through genomic and non-genomic mechanisms [11]. MR and GR are present in the cytoplasm before binding to their corticosteroid targets, and when the binding takes place, ligand-receptor complexes are translocated to the nucleus [11]. Corticosteroids, once they are in the nucleus, can alter gene transcription directly or indirectly via DNA binding or through interaction with transcriptional elements [11]. For instance, in rat CA1 pyramidal neurons, a brief application of Cort raises the amplitude of high-voltage activated sustained Ca^{2+} currents, primarily through a change in L-type Ca^{2+} currents [12], which requires GR-mediated protein synthesis. However, Corticosteroid-mediated' MR activation affects L-type Ca^{2+} channels densities in a dose-dependent manner [13]. P/Q-, N-, R- and T- types of Ca^{2+} channels are also associated with intracellular calcium modulation by increased levels of Cort [14]. The dose-dependent activation of GR or MR affects the synaptic transmission through distinct mechanisms. In the short term, the amplitude of the miniature excitatory postsynaptic currents (mEPSC) is increased although mEPSCs decay faster after corticosteroid application [15]. In the longer term, the membrane is depolarized via a transcription-dependent increase in intracellular calcium, which increases the amplitude of mEPSCs [15]. As both influx and efflux of Ca^{2+} are regulated by GRs it is not surprising that GRs potently modulate neuronal communication and synaptic plasticity in a wide range of synaptic circuits [11].

Given the highly non-linear compartmental dynamics of the calcium signaling in the neocortex [16,17], Cort action in regulation of calcium signaling in the neocortex might be critical in shaping communication across the network. Therefore, in this study, I addressed the Cort action on calcium signaling using genetically encoded calcium indicators and inorganic dyes. The results showed that Cort regulates calcium dynamics in soma, but not dendrites, suggesting that Cort might alter cellular excitability, plausibly controlling spike timing in sensory neurons.

Materials and Methods

Animals

Eight weeks old male Sprague Dawley rats (Charles River Laboratories) were given *ad libitum* access to food and water and housed on a 12-hour light/dark cycle. They were anesthetized (Isoflurane) and perfused with iced and oxygenated (95% O_2/5% CO_2) slicing medium (SM) containing, in mM: 10.8 ChCl, 0.3 KCl, 2.6 $NaHCO_3$, 0.125 $NaH_2PO_4.H_2O$, 2.5 Glucose.H_2O, 0.1 $CaCl_2.2H_2O$, 0.6 $MgSO_4.7H_2O$, 0.3 Na-Pyruvate.

Cultures of dissociated cortical neurons were prepared from prenatal E18 Wistar rats. The mother was sacrificed by cervical dislocation, pups by decapitation, and pup brains were rapidly removed. All experimental procedures were approved by the Ethical Committee for

Animal Experimentation of Radboud University.

Experimental procedures

Acute coronal sections (400 μm) of the barrel cortex were sliced in cold and carbonated SM. Sections were then incubated for 30 min in a chamber filled with carbonated (95/5% O_2/CO_2) artificial cerebrospinal fluid (ACSF) containing, in mM: 120 NaCl, 3.5 KCl, 1.3 $MgSO_4.7H_2O$, 2.5 $CaCl_2.2H_2O$, 10 Glucose.H_2O, 1.25 $NaH_2PO_4.H_2O$, 25 $NaHCO_3$) at 37°C for 1 hour. The temperature was subsequently gradually reduced to room temperature and slices were transferred to a recording chamber where they were perfused continuously with oxygenated ACSF at the room temperature. Three injections of Fluo4AM were made in layer 2/3 of the barrel cortex where calcium dynamics were studied upon electrical stimulation of layer 4 using a bipolar electrode.

The protocol consisted of three repetitions of a voltage series between 0.5 - 4V delivered with an interstimulus interval of 20 sec, which was repeated a second time 30 minutes later. After that, each slice was perfused with one of the six pharmacological agents: ACSF containing 0.05% ethanol; 10 μM, 100 nM, or 20 nM isoproterenol (ISO); 5 μM NE; 1 μM Cort; 10 μM ISO with 100 nM Cort; or 10 μM ISO with 0,05% ethanol for 20 min to regulate α-1, β-2 and GR receptors. The stimulus protocol was repeated a third time after the pharmacological intervention and the bath solution was immediately changed back to ACSF to wash the agents off of the slice for 30 min. Finally, the stimulation protocol was repeated a fourth time. Data acquisition was performed using Q-imaging Exi blue camera controlled through Master-8 and micromanager.

Cell culture preparation: After animals were euthanized by decapitation on E18, brains were isolated and cooled ice-cold Hank's balanced salts solution (HBBS) containing 10% HBSS without Mg or Ca (Gibco/Invitrogen), 100 U/ml penicillin (LifeTechnologies), 100 μg/ml streptomycin (LifeTechnologies), 500 μM glutamine and 12.5 μM glutamate (Sigma, pH 7.3). Cortices were removed and incubated in HBSS with 5% trypsin solution (Gibco/Invitrogen). The solution was removed, and the cells were dissociated using a fire-polished Pasteur's pipette.

Dissociated neurons were plated onto 24 mm coverslips, coated with 1% poly-D-lysine (Fisher Scientific), with a density of $1.6*10^5$/coverslip. Cultures were maintained at 37°C in a humidified atmosphere (95% O_2/5% CO_2) in a culture medium comprising neurobasal medium (Gibco/Invitrogen), supplemented with 2% B27 Supplement (Gibco/Invitrogen), 500 μM glutamine and 12.5 μM glutamate. After five days, the culture medium was replaced with the same medium but without glutamate. Half the medium was changed twice per week. Cultures were used for 13-17 days after plating. Calcium imaging in cultured neurons was

performed using GCaMP6s (see below). Neurons were virally transfected two days after the plating.

Prior to calcium imaging cells were incubated with Cort (100 nM, dissolved in 20 µM Ethanol, N=10), Ethanol (EtOH, 20 µM, Vehicle group, N=9) or Ringer's (Control group, N=10) solution for 20 min in room temperature protected in a light-tight environment. The plate was then washed with Ringers before it was placed under the microscope (Nikon FN-2SN) and kept perfused continuously with carbonated ACSF 2 mL per minute, at room temperature for one hour before imaging started. Evoked calcium transients were triggered using KCl (60 mM) puffs (1.6 mL/each for a total duration of 10 sec).

Preparation of GCamp6 and transfection

AAV-HEK293 cells (ATTC, < p+25) were maintained in Culture Medium (DMEM supplemented with 10% FCS, 1 mM Na-Pyruvate and Pen/Strep). For GCamp6s-AAV virus production, 48 hours prior transfection AAV-HEK293 cells were plated onto poly-L-Lysine-coated 15-cm cultures dishes and cultured until a confluence of ~80% was reached. For $CaPO_4$-transfection, 37.5 µg pRVl (AAV2); 37.5 µg pH21 (AAV1); 150 µg pFdelta6 (Ad Helper), and 75 µg pAAV-CaMKIIa-GCamp6 plasmid DNA were mixed with 1.44 ml 2.5 M $CaCl_2$ and 12 ml of MQ water. Then, while mixing the solution, 13 ml of 2xHBS (280 mM NaCl, 50 mM HEPES, 1.42 mM Na_2HPO_4, pH 7.05) was added gradually. This mixture (5 ml/plate) was added to the plate and 16 hours later cells were supplied with fresh culture medium. Virus production continued 48-72 hours after transfection.

Viral particles were isolated from the cells essentially as previously described [18]. In short, cells were collected in warm PBS, lysed in Lysis buffer (150 mM NaCl, 20 mM Tris, pH 8.0) supplemented with 0.5% deoxycholate and 50 u/ml Benzonase. After clearing the lysate by centrifugation, AAV virus was isolated using a HiTrap heparin column (GE Healthcare, #17-0406-01) and afterward concentrated in PBS using Ultracel-100K centrifugal filter units (Amicon, #UFC810024). Batches #2 (physical titer: 4.92*1012 genomes/ml) and #4 (physical titer: 1.86*1012 genomes/ml) were used to transduce dissociated cortical neuronal cultures.

Data analysis

The data analysis was performed using in-house software written in MATLAB (MathWorks). The fractional change in fluorescence was calculated and normalized to the baseline illumination in single pixel resolution and data are represented as df/F=(f-F)/F, where f is evoked responses and F is the illumination prior to the onset of stimulus.

Results

Here we addressed the role of corticosterone in controlling calcium dynamics in acute slices of the primary somatosensory cortex and in cultures of dissociated neocortical neurons. Epifluorescence imaging in acute slices allowed visualization of population dynamics (Figure 1), at the expense of spatial resolution, while imaging in dissociated cultures provided high resolution, compartmental analysis of the changes in calcium, using single-photon excitation (Figure 2).

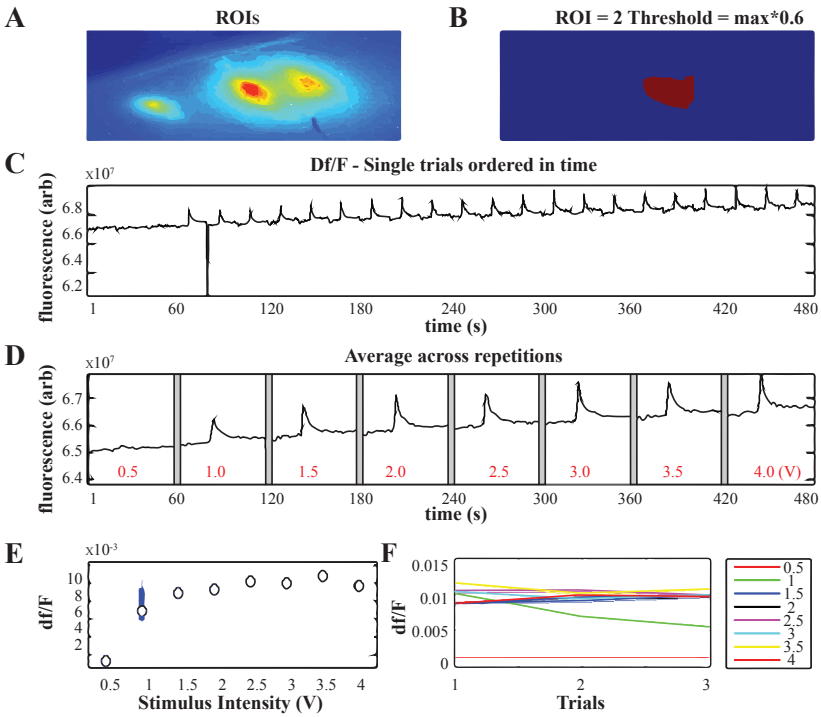

Figure 1. Visualization of population calcium dynamics in acute slices of the barrel cortex. Calcium transients were detected using Fluo4 injected in three locations in layers (L) 2/3 of the barrel cortex, while electrical stimulation was delivered to the L4 using bipolar electrodes. (A) Three injection sites and magnitude of basal fluorescence amplitude in pseudo colors. Warmer colors represent higher fluorescence. A single image was acquired in the absence of electrical stimulation. (B) ROI (Region of Interest) identified by thresholding, in this example 60% of the global maximum fluorescence. (C) The intensity of the fluorescence over repetitive electrical stimulation. Increase in fluorescence intensity (calcium influx) is seen due to consecutive electrical stimulations. (D) Average of the fluorescence after three repetitions, across voltage steps of 0.5 V. (E) Average df/F as a function of stimulus intensity. Incremental elevation in stimulation intensity led to an increase in df/F, indicating more calcium influx. (F) There was small to no variation across the three repetitions of the experiment. Color code indicates the stimulus intensity (in V).

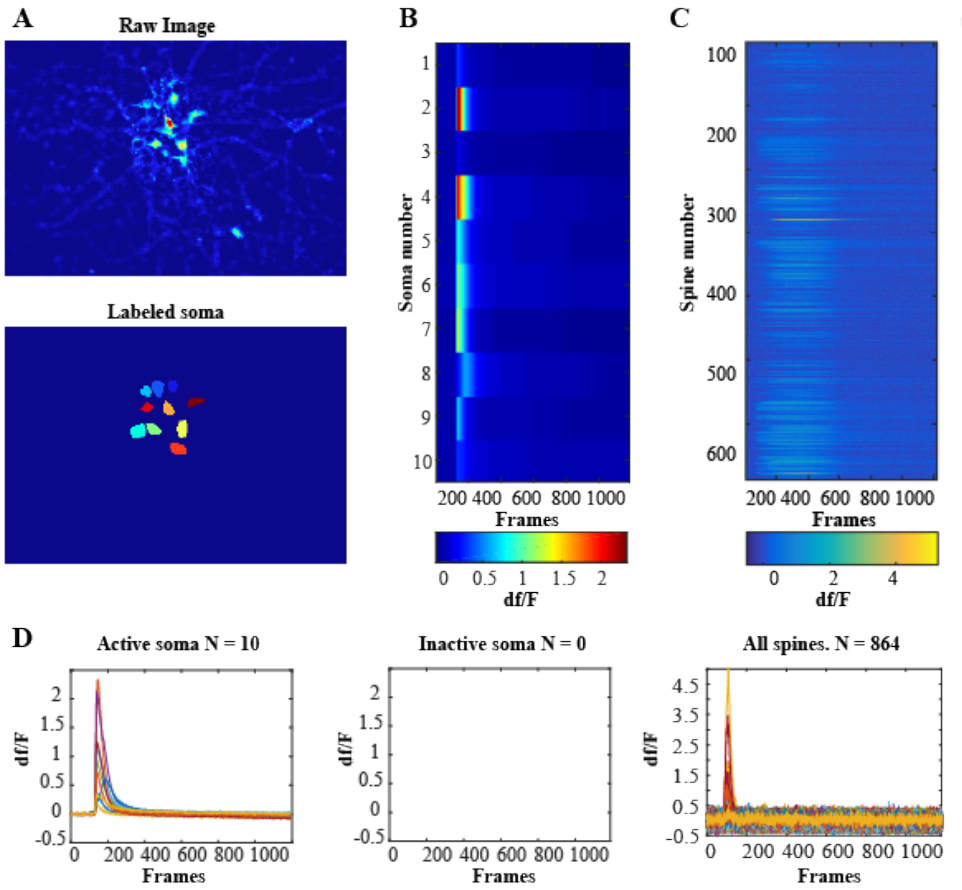

Figure 2. Compartmental visualization of the calcium dynamics in slice cultures. (A) Top: Raw GCaMP6s signal displayed as an intensity image. Bottom: Isolated and labeled soma after image segmentation. (B) Time course of the evoked response in identified soma in a single trial. The stimulus was delivered 20 sec into the trial. Data recorded at 10 fps. (C) Same as in B but data from identified spines. (D) Normalized change in fluorescence (df/F) in active and inactive soma, classified statistically based on whether stimulus evoked significant response above background in a given soma, and spines (right).

Acute application of Cort with ISO suppresses population calcium activity in S1

As expected, neuronal excitability, as measured by evoked calcium signals, were increased in proportion to the stimulus intensity (Figure 3, 2-way-ANOVA, $p < 0.001$, $\eta^2 = 0.218$). However, the change in excitability calculated by the df/F was minimal across all conditions in acute cortical slices. The exception was the reduced excitability observed in Cort combined with ISO (Figure 3B, 2-way-ANOVA, $p < 0.001$), but with a small effect size ($\eta^2 = 0.036$).

The significant reduction was specific to stimuli above 3V (Student's t test, $p<0.001$), when compared to Control. The experiments with Ethanol-only treatment showed the lowest df/F values, while experiments with ISO (including combined with ethanol or combined with Cort) had the highest change in evoked calcium amplitude (Figure 3).

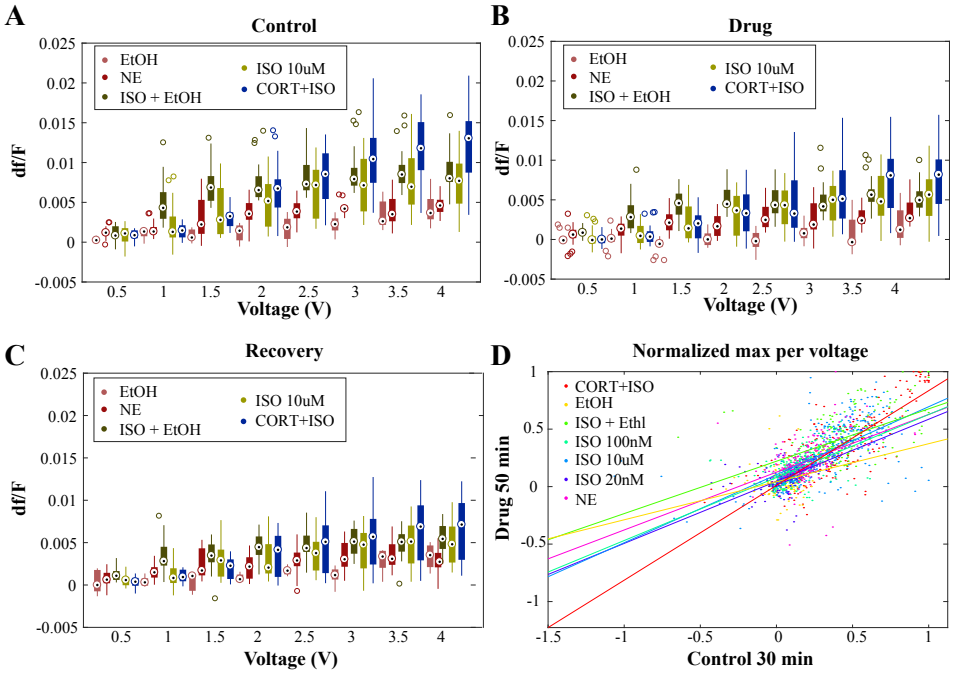

Figure 3. Reduction in evoked calcium transients in the acute slices of the barrel cortex (Layer 2/3). Each slice was studied prior to administration of pharmacological agents (*Control*), during the application (*Drug*) of norepinephrine (NE), isoproterenol (ISO), ethanol (EtOH), and corticosterone (Cort), and after reperfusion with ACSF (*Recovery*). (A) Data were normalized to the maximum df/F across stimuli. In all drug conditions the amplitude of evoked calcium transients increased in proportion to the stimulus intensity (ANOVA repeated measures, $p<0.001$). (B) Evoked calcium transients were reduced across all drug conditions compared to *Control*, but only significantly in acute treatment of Cort+ISO, above 3V stimuli (2-way-ANOVA, $p<0.001$, $\eta^2=0.036$, Bonferroni, $p<0.001$). No significant differences were found in any other experimental conditions in comparison to control. (C) This reduction in calcium transient was sustained for at least 50 min including during *recovery* (Cort+ISO in comparison to *Control*, Bonferroni, $p<0.001$). A tendency of reduction observed in ISO (ANOVA repeated measures, $p=0.04$) was not confirmed by post-hoc statistics in comparison to *Control* (Bonferroni, $p=0.098$), or *Drug* (Bonferroni, $p=0.202$). (D) Scatter plot of normalized df/F before and after pharmacological administrations. The control showed here was the second stimulation (t = 30 min) before drug application.

To ensure that the comparison is not biased due to within experiment variability, the evoked calcium transients were normalized to the global maximum in each stimulus intensity (voltage) (Figure 3A, B and C), which showed

that at the population level corticosterone reduces excitability via regulation of calcium dynamics, specifically at higher stimulations. These results suggest that only Cort in combination with ISO changes calcium dynamics at the population level, indicating that glucocorticoid and adrenergic receptors activation combined regulate the calcium signaling in the somatosensory cortex.

Compartmental analysis of calcium dynamics

Compartmental analysis was performed in dissociated cultures using a genetically encoded calcium indicator, GCaMP6s. Soma and spines were identified, and three independent groups (Corticosterone, Ethanol and Control) were studied. Somatic (Cort = 214; vehicle (Ethanol) = 178) and spine dynamics of evoked calcium transients were quantified (Cort = 2881; vehicle (Ethanol) = 2402).

Peak amplitude and latency were quantified at the highest point of calcium influx after df/F normalization. The evoked calcium response was calculated as the area under the curve of change in fluorescence (df/F). Figure 4 details the evoked somatic responses across a period of three hours. Within one hour after the administration, Cort significantly delays evoked responses as measured by latency to the peak amplitude of the calcium influx, in soma (Student's t test, $p < 0.0001$). Despite the slower transients, the peak amplitude of the response ($p = 0.04$) and the total evoked amplitude ($p = 0.004$) were significantly enhanced after Cort administration in comparison to vehicle-treated cultures (see the first row of Figure 4). Long-term exposure to Cort further delayed the evoked somatic calcium transients as the peak latency was reached systematically later when measured 2h (~45%, Bonferroni post-hoc comparisons, $p <0.001$) and 3h (~30%, Bonferroni post-hoc comparisons, $p = 0.006$) after the first administration (see Figure 4 the middle row, ANOVA repeated measures, $p < 0.001$). Long-term exposure to Cort did not result in sustained elevated amplitudes of evoked transients, rather both the peak amplitude ($p = 0.021$) and the total evoked amplitude of the calcium transients ($p = 0.022$) were gradually reduced by the 3rd hour (Figure 4 middle row). Long-term consequences of the exposure to the vehicle (Ethanol) were limited to a gradual change in the total evoked calcium levels after three hours ($p = 0.026$), although there were no significant changes in peak latency and amplitude.

These results show that Cort potently regulates calcium dynamics in soma. Cort administration causes sustained delays in evoked somatic calcium transients while the amplitude of the calcium response is only transiently up-regulated.

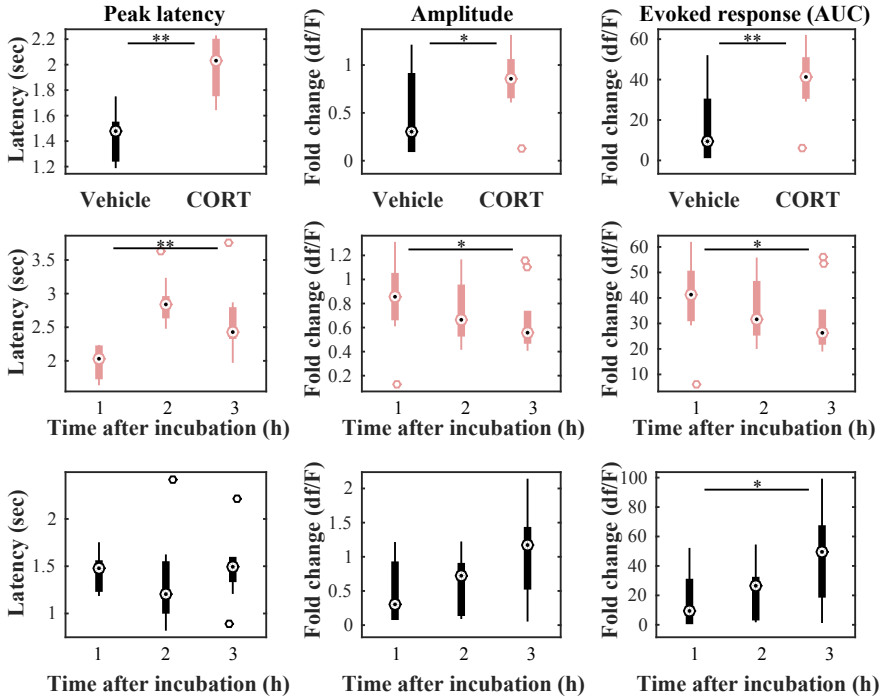

Figure 4. Group analysis of the somatic calcium transients. Top row: application of corticosterone increases peak latency, amplitude and evoked response in soma in the first hour (Student's t-test, respectively: $p < 0.001$, $p = 0.04$, $p = 0.004$). Middle row: corticosterone continues increasing the latency of evoked calcium transients but reduces the amplitude and the evoked response over time (ANOVA repeated measures, respectively: $p < 0.001$, $p = 0.021$, $p = 0.022$). Third row: Vehicle (Ethanol) administration alone does not change calcium dynamics with the exception that, without corticosterone, the evoked response in the soma increases significantly over time (ANOVA repeated measures, $p = 0.026$). ** = $p < 0.01$; * = $p < 0.05$).

To address whether Cort mediated regulation of calcium dynamics was specific to soma, we have studied the calcium dynamics in identified spines (Figure 5). Cort administration did not change spine calcium dynamics in respect to vehicle condition within the first hour after the administration (Figure 5, top row), neither does it alter the calcium dynamics in the long-term (pairwise comparisons after Bonferroni $p>0.05$). Neither the peak latency nor total evoked calcium amplitude changed at any point after Cort administration (see Figure 5 middle row). These results were mirrored in the vehicle group as ethanol treatment did not change spine calcium dynamics significantly (ANOVA repeated measures, $p>0.05$) at any time points (see Figure 5, bottom row). Taken together the results show a compartmentalized role for corticosteroids in controlling calcium dynamics in the neocortex, affecting the timing and the intensity of intracellular calcium activity in soma but not across spines.

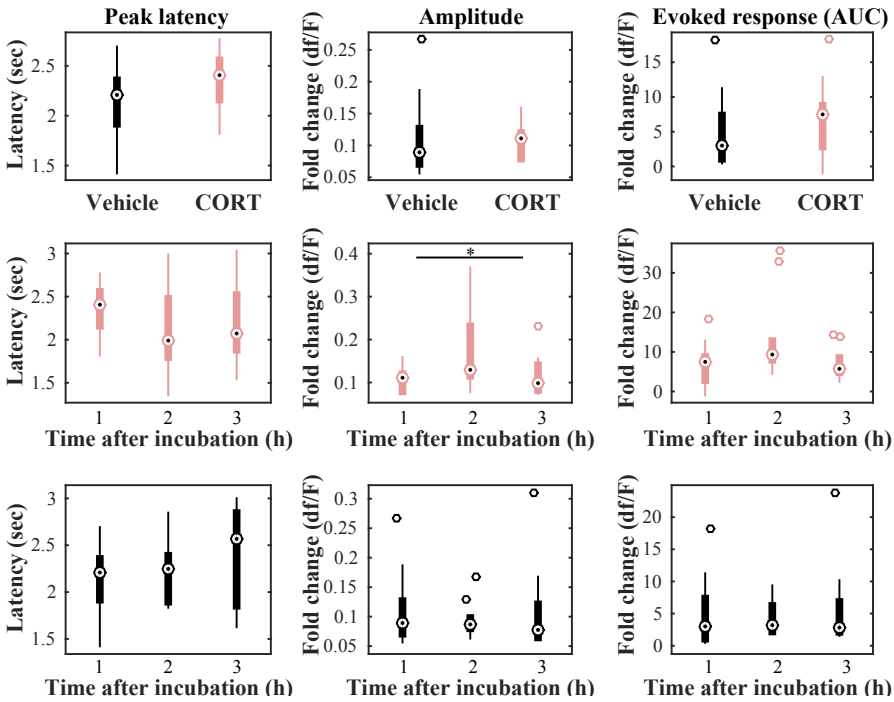

Figure 5. Cort does not regulate calcium dynamics in spines. First row: application of corticosterone does not alter the peak latency, amplitude or the evoked response in spines within the first hour (Student's t-test, respectively: p = 0.15, p = 0.88, p = 0.49). Second row: corticosterone does not affect the latency of the peak calcium excitability in spines (left), but marginally changes the peak amplitude of the evoked transients (middle) without altering the total calcium entry (right). ANOVA repeated measures, respectively: p = 0.179, p = 0.028, p = 0.054. Third row: No significant changes in peak latency, amplitude or in the calcium evoked transients were noted in the vehicle (Ethanol) condition in the spines. (ANOVA repeated measures, p = 0.197, p = 0.838, p = 0.852). ** = p < 0.01; * = p < 0.05.

Discussion

The findings suggest that stress regulates the information transfer and timing on the neocortical network. This study demonstrated that corticosterone is able to modulate calcium dynamics in a subcellular specific manner, targeting the somatic neuronal excitability in a time-span of hours. Cort affects the stimulus evoked calcium dynamics for a long period after the stress onset, as indicated by the specific control of latency and intensity of the calcium response in soma.

It is known that increased calcium influx induced by corticosteroids leads to higher spike threshold and firing frequency adaptation within hours, which is important for

the accommodation of the stress response in the limbic system [1]. However, the threshold between adaptive and non-adaptive responses to stress might be due to long-lasting effects of corticosteroids in the synaptic plasticity and in the excitatory transmission [19], the latter relying heavily on calcium signaling. The compartmentalized effect of Cort indicates that this stress hormone is a potential top-down neuromodulator because it can target the somatic excitability, thus potentially controlling the generation of action potential at the axonal hillock.

Cort as a top-down regulator of cortical dynamics with long-term consequences

GR receptors are widespread throughout the brain, however, their expression is greater in the hippocampus, the lateral septum and the paraventricular nucleus (PVN) [2]. MR receptors are highly expressed in the lateral septum and in the hippocampal formation, but also in the amygdala, PVN and locus coeruleus (LC) [2]. Those receptors have complementary roles in suppressing the elevating excitability, helping with recovery from the stressful experience and storage of this information for the future [25]. Therefore, activation of GR and MR coordinate a broad behavioral response and ensure emotional, cognitive and neuroendocrine processing of stressful experiences [2]. In the principal neurons of the basolateral amygdala, Cort gradually increases the amplitude of sustained, high-voltage Ca^{2+} currents [26], similar to what happens in CA1, although the downstream targets after calcium binding varies across neural structures [1]. Similarly, in the amygdala, the activation of GR is primarily related with modulation of excitability rather than promoting inhibition [2]. Cort does not exert any significant control over Ca^{2+} currents in the dentate gyrus [27], although it controls transcription in DG neurons [1]. This may explain the role of Cort in underlying learning and memory processes.

Since those processes are highly associated with sensory mechanisms, similar mechanisms could be shared in the somatosensory system, along with other sensory systems. The barrel cortex receives noradrenergic projections from the locus coeruleus [20] and therefore is likely to undergo rapid (and potentially long-lasting) modulation of sensory representations upon stress. In support of this hypothesis, earlier studies have already shown that the connectivity within the bilateral visual and primary somatosensory network is increased after chronic stress exposure [21], and repeated exposure to maternal separation stress [22] results in neuronal hypertrophy in the rodent's somatosensory cortex. Adrenergic receptors (specifically α_1-receptors) in the barrel cortex are modulated by sensory experience, their expression is down-regulated upon sensory deprivation (vibrissectomy) and up-regulated following noradrenergic input blockage (locus coeruleus lesion) [23]. Dysregulation of noradrenergic neurotransmission, e.g. upon chronic stress, for example, could influence the somatosensation. In layer 5 of the somatosensory cortex, NE has been observed increasing the excitability

of the regular spiking neurons, showing a modulatory role in facilitating the response to stimulation of the afferent pathway, while simultaneously reducing the activity of intrinsic burst neurons [24].

Surprisingly, the application of the β-2 adrenergic receptor agonist ISO also resulted in reduced calcium activity, even when combined with Cort. This observation cannot be explained by the lack of receptors, as β-2 receptors have been localized in the S1 [28]. However, some clear limitations are the population imaging that prevents us to distinguish neuronal subtypes, and the lack of electrophysiological assessment. Nonetheless, the reported research leads to the conclusion that Cort does not acutely control the excitability of somatosensory cortical neurons through calcium regulation. Corticosteroids are also potent regulators of vasculature and blood pressure [29] and might alter neuronal representations by regulating neuro-epithelial coupling. The acute effects of Cort in sensory excitability might therefore be associated with its regulation of cortical blood supply as supported by intrinsic optical imaging of whisker evoked representations (Figure 6).

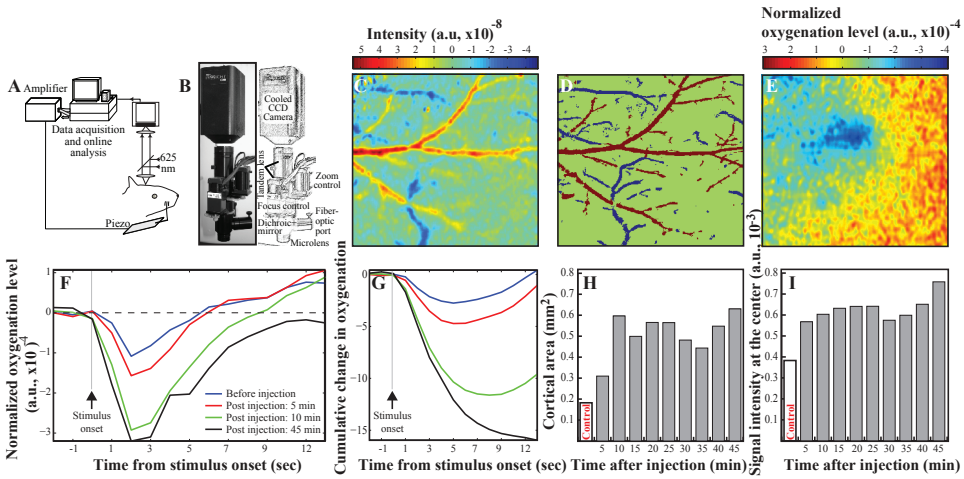

Figure 6. Corticosterone administration alters oxygen utilization in the neocortex. Changes in reflectance of 625 nm wavelength light enable spectroscopic visualization of deoxyhemoglobin concentration with a spatial resolution < 40 μm [30]. (A) Experimental set-up. Monochromatic light is generated using a LED and haptic stimuli are delivered using a piezoelectric wafer in contact with facial whiskers under anesthesia. (B) Custom-made macroscope for intrinsic optical imaging. (C) Spontaneous low-frequency oscillations in mean pixel reflectance over a 60 second (sec) period depict the signal localization to the blood vessels. (D) Binary classification of the blood vasculature by visualizing the positive and negative peak oxygen utilization. Red: Arteries; Blue: Venules. (E) During stimulus delivery spectroscopic signal originates both from within and outside the vasculature. Stimulus-evoked changes in the oxygenation show that single whisker stimulation results in a spatially restricted change in signal intensity. Field

of view: 2.5 x 2.5 mm. (F) Time course of the change in oxygenation level before and during stimulus delivery. The signal develops over a period of ~2 sec after stimulus delivery and lasts for ~3 sec under control conditions, i.e. no corticosterone. Subcutaneous Corticosterone administration (concentration: 3 mg/kg volume: 10 ml/kg) increases the deoxygenation of the hemoglobin gradually which lasts > 45 min. Note that deoxygenation is altered only during stimulus processing. (G) Total hemoglobin deoxygenation and its time course altered after corticosterone injection. (H) Deoxygenation is spatially restricted and the cortical area where deoxygenation is observed is enlarged upon Corticosterone administration. (I) Enlargements of the deoxygenation are accompanied by the change in peak signal intensity, as determined at the center of mass of the hemoglobin deoxygenation. The data is kindly contributed by Dr. Chao Huang at the Department of Neurophysiology, Donders Institute.

Subcellular differences in Cort mediated calcium dynamics

Corticosterone modulates calcium transients possibly through transcriptional regulation, appearing at least 1 hour after the corticosterone exposure, as described in our compartmentalized imaging results. While our results indicate that Cort action in somatosensory neurons might be limited to genomic modulation in the soma, in the hippocampus, for example, corticosterone increases the spine density through non-genomic processes, via MAPK and PKA pathways [31]. This fast regulation of synaptic plasticity following acute stress may affect memory. Chronic corticosterone administration also impacts the dendritic morphology in the medial prefrontal cortex, increasing the spine density in the apical dendrites located in the proximal region of the soma [32]. The majority of the spines altered by corticosterone were located in pyramidal neurons of layers II/III, thus likely mediating excitatory inputs in the PFC [33]. This specific control of calcium transients that differs in the hippocampus and in cortical areas indicate that Cort can target specific networks helping in stress adaptation but potentially contributing to cognitive impairments caused by chronic stress.

In the hypothalamus, the negative feedback mediated by Cort occurs rapidly and may have long-lasting consequences. Cort decreases excitability on PVN neurons through both non-genomic and genomic mechanisms [11]. In the pituitary, for example, after a stressful event ACTH release is inhibited within minutes and lasts for several hours [11]. Thus, a possible explanation for the observed somatic effects of corticosterone can be the time needed for transcriptional regulation in spines, as the proteins should either be transported to the spine, or the RNAs should be delivered to the spine for local translation [34]. This transportation requirement suggests that if we were to look at the spine dynamics at a later point (e.g. 5h after) we might actually see similar results in the soma versus dendrites.

The results add further complexity to differences in Cort effects in different regions of the brain. Expanding this work would require focusing on the mechanisms by which calcium currents control Cort. As these targets are likely to involve L-P/Q, N, R and T-type calcium channels [35], future systematic analysis would need to include whole-cell voltage clamp

recordings. In summary, the conclusion here outlined is that Cort has a time-dependent somatic effect on evoked calcium transients and does not acutely modulate neuronal excitability in the somatosensory cortex.

Bibliography

1. Joëls, M. & Karst, H. Corticosteroid effects on calcium signaling in limbic neurons. *Cell Calcium* **51,** 277–283 (2012).
2. Joëls, M. & Baram, T. Z. The neuro-symphony of stress. *Nat. Rev. Neurosci.* **10,** 459–466 (2009).
3. Butler, L. K., Bisson, I.-A., Hayden, T. J., Wikelski, M. & Romero, L. M. Adrenocortical responses to offspring-directed threats in two open-nesting birds. *Gen. Comp. Endocrinol.* **162,** 313–318 (2009).
4. Joëls, M., Karst, H., Krugers, H. J. & Lucassen, P. J. Chronic stress: implications for neuronal morphology, function and neurogenesis. *Front. Neuroendocrinol.* **28,** 72–96 (2007).
5. Raubenheimer, P. J., Young, E. A., Andrew, R. & Seckl, J. R. The role of corticosterone in human hypothalamic-pituitary-adrenal axis feedback. *Clin Endocrinol (Oxf)* **65,** 22–26 (2006).
6. Adamo, S. A. The effects of stress hormones on immune function may be vital for the adaptive reconfiguration of the immune system during fight-or-flight behaviour. *Integr. Comp. Biol.* **54,** 419–426 (2014).
7. Ota, K. Fight, fatigue and flight: narrowing of attention to a threat compensates for decreased anti-predator vigilance. *J. Exp. Biol.* **221,** (2018).
8. Matt, K. S., Moore, M. C., Knapp, R. & Moore, I. T. Sympathetic mediation of stress and aggressive competition: plasma catecholamines in free-living male tree lizards. *Physiol. Behav.* **61,** 639–647 (1997).
9. de Kloet, E. R., Joëls, M. & Holsboer, F. Stress and the brain: from adaptation to disease. *Nat. Rev. Neurosci.* **6,** 463–475 (2005).
10. Oakley, R. H. & Cidlowski, J. A. Cellular processing of the glucocorticoid receptor gene and protein: new mechanisms for generating tissue-specific actions of glucocorticoids. *J. Biol. Chem.* **286,** 3177–3184 (2011).
11. Groeneweg, F. L., Karst, H., de Kloet, E. R. & Joëls, M. Rapid non-genomic effects of corticosteroids and their role in the central stress response. *J. Endocrinol.* **209,** 153–167 (2011).
12. Chameau, P., Qin, Y., Spijker, S., Smit, A. B. & Joëls, M. Glucocorticoids specifically enhance L-type calcium current amplitude and affect calcium channel subunit expression in the mouse hippocampus. *J. Neurophysiol.* **97,** 5–14 (2007).
13. Nair, S. M. *et al.* Corticosteroid regulation of ion channel conductances and mRNA levels in individual hippocampal CA1 neurons. *J. Neurosci.* **18,** 2685–2696 (1998).
14. Bali, A., Gupta, S., Singh, N. & Jaggi, A. S. Implicating the role of plasma membrane localized calcium channels and exchangers in stress-induced deleterious effects. *Eur. J. Pharmacol.* **714,** 229–238 (2013).
15. Chatterjee, S. & Sikdar, S. K. Corticosterone targets distinct steps of synaptic transmission via concentration specific activation of mineralocorticoid and glucocorticoid receptors. *J. Neurochem.* **128,** 476–490 (2014).
16. Reuveni, I., Friedman, A., Amitai, Y. & Gutnick, M. J. Stepwise repolarization from Ca2+ plateaus in neocortical pyramidal cells: evidence for nonhomogeneous distribution of HVA Ca2+ channels in dendrites. *J. Neurosci.* **13,** 4609–4621 (1993).
17. Antic, S. D. Action potentials in basal and oblique dendrites of rat neocortical pyramidal neurons. *J Physiol (Lond)* **550,** 35–50 (2003).
18. McClure, C., Cole, K. L. H., Wulff, P., Klugmann, M. & Murray, A. J. Production and titering of recombinant adeno-associated viral vectors. *J. Vis. Exp.* e3348 (2011). doi:10.3791/3348
19. Timmermans, W., Xiong, H., Hoogenraad, C. C. & Krugers, H. J. Stress and excitatory synapses: from health to disease. *Neuroscience* **248,** 626–636 (2013).

20. Ungerstedt, U. Stereotaxic mapping of the monoamine pathways in the rat brain. *Acta Physiol. Scand. Suppl.* **367,** 1–48 (1971).
21. Henckens, M. J. A. G. *et al.* Stress-induced alterations in large-scale functional networks of the rodent brain. *Neuroimage* **105,** 312–322 (2015).
22. Bock, J., Gruss, M., Becker, S. & Braun, K. Experience-induced changes of dendritic spine densities in the prefrontal and sensory cortex: correlation with developmental time windows. *Cereb. Cortex* **15,** 802–808 (2005).
23. Dunn-Meynell, A. A. & Levin, B. E. Alpha 1-adrenoceptors in the adult rat barrel field: effects of deafferentation and norepinephrine removal. *Brain Res.* **623,** 25–32 (1993).
24. Waterhouse, B. D., Mouradian, R., Sessler, F. M. & Lin, R. C. Differential modulatory effects of norepinephrine on synaptically driven responses of layer V barrel field cortical neurons. *Brain Res.* **868,** 39–47 (2000).
25. de Kloet, E. R., Karst, H. & Joëls, M. Corticosteroid hormones in the central stress response: quick-and-slow. *Front. Neuroendocrinol.* **29,** 268–272 (2008).
26. Karst, H. *et al.* Glucocorticoids alter calcium conductances and calcium channel subunit expression in basolateral amygdala neurons. *Eur. J. Neurosci.* **16,** 1083–1089 (2002).
27. van Gemert, N. G. *et al.* Dissociation between rat hippocampal CA1 and dentate gyrus cells in their response to corticosterone: effects on calcium channel protein and current. *Endocrinology* **150,** 4615–4624 (2009).
28. Vos, P., Kaufmann, D., Hand, P. J. & Wolfe, B. B. Beta 2-adrenergic receptors are colocalized and coregulated with “whisker barrels” in rat somatosensory cortex. *Proc Natl Acad Sci USA* **87,** 5114–5118 (1990).
29. Scheuer, D. A. Regulation of the stress response in rats by central actions of glucocorticoids. *Exp. Physiol.* **95,** 26–31 (2010).
30. Stewart, R. S., Huang, C., Arnett, M. T. & Celikel, T. Spontaneous oscillations in intrinsic signals reveal the structure of cerebral vasculature. *J. Neurophysiol.* **109,** 3094–3104 (2013).
31. Murakami, G. *et al.* Rapid nongenomic modulation by neurosteroids of dendritic spines in the hippocampus: Androgen, oestrogen and corticosteroid. *J. Neuroendocrinol.* **30,** (2018).
32. Wellman, C. L. Dendritic reorganization in pyramidal neurons in medial prefrontal cortex after chronic corticosterone administration. *J. Neurobiol.* **49,** 245–253 (2001).
33. Seib, L. M. & Wellman, C. L. Daily injections alter spine density in rat medial prefrontal cortex. *Neurosci. Lett.* **337,** 29–32 (2003).
34. Smrt, R. D. & Zhao, X. Epigenetic regulation of neuronal dendrite and dendritic spine development. *Front Biol (Beijing)* **5,** 304–323 (2010).
35. Catterall, W. A. Structure and regulation of voltage-gated Ca2+ channels. *Annu. Rev. Cell Dev. Biol.* **16,** 521–555 (2000).

Chapter 7

Implications of the dopaminergic modulation on sensory representations

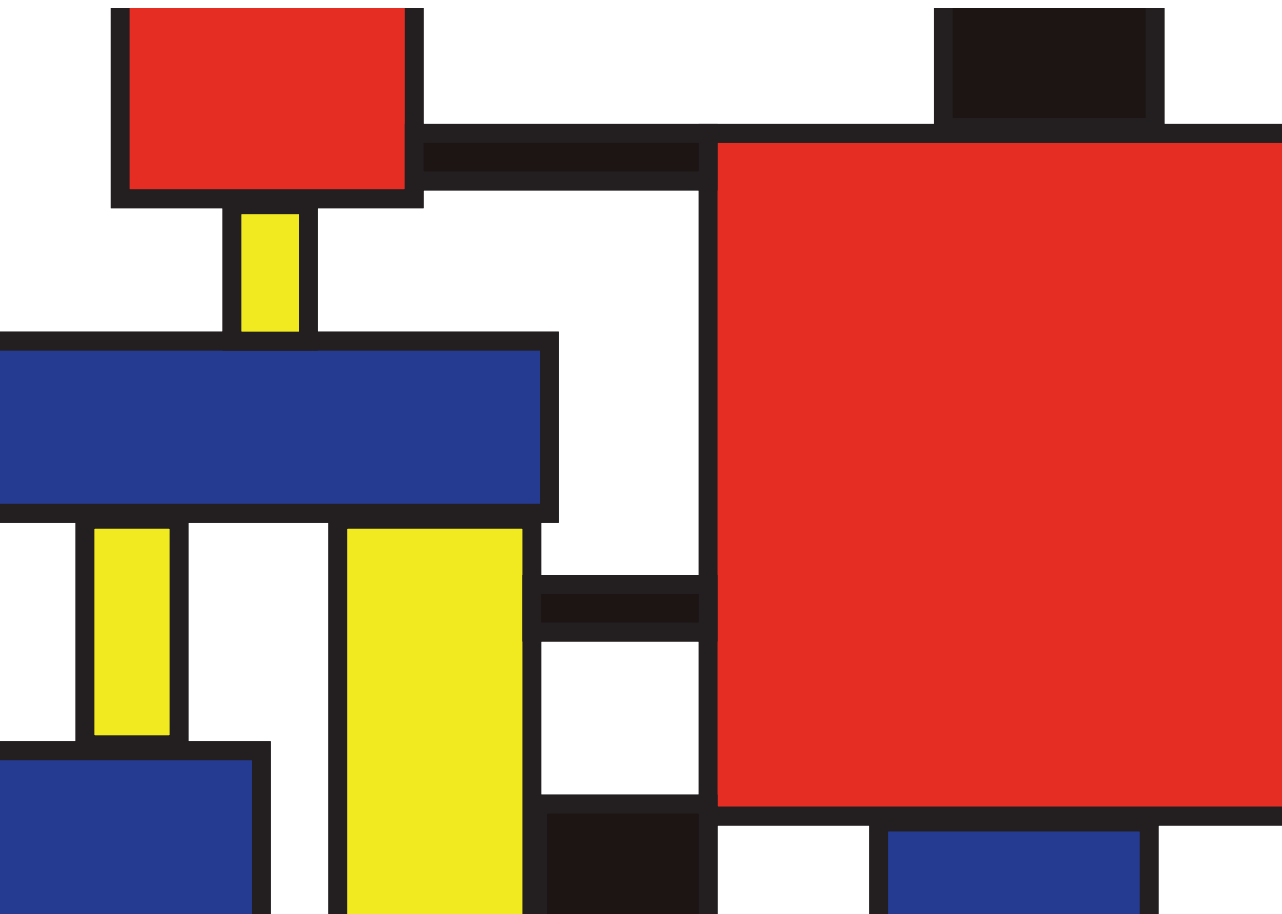

The sensory perception requires the integration of bottom-up sensory information with top-down predictions of the brain for making sense of the environment. Neuromodulatory neurotransmitters, such as dopamine, are known temporal and contextual regulators of the neuronal sensory processing. They facilitate the information transfer between neurons through regulation of firing rate, action potential timing, and cellular excitability. The goal of this thesis was to investigate how dopamine might control cellular information processing in the somatosensory system, addressing the dopaminergic top-down modulation of the sensory processing at the synaptic level. The results outlined in the preceding chapters showed that dopamine suppresses the neuronal excitability via regulation of voltage-gated sodium channels, thus determining the spike threshold in the single-neuron level. Focusing on the D1-like dopaminergic receptors (D1R) to address the cell-type specific regulation of excitability, we further showed that D1R activation improves information processing in inhibitory neurons while suppressing the information transferred by excitatory neurons. Transcriptional mapping of the dopaminergic signaling in a cortical layer and column specific manner showed that molecules involved with dopaminergic action in the somatosensory cortex are regulated by sensory experience. These results argue that there is a close-loop regulatory interaction between sensory signaling and dopaminergic pathways, and propose the primary somatosensory cortex as a model system to study the integration of bottom-up and top-down information at a synaptic level.

Dopamine has been studied as a part of the reward system for decades, but only a few studies investigated the dopaminergic modulation of sensory processing, including 1) dopamine increases the excitability of thalamic neurons projecting to the sensory cortex via complimentary activation of D1 and D2 receptors [1]; 2) D1 activation in A1 improves auditory stimulus discrimination in awake rodents [2]; and 3) systemic increase of dopaminergic neuromodulation increases visual information encoding in V1, especially in supragranular layers projecting to higher cortical areas [3]. Thus, dopamine is believed to facilitate sensory processing across modalities. Here, we have shown in S1 that dopamine suppresses excitability and regulate information transfer in a cell-type specific manner.

We found that activation of the D1-like or D2-like dopaminergic receptors regulate excitability in different ways: D1 activation decreases spiking in higher frequencies, D2-like receptors do so mainly in lower frequencies. These observations contribute to ever growing literature that proposes a modulatory, and plausibly an instructive, role for dopamine in shaping neuronal excitability along the sensorimotor circuits in the brain (see Chapter 1 for details).

Reward and sensorimotor circuits of the brain are reciprocally coupled (Chapter 1). Besides modulating the signal amplitude, dopamine regulates action potential latency in order to transfer information related to reward. Dopaminergic neurons make glutamatergic connections to accumbens neurons, and D2 inhibits the early response in the ventral tegmental area (VTA) increasing the spike threshold [4], therefore controlling the duration of the excitability. Moreover, D2 inhibits action potential initiation not only in the VTA but also in the substantia nigra compacta (SNc) [5,6]. Bidirectional control of excitability between the GP and the STN seems to be mediated by D2. The firing mediated by D2 activation in the GP [7] prevents the firing of STN and SNr neurons [8]. Microstimulation of STN produces monosynaptic subthreshold EPSPs and reduces spike latency in the VTA [9]. Via bidirectional control of cellular excitability and spike timing, dopamine is believed to gate the information transfer within the reward circuit, potentially shaping the sensorimotor control during goal-directed behaviors.

The dopaminergic control of sensory processing in single neurons

Results in Chapter 5 showed that dopamine regulates the excitability of pyramidal and interneurons by voltage-gated sodium channels inactivation (Na_V). Because Na_V opening is an obligatory step in action potential generation, and define the spike threshold, dopamine powerfully shapes action potential and spike timing [10,11]. These observations do not exclude the possibility that voltage-gated potassium channels (K_v) might contribute to the dopaminergic regulation of sensorimotor excitability. At least in the thalamic somatosensory neurons while

D2 receptor activation regulates α-DTX sensitive K^+ channels the D1 receptor agonists depolarize the membrane via G protein inward rectifying K^+ (GIRK) currents [1,12].

On the contrary to our findings, dopamine facilitate the excitability of PFC pyramidal neurons by increasing the spike frequency without any change in the spike amplitude or timing of inward or outward rectifications [13]. This regulation is mediated through D1 receptor activation, at least in the neocortical layer 3, and is caused by a decrease in the spike threshold and action potential latency [13]. However, the activation of D1 also increases the excitability of the interneurons in the same circuit [14] while decreasing excitability in Layer 5 via activation of D2-like receptors [15]. One potential explanation for these findings is the cross coupling between the glutamatergic and dopaminergic neurotransmission. The impairment of the glutamatergic transmission, in an NMDAR knockout model, increases the synaptic dopamine available chronically, leading to suppression of D2 activation which results in higher firing rate in the dopaminergic neurons [16]. GABAergic transmission is also regulated by dopamine, as D4 activation inhibits $GABA_A$ receptor inhibitory postsynaptic currents (IPSCs) via a presynaptic mechanism that regulates the GP efferents [1,12]. Considering the dopaminergic interaction with the principal excitatory (glutamatergic [17]) and inhibitory (GABAergic [18]) drive in the central nervous system, it would be necessary to systematically study the synergistic interactions across neurotransmitters.

Our experiments have shown that D1 and D2 receptor activation regulates the calcium signaling differentially in the soma and spines during somatic depolarization. As calcium stimulates dopamine release via potassium-dependent depolarization of neurons which only occurs in the presence of calcium [19], dopamine controls calcium dynamics through the signaling cascade activated when binding to one of its five receptor types. Already debated in Chapter 1, the intracellular effects of dopaminergic binding can go beyond the soma and potentially include differential modulation of the spines and dendrites of the neurons. This means that dopamine could direct the information flow, and perhaps suppress or activate different parts of the neuronal network, therefore, exerting control over the information transferred across different cortical layers. Because dopamine can control the excitability of the dendrites through activation of T-type calcium (Ca^{2+}) channels, at least in the substantia nigra (SN) [20], dopamine might contribute to gating of synaptic information from spines to soma.

Computational modeling corroborates calcium dynamics dependent on L-type and T-type channels influencing the synaptic plasticity in striatal neurons, there altering the direction of pre/post- synaptic plasticity if combined with GABAergic activation [21]. Dopaminergic activation of D4 also modulates the information transfer via calcium release after direct activation of IP_3 [22], in this case, independent from L-type Ca^{2+} channels or α-nicotinic Ach

receptors [22]. Ultimately, this dynamic influence between calcium and dopamine influences the action potential rate and timing.

Dopamine as a gain-modulator of bottom-up sensory information

Dopamine might perform synchronization of top-down and bottom-up circuits. The top-down input originating from the medial ion prefrontal cortex (mPFC), for example, represents uncertainty [23]. Dopamine neurons in the VTA, on the other hand, encode reward expectation. Given that prediction error originating from mPFC computations are required for the brain to create an internal state of action outcomes dopamine might help to coordinate the activity across sensory and frontal circuits to regulate propagation of bottom-up information from the periphery [23]. Furthermore, because the cortical pyramidal neurons excitability is regulated by GABA and dopamine, with the former preventing firing backpropagation in distal sites and the latter suppressing calcium signals [24], simultaneous dopaminergic and GABAergic neurotransmission in the mPFC might facilitate reward prediction. A direct outcome of this signaling would be enhanced top-down communication as the dopamine release is elevated [25]. In this context, bottom-up information passing through the ventrobasal (VB) thalamus dictates the rate of sensory information transfer to the somatosensory cortex via D1, which controls membrane depolarization, and D2, which elicits firing, receptor activation [1].

Our results on the bidirectional control of neuronal excitability by dopamine in the somatosensory cortex support the observations previously made in the basolateral amygdala (BLA)[26]. In BLA dopamine increases the firing rate of fast-firing interneurons while suppressing the spiking of regularly-firing (presumably excitatory) projection neurons [26]. Moreover, the dopaminergic receptor activation suppresses short-latency spikes evoked by electrical stimulation of the prefrontal and mediodorsal thalamic inputs to the BLA while potentiating the responses evoked by electrical stimulation of sensory association cortex [26]. Thus, it is plausible to assume that D1 and D2 activation facilitate sensory input (bottom-up) processing while attenuating mPFC (top-down) inputs. Overall, the systemic presence of dopamine from subcortical structures to sensory and higher cortices, and its role on the modulation of bottom-up and top-down processing argue that dopamine selectively modulates the gain in the sensory information propagating from the periphery.

Experience-dependent regulation of the somatosensory processing and behavior

During the brain development, dopaminergic neurons undergo experience dependent plasticity [27–29]. Our findings demonstrated that tactile sensory deprivation alters the transcription of genes in the dopaminergic signaling pathway in a cortical layer-specific manner (see Chapter 4). In L4, the main recipient of thalamic information in the S1, the genes regulated by

experience are involved in presynaptic dopaminergic signaling, localization, and transport. In L2/3, they are mostly responsible for postsynaptic changes and regulation of network excitability. Genes responsible for dopamine receptor trafficking, localization and metabolic control of dopamine synthesis and turnover were downregulated across all granular and supragranular layers. These findings are consistent with the observations in the olfactory system, where persistent odor enrichment leads to an increased number of dopaminergic cells in the glomerular layer [30]. This enrichment is likely to be modulated through regulation of neurogenesis as dopaminergic bulbar neurons are known to be involved in the olfactory sensory processing, especially in the signaling of innate olfactory-driven behaviors and the restorative functions of the adult olfactory bulb through neurogenesis [31].

Stimulus representations are regulated by dopaminergic modulation of the neuronal communication in cortical and subcortical areas of the brain. Dysregulation of the dopaminergic signaling is often linked to neuropsychiatric disorders associated with distorted perception such as addiction, depression and schizophrenia [32]. Therefore experience dependent regulation of dopaminergic signaling in sensory cortices might have far reaching consequences in neural computations that are known to be regulated by dopamine, e.g. reward prediction [33,34], reward delivery and representation [35], motor control [36], sensory mapping [37], selectivity to stimulus [38], sensory filtering in the amygdala [26], integration of newly born cells [30], sensory processing [31,39], sensorimotor gating [40,41] and memory formation [42,43]. Providing information about the outcome options is fundamental for decision making, and such predictions must be stored in the higher brain center so they can be evaluated together with the lower brain centers whenever new environmental information comes (updating predictions) [44]. As dopamine controls the excitability depending on the sensory input, it is possible that it might contribute to formation of sensory and perceptual memories in the sensory cortices.

Conclusions

Studies on the dopaminergic modulation of sensory processing in the visual circuitry (dopamine improves the transmission of the sensory signal by decreasing latency to response onset and increasing peak intensity and area of the primary response [45]; major depression [46] and schizophrenia [47] impairs visual processing), in the hippocampus (dopaminergic receptors work together for memory consolidation [48], spatial learning [49,50], and episodic memory [51]) and the complex modulation of intracellular resources by dopamine (see Chapter 1), suggest a neuromodulatory role for dopamine in sensory processing. Here we show that dopamine also controls information transfer in a cell type specific manner while providing a unique insight on the molecular, cellular and systemic role of dopamine in controlling sensory processing in the somatosensory cortex.

Dopamine influences the neuronal communication of the input regulating the spike threshold of pyramidal and interneurons differentially, through voltage-gated sodium channels activation. The intracellular calcium is another target after the activation of the dopaminergic receptors, leading to the specialized control of activation of subcellular structures, such as the dendritic spines. At the network level, this dopaminergic signaling filters the relevant information from the stimulus that is communicated with higher processing centers in the brain. It should be noted that this study has been primarily concerned with the electrophysiological properties of the neurons in the supragranular layers of the somatosensory cortex after pharmacological application of dopaminergic agonists and antagonists. The dopamine receptor localization was not directly quantified. However, there is evidence in the literature that shows their expression in the somatosensory cortex [52–54]. Moreover, in Chapter 4 we confirm these observations through RNA sequencing (also see barrelomics.science.ru.nl). Dopamine is related to many top-down factors such as reward, pleasure and movement generation, being a suitable candidate for the integration of the information that is transferred across neurons in different layers and brain regions. The dopamine receptors present in central and peripheral sensory systems are likely performing bidirectional control of the information processing, closing the neuromodulatory loop between the sensory processing and the dopaminergic signaling. Besides, simultaneous integration of top-down and bottom-up signals are expected in some cortical sensory neurons, such as the ones located in L2/3 of the somatosensory cortex. Overall, preparation for an action depends on the perception of object associated cues, for instance, and this process is highly coordinated between sensory and dopaminergic pathways simultaneously, leading to the conclusion that dopamine controls sensory representation and is likely involved in prior expectations and predictions, which should be object for further investigation.

Bibliography

1. Govindaiah, G., Wang, Y. & Cox, C. L. Dopamine enhances the excitability of somatosensory thalamocortical neurons. *Neuroscience* **170,** 981–991 (2010).
2. Schicknick, H. *et al.* Dopamine modulates memory consolidation of discrimination learning in the auditory cortex. *Eur. J. Neurosci.* **35,** 763–774 (2012).
3. Zaldivar, D., Goense, J., Lowe, S. C., Logothetis, N. K. & Panzeri, S. Dopamine Is Signaled by Mid-frequency Oscillations and Boosts Output Layers Visual Information in Visual Cortex. *Curr. Biol.* **28,** 224–235.e5 (2018).
4. Chuhma, N. *et al.* Dopamine neurons mediate a fast excitatory signal via their glutamatergic synapses. *J. Neurosci.* **24,** 972–981 (2004).
5. Werkman, T. R., Kruse, C. G., Nievelstein, H., Long, S. K. & Wadman, W. J. Neurotensin attenuates the quinpirole-induced inhibition of the firing rate of dopamine neurons in the rat substantia nigra pars compacta and the ventral tegmental area. *Neuroscience* **95,** 417–423 (2000).
6. Werkman, T. R. *et al.* Quetiapine increases the firing rate of rat substantia nigra and ventral tegmental area dopamine neurons in vitro. *Eur. J. Pharmacol.* **506,** 47–53 (2004).
7. Zhu, H. *et al.* Parkinson's disease-like forelimb akinesia induced by BmK I, a sodium channel modulator. *Behav. Brain Res.* **308,** 166–176 (2016).
8. Mamad, O., Delaville, C., Benjelloun, W. & Benazzouz, A. Dopaminergic control of the globus pallidus through activation of D2 receptors and its impact on the electrical activity of subthalamic nucleus and substantia nigra reticulata neurons. *PLoS ONE* **10,** e0119152 (2015).
9. Kang, Y. & Futami, T. Arrhythmic firing in dopamine neurons of rat substantia nigra evoked by activation of subthalamic neurons. *J. Neurophysiol.* **82,** 1632–1637 (1999).
10. Naundorf, B., Wolf, F. & Volgushev, M. Unique features of action potential initiation in cortical neurons. *Nature* **440,** 1060–1063 (2006).
11. Mainen, Z. F., Joerges, J., Huguenard, J. R. & Sejnowski, T. J. A model of spike initiation in neocortical pyramidal neurons. *Neuron* **15,** 1427–1439 (1995).
12. Govindaiah, G., Wang, T., Gillette, M. U., Crandall, S. R. & Cox, C. L. Regulation of inhibitory synapses by presynaptic D_4 dopamine receptors in thalamus. *J. Neurophysiol.* **104,** 2757–2765 (2010).
13. Henze, D. A., González-Burgos, G. R., Urban, N. N., Lewis, D. A. & Barrionuevo, G. Dopamine increases excitability of pyramidal neurons in primate prefrontal cortex. *J. Neurophysiol.* **84,** 2799–2809 (2000).
14. Gorelova, N., Seamans, J. K. & Yang, C. R. Mechanisms of dopamine activation of fast-spiking interneurons that exert inhibition in rat prefrontal cortex. *J. Neurophysiol.* **88,** 3150–3166 (2002).
15. Gulledge, A. T. & Jaffe, D. B. Dopamine decreases the excitability of layer V pyramidal cells in the rat prefrontal cortex. *J. Neurosci.* **18,** 9139–9151 (1998).
16. Ferris, M. J. *et al.* Sustained N-methyl-d-aspartate receptor hypofunction remodels the dopamine system and impairs phasic signaling. *Eur. J. Neurosci.* **40,** 2255–2263 (2014).
17. Tseng, K. Y. & O'Donnell, P. Dopamine-glutamate interactions controlling prefrontal cortical pyramidal cell excitability involve multiple signaling mechanisms. *J. Neurosci.* **24,** 5131–5139 (2004).
18. Tepper, J. M. & Lee, C. R. in *Gaba and the Basal Ganglia - From Molecules to Systems* **160,** 189–208 (Elsevier, 2007).
19. Yarom, M., Zurgil, N. & Zisapel, N. Calcium permeability changes and neurotransmitter release in cultured

brain neurons. II. Temporal analysis of neurotransmitter release. *J. Biol. Chem.* **260,** 16294–16302 (1985).

20. Evans, R. C., Zhu, M. & Khaliq, Z. M. Dopamine Inhibition Differentially Controls Excitability of Substantia Nigra Dopamine Neuron Subpopulations through T-Type Calcium Channels. *J. Neurosci.* **37,** 3704–3720 (2017).
21. Jędrzejewska-Szmek, J., Damodaran, S., Dorman, D. B. & Blackwell, K. T. Calcium dynamics predict direction of synaptic plasticity in striatal spiny projection neurons. *Eur. J. Neurosci.* **45,** 1044–1056 (2017).
22. Wang, Y.-L. *et al.* Selective dopamine receptor 4 activation mediates the hippocampal neuronal calcium response via IP3 and ryanodine receptors. *Brain Res.* **1670,** 1–5 (2017).
23. Starkweather, C. K., Babayan, B. M., Uchida, N. & Gershman, S. J. Dopamine reward prediction errors reflect hidden-state inference across time. *Nat. Neurosci.* **20,** 581–589 (2017).
24. Zhou, W.-L. & Antic, S. D. Rapid dopaminergic and GABAergic modulation of calcium and voltage transients in dendrites of prefrontal cortex pyramidal neurons. *J Physiol (Lond)* **590,** 3891–3911 (2012).
25. Jo, Y. S., Lee, J. & Mizumori, S. J. Y. Effects of prefrontal cortical inactivation on neural activity in the ventral tegmental area. *J. Neurosci.* **33,** 8159–8171 (2013).
26. Rosenkranz, J. A. & Grace, A. A. Modulation of basolateral amygdala neuronal firing and afferent drive by dopamine receptor activation in vivo. *J. Neurosci.* **19,** 11027–11039 (1999).
27. Michel, P. P. *et al.* Role of activity-dependent mechanisms in the control of dopaminergic neuron survival. *J. Neurochem.* **101,** 289–297 (2007).
28. Barr, H. J. & Woolley, S. C. Developmental auditory exposure shapes responses of catecholaminergic neurons to socially-modulated song. *Sci. Rep.* **8,** 11717 (2018).
29. Bonzano, S., Bovetti, S., Gendusa, C., Peretto, P. & De Marchis, S. Adult Born Olfactory Bulb Dopaminergic Interneurons: Molecular Determinants and Experience-Dependent Plasticity. *Front. Neurosci.* **10,** 189 (2016).
30. Bonzano, S., Bovetti, S., Fasolo, A., Peretto, P. & De Marchis, S. Odour enrichment increases adult-born dopaminergic neurons in the mouse olfactory bulb. *Eur. J. Neurosci.* **40,** 3450–3457 (2014).
31. Lazarini, F. *et al.* Adult neurogenesis restores dopaminergic neuronal loss in the olfactory bulb. *J. Neurosci.* **34,** 14430–14442 (2014).
32. Berridge, K. C. & Kringelbach, M. L. Affective neuroscience of pleasure: reward in humans and animals. *Psychopharmacology (Berl)* **199,** 457–480 (2008).
33. Asaad, W. F. & Eskandar, E. N. Encoding of both positive and negative reward prediction errors by neurons of the primate lateral prefrontal cortex and caudate nucleus. *J. Neurosci.* **31,** 17772–17787 (2011).
34. Kobayashi, S. & Schultz, W. Reward contexts extend dopamine signals to unrewarded stimuli. *Curr. Biol.* **24,** 56–62 (2014).
35. Wilson, D. I. G. & Bowman, E. M. Neurons in dopamine-rich areas of the rat medial midbrain predominantly encode the outcome-related rather than behavioural switching properties of conditioned stimuli. *Eur. J. Neurosci.* **23,** 205–218 (2006).
36. Wang, H. & Pickel, V. M. Dopamine D2 receptors are present in prefrontal cortical afferents and their targets in patches of the rat caudate-putamen nucleus. *J. Comp. Neurol.* **442,** 392–404 (2002).
37. Cho, J., Duke, D., Manzino, L., Sonsalla, P. K. & West, M. O. Dopamine depletion causes fragmented clustering of neurons in the sensorimotor striatum: evidence of lasting reorganization of corticostriatal input. *J. Comp. Neurol.* **452,** 24–37 (2002).
38. Bao, S., Chan, V. T. & Merzenich, M. M. Cortical remodelling induced by activity of ventral tegmental dopamine neurons. *Nature* **412,** 79–83 (2001).

39. Ongini, E., Bo, P., Dionisotti, S., Trampus, M. & Savoldi, F. Effects of remoxipride, a dopamine D-2 antagonist antipsychotic, on sleep-waking patterns and EEG activity in rats and rabbits. *Psychopharmacology (Berl)* **107,** 236–242 (1992).
40. Kucinski, A. *et al.* α7 neuronal nicotinic receptor agonist (TC-7020) reverses increased striatal dopamine release during acoustic PPI testing in a transgenic mouse model of schizophrenia. *Schizophr. Res.* **136,** 82–87 (2012).
41. Vuillermot, S., Feldon, J. & Meyer, U. Relationship between sensorimotor gating deficits and dopaminergic neuroanatomy in Nurr1-deficient mice. *Exp. Neurol.* **232,** 22–32 (2011).
42. Aso, Y. *et al.* Three dopamine pathways induce aversive odor memories with different stability. *PLoS Genet.* **8,** e1002768 (2012).
43. Wang, M., Vijayraghavan, S. & Goldman-Rakic, P. S. Selective D2 receptor actions on the functional circuitry of working memory. *Science* **303,** 853–856 (2004).
44. Schultz, W. Multiple functions of dopamine neurons. *F1000 Biol. Rep.* **2,** (2010).
45. Navarra, R. L., Clark, B. D., Zitnik, G. A. & Waterhouse, B. D. Methylphenidate and atomoxetine enhance sensory-evoked neuronal activity in the visual thalamus of male rats. *Exp. Clin. Psychopharmacol.* **21,** 363–374 (2013).
46. Fitzgerald, P. J. Gray colored glasses: is major depression partially a sensory perceptual disorder? *J. Affect. Disord.* **151,** 418–422 (2013).
47. Gracitelli, C. P. B. *et al.* Ophthalmology issues in schizophrenia. *Curr. Psychiatry Rep.* **17,** 28 (2015).
48. Furini, C. R. G., Myskiw, J. C., Schmidt, B. E., Marcondes, L. A. & Izquierdo, I. D1 and D5 dopamine receptors participate on the consolidation of two different memories. *Behav. Brain Res.* **271,** 212–217 (2014).
49. Kempadoo, K. A., Mosharov, E. V., Choi, S. J., Sulzer, D. & Kandel, E. R. Dopamine release from the locus coeruleus to the dorsal hippocampus promotes spatial learning and memory. *Proc Natl Acad Sci USA* **113,** 14835–14840 (2016).
50. Rocchetti, J. *et al.* Presynaptic D2 dopamine receptors control long-term depression expression and memory processes in the temporal hippocampus. *Biol. Psychiatry* **77,** 513–525 (2015).
51. Chowdhury, R., Guitart-Masip, M., Bunzeck, N., Dolan, R. J. & Düzel, E. Dopamine modulates episodic memory persistence in old age. *J. Neurosci.* **32,** 14193–14204 (2012).
52. Rivera, A. *et al.* Cellular localization and distribution of dopamine D(4) receptors in the rat cerebral cortex and their relationship with the cortical dopaminergic and noradrenergic nerve terminal networks. *Neuroscience* **155,** 997–1010 (2008).
53. Gurevich, E. V. & Joyce, J. N. Dopamine D(3) receptor is selectively and transiently expressed in the developing whisker barrel cortex of the rat. *J. Comp. Neurol.* **420,** 35–51 (2000).
54. Lidow, M. S. & Rakic, P. Scheduling of monoaminergic neurotransmitter receptor expression in the primate neocortex during postnatal development. *Cereb. Cortex* **2,** 401–416 (1992).

Summary

Summary

One of the most important functions of the brain is to process sensory information. All the time sensory inputs are being integrated with previous experiences and predictions, having the chance to define the best motor responses to the constantly changing environment. Spatial and temporal modulations of spike activity on sensory areas are required for the selectivity of stimulus-response patterns in the brain. The hypothesis that dopamine, in particular, and other neurotransmitters, in general, could regulate stimulus-evoked representations during adulthood has not been deeply addressed so far. Therefore, this thesis has focused on the neuromodulatory role of dopamine in integrating top-down and bottom-up inputs within the rodent brain somatosensory cortex, specialized in tactile inputs. More specifically, the dopaminergic control of sensory neuronal excitability was explored in detail.

Throughout the study, the main conclusions found were that **1)** Dopamine suppresses neuronal excitability; **2)** D1 and D2 receptor-mediated control of excitability is mediated through voltage-gated sodium channels and results in modulation of the action potential threshold; **3)** D1-mediated control of excitability is cell-type specific: upon D1 receptor activation, excitatory neuron firing rate is decreased while inhibitory neuronal firing rate is increased; **4)** Sensory deprivation alters transcription of genes in the dopaminergic signaling pathway in a cortical layer-specific manner suggesting that there is a functional close-loop between the dopaminergic signaling and sensory experience, and **5)** Dopamine is not the only neuromodulator to cause significant changes in neuronal activity, as Corticosterone controls evoked calcium transients in vitro and sensory representations in vivo.

Chapter 1 provided a critical review of the literature on dopaminergic regulation of neuronal excitability throughout the brain, arguing that sensorimotor circuits and dopaminergic neurons form a closed-loop circuit in the adult brain. To study the dopaminergic regulations of sensory neuron excitability, one first needs to define the biophysical properties of somatic integration. However, the integrative properties of the sensory cortical neurons are thus far studied only during the first weeks of the postnatal development. To provide an all-inclusive insight into the adult cortical neurons, **Chapter 2** presented our open source database including voltage-clamp and current-clamp recordings from the primary somatosensory cortex in animals 9-45 weeks old. **Chapter 3** determined the basic integrative properties of the excitatory and inhibitory neurons in the upper layers of the barrel cortex and identified electrically distinguishable subclasses in the adult neocortex. **Chapter 4** demonstrated that dopaminergic signaling in these layers undergo experience-dependent plasticity, arguing that sensory experience modulates the top-down dopaminergic drive impinging onto these sensory neurons. **Chapter 5** provided in-depth evidence that dopaminergic activation of the sensory neurons controls neuronal excitability in a cell-type specific manner by regulating

the voltage-gated sodium channel conductance to control spike-timing. **Chapter 6** showed that top-down regulation of the synaptic integration is not specific to the dopaminergic signaling by studying stimulus-evoked representations upon corticosterone application. Finally, **Chapter 7** provided an overview of how top-down regulation can modulate sensory representations. This mechanistic understanding of the contextual control over sensory representations will help to determine how neural representations of the world are shaped by behavioral and perceptual priors.

List of abbreviations

List of abbreviations

α-1: alpha-1 adrenergic receptor
AC: adenylate cyclase
Ach: acetylcholine
aCSF: artificial cerebrospinal fluid
ACTH: adrenocorticotropic hormone
ADHD: Attention Deficit Hyperactivity Disorder
α-DTX : alpha-dendrotoxin
AHP: afterhyperpolarization peak
AKAP-15: 15 kDa cAMP-dependent protein kinase-anchoring protein
AMPAr: α-amino-3-hydroxy-5-methyl-4-isoxazolepropionic acid receptor
ANOVA: analysis of variance
AP: action potential
ATP: adenosine triphosphate
AVP: vasopressin
β-2: beta-2 adrenergic receptor
βArrII: β arrestin II
BLA: basolateral amygdala
CA1: cornu ammonis 1 (first region hippocampus)
Ca^{2+}: calcium
CaM: calmodulin
CaMKII: Ca2+/calmodulin-dependent protein kinase II
Cat.nr.: category number
cAMP: cyclic adenosine monophosphate
CC: current clamp
Cort: corticosterone
CREB: cAMP response element-binding protein
CRH: corticotropin-releasing hormone
D1R: D1 receptor
D2R: D2 receptor
D3R: D3 receptor
D4R: D4 receptor
D5R: D5 receptor
DA: dopamine
DAG: diacylglycerol
DARPP-32: dopamine and cAMP regulated neuronal phosphoprotein

DSP: dopamine signaling pathway
EGTA: egtazic acid
EPSP: excitatory postsynaptic potentials
EtOH: ethanol
FN: frozen noise
FoxP2: forkhead box protein P2
GABA: gamma-Aminobutyric acid
GB: globus pallidus
Gi: G-protein subunit alpha i
GIRK: G-protein coupled inwardly rectifying potassium channel
GP: globus pallidus
GPCR: G-protein coupled receptors
G-proteins: guanosine triphosphate-binding proteins
Gq: G-protein subunit q
GR: glucocorticoids receptor
Gs: G-protein subunit alpha s
GSK-3: glycogen synthase kinase 3
GTP: guanosine-5'-triphosphate
HBBS: Hank's balanced salts solution
HCN: hyperpolarization-activated, cyclic nucleotide-modulated
HEPES: 4-(2-hydroxyethyl)-1-piperazineethanesulfonic acid
HPA: hypothalamic-pituitary-adrenal
ISO: isoproterenol
I/V: current/voltage
IK(Ca): calcium-activated potassium after-hyperpolarization current
IP3: inositol triphosphate;
ISI: interspike intervals
K^+: potassium
K_v: voltage-gated potassium channel
L1: cortical layer 1
L2/3: cortical layer 2/3
L4: cortical layer 4
L5: cortical layer 5
L6: cortical layer 6
LTD: long term depression
LTP: long term potentiation

M1: primary motor cortex
MAPK: mitogen-activated protein kinase
mPFC: medial prefrontal cortex
ML: maximum likelihood
MR: mineralocorticoids receptor
mRNA: messenger ribonucleic acid
Na^+: sodium
NaV: voltage-gated sodium channel
NE: norepinephrine
NMDA: N-Methyl-D-aspartic acid
NMDAr: N-methyl-D-aspartate receptor
P2P: peak-to-peak
PCA: principal component analysis
PD: Parkinson's Disease
PFC: prefrontal cortex
PKA: protein kinase A;
PKC: protein kinase C
PLC: phospholipase C
P*n*: postnatal day *n*
POMC: pro-opiomelanocortin
PP-1: protein phosphatase 1
PP2A: protein phosphatase 2
PPN: pedunculopontine nucleus
PPP1R1B: protein phosphatase 1 regulatory subunit 1B
PSP: postsynaptic potentials
Pval: Parvalbumin
PVN: portal vessel system
RNA: ribonucleic acid
RPE: reward prediction error
S1: primary sensory cortex
SK: calcium activated potassium channels
SM: slicing medium
SNc: Substantia nigra pars compacta
SNr: Substantia nigra pars reticulata
SSt: somatostatin
ST: sawtooth

STN: subthalamic nucleus
TAAR1: Trace Amine Associated Receptor 1
TTX: tetrodotoxin
V1: primary visual cortex
VB: ventrobasal thalamus
VC: voltage clamp
VGCC: voltage-gated calcium channel
VTA: Ventral tegmental area

Samenvatting

Samenvatting

Een van de belangrijkste functies van de hersenen is het verwerken van sensorische informatie. Voortdurend worden sensorische *inputs* geïntegreerd met eerdere ervaringen en voorspellingen, waardoor de best passende motorische reacties op de constant veranderende omgeving gedefinieerd kunnen worden. Ruimtelijke en temporele modulaties van spike-activiteit op sensorische gebieden zijn vereist voor de selectiviteit van stimulus-responspatronen in de hersenen. De hypothese dat voornamelijk dopamine en andere neurotransmitters, stimulus representaties tijdens volwassenheid kunnen reguleren, is tot nu toe niet diepgaand aangepakt. Daarom heeft dit proefschrift zich gericht op de neuromodulerende rol van dopamine bij het integreren van top-down en bottom-up *inputs* in de somatosensorische hersenschors van knaagdieren, gespecialiseerd in tactiele ingangen. Met name de dopaminerge controle van sensorische neuronale exciteerbaarheid werd in detail onderzocht.

Gedurende de gehele studie waren de belangrijkste conclusies dat **1)** dopamine de neuronale prikkelbaarheid onderdrukt; **2)** D1- en D2-receptor-gemedieerde controle van de exciteerbaarheid wordt gemedieerd door spanningsafhankelijke natriumkanalen en resulteert in modulatie van de actiepotentiaalgrens; **3)** D1-gemedieerde controle van de exciteerbaarheid celtype specifiek is: na D1-receptoractivering is de excitatorische neuron afvuursnelheid verlaagd terwijl de remmende neuronale afvuursnelheid wordt verhoogd; **4)** Sensorische deprivatie de transcriptie van genen in de dopaminerge signaalroute op een corticale laag-specifieke manier verandert, wat suggereert dat er een functionele close-loop is tussen de dopaminerge signalering en sensorische ervaring, en **5)** Dopamine niet de enige neuromodulator is die significante veranderingen veroorzaakt in neuronale activiteit, aangezien corticosteron in vitro opgewekte calcium transiënten en *in vivo* sensorische representaties regelt.

Hoofdstuk 1 gaf een kritische beoordeling van de literatuur over dopaminerge regulatie van neuronale exciteerbaarheid in de hersenen, met als discussiepunt dat sensorimotorische circuits en dopaminerge neuronen een gesloten circuit vormen in het volwassen brein. Om de dopaminergische voorschriften van sensorische neuron-exciteerbaarheid te bestuderen, moet men eerst de biofysische eigenschappen van somatische integratie definiëren. De integrerende eigenschappen van de sensorische corticale neuronen zijn echter tot nu toe alleen bestudeerd gedurende de eerste weken van de postnatale ontwikkeling. Om volledig inzicht te bieden in de volwassen corticale neuronen, presenteerde **Hoofdstuk 2** onze open source database met spannings- en stroomklem opnames van de primaire somatosensorische cortex bij muizen van 9-45 weken oud. **Hoofdstuk 3** bepaalde de basale integrerende eigenschappen van de excitatoire en remmende neuronen in de bovenste lagen van de *barrel cortex* en identificeerde elektrisch te onderscheiden subklassen in de volwassen neocortex. **Hoofdstuk 4** bewijst dat

dopaminerge signalering in de bovenste lagen van de barrel cortex ervaringsafhankelijke plasticiteit ondergaat, met onderbouwing dat de top-down dopaminerge aandrijving op deze sensorische neuronen wordt gereguleerd door sensorische ervaringen. **Hoofdstuk 5** leverde diepgaand bewijs dat dopaminerge activering van de sensorische neuronen neuronale exciteerbaarheid regelt. De wijze waarop dit gebeurt is afhankelijk van het celtype. Dit gebeurt op een celspecifieke manier door de spanningsafhankelijke natriumkanaalgeleidbaarheid te reguleren wat invloed heeft op de spike-timing. Door het bestuderen van stimulus-opgewekte representaties bij toepassing van corticosteron laat **Hoofdstuk 6** zien dat top-down regulatie van de synaptische integratie niet specifiek is voor de dopaminerge signalering. Ten slotte gaf H**oofdstuk 7** een overzicht van de wijze waarop top-down regulatie sensorische representaties kan moduleren. Het begrip van de contextuele controle wat betreft sensorische representaties zal helpen bepalen hoe neurale representaties van de wereld worden gevormd door gedrags- en perceptuele *priors*.

Acknowledgements

Acknowledgements

Many people contributed to this thesis and my survival as a researcher in the Netherlands. First, I would like to thank the opportunity granted to me by Benno Rozendaal and Tansu Celikel, after accepting my application as a Ph.D. candidate of the Donders Institute, and to the National Council for Scientific and Technological Development of Brazil (CNPq) for providing the financial support.

Tansu not only was my daily supervisor but mainly gave me all the assistance I needed to embrace new challenges and to overcome each limitation, besides holding my dopaminergic levels raised at our weekly meetings (with a lot of chocolate). During these four years, I have acquired so much knowledge working with you, that it seems like a lifetime. You constantly motivated me to go further than I thought it was possible. Thanks for being patient and doing everything you could to make this production happen.

In the Department of Neurophysiology, it was difficult to say goodbye to several people who have worked with me throughout the years. Specially, I would like to thank the contributions of Lorena, Max, Sabine, Francisco, Michel and Ate (this one I did not have to say goodbye yet, as he is part of the furniture). I hope I have contributed to your learning and future careers as much as you presented me with your curiosity and dedication during your internships. Ate, in particular, helped me to persevere on the patch-clamp experiments by regularly playing an uplifting playlist including from Backstreet Boys to *Nederhop*. Still, seriously, you can count on me as a friend. Thank you for everything. Debbie, Ron and Eric, it was a pleasure to work with you! From preparing perfusions and ordering drugs to professional photography's and organizing parties, you were always there! Thanks for the *gezelligheid*. My colleagues Jesse, Koen, Ali, Úrzula, Yiping, Niccolo, Ashutosh, and Xuan, thanks for the inspiring talks about neuroscience and beyond. It was a delight to go through these years with you guys. Rémi, Yutaro, Fleur, Bernhard, and Wim, I have learned so much from you and know I am proud of eventually being part of the same team as all of you. Tido, Thijs G., Thijs R., Lynn, Judith, David, and Leonhard, what a busy department we had then! You were always so chill and friendly that I could even forget we were in the Science Faculty sometimes. Thanks for the friendship. Maaike, Melanie, Judith, Mark, Merijn, Fei Ma, and Zhengyu Tang, who I met in the past year, sorry I could not socialize more, but it was great meeting you.

The Donders Institute enabled rich scientific discussions, by promoting excellent events, lectures, and courses, offering all the means for me to become a complete neuroscientist. I could lunch with the most prominent Brazilian neuroscientist, Miguel Nicolelis, and organize scientific talks as a member of the Donders Sessions committee, and of the Donders Discussions organizing committee. Besides, I met excellent colleagues who I ended

up joining for a project in neuroscience education for children. Thanks for the refreshing meetings with *OCEANA*, specially Roselyne, Izabella, Sophie, Ella, and Joao. Special thanks to the *Radboud Sportcentrum*: their cheap fee and wonderful courses really helped me to have the best shape of my life (it is not the case anymore), and also sustained my mental health.

I must acknowledge the support of my close friends in the Netherlands, that became a family during this period. Thank you Bia, Edu and Joames, you know how much I have struggled, and you helped it to be lighter by dancing with me "to the floor", even in the cold, dark and snowy days. Bia, you know how strong our friendship became. You can deny you are Brazilian and pretend you do not like to dance Brazilian funk but stop lying that you never met me in Sao Paulo before. We are sisters! Thank you for daily encouragement and support. Edu, every year that passes you get younger! It is amazing, I want to be like you when I grow up. Now thanks for listening to my never-ending stories from the lab and managing not to steal any of my boyfriends from me. Joames, you know you can count on me and I know you are one of the most trustworthy people I have met. Thanks for being here.

My Brazilian friends and family, I am sorry I have left you! I can never feel guiltier from missing the time I could have spent with you in the past years. However, we were never really apart, right? My friends from high-school, *as F*úteis (Rafa, Thalita, Marcia, Mariana, Loira, Nathi, Debora), and many others from São Paulo, I can always feel your love and care even by text messages. Some of you came to Europe during this time, and we met when I went to Brazil, and it is always as if we were never missing each other. Thanks for the long-distance motivation. I love you forever. My close family consists in the majority of lovely and strong women. Without my great-grandmothers (Bisa Anália and Bisa Inácia), my grandmother (Vó Dalva), and my mother (Mamis), I would never be here, for obvious genetic reasons, and for their intense and unconditional love.

Bisa Inácia (*in memorian*) taught me since early age to be independent and care for my education. Vó Dalva, a senhora é mãe, é pai, é avó, é amiga, é o maior presente na nossa família. Sustenta tudo sozinha, o mundo pode desabar, mas sua força nos mantém. Quero muito que a senhora se cuide também, não esquece. Aquela cartinha que encontrei na minha mala quando cheguei aqui me ajudou muitas vezes, e sempre esteve na minha parede. Obrigada por superar seu medo de avião para vir na minha defesa mesmo sem a gente saber se vai mesmo acontecer, se estiver lendo isso, é porque eu consegui. Eu te amo muito e agradeço demais o apoio que me deu desde o início. Mãe, Sheila, você é a melhor mãe que eu poderia sonhar em ter. É *pãe*, como se diz agora, me criou tão jovem, e do seu jeito e com tanto amor e respeito, que eu só tenho a agradecer. As aulas de inglês no carro, ao som do *Offspring*, me motivaram a falar inglês melhor, a independência com que me ensinou a

viver, a amizade, a persistência, e a honestidade. Não seria possível eu estar aqui sem você. Te amo demais, obrigada. Léo e Bia, meus irmãos lindos, eu sinto muito o tempo perdido em que poderia ter brincado com vocês, e ter testemunhado seu desenvolvimento de perto. Mas vocês sempre poderão contar comigo. O amor supera todas as distâncias. Minhas tias: Monica, Tita (*in memorian*), e Mariane (*in memorian*), vocês me motivaram a estudar, porque eu tinha vocês como inspirações. Sempre estudiosas, mas com equilíbrio, nunca deixando de se divertir e vivendo a vida com leveza. Amo todas vocês e sinto muita saudade das que se foram… Vô Dilson, o senhor foi um suporte muito importante durante toda a minha vida acadêmica e até hoje. Sempre disponível. Obrigada por tudo. Nossa viagem mais recente ao Rio de Janeiro vai ficar para sempre no meu coração. Laura, Cecília, Fe e Taís, eu não podia esperar primos mais fofos e maravilhosos. Orgulho de vocês. Laura e Ce, obrigada por terem vindo. Tia Nélia, obrigada pelo apoio como representante da minha família paterna. À minha família extensa: tios-avós, primas e primos, muito obrigada também pelo apoio, mesmo que de longe.

Tot slot zou ik mijn liefje Luc willen bedanken, die tijdens de moeilijkste dagen aan mijn zijde heeft gestaan. Sorry mijn Nederlands is nog niet perfect. Maar bedankt voor je kalmte, geduld en warmte. Bedankt voor het bereiden van evenwichtige en vegetarische maaltijden voor mij (toen ik zelfs vergat dat ik ook moest eten), voor het kopen van een Braziliaans gedichtboek zodat ik me thuis voelde en voor me kon zorgen. Je bent de meest liefdevolle persoon die ik ooit heb ontmoet. Ik hou van je.

Finally, I will leave a piece of my favorite Brazilian poem, from Carlos Drummond de Andrade, A máquina do mundo:

"O que procuraste em ti ou fora de
teu ser restrito e nunca se mostrou,
mesmo afetando dar-se ou se rendendo,

e a cada instante mais se retraindo,
olha, repara, ausculta: essa riqueza
sobrante a toda pérola, essa ciência

sublime e formidável, mas hermética,
essa total explicação da vida,
esse nexo primeiro e singular,

que nem concebes mais, pois tão esquivo

se revelou ante a pesquisa ardente
em que te consumiste... vê, contempla,
abre teu peito para agasalhá-lo."

Curriculum Vitae

Curriculum Vitae

Angelica da Silva Lantyer was born in Sao Paulo, Brazil and finished her bachelor's in psychology in the Federal University of Sao Paulo. At the same university, she completed her Master thesis on stress and anxiety among university students and subsequently worked as a social psychologist in Campinas. She moved to the Netherlands to study the complex neuromodulatory mechanisms involved in sensory perception at the Donders Institute. She is currently assistant coordinator of the Human Brain Project, located in the Department of Systems and Cognitive Neurosciences, University of Amsterdam.

Donders Series

Donders Graduate School for Cognitive Neuroscience

For a successful research Institute, it is vital to train the next generation of young scientists. To achieve this goal, the Donders Institute for Brain, Cognition and Behaviour established the Donders Graduate School for Cognitive Neuroscience (DGCN), which was officially recognised as a national graduate school in 2009. The Graduate School covers training at both Master's and PhD level and provides an excellent educational context fully aligned with the research programme of the Donders Institute.

The school successfully attracts highly talented national and international students in biology, physics, psycholinguistics, psychology, behavioral science, medicine and related disciplines. Selective admission and assessment centers guarantee the enrolment of the best and most motivated students.

The DGCN tracks the career of PhD graduates carefully. More than 50% of PhD alumni show a continuation in academia with postdoc positions at top institutes worldwide, e.g. Stanford University, University of Oxford, University of Cambridge, UCL London, MPI Leipzig, Hanyang University in South Korea, NTNU Norway, University of Illinois, North Western University, Northeastern University in Boston, ETH Zürich, University of Vienna etc.. Positions outside academia spread among the following sectors: specialists in a medical environment, mainly in genetics, geriatrics, psychiatry and neurology. Specialists in a psychological environment, e.g. as specialist in neuropsychology, psychological diagnostics or therapy. Positions in higher education as coordinators or lecturers. A smaller percentage enters business as research consultants, analysts or head of research and development. Fewer graduates stay in a research environment as lab coordinators, technical support or policy advisors. Upcoming possibilities are positions in the IT sector and management position in pharmaceutical industry. In general, the PhDs graduates almost invariably continue with high-quality positions that play an important role in our knowledge economy.

For more information on the DGCN as well as past and upcoming defenses please visit: http://www.ru.nl/donders/graduate-school/phd/